Consejo Superior de Investigaciones Científicas
Universidad Miguel Hernández
Instituto de Neurociencias

PROPIEDADES BIOFÍSICAS Y FARMACOLOGÍA DE LOS CANALES IÓNICOS TRP SENSIBLES A TEMPERATURA: TRPV1, TRPA1 Y TRPM8

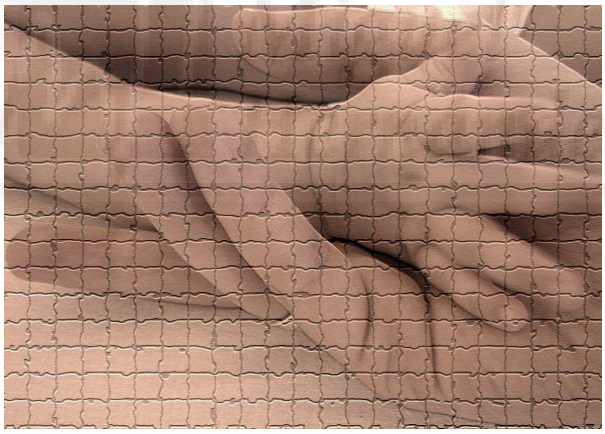

Tesis para optar al grado de Doctor en Neurociencias presentada por:

Víctor M. Meseguer Vigueras

Director:

Dr. Félix Viana de la Iglesia

San Juan de Alicante, Junio de 2009

UNIVERSITAS
Miguel
Hernández

A Luisa y nuestra pequeña Esther,
a mis padres Manolo y Loli,
a mi hermana Elisa, a Carmen,a Kini,
a toda mi familia, amigos y compañeros.

Por vuestro apoyo incondicional

UNIVERSITAS
Miguel
Hernández

ÍNDICE

UNIVERSITAS
Miguel
Hernández

ABREVIATURAS

1. INTRODUCCIÓN

2. OBJETIVOS

3. MATERIALES Y MÉTODOS

UNIVERSITAS
Miguel
Hernández

ABREVIATURAS

AA: ácido araquidónico
AEA: anandamida
AINE: antiinflamatorios no esteroideos
AITC: alil-isotiocianato
4α -PDD: 4α-forbol 12,13-didecanoato
ANKTM1: “Ankyrin like protein with transmembrane domains 1”
AP18: 4-(4-Clorofenil)-3-metil-3-buten-2-ona oxima
2-APB: 2- Aminoetoxidifenil borato
AS-ODN: oligonucleótido antisentido
ATP: adenosin trifosfato
$ATPNa_2$: ATP disódico
BAYK8644: metil 2,6-dimetil-5-nitro-4-[2-(trifluorometil)fenil]-1,4-dihidropiridina-3-carboxilato.
BCTC: N-(4-tertiaributilfenil)-4-(3-cloropiridin-2-il) tetrahidropirazina-1(2H)-carboxamida
$[Ca^{2+}]_i$: concentración intracelular de calcio
CaM: calcio/calmodulina
CaMKII: quinasa II dependiente de calcio calmodulina
Caps: capsaicina
CB1: receptor canabinoide de tipo 1
CCD: dispositivo de cargas eléctricas acopladas
CGRP: peptido relacionado con el gen de la calcitonina
CLT: clotrimazol
CM: cinamaldehído
CMH: fibras C nociceptivas sensibles a estímulo mecánico y calor
CMR1: receptor de mentol y frío 1
CR#1: linea celular “cold receptor 1”
CTPC: (2R)-4-(3-cloro-2-piridinil)-2-metil-N-(4-[trifluorometil]fenil)-1-piperazinacarboxamida
Ctrl: control
Cu-Phe: complejo cobre:fenantrolina
CHO: linea celular “Chinese Hamster Ovary”
CHO-K1/FRT: células CHO con expresión inducible con tetraciclina
CHO-TRPA1: células CHO con expresión estable de TRPA1
DAG: diacilglicerol
DMEM: “Dulbecco's Modified Eagle Medium”
DMSO: Sulfóxido de dimetilo
EGTA: Ácido etilenglicol-bis (2 aminoetiléter)–. N, N, N’, N’- tetra-acético
F: frío
F_{340}: Fluorescencia emitida por el Fura-2 excitado con luz de longitud de onda de 340 nm
F_{380}: Fluorescencia emitida por el Fura-2 excitado con luz de longitud de onda de 380 nm
fura 2-AM: Fura-2 acetoximetil ester
GFP: proteína fluorescente verde
G_{max}: conductancia máxima
HC-030031: 2-(1,3-dimetil-2,6-dioxo-1,2,3,6-tetrahidro-7H-purin-7 -il)-N-(4-isopropilfenil)acetamida

HEK293: linea celular “Human embryonic Kidney 293”
HEPES: ácido N-(2-hidroxietil)piperazina-N’-(4-butasulfónico)
5 –HETE: ácido 5 hidroxieicosatetraenoico
15 –HETE: ácido 15 hidroxieicosatetraenoico
HETEE: HETE etanolamida
4-HNE: 4-Hidroxinonenal
HPETEE: HPETE etanolamida
15-HPETE: ácido 15 hidroperoxieicosatetraenoico
12-HPTE: ácido 12 hidroperoxieicosatetraenoico
IC_{50}: valor medio de la concentración inhibitoria máxima
I_{cola}: corriente de cola
IK (Ca^{2+}): “intermediate conductance Ca^{2+}-activated K^+ channels”
I_{max}: corriente máxima
IP3: inositol 1,4,5 trifosfato
iPLA2: fosfolipasa A2 insensible a calcio
I_{ss}: corriente en estado estacionario
IUSP: Asociación Internacional para el Estudio del Dolor
I-V: curva corriente-voltaje
K: pendiente de la curva de activación
LBT4: leucotrieno B4
LNCaP: linea celular “androgen-sensitive human prostate adenocarcinoma”
LOX: lipooxigenasa
LPL: lisofosfolípido
M: mentol
ML1: “mucolipin 1”
ML2: “mucolipin 2”
ML3: “mucolipin 3”
MO: aceite de mostaza
mTRPC2: “transient receptor potential” de ratón tipo C2
$[Na^+]_i$: concentración intracelular de sodio
NADA: N- araquidonildopamina
NGF: factor de crecimiento neuronal
Nif: nifedipina
0 Ca^{2+}: solución sin Ca^{2+}
$P_{apertura}$: probabilidad de apertura
PBS: tampón fosfato salino
P_{Ca}: permeabilidad a Ca^{2+}
P_{Cs}: permeabilidad a Cs^+
PGE_2: prostaglandina E_2
PIP_2: inositol 4,5 bifosfato
PKA: proteína quinasa A
PKC: proteína quinasa C
PKD2: “Polycystic Kidney disease protein”
PKD2L1: “PKD-like protein” tipo 1
PKD2L2: “PKD-like protein” tipo 2
PLC: fosfolipasa C
P_{Na}: permeabilidad a Na^+
PUFA: ácidos grasos poliinsaturados
RR: rojo de rutenio
RTX: resiniferatoxina

SB-452533: N-(2-bromofenil)-N´-(2-[etil{3-metilfenil}amino]etil)-urea
SKF96365:1-[β-[3-(4-methoxifenil)propoxi]-4-methoxifenetil]-1H-imidazol hidroclorito
SP: substancia P
TG: ganglio trigémino
Δ9-THC: Δ9-tetrahidrocanabiol
TM2: segundo dominio transmembrana
TM3: tercer dominio transmembrana
TRP: “transient receptor potential”
TRPA: “transient receptor potential” tipo A
Trpa1-/-: genotipo nulo para TRPA1
TRPA1: “transient receptor potential” tipo A1
TRPC: “transient receptor potential” tipo C
TRPM: “transient receptor potential” tipo M
TRPM2: “transient receptor potential M2”
TRPM4: “transient receptor potential” tipo M4
TRPM5: “transient receptor potential” tipo M5
TRPM8: “transient receptor potential” tipo M8
TRPML: “transient receptor potential” tipo ML
TRPN: “transient receptor potential” tipo N
TRPP: “transient receptor potential” tipo P
TRP-p8: “transient receptor potential” tipo p8
TRPV: “transient receptor potential” tipo V
$TRPV1^{-/-}$: genotipo nulo para TRPV1
TRPV1: “transient receptor potential” tipo V1
$TRPV1^{+/+}$: genotipo homocigótico para TRPV1
TRPV2: “transient receptor potential” tipo V2
TRPV3: “transient receptor potential” tipo V3
TRPV4: “transient receptor potential” tipo V4
TRPV6: “transient receptor potential” tipo V6
TRPY: “transient receptor potential” tipo Y
V: potencial de membrana
$V_{1/2}$: potencial de membrana en el que la probabilidad de apertura de un canal iónico es del 50%.
V_m: potencial de membrana
VR-1: receptor vaniloide de tipo 1
V_{rev}: potencial de reversión
WT: genotipo silvestre
zTRPN1: “transient receptor potential” de pez cebra tipo N1

UNIVERSITAS
Miguel
Hernández

1 INTRODUCCIÓN

UNIVERSITAS
Miguel
Hernández

Los receptores sensoriales son el conjunto de células periféricas especializadas en proporcionar al sistema nervioso información sobre la naturaleza e intensidad de los diferentes estímulos que alcanzan nuestro organismo. Estos estímulos pueden ser de naturaleza química o física, como las fuerzas mecánicas y la temperatura. Hasta hace pocos años existía un desconocimiento casi absoluto sobre los mecanismos moleculares responsables de la detección de los estímulos térmicos, a diferencia de la transducción de estímulos luminosos, gustativos, olfatorios y auditivos, para los que ya se había identificado la proteína receptora y se habían descrito los mecanismos iónicos que conducen a la generación del potencial receptor. Esta situación cambió con la identificación de distintos canales iónicos que muestran una gran sensibilidad (Q10 >5) en su actividad durante los cambios de temperatura (Jordt et al. 2003). Entre dichos canales termosensibles destacan algunos de la familia de los canales iónicos TRP, que deben su nombre al potencial receptor transitorio ("transient receptor potential") característico de los fotorreceptores en un mutante de *Drosophila*, el cual permitió la identificación del primer miembro de dicha familia. Actualmente a los canales iónicos TRP se les atribuye un papel fundamental en los procesos de transducción sensorial de distintos estímulos, incluyendo el tacto, la percepción de temperatura (frío y calor) y del dolor (Wissenbach et al. 2004).

En las últimas décadas el desarrollo de dos herramientas metodológicas, las técnicas de "patch-clamp" y las técnicas de biología molecular han contribuido de manera decisiva a ampliar el conocimiento sobre la distribución, estructura, funcionamiento y el papel fisiológico de los canales iónicos en los organismos vivos. Además, la modulación farmacológica de la actividad de los canales iónicos ha enriquecido el conocimiento de los mecanismos moleculares de comunicación tanto de tipo eléctrico (potencial de acción) como químico (neurotransmisores y hormonas) entre células.

1.1. Canales iónicos.

El genoma humano codifica cientos de canales iónicos que regulan el paso de iones a través de la bicapa lipídica (Hille 2001). Mientras que los transportadores requieren energía para la generación de gradientes electroquímicos a través de la membrana, los canales iónicos gastan esta energía almacenada, como si se tratase de interruptores que liberan la energía eléctrica acumulada en una batería. La apertura y cierre de estos canales iónicos se debe a cambios de conformación, lo que permite el paso regulado de iones a través de su poro. El flujo de iones a través de la membrana plasmática genera señales eléctricas en las células excitables. Estas señales se suelen acoplar a un aumento transitorio del calcio intracelular, y controlan procesos fisiológicos tan diversos como la contracción muscular, la secreción de hormonas, la expresión de genes, la división celular, las sensaciones y el procesamiento de información.

En función de su mecanismo de apertura, los canales iónicos se pueden clasificar en tres grandes grupos: canales abiertos por cambio del voltaje transmembrana, canales abiertos por ligandos extra o intracelulares y canales abiertos por fuerzas físicas (estímulos mecánicos, temperatura), aunque también se usan otros criterios para su clasificación como pueden ser la selectividad iónica (canales de sodio, de potasio, de calcio, etc.) o criterios filogenéticos como la homología de las secuencias de aminoácidos.

1.2. Canales iónicos TRP

Como ya he mencionado, los llamados canales iónicos TRP constituyen una superfamilia de canales iónicos que debe su nombre a una mutación en una proteína de *Drosophila melanogaster* asociada a la fototransducción. En el ojo complejo de Drosófila, estos mutantes presentan, a diferencia del fenotipo silvestre, un potencial receptor transitorio (*trp;* transient receptor potential) a la estimulación lumínica prolongada. Los mutantes *trp* se conocen desde 1969 (Cosens et al. 1969), aunque hasta el año 1989 no se caracterizó el defecto genético subyacente al fenotipo mutante *trp* de Drosófila (Montell et al. 1989), y hasta 1992 no se identificaron las proteínas TRP como canales iónicos (Hardie et al. 1992). Desde entonces, muchos nuevos canales iónicos han sido identificados

como pertenecientes a la superfamilia de canales iónicos TRP, exclusivamente en organismos eucariotas, y más concretamente en animales y hongos.

La presencia de los canales iónicos TRP en levaduras sitúa su origen evolutivo en organismos unicelulares anteriores a la aparición de los metazoos. En estos organismos unicelulares los TRP son imprescindibles para la interacción y adaptación al entorno, así por ejemplo permiten a levaduras percibir y responder a cambios osmóticos del medio (Wissenbach et al. 2004). Mientras que la presencia de los TRP en células especializadas de organismos pluricelulares permite la existencia entre otras funciones de procesos sensoriales complejos como la visión y el oído, además de la percepción de la temperatura, el dolor, el gusto y las feromonas.

Los canales iónicos TRP median el paso de cationes a través de la membrana plasmática. De este modo, los cationes Ca^{2+} y Na^{+} que forman parte del medio extracelular pasan al interior celular a favor de un gradiente electroquímico, lo que genera un incremento de las concentraciones intracelulares de calcio $[Ca^{2+}]_i$ y de sodio $[Na^{+}]_i$ respectivamente, y esto conlleva el cambio del potencial de la membrana plasmática (V_m) hacia valores más positivos o despolarizados. En células excitables como las neuronas, el cambio en el V_m determina la generación y propagación del potencial de acción, mientras que en células no neuronales y excitables como son las fibras musculares participa en la contracción muscular. El papel del voltaje en células no excitables es fundamental para establecer la fuerza electromotriz que favorece la entrada de calcio a la célula, así como para la apertura de canales de Ca^{2+}, K^{+} y Cl^{-} dependientes de voltaje. Además, el incremento de calcio intracelular es un mecanismo de señalización celular *per se*.

1.2.1. Clasificación y distribución filogenética

La superfamilia de canales iónicos TRP se expresa en una gran variedad de organismos multicelulares que incluye anélidos, mosca del vinagre, pez cebra ratones y humanos. Dependiendo del organismo en donde se expresan el número de miembros que conforman la superfamilia de los canales TRP comprende entre 17 y 28. Los canales TRP se dividen en dos grandes grupos, grupos 1 y 2, que a su vez se dividen en siete familias. La clasificación se ha realizado en base a la homología de las secuencias primarias de aminoácidos debido a la enorme variabilidad existente en cuanto a selectividad catiónica, tipo

de ligando, regulación, función, etc. (Clapham 2003). Además, en levaduras existe una octava familia llamada TRPY, pero no está incluida en los dos grupos mencionados debido a la gran diferencia que existe en sus secuencias primarias.

Como se muestra en la figura 1, el grupo 1 de canales iónicos TRP está formado por cinco familias entre las que se encuentran los miembros que presentan el mayor grado de homología respecto del miembro fundador de los TRP, el TRP originalmente hallado en Drosófila (Hardie et al. 1992). Estos TRP son conocidos con el nombre de TRPC, donde la letra C hace alusión a clásico o canónico. Este grupo 1 lo completan las familias TRPV, TRPM, TRPA y TRPN. La familia TRPN no se ha encontrado en mamíferos aunque sí en otros vertebrados como el pez cebra. La familia TRPV (V; vaniloide), formada por seis miembros, debe su nombre al primer miembro identificado, el receptor vaniloide (VR-1; vanilloid receptor), actualmente también conocido como TRPV1. La familia TRPM (M, melastatina), comprende ocho miembros y debe su nombre a que el canal iónico TRPM1, el primero de la familia en ser identificado, fue originariamente llamado melastatina. Por último, la familia TRPA, formada por un único miembro en mamíferos, llamado ANKTM1 o TRPA1.

El grupo 2 lo conforman las familias TRPP y TRPML. Los miembros pertenecientes a la familia TRPP lo forman la proteína conocida como PKD2 (Polycystic Kidney disease protein), que en su forma mutante está relacionada con la enfermedad hereditaria del riñón poliquístico, más otras dos proteínas semejantes, “PKD-like proteins”, llamadas. PKD2L1 y PKD2L2. La familia TRPML está formada por tres proteínas (ML1, ML2 y ML3) relacionadas con la proteína MCOLN1, implicada en la enfermedad hereditaria Mucolipidosis Tipo IV (Venkatachalam et al. 2007).

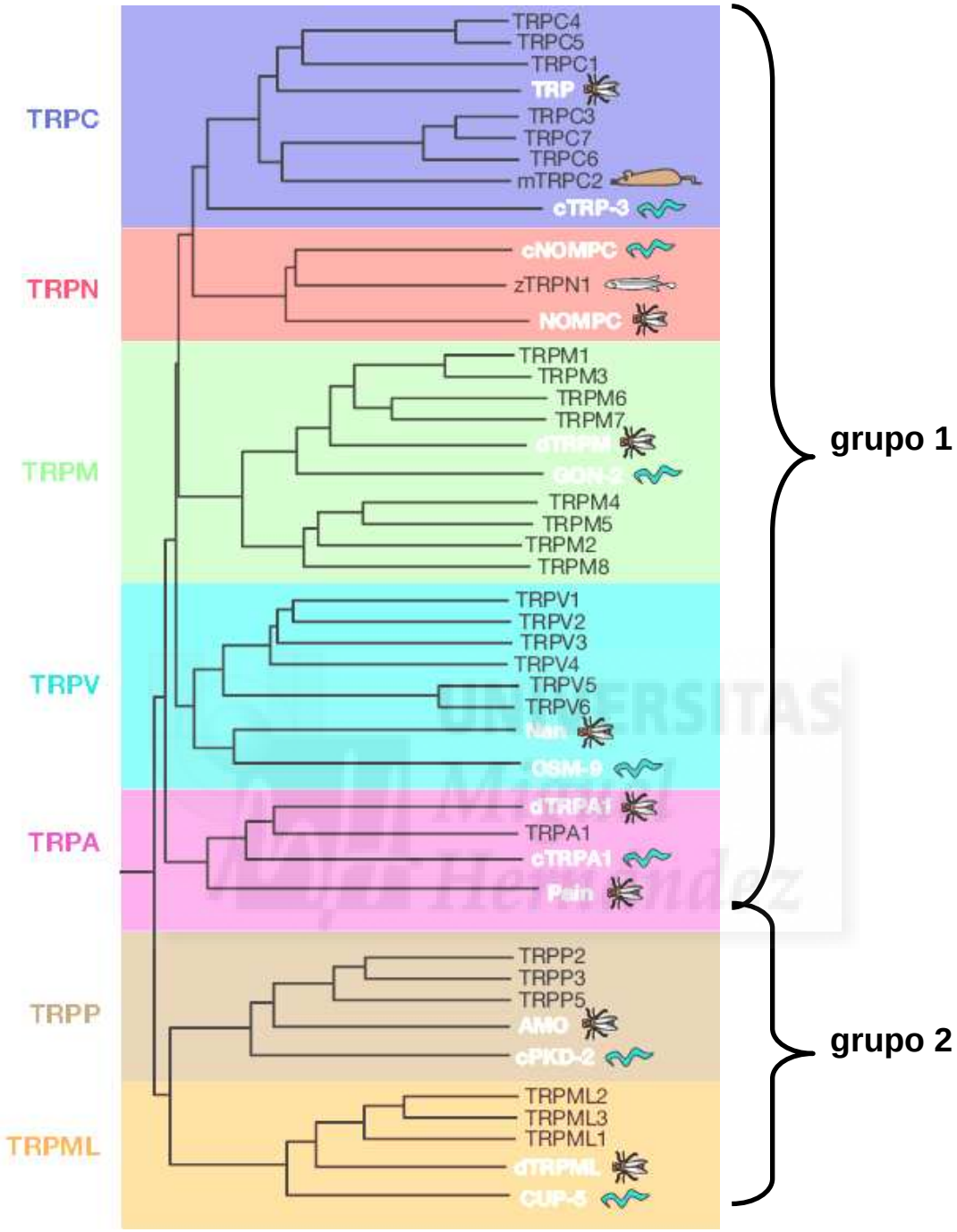

Figura 1. Dendrograma filogenético de las proteínas TRP basado en la homología de las secuencias primarias de aminoácidos. El uso de caracteres negros indica que son proteínas TRP de vertebrados, en todos los casos de humano, excepto para mTRPC2, que es de ratón (señalada con el correspondiente dibujo) y zTRPN1, que es de pez cebra (señalada con el correspondiente dibujo). El uso de caracteres blancos indica proteínas TRP de invertebrados, Cada familia incluye un miembro de *Drosophila melanogaster* y un miembro de *Caenorhabditis elegans*, señalados con el respectivo dibujo de una mosca y un gusano (Figura tomada de (Venkatachalam et al. 2007)).

1.2.2. Estructura

Las proteínas TRP están formadas por seis dominios α hélice transmembrana (S1-S6) unidos a los extremos amino y carboxilo terminal intracelulares (ver figura 2). Los canales funcionales, en analogía a los canales de potasio dependientes de voltaje, se cree que forman estructuras tetraméricas.

El poro del canal estaría formado por el ensamblaje de cada uno de los cuatro dominios transmembrana S5, S6 y el lazo de aminoácidos situado entre ambos. El lazo de aminoácidos formaría también el filtro de selectividad iónica en la parte extracelular del poro del canal, mientras que en la parte citoplasmática del poro, se cree que los dominios S6 forman la puerta que mediante su apertura y cierre, regula la entrada de cationes. Los dominios S4 tienen residuos de arginina que les confieren cargas positivas, los cuáles estarían implicados en sensibilidad a cambios de voltaje transmembrana. Todos los elementos situados fuera de la región formada por los elementos S5-lazo-S6, proporcionan o bien la capacidad de asociación entre subunidades, pudiendo formar homotetrámeros o heterotetrámeros, o actúan como elementos de unión para el control de la apertura del canal. De este modo, los canales TRPC, TRPM y TRPN tienen el llamado dominio TRP situado a partir del segmento S6 en el extremo C terminal. Las regiones más conservadas dentro del domino TRP reciben el nombre de “TRP box” y consisten en secuencias de entre 23 y 25 aminoácidos. Se cree que los dominios anquirina sirven de anclaje y/o para la interacción de proteínas y dependiendo del tipo de TRP presentan entre 0 y 14 repeticiones (entre 3 y 4 en TRPV y TRPC, 14 en TRPA1) (Clapham 2003).

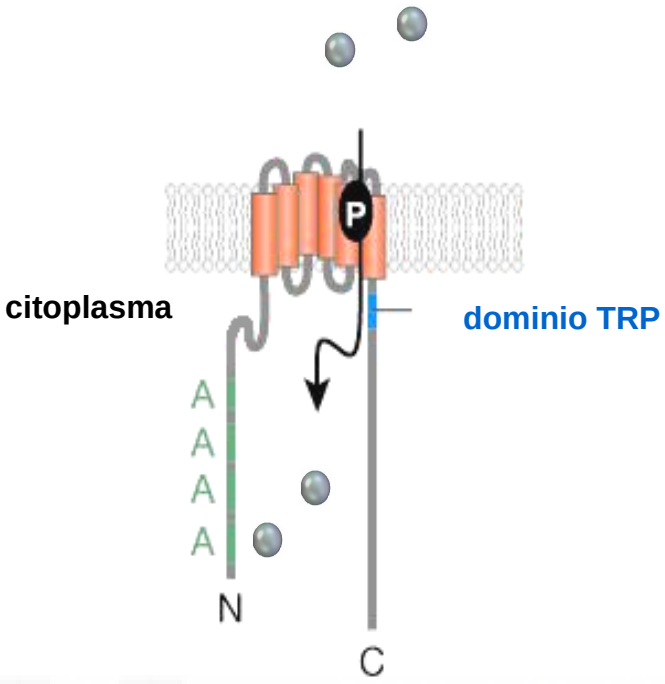

Figura 2. Estructura general de una subunidad TRP. Los seis dominios transmembrana están representados por cilindros de color naranja. N y C señalan respectivamente las regiones amino y carboxilo intracelulares. Los segmentos en color verde indicados con la letra A representan los dominios de anquirina y el segmento en color azul ilustra el dominio TRP. El dominio del poro está señalado por la letra P y las esferas representan iones catiónicos. (Figura adaptada de (Venkatachalam et al. 2007)).

1.2.3. Distribución tisular

Los canales iónicos TRP están ampliamente distribuidos por el organismo. Se expresan de forma ubicua en casi todos los tipos celulares, en donde presentan distintas isoformas. Se ha descrito la expresión de los canales iónicos TRPC en el sistema nervioso central, sistema vascular, músculo esquelético y pulmones; de los canales iónicos TRPV en el sistema nervioso periférico, corazón, piel, vejiga, músculo esquelético, riñón e intestino; y de los canales iónicos TRPM en el sistema nervioso periférico, sistema inmune, piel, próstata, riñón, páncreas e hígado (Clapham 2009).

1.2.4. Selectividad iónica

Los canales iónicos TRP son permeables a cationes de forma no selectiva Excepto TRPM4 y TRPM5, todos los TRP son permeables a Ca^{2+}, y algunos de ellos, como TRPV5 y TRPV6, son muy selectivos a este catión (Owsianik et al. 2006b).

1.2.5. Funciones biológicas

Las funciones de los distintos canales iónicos TRP son muy diversas (Nilius et al. 2005b). Así por ejemplo, miembros de la familia TRPC realizan funciones o están implicados en procesos tales como cambios en la permeabilidad endotelial, recepción de feromonas en ratones, diferenciación celular, desarrollo del cerebro, permeabilidad microvascular o agregación plaquetaria. Los canales iónicos TRP pertenecientes a la familia TRPV están implicados en percepción de la temperatura, de estímulos picantes, nocicepción, detección de cambios osmóticos o reabsorción de calcio en intestino y riñón; mientras que miembros de la familia TRPM actúan como supresor oncogénico, detección de estrés oxidativo en el sistema inmune, transducción de sabores, reabsorción de magnesio en intestino y riñón, regulación del ciclo celular o percepción de frío y dolor. El único miembro de la familia TRPA media recepción de estímulos picantes (wasabi o aceite de mostaza), transducción de estímulo mecánico, oído y percepción de dolor y frío intenso. Los canales iónicos TRP pertenecientes a las dos familias restantes están implicados en transporte intracelular de proteínas, regulación de la pigmentación o desarrollo de músculo esquelético, corazón y riñón (Nilius et al. 2005b).

1.2.6. Patologías asociadas a los canales TRP

Las enfermedades en cuya patogénesis están implicadas alteraciones de la función de canales iónicos se conocen como canalopatías. Se estima que el genoma humano codifica para unos 300 canales iónicos diferentes, y aunque relativamente pocos se han relacionado de forma directa con enfermedades en humanos, el número de canalopatías identificadas está en continuo aumento.

Entre las canalopatías asociadas a mutaciones en los genes que codifican canales iónicos TRP se encuentran la Glomeruloesclerosis Focal y Segmentaria,

asociada a un defecto genético en TRPC6, Hipomagnesemia con Hipocalcemia Secundaria en TRPM6, Riñón Poliquístico Dominante Autosómico en TRPP2 y Mucolipidosis tipo IV en TRPML1. Además de estas enfermedades hereditarias, defectos en el TRPM7 incrementan el riesgo de padecer Esclerosis Lateral Amiotrófica de Guam asociada a Parkinsonismo –Demencia.

Sin embargo, la contribución de los TRP a la etiología o progresión de enfermedades no pasa necesariamente por defectos en los genes que los codifican, ya que alteraciones en la expresión, o en la sensibilización o desensibilización de su actividad, aumentan potencialmente la relevancia e implicación de éstos en las alteraciones de las funciones fisiológicas. Por ejemplo, en un proceso inflamatorio, la presencia de mediadores de la inflamación en el entorno de un determinado canal iónico TRP puede modificar su actividad de modo que contribuya al desarrollo de la enfermedad.

De acuerdo con Nilius y colaboradores (Nilius 2007), la alteración de la función de un canal iónico TRP puede llevar al desarrollo de una patología por uno o por varios de los siguientes mecanismos:

- La mayor parte de los TRP son permeables a Ca^{2+}, lo que les convierte en importantes reguladores de la concentración intracelular de esta molécula de señalización. Por lo tanto, la alteración de la funcionalidad de los TRP puede tener grandes efectos tanto a nivel celular como sistémico.
- Los TRP pueden actuar como receptores polimodales para diferentes estímulos físicos y químicos en la célula. Esta característica permite a las células y organismos percibir y elaborar repuestas a cambios en el medio, por lo que modificaciones de la actividad de estos canales pueden provocar disfunciones por ejemplo en el sistema somatosensorial.
- Algunos TRP están implicados en la absorción y reabsorción selectiva de los cationes Mg^{2+} y Ca^{2+}, lo que resulta imprescindible para la homeostasis de estos iones en el organismo.
- Los TRP se localizan también en las membranas de organelas intracelulares donde alteraciones de su actividad llevan a disfunciones por ejemplo de los lisosomas, como es el caso de mutaciones en el TRPML1.
- Existen canales iónicos TRP implicados en procesos de proliferación y crecimiento celular. En este caso, disfunciones de los TRP se relacionan

con alteraciones en el crecimiento, formación de órganos y el desarrollo de tumores.

- Otro mecanismo por el que defectos en los TRP puede contribuir a la génesis de una enfermedad es a través de su implicación en procesos de interacción entre proteínas.
- En las células excitables del sistema nervioso y del corazón, los TRP modulan la actividad eléctrica, por lo que alteraciones de su actividad pueden conllevar disfunciones importantes.

1.2.7. Canales iónicos TRP y percepción de la temperatura

La transducción sensorial es el mecanismo por el que cambios físicoquímicos en el medio ambiente son transformados en señales bioquímicas y/o eléctricas por regiones especializadas de neuronas sensoriales (receptores sensoriales), las cuáles se diferencian entre sí por su capacidad de responder preferentemente a una determinada forma de energía, como por ejemplo un estímulo térmico.

En el sistema somatosensorial de mamíferos, los termorreceptores detectan cambios de la temperatura ambiental en un amplio rango de temperaturas. Este proceso se inicia cuando el estímulo térmico (calor o frío) excita las fibras nerviosas sensoriales que son proyectadas hacia tejidos periféricos desde neuronas sensoriales primarias de los ganglios raquídeos y trigéminos, las cuáles inervan regiones del tronco y cabeza respectivamente. Estas neuronas termorreceptoras convierten los estímulos térmicos en señales eléctricas, es decir, en potenciales de acción, y relevan esta información sensorial a la médula espinal y cerebro, donde es integrada e interpretada, con resultado de las adecuadas respuestas reflejas y cognoscitivas al estímulo térmico (Fields 1987; Julius et al. 2001).

Numerosas evidencias sugieren que los principales detectores de temperatura de las terminaciones nerviosas sensoriales de mamífero pertenecen a la superfamilia de canales catiónicos TRP (Clapham 2003; Voets et al. 2003). Hasta el momento, seis miembros de esta superfamilia han sido descritos como canales iónicos sensibles a temperatura, cubriendo juntos un amplio rango de las temperaturas que los mamíferos son capaces de detectar. Cuatro de estos canales TRP, pertenecientes a la subfamilia TRPV, se activan por calor, con temperaturas de

activación características comprendidas entre temperaturas moderadas (> 25 °C para TRPV4; > 31 °C para TRPV3) (Watanabe et al. 2002; Xu et al. 2002) y calor intenso (> 43 °C para TRPV1; > 52 °C para TRPV2) (Caterina et al. 1997; Caterina et al. 1999). Mientras que TRPM8 y TRPA1 (ANKTM1) se activan por frío (< 28 °C para TRPM8; < 18 °C para TRPA1) (Mc Kemy et al. 2002; Story et al. 2003).

1.2.8. Canales iónicos TRP y dolor

El dolor es una percepción que consiste en una experiencia sensorial y emocional desagradable asociada con una lesión tisular presente o expresada como si tal lesión existiera. El dolor es una submodalidad dentro de las sensaciones somáticas que tiene una importante función protectora, ya que nos avisa de una lesión que debe ser evitada o tratada.

La nocicepción es la recepción de señales bioquímicas y/o eléctricas en el sistema nervioso central que resulta de la estimulación selectiva de ciertos receptores sensoriales (nociceptores) por estímulos que pueden lesionar los tejidos. Los nociceptores responden de forma directa a algunos estímulos nocivos como son los estímulos mecánicos y térmicos intensos y substancias químicas irritantes. Además, pueden ser sensibilizados o activados por substancias químicas liberadas por las células del tejido lesionado, como por ejemplo: histamina, bradiquinina, substancia P, ATP, acidez (disminución del pH alrededor de la terminal nerviosa), serotonina, etc. Los estímulos dolorosos de la piel o el tejido subcutáneo, como las articulaciones o los músculos, activan varias clases de terminales de nociceptoras que son las terminaciones periféricas de neuronas sensoriales primarias, y cuyos cuerpos celulares se encuentran en los ganglios raquídeos y trigéminos. Estas fibras nociceptoras aferentes terminan en neuronas de proyección del asta posterior de la médula espinal, las cuáles transmiten información nociceptiva al tálamo y la corteza cerebral (Basbaum et al. 2004).

Numerosas evidencias relacionan a diversos miembros de la superfamilia de canales iónicos TRP con la detección de estímulos intensos de origen térmico y mecánico, así como de estímulos químicos.

Las temperaturas superiores a 43 °C (calor intenso) e inferiores a 15 °C (frío intenso), además de la correspondiente sensación térmica, evocan sensaciones dolorosas. Estudios neurofisiológicos demuestran que la actividad de los

nociceptores conocidos como CMH (C-fiber mechano-heat nociceptors), en respuesta a los estímulos mecánico y térmico, evoca a través de fibras aferentes C sensación de dolor quemante (LaMotte et al. 1978). El frío intenso también activa una subpoblación de neuronas nociceptoras, sin embargo, la fisiología del dolor evocado por frío intenso es menos conocida que la evocada por calor intenso.

Es bien conocido que las terminaciones nerviosas de los nociceptores detectan la temperatura y otros estímulos físicos por medio de canales iónicos sensibles a estos estímulos. El primer apoyo a esta hipótesis vino de la identificación de canales iónicos en neuronas sensoriales primarias (Cesare et al. 1996; Reichling et al. 1997) y del posterior clonaje y reconocimiento del receptor de capsaicina TRPV1 (VR1) como un nociceptor de mamíferos activado por temperaturas elevadas con un umbral de 43 ° C (Caterina et al. 1 997; Caterina et al. 2001). Aunque otros tres canales iónicos pertenecientes a la subfamilia TRPV son activados por calor, únicamente TRPV1 y TRPV2 presentan umbrales de activación dentro de un rango de calor intenso.

En cuanto a la nocicepción evocada por frío intenso, actualmente existe la hipótesis de que TRPM8 media la transducción sensorial del frío inocuo, mientras que TRPA1 media la transducción sensorial del frío intenso. Si bien, es un tema de enorme controversia, y numerosos trabajos recientes atribuyen a TRPM8, un papel principal como base molecular para la respuesta de los termorreceptores, no solamente al frío inocuo sino también al frío intenso (Bautista et al. 2007; Colburn et al. 2007; Dhaka et al. 2007; Green et al. 2007; Takashima et al. 2007; Madrid et al. 2009).

Además, otros canales iónicos no pertenecientes a la superfamilia de los TRP estarían también implicados en la transducción sensorial del frío. En este sentido existen estudios que demuestran que el frío cierra distintas conductancias de potasio en neuronas de ganglio trigémino de ratón, conduciendo a una despolarización de la membrana y a un incremento de la tasa de disparo de potenciales de acción (Viana et al. 2002). Por lo que existe en la terminal nerviosa un contexto iónico más complejo que el ofrecido simplemente por TRPM8 y TRPA1, en el que otros mecanismos moleculares contribuyen a modular la excitabilidad de los termorreceptores en respuesta a frío.

1.2.9. Mecanismo de apertura de los canales iónicos TRP termosensibles

Un principio termodinámico fundamental de la Química es que la velocidad de una reacción química aumenta con el incremento de la temperatura. Esto nos llevaría a intuir que los canales iónicos, como otras proteínas, deberían funcionar más eficazmente a temperaturas más elevadas. Pero paradójicamente, entre los canales iónicos TRP sensibles a temperatura, el TRPM8 se activa con el descenso de la temperatura, mientras que TRPV1 se activa con el incremento de ésta. Hace unos pocos años, se publicó que ambos canales iónicos tienen en común una activación dependiente del potencial de membrana (Gunthorpe et al. 2000; Voets et al. 2004a). En respuesta a sus respectivos estímulos, ambos canales muestran una relación corriente-voltaje con una acentuada rectificación de salida (ver figura 4), lo que implica una mayor activación del canal iónico a valores de potencial de membrana más positivos que a los cercanos al potencial de reposo de la célula.

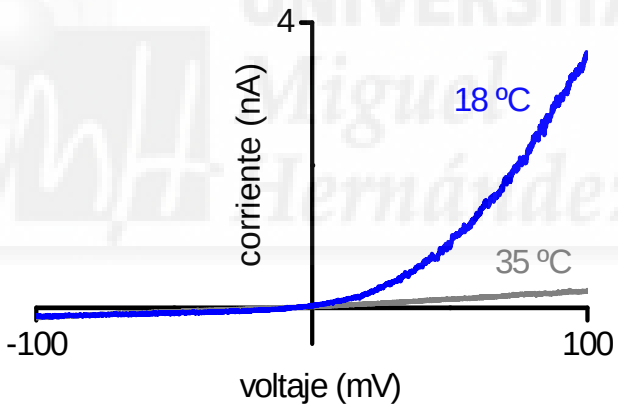

Figura 4. Ejemplo de relación corriente-voltaje a 35 ºC (trazo gris) y a 18 ºC (trazo azul) mediada por TRPM8 en un sistema de expresión heteróloga.

Para entender cómo los cambios de temperatura modulan la actividad de ambos canales iónicos, Voets y colaboradores (Voets et al. 2004a) propusieron un modelo de apertura basándose únicamente en dos estados (abierto y cerrado), y en el que al mismo tiempo que las constantes cinéticas de apertura y cierre son sensibles a los cambios de temperatura, las transiciones entre los dos estados son sensibles al voltaje. De este modo, un potencial de membrana hacia valores más positivos incrementa la probabilidad de que el canal iónico esté en estado abierto (ver figura 5).

En el caso de TRPV1, la constante cinética de apertura es muy sensible al incremento de la temperatura, mientras que la constante cinética de cierre es mucho menos sensible, por lo que el incremento de la temperatura desplaza el equilibrio hacia la apertura, y a la vez desplaza el potencial de membrana al que la probabilidad de apertura es del 50% ($V_{1/2}$) hacia valores más negativos o fisiológicos. Por el contrario, la constante cinética de apertura de TRPM8 es mucho menos sensible al incremento de temperatura que la constante cinética de cierre, por lo que el incremento de temperatura desplaza el equilibrio hacia el cierre del canal, y es el descenso de la temperatura lo que conduce a la apertura.

Según este modelo, la apertura por cambio de temperatura es inherente a la apertura por voltaje, por lo que los cambios de temperatura se acompañan siempre de un desplazamiento de la dependencia de voltaje de la activación de ambos canales iónicos.

En el mismo trabajo, Voets y colegas proponen que los agonistas químicos capsaicina y mentol, agonistas de TRPV1 y TRPM8 respectivamente, actúan como moduladores de la apertura de ambos canales iónicos por medio de un cambio en la dependencia de voltaje hacia valores de potencial de membrana más negativos o fisiológicos.

Otros ejemplos de canales iónicos TRP termosensibles, cuyos datos de cinética de apertura por temperatura se ajustan a este modelo de dos estados son TRPM4 y TRPM5 (Talavera et al. 2005).

Existe otro modelo, propuesto por Brauchi y colaboradores (Brauchi et al. 2004), en el que la apertura de TRPM8 por frío implica la interacción alostérica entre el dominio estructural sensible a voltaje, que en este caso no es inherentemente sensible a temperatura, y un cambio conformacional en otro domino estructural del canal iónico, el cuál es altamente sensible a temperatura.

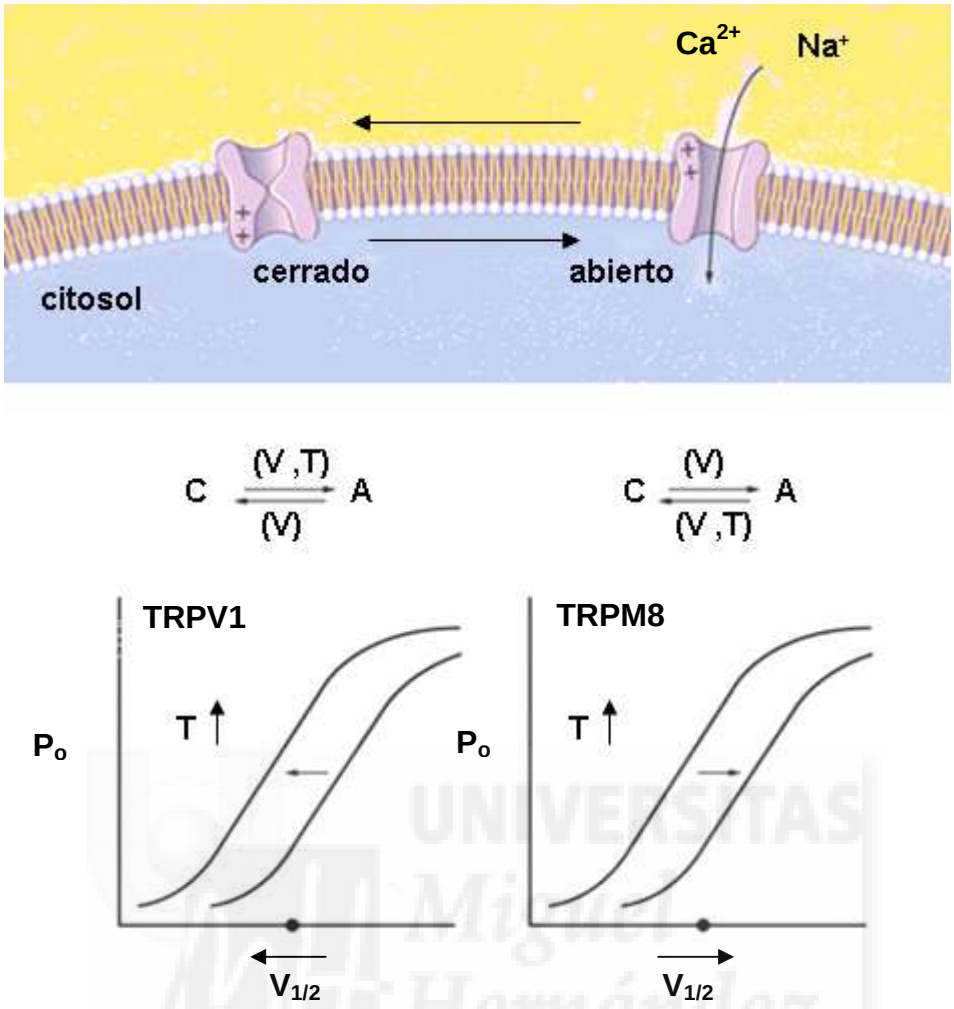

Figura 5. Modelo para la apertura por cambios de temperatura de los canales iónicos TRPV1 y TRPM8. En este modelo, el canal iónico presenta solo dos estados (abierto y cerrado), y las transiciones entre los dos estados son dependientes de voltaje. Para el canal iónico TRPV1, la constante cinética de apertura es más sensible al incremento de temperatura que la constante cinética de cierre, mientras que para TRPM8 es al contrario. Este modelo predice que la dependencia de voltaje (expresada como $V_{1/2}$) de la activación de TRPV1 por calor se desplaza hacia la izquierda en el eje del potencial de membrana, mientras que en el caso de TRPM8 se desplaza hacia la derecha en presencia del mismo estímulo (Figura adaptada de (Liman 2006)).

1.3. El canal iónico TRPV1

El canal TRPV1 fue clonado en el año 1997 (Caterina et al. 1997) y se le llamó receptor de capsaicina o receptor vaniloide, ya que se activa de forma selectiva por la capsaicina, un compuesto presente en determinadas especies de vegetales del género *Capsicum sp.*, y que ya era conocido por evocar una sensación de quemazón mediante la excitación de terminales sensoriales polimodales (Szolcsanyi 1977; Caterina et al. 1997; Szolcsanyi 2004).

Entre los numerosos miembros de la superfamilia de los canales iónicos TRP, TRPV1 es el mejor caracterizado hasta la fecha desde el punto de vista

farmacológico, de sus mecanismos de regulación y función. Este canal iónico es permeable preferentemente a Ca^{2+} y en menor medida a otros cationes. La permeabilidad a calcio es 10 veces mayor que a sodio y la permeabilidad a magnesio es 5 veces mayor que a sodio. La permeabilidad a sodio, potasio y cesio es similar (Caterina et al. 1997).

Al igual que el resto de canales iónicos TRP, se predice que la estructura funcional de TRPV1 es un tetrámero en el que cada subunidad consta de seis dominios α hélice transmembrana y un corto lazo de residuos hidrofóbicos entre los dominios transmembrana quinto y sexto que conforman el poro (ver figura 6). TRPV1 tiene tres dominios de anquirina en el extremo N terminal que estarían implicados en la modulación endógena de TRPV1 por ser el sitio de unión a calmodulina y ATP (Lishko et al. 2007). Además, existe otro sitio de unión a calmodulina en el extremo C terminal (Caterina et al. 1997; Numazaki et al. 2003a). Por otro lado se han identificado residuos susceptibles de ser fosforilados por la proteina quinasa A (PKA) (De Petrocellis et al. 2001; Bhave et al. 2002; Rathee et al. 2002), la proteína quinasa C (PKC) (Bhave et al. 2003; Dai et al. 2004; Premkumar et al. 2004) y la proteína quinasa II dependiente de Ca^{2+}/Calmodulina. PIP_2 se une en una región del extremo C terminal llamada dominio TRP. Los aminoácidos del poro son protonables y existen residuos cisteínas susceptibles de ser reducidos.

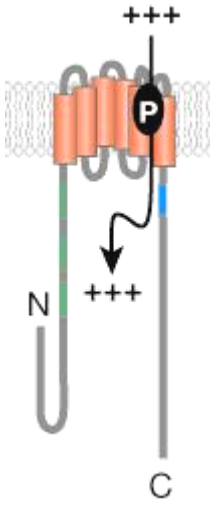

Figura 6. Estructura general de una subunidad TRPV1. Los seis dominios transmembrana están representados por cilindros de color naranja. N y C señalan respectivamente las regiones amino y carboxilo intracelulares. Los segmentos en color verde representan los dominios de anquirina y el segmento en color azul ilustra el dominio TRP. El dominio del poro está señalado por la letra P y el símbolo + representa iones catiónicos. (Figura adaptada de (Venkatachalam et al. 2007)).

TRPV1 se expresa en fibras nerviosas sensoriales de tipo C, las cuáles además contienen diversos neuropéptidos como son la sustancia P (SP) y el péptido relacionado con el gen de la calcitonina (CGRP), los cuáles están implicados en el proceso de inflamación neurogénica. Estas fibras nerviosas inervan entre otros tejidos la piel, vejiga urinaria y la mucosa gástrica. En el sistema nervioso central también se ha identificado expresión de TRPV1 en el hipocampo, cortex y bulbo olfatorio de rata (Toth et al. 2005), aunque su función en estas estructuras no es bien conocida.

El aspecto funcional fundamental del canal TRPV1 es su polimodalidad. Fue el primer canal iónico TRP implicado en la detección de estímulos irritantes en el sistema somatosensorial (Caterina et al. 1997), pero además es también activado por calor intenso, a partir de temperaturas superiores a 43 °C, y por pH ácido, por debajo de 5.9 en el medio extracelular (Caterina et al. 1997; Tominaga et al. 1998).

Los estudios de ratones TRPV1$^{-/-}$ muestran que TRPV1 es esencial para las respuestas nociceptivas a la aplicación de sustancia irritantes como la capsaicina y resiniferatoxina, y para la hiperalgesia térmica que se produce durante un proceso inflamatorio. El papel del TRPV1 en la detección del calor nociceptivo es controvertido. En un trabajo se demostró que TRPV1 contribuye a la detección del calor intenso (Caterina et al. 2000) mientras que otro muestra que no es necesario y sugiere la implicación de otros mecanismos moleculares en este proceso sensorial (Davis et al. 2000).

1.3.1. Agonistas exógenos de TRPV1

Además de la capsaicina, se han identificado otros compuestos vaniloides, que también activan el canal TRPV1. Así, la resiniferatoxina (RTX), un diterpeno relacionado con los esteres de forbol, es un potente análogo de la capsaicina presente en el cactus *Euphorbia resinifera* y que destaca por tener una mayor potencia irritadora (Szolcsanyi et al. 1990). En el polo opuesto, otro análogo de la capsaicina bien caracterizado, pero que destaca por su reducida eficacia para excitar las terminales sensoriales nociceptoras es el olvanilo (Liu et al. 1997). Piperina y zingerona, dos compuestos presentes en el pimiento negro y gengibre también activan TRPV1 (Liu et al. 1996a; McNamara et al. 2005). Otros estímulos

químicos que activan TRPV1 son el eugenol, el alcanfor, el 2-APB y el hidroxi-alfa-sanshool, el componente activo de la pimienta de Sichuan.

TRPV1 también es activado por extractos de ajo y de cebolla, además de por alicina, el principal componente activo de estos extractos. Este compuesto activa TRPV1 a través de la modificación covalente de una única cisteína (C157) localizada en el extremo N Terminal (Salazar et al. 2008).

1.3.2. Antagonistas exógenos de TRPV1

Dado su potencial interés terapéutico, el listado de antagonistas de TRPV1 es muy largo (Messeguer et al. 2006; Szallasi et al. 2007; Belmonte et al. 2008). Entre los antagonistas de TRPV1 se encuentran el Rojo de Rutenio (RR), la capsazepina, N-(4-tertiaributilfenil)-4-(3-cloropiridin-2-il) tetrahidropirazina-1(2H)-carboxamida (BCTC), (2R)-4-(3-cloro-2-piridinil)-2-metil-N-(4-[trifluorometil]fenil)-1-piperazinacarboxamida (CTPC), DDO1050, yodo-resiniferatoxina, N-(2-bromofenil)-N´-(2-[etil{3-metilfenil}amino]etil)-urea (SB-452533) así como el complejo Cu:fenantrolina y N-arilcinamidas.

1.3.3. Modulación endógena de la actividad de TRPV1

Entre los ligandos naturales que activan de forma endógena TRPV1 se encuentra la anandamida (AEA) (Zygmunt et al. 1999), que es conocida además como un activador del receptor canabinoide de tipo 1 (CB1) y los metabolitos lipídicos producto de la acción enzimática de la lipooxigenasa (LOX) sobre el ácido araquidónico (AA) que son 12 y 15 hidroperoxieicosatetraenoico (12 y 15-HPETEs), ácidos 5 y 15 hidroxieicosatetraenoico (5 y 15 HETEs) y leucotrienos B4 (LBT4) (Hwang et al. 2000) y sobre la anandamida, que son HPETE etanolamidas (HPETEE) y HETE etanolamidas (HETEE) (Craib et al. 2001). Otro compuesto endógeno presente en el cerebro y estructuralmente parecido a la capsaicina con capacidad agonista sobre TRPV1 es la N- araquidonildopamina (NADA) (Premkumar et al. 2004).

Los lípidos de membrana regulan la función de algunos canales iónicos, incluido TRPV1. El inositol 4,5 bifosfato (PIP_2) fue propuesto inicialmente como un modulador inhibitorio de la actividad de TRPV1. La activación de receptores metabotrópicos activa a la fosfolipasa C (PLC) que usa a PIP_2 como sustrato y lo hidroliza produciendo diacilglicerol (DAG) e inositol trifosfato (IP3). Esta hidrólisis

de PIP_2 conduciría a la activación de TRPV1 (Chuang et al. 2001). Sin embargo, estudios posteriores mostraron que la aplicación directa de PIP_2 sobre TRPV1 produce su activación (Stein et al. 2006; Lukacs et al. 2007) y que la sensibilización de TRPV1 por PIP_2 depende de la concentración del estímulo (Lukacs et al. 2007).

Al igual que ocurre con otros canales iónicos, TRPV1 es modulado por moléculas tales como calcio/calmodulina (CaM), la cuál estaría implicada en la desensibilización de TRPV1 (Numazaki et al. 2003b; Rosenbaum et al. 2004). Además puede ser fosforilado por quinasas que incluyen PKA (De Petrocellis et al. 2001; Rathee et al. 2002; Vlachova et al. 2003), PKC (Bhave et al. 2003; Premkumar et al. 2004; Tominaga et al. 1998; Varga et al. 2006), quinasa II dependiente de calcio calmodulina (CaMKII) (Jung et al. 2004), o la quinasa Src (Jin et al. 2004). Estas fosforilaciones sensibilizan las respuestas de TRPV1 a los agonistas mientras que las desfosforilaciones producidas por fosfatasas como la calcineurina se relacionan con una disminución de la actividad del canal iónico.

Los mediadores de la inflamación, como la bradiquinina, la prostaglandina E_2 (PGE_2), el factor de crecimiento neuronal (NGF), sensibilizan la respuesta de TRPV1 a sus agonistas naturales (p.e. capsaicina, calor, protones) a través de vías de señalización que implican la fosforilación de residuos específicos del canal iónico (Cesare et al. 1999; Premkumar et al. 2000; Vellani et al. 2001; Zhang et al. 2008). Por otro lado, se ha propuesto que dicha sensibilización se debe al descenso del nivel de PIP_2 en la membrana (Chuang et al. 2001; Prescott et al. 2003),como consecuencia de la activación de los respectivos receptores metabotrópicos por parte de los mediadores de la inflamación. No obstante, esta última hipótesis es controvertida porque existen numerosos datos experimentales que no son consistentes con un papel de modulación negativa de la actividad de TRPV1 por PIP_2 (Zhang et al. 2005; Stein et al. 2006; Lukacs et al. 2007).

1.3.4. TRPV1 y patologías asociadas

En los últimos años numerosos estudios han vinculado el aumento de expresión de TRPV1, su síntesis *de novo*, o su desregulación con numerosas patologías. Este canal parece estar implicado en la patogénesis del dolor neuropático, en el que se presentan síntomas tales como la hiperestesia (sensibilidad potenciada a un estímulo natural del tacto), hiperalgesia (sensibilidad anormal del dolor),

alodinia (sensaciones dolorosas en respuesta a estímulos inocuos) y dolor ardiente espontáneo.

En humanos, el dolor neuropático es crónico y debilitante, y se manifiesta en condiciones de neuralgia trigeminal, neuropatía diabética, neuralgia post-herpética, cáncer, amputaciones, o daños físicos en los nervios. La alodinia se debe a una actividad y/o sensibilidad de TRPV1 como resultado de la activación de la proteína quinasa C, pH ácido y mediadores inflamatorios.

La sobreexpresión de TRPV1 también se ha relacionado con la irritación, la sensación de dolor o hipersensibilidad que se manifiestan en determinadas condiciones patológicas como enfermedades gastrointestinales, vulvodinia, mastalgia, asma, pancreatitis, etc (Nilius 2007).

1.4. El canal iónico TRPM8

En el año 2001, Tsavaler y colaboradores identificaron y secuenciaron un gen desconocido hasta entonces a partir de una genoteca de ADN de próstata humana. Este gen codificaba una proteína de 130 kDa con una gran homología de secuencia con los canales iónicos TRP y la llamaron TRP-p8 (Tsavaler et al. 2001). Un año más tarde se unificó la nomenclatura de los canales iónicos pertenecientes a la superfamilia de los TRP y fue incluido en la familia de los canales iónicos TRPM como TRPM8 (Montell et al. 2002). Este mismo año se identificó el gen que expresa un receptor de mentol que es además activado por frío, a partir de una genoteca de ADN de ganglio trigémino de rata (McKemy et al. 2002) y al que llamaron CMR1 (las siglas en inglés de receptor de mentol y frío 1). Este nuevo canal iónico resultó ser el ortólogo en rata de Trp-p8 (TRPM8). Otro grupo, gracias a técnicas de análisis bioinformáticas, basadas en la búsqueda de secuencias homólogas al canal iónico TRPV1, identificó la misma secuencia, y la clonó a partir de ganglio raquídeo de ratón. Mediante su expresión en un sistema de expresión heteróloga identificaron su actividad como canal iónico sensible a compuestos químicos (mentol, eucaliptol, etc) y frío (Peier et al. 2002).

En consonancia con otros TRP, la estructura funcional de TRPM8 es la de un tetrámero (Owsianik et al. 2006a) en el que cada subunidad consta de seis dominios α hélice transmembrana flanqueada por dos largos dominios terminales citoplasmáticos N y C (ver figura 7). Además, un pequeño lazo de residuos

hidrofóbicos entre los dominios transmembrana quinto y sexto forman el filtro de selectividad iónica en la región extracelular del poro (Voets et al. 2004b; Nilius et al. 2005a; Owsianik et al. 2006a).

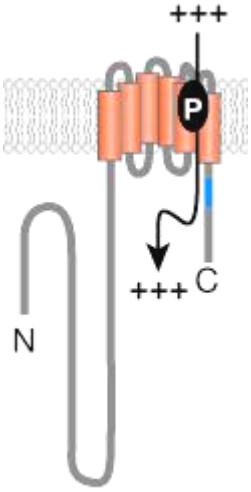

Figura 7. Estructura general de una subunidad TRPM8. Los seis dominios transmembrana están representados por cilindros de color naranja. N y C señalan respectivamente las regiones amino y carboxilo intracelulares. El segmento en color azul ilustra el dominio TRP. El dominio del poro está señalado por la letra P y el símbolo + representa iones catiónicos (Figura adaptada de (Venkatachalam et al. 2007)).

No se conocen con detalle los mecanismos de oligomerización del canal TRPM8. Un estudio implica el domino C terminal de la proteína, en concreto una región conocida como "coiled coil" (Tsuruda et al. 2006). Sin embargo, un estudio posterior generó mutantes de TRPM8 con deleciones de los extremos C terminal y N terminal que oligomerizan adecuadamente, indicando que los dominios transmembrana son suficientes para este proceso (Phelps et al. 2007), aunque los mutantes con deleciones del extremo C terminal resultan ser formas inactivas, afectadas en el mecanismo de apertura y/o el reconocimiento del estímulo.

TRPM8 es un canal catiónico permeable a cationes monovalentes y divalentes de forma no selectiva (McKemy et al. 2002; Peier et al. 2002). La permeabilidad relativa del calcio versus al sodio (P_{Ca}/P_{Na}) es de entre 0.97 y 3.3 y en menor medida a cationes monovalentes, cuya secuencia de permeabilidad es $Cs^+ > K^+ > Na^+$, con una permeabilidad muy similar para todos ellos ($P_{Cs}/P_{Na} \sim 1.4$).

En un principio el conocimiento de la expresión de TRPM8 se limitaba a la próstata y tumores primarios de mama, colon, pulmón y piel (Tsavaler et al. 2001). Posteriormente se identificó la presencia de ARN mensajero de TRPM8 o la proteína en una subpoblación de neuronas sensoriales de ganglios trigéminos

y raquídeos (McKemy et al. 2002; Peier et al. 2002), en ganglio nodoso (Zhang et al. 2004), fundus gástrico (Mustafa et al. 2005), músculo liso vascular (Yang et al. 2006), hígado (Henshall et al. 2003), y en la vejiga (Stein et al. 2004).

El enfriamiento de la solución extracelular activa el canal iónico TRPM8 tanto en sistemas de expresión heteróloga, como en una subpoblación de neuronas sensoriales en cultivo de ganglios raquídeos y trigéminos de rata y ratón (McKemy et al. 2002; Okazawa et al. 2002; Reid et al. 2002b; Nealen et al. 2003; Madrid et al. 2006). Estos estudios, junto con otros en los que se caracteriza la sensibilidad al frío de ratones transgénicos que carecen de TRPM8, presentan numerosas evidencias que le atribuyen a este canal iónico un papel fundamental en la transducción sensorial del frío moderado e intenso (Reid et al. 2002a; Madrid et al. 2006; Bautista et al. 2007; Colburn et al. 2007; Dhaka et al. 2007; Green et al. 2007; Takashima et al. 2007; Madrid et al. 2009).

1.4.1. Agonistas químicos de TRPM8

Entre los agonistas químicos, los mejor estudiados son el mentol, el componente activo de la planta de la menta que evoca una sensación refrescante, y la icilina, un agente refrescante sintético conocido hasta ahora por ser el agonista más potente de TRPM8 (McKemy et al. 2002; Peier et al. 2002). Existen también derivados sintéticos del mentol como son Frescolat ML, Coolact P, agente refrescante 10 y WS-3 que activan TRPM8 con una eficacia parecida a la del mentol (Behrendt et al. 2004). Otros compuestos naturales estructuralmente diferentes al mentol, como son eucaliptol, linalol, hidroxi-citronelal y geraniol también activan TRPM8, pero con una menor eficacia (McKemy et al. 2002; Behrendt et al. 2004).

Mediante la generación de quimeras de TRPM8 y TRPV1, en las que se intercambiaron la región C terminal de ambos canales entre sí, se pudo demostrar que esta región confiere a ambos canales iónicos la propiedad de ser activados por los cambios de temperatura y que esta activación es independiente de la región sensible a cambios de voltaje localizada en el segmento transmembrana S4 y en el lazo de aminoácidos entre S4 y S5 (Brauchi et al. 2006). Sin embargo, un estudio posterior, en el que se mutó la región sensible a voltaje de TRPM8, muestra que estos mutantes tienen una menor afinidad por mentol y una sensibilidad al frío alterada, lo que indica la interacción de la

activación de TRPM8 por voltaje, frío y el agonista químico mentol (Voets et al. 2007).

El uso de quimeras de TRPM8 de rata y de pollo, y mutaciones puntuales permitieron la identificación de residuos implicados en la activación de TRPM8 por icilina en el tercer dominio transmembrana (TM3) y en la región de aminoácidos que une el segundo (TM2) y TM3 (Chuang et al. 2004). Esta región también está implicada en la activación de TRPV1 por compuestos vaniloides y capsazepina (Jordt et al. 2002; Gavva et al. 2004) y en la activación de TRPV4 por 4-α-PDD (Vriens et al. 2004). Además, en la activación por mentol también están implicados residuos del dominio TM2 (Bandell et al. 2006), lo que sugiere un mecanismo conservado para la apertura de canales iónicos TRP por agonistas químicos.

1.4.2. Antagonistas exógenos de TRPM8

La farmacología del canal TRPM8 es todavía incipiente y no se conocen antagonistas específicos. Los inhibidores conocidos más potentes de TRPM8 son el N-(4-tertiatibutil-fenil)-4-(3-cloropiridin-2-il) tetrahidropirazina-1(2H)-carboxamida (BCTC) y su derivado tio-BCTC, los cuáles inhiben de manera dosis-dependiente la señal de calcio intracelular y la corriente inducida por frío y mentol. Estos compuestos son a su vez antagonistas muy potentes de TRPV1 (Valenzano et al. 2003; Behrendt et al. 2004).

Otro antagonista de TRPM8 es el 2-aminoetoxidifenil borato (2-APB) (Hu et al. 2004), no obstante, su especificidad es baja ya que también es conocido como un inhibidor de receptores de inositol 1,4,5 trifosfato (Maruyama et al. 1997), bombas Ca^{2+} -ATPasas del retículo endoplasmático (Bilmen et al. 2002) y canales iónicos TRP de la familia TRPC (Hu et al. 2004). Además, 2-APB activa y/o sensibiliza a TRPV1, TRPV2, TRPV3 y TRPV6 (Voets et al. 2001; Chung et al. 2004; Hu et al. 2004).

La acidificación del pH intracelular también inhibe la actividad de TRPM8. Un trabajo indica que esta acidificación inhibe la respuesta de TRPM8 a frío e icilina, aunque describe la respuesta a mentol como insensible a este cambio de pH (Andersson et al. 2004). Sin embargo otro trabajo describe que la acidificación del pH intracelular inhibe la respuesta inducida por mentol (Behrendt et al. 2004).

1.4.3. Modulación endógena de la actividad de TRPM8

La activación de TRPM8 por frío, mentol e icilina se acompaña de la desensibilización de la actividad de este canal iónico de manera dependiente del calcio intracelular (McKemy et al. 2002). Estudios posteriores han demostrado la implicación del lípido de membrana PIP_2 en este proceso. PIP_2 actúa como un modulador positivo de la actividad de TRPM8, de modo que la entrada de calcio a través de TRPM8 lleva a la activación de la fosfolipasa C dependiente de calcio y a la subsiguiente hidrólisis de PIP_2, lo que favorece la desensibilización de TRPM8 (Rohacs et al. 2005; Liu et al. 2005).

Existen evidencias de que el extremo C terminal está implicado en la unión de TRPM8 con el lípido de membrana PIP_2, en concreto residuos con carga positiva del dominio TRP localizado en esta región (Rohacs et al. 2005; Brauchi et al. 2006).

Por otro lado, la activación de la proteína quinasa C (PKC) dependiente de calcio también produce la desensibilización de TRPM8 (Premkumar et al. 2005; Abe et al. 2006). La activación de la PKC produce de forma indirecta desfosforilaciones de TRPM8 que conducen a una menor actividad del canal iónico (Premkumar et al. 2005).

Un estudio reciente muestra como los productos de la actividad de un tipo de enzima fosfolipasa A2, la fosfolipasa A2 insensible a calcio (iPLA2), modulan la actividad de TRPM8. Estos productos son los lisofosfolípidos (LPLs), entre los que se encuentra la lisofosfatidilcolina, la cuál modula positivamente la actividad de TRPM8, y los ácidos grasos poliinsaturados (PUFAs), entre los que se encuentra el ácido araquidónico, el cuál modula de forma inhibitoria la actividad de TRPM8 (Andersson et al. 2007).

1.4.4. TRPM8 y patologías asociadas

La expresión de TRPM8 está incrementada en tumores malignos de próstata, además de en tumores de mama, colon, pulmón y piel (Tsavaler et al. 2001). En la línea celular LNCaP, una línea de células tumorales de próstata, TRPM8 se expresa en el retículo endoplasmático y en la membrana plasmática, donde funciona como un canal iónico permeable a Ca^{2+}, y su expresión es incrementada por andrógenos. TRPM8 contribuye a la homeostasis de Ca^{2+} en células epiteliales de próstata y podría ser una diana potencial para la acción de drogas

contra el desarrollo del cáncer de próstata (Bodding et al. 2007; Prevarskaya et al. 2007).

Además, datos experimentales obtenidos con ratones nulos para TRPM8 (Colburn et al. 2007), sugieren que TRPM8 podría estar implicado en alodinia por frío, una hipersensibilidad al frío experimentada por pacientes con lesiones nerviosas periféricas.

1.5. El canal iónico TRPA1

El canal iónico TRPA1 fue clonado por primera vez a partir de cultivos de fibroblastos humanos y en un principio se le relacionó con alteraciones de la división celular al estar aumentada su expresión en células tumorales (Jaquemar et al. 1999). Varios años más tarde fue clonado de nuevo a partir de una genoteca de ganglio raquídeo de ratón (Story et al. 2003).

Desde el punto de vista estructural, TRPA1 está formado por seis dominios transmembrana flanqueados por las regiones N y C terminales citoplasmáticas (ver figura 8). Una característica peculiar de la estructura de TRPA1 es una larga región N terminal la cuál presenta 14 repeticiones de anquirina (Story et al. 2003), que podrían servir para la interacción con otras proteínas (Mosavi et al. 2004).

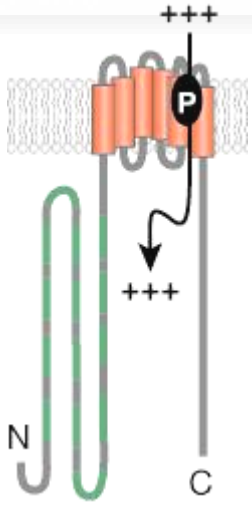

Figura 8. Estructura general de una subunidad TRPA1. Los seis dominios transmembrana están representados por cilindros de color naranja. N y C señalan respectivamente las regiones amino y carboxilo intracelulares. Los segmentos en color verde representan los dominios de anquirina. El dominio del poro está señalado por la letra P y el símbolo + representa iones catiónicos (Figura adaptada de (Venkatachalam et al. 2007)).

TRPA1 es permeable a cationes monovalentes y divalentes de forma no selectiva. La permeabilidad relativa al calcio versus al sodio (P_{Ca}/P_{Na}) es 1.4. Además presenta una permeabilidad similar a calcio y a magnesio.

Mediante hibridación *in situ* se ha encontrado que la expresión de TRPA1 se restringe al oído interno y a los ganglios sensoriales (raquídeo, trigémino y nodoso) (Nagata et al. 2005), lo que sugiere funciones específicas a nivel sensorial.

Inicialmente se le atribuyó el papel de mediar la transducción sensorial de los estímulos de frío intenso (umbral < 17 °C) en neur onas nociceptoras (Story et al. 2003). Esta función ha sido discutida en los años posteriores, en los que han aparecido trabajos que negaban esta propiedad de TRPA1 en su expresión heteróloga (Nagata et al. 2005; Bautista et al. 2006). Además, no han existido evidencias firmes sobre la activación por frío de TRPA1 en su expresión nativa en neuronas sensoriales hasta la aparición de un trabajo reciente que describe respuestas a frío mediadas por TRPA1 en neuronas sensoriales de ganglio nodoso (Fajardo et al. 2008a), y posteriormente de ganglio trigémino (Karashima et al. 2009). La caracterización de dos líneas diferentes de ratones nulos para TRPA1 tampoco resolvió la controversia debido a que un trabajo no encontró una reducción de la respuesta a frío (Bautista et al. 2006), mientras que el otro encontró una moderada reducción restringida a las hembras (Kwan et al. 2006).

Además, se ha postulado que TRPA1 podría estar implicado en la transducción sensorial del estímulo mecánico y tener un papel en la audición (Corey et al. 2004). Existe un modelo que predice que los dominios de anquirina formarían un resorte molecular que se uniría a proteínas del citoesqueleto, proporcionándole elasticidad a un sistema molecular que serviría para acoplar los cambios de tensión de la membrana en respuesta a un estímulo mecánico con la activación de este canal iónico (Corey et al. 2004; Howard et al. 2004; Lee et al. 2006). El estudio de los ratones nulos para TRPA1 revela una nocicepción mecánica reducida (Kwan et al. 2006), sin embargo no presentan alteraciones auditivas (Bautista et al. 2006; Kwan et al. 2006).

Por otro lado, las neuronas sensoriales procedentes de ratones nulos de *trpa1* no muestran respuestas a la aplicación de aceite de mostaza, compuestos azufrados o acroleína, ni tampoco muestran signos de dolor tras la inyección de aceite de mostaza en la pata, por lo que se le atribuye a TRPA1 un papel fundamental en la

transducción sensorial de estímulos químicos irritadores (Bautista et al. 2006; Garcia-Anoveros et al. 2007; Peterlin et al. 2007).

1.5.1. Agonistas exógenos de TRPA1

El aceite de mostaza (alil isocianato) es un compuesto presente en plantas del género *Brassica*, y es conocido desde hace muchos años por inducir dolor e irritación al ser aplicado de forma tópica sobre la piel (Guimaraes et al. 2007) además de producir inflamación neurogénica (Louis et al. 1989). No ha sido hasta hace pocos años que se ha conocido la base molecular de estos efectos sensoriales al identificarse el aceite de mostaza como un activador específico de TRPA1 (Jordt et al. 2004).

Además de por aceite de mostaza, el canal iónico TRPA1 se activa por otros compuestos procedentes de plantas y conocidos por sus propiedades irritantes. Estos compuestos incluyen el cinamaldehído, el eugenol, el gingerol y el metil salicilato (Bandell et al. 2004).

Las plantas del género *Allium sp* contienen distintos compuestos azufrados, como la alicina y el dialil disulfido, y ambos son potentes agonistas de TRPA1 (Bautista et al. 2005; Macpherson et al. 2005).

Otro agonista de TRPA1 es la acroleína (2-propenal) (Bautista et al. 2006), un aldehído conocido por sus propiedades irritantes tras ser inhalado y por producir lagrimeo. Se puede formar y dispersarse por el aire, cuando se queman aceites, tabaco y otras plantas, gasolina y petróleo.

Recientemente se ha descrito que la activación de TRPA1 por aceite de mostaza, cinamaldehído, dialil disulfido, y acroleína tiene lugar a través de la modificación covalente de residuos de cisteína localizados en el extremo N terminal de este canal iónico (Hinman et al. 2006; Macpherson et al. 2007a). Estas substancias tienen en común ser reactivos electrófilos que tienen la capacidad de reaccionar covalentemente con el grupo tiol de los residuos cisteína.

El mentol y la icilina, dos conocidos agonistas de TRPM8 también activan TRPA1. En el caso del mentol, existe un efecto opuesto sobre el TRPA1 de ratón en función de la concentración, de modo que a concentraciones submicromolares o bajas concentraciones micromolares tiene un efecto activador (Karashima et al. 2007) mientras que a concentraciones micromolares altas o milimolares, el efecto

es inhibidor (Story et al. 2003; Karashima et al. 2007). Sin embargo, el efecto del mentol sobre el TRPA1 humano es únicamente agonista (Xiao et al. 2008).

Debido al efecto dual del mentol sobre la actividad de TRPA1 y a la rápida reversibilidad, junto con datos que implican a residuos situados en TM5 como necesarios para la activación de TRPA1 por mentol (Xiao et al. 2008), es improbable que la interacción del mentol con este canal iónico implique la modificación covalente de los residuos de cisteina situados en el extremo N terminal.

Otros agonistas de TRPA1 son el Δ9-tetrahidrocanabiol (Δ9-THC) (Jordt et al. 2004) presente en plantas del género *Cannabis sp* y conocido por sus propiedades psicoactivas, el trinitrofenol, un compuesto anfipático aniónico con la capacidad de modificar la curvatura de la membrana plasmática, el GsMTx-4, un tipo de toxina de tarántula (Hill et al. 2007), hidroxi-alfa-sanshool (Hill et al. 2007), 2-APB (Hinman et al. 2006), acetaldehído (Bang et al. 2007), metil p-hidroxibenzoato (Fujita et al. 2007), formaldehído (Macpherson et al. 2007a) y la formalina (McNamara et al. 2007).

1.5.2. Antagonistas exógenos de TRPA1

Entre los inhibidores de la actividad de TRPA1 se encuentran compuestos de origen natural como son el alcanfor (Xu et al. 2005) y el mentol (Story et al. 2003), aunque el efecto se produce a concentraciones altas. El elemento químico gadolinio, el rojo de rutenio, conocido como un bloqueante inespecífico de canales iónicos, el antibiótico gentamicina, el fármaco diurético amilorida (Nagata et al. 2005) y los compuestos sintéticos HC-030031 (McNamara et al. 2007) y AP18 (Petrus et al. 2007).

1.5.3. Modulación endógena de TRPA1

El mediador de la inflamación bradiquinina produce la activación de TRPA1 a través de la activación de su receptor acoplado a proteína G y los subsiguientes efectos mediados por la fosfolipasa C en neuronas sensoriales de ganglio raquídeo (Bandell et al. 2004).

Trabajos más recientes atribuyen a PIP_2 un papel modulador de la actividad de TRPA1, sin embargo, existen evidencias controvertidas sobre el signo positivo o negativo de esta modulación. Existen dos trabajos que atribuyen a PIP_2 un control

inhibidor de la actividad de TRPA1 (Dai et al. 2007; Kim et al. 2008), por lo que la hidrólisis de PIP_2 conlleva la activación de TRPA1, mientras que existen otros dos trabajos que aportan evidencias sobre la modulación positiva de PIP_2 sobre la actividad de TRPA1 (Akopian et al. 2007; Karashima et al. 2008).

Por otro lado se ha descrito recientemente la activación directa de TRPA1 por el ión Ca^{2+}. Esta activación estaría mediada por un dominio "EF hand" implicado en la unión a Ca^{2+} localizado en el extremo N terminal citoplasmático (Doerner et al. 2007; Zurborg et al. 2007). Además, un trabajo reciente (Wang et al, 2008), sugiere que el incremento de calcio intracelular, potencia la actividad de TRPA1, y posteriormente lo inactiva.

Otro estudio sugiere que TRPA1 precisa de un factor soluble intracelular para mantener una conformación funcional y que los polifosfatos inorgánicos pueden actuar como este factor (Kim et al. 2007).

Además, 4-Hidroxinonenal (4-HNE), un reactivo químico endógeno que se produce en procesos de estrés oxidativo y otros aldehídos relacionados también activan TRPA1 *in vitro* (Macpherson et al. 2007b).

Todos estos datos indican múltiples factores convergentes en la modulación endógena de TRPA1.

1.5.4. TRPA1 y patologías asociadas

La hiperalgesia al frío es un síntoma de dolor inflamatorio y neuropático. Existen evidencias experimentales que relacionan al canal TRPA1 con la hiperalgesia al frío. Por ejemplo, ratones con una expresión disminuida de TRPA1 al ser tratados con AS-ODN (oligonucleótido antisentido) mostraron una reducción de la hiperalgesia al frío consecuencia de la ligación de nervios espinales. Dicho tratamiento no modificó, ni la alodinia mecánica ni la hiperalgesia al calor secundaria a la ligadura nerviosa. Además, la regulación al alza de TRPA1 que se produce en neuronas sensoriales en el contexto de inflamación y daño tisular contribuye a la hiperalgesia al frío (Obata et al. 2005; Katsura et al. 2006).

Existe un estudio que usa ratones nulos para TRPA1 e implica a este canal iónico en la hiperalgesia mecánica (Kwan et al. 2006), mientras que otro trabajo coetáneo que usa otra línea de ratones $trpa1^{-/-}$ concluye que TRPA1 no es

necesario para la nocicepción mecánica. Estudios anteriores atribuyeron a TRPA1 un papel fundamental en el proceso de audición en vertebrados (Corey et al. 2004; Nagata et al. 2005), sin embargo ninguna de las líneas modificadas genéticamente presentaron déficits auditivos

1.6. Tabla resumen de la farmacología de TRPV1, TRPM8 y TRPA1

Canal iónico	Agonistas	Antagonistas
TRPV1	Capsaicina, resiniferatoxina, olvanilo, piperina, zingerona, eugenol, alcanfor, 2-APB, hidroxi-alfa-sanshool, alicina.	Capsazepina, rojo de rutenio, BCTC, CTPC, DDO1050, yodo-resiniferatoxina, SB-452533, Cu:fenantrolina, N-arilcinamidas
TRPM8	Mentol, icilina, Frescolat ML, coolact P, agente refrescante 10, WS-3, eucaliptol, linalol, hidroxi-citronelal, geraniol.	BCTC, tio-BCTC, 2-APB
TRPA1	Aceite de mostaza cinamaldehído, eugenol, gingerol, metilsalicilato, alicina, dialil disulfido, acroleína, mentol, icilina, Δ9- THC, trinitrofenol, GsMTx-4, hidroxi-alfa-sanshool, 2-APB, acetaldehído, metil-p-hidroxibenzoato, formaldehído, formalina.	Alcanfor, HC-030031, AP18, mentol, gadolinio, rojo de rutenio, gentamicina, amilorida.

1.7. Solapamiento de la farmacología de TRPV1, TRPM8 y TRPA1

Existen numerosos ejemplos del solapamiento de la farmacología de los tres canales iónicos TRPM8, TRPV1 y TRPA1. De este modo, compuestos como capsazepina, BCTC, tio-BCTC, CTPC o SB-452533 inhiben las corrientes mediadas tanto por TRPV1 como por TRPM8 (Weil et al. 2005). Otro ejemplo de solapamiento farmacológico es la activación de TRPM8 y TRPA1 por mentol e icilina. Mientras que alicina, hidroxi-alfa-sanshool, 2-APB y eugenol activan a

TRPA1 y a TRPV1. Todo esto dificulta la identificación funcional de estos canales iónicos en sus sistemas de expresión nativa.

Aunque los canales iónicos TRP están bien caracterizados en sistemas de expresión heteróloga, los trabajos sobre la función en un contexto nativo son aún limitados, por lo que se hace necesaria la búsqueda de nuevos agonistas y antagonistas que puedan ser usados como herramienta para el desarrollo de experimentos fisiológicos. También es importante una mejor caracterización de los mecanismos de acción de los fármacos utilizados hasta ahora como agonistas o antagonistas.

1.8. Potencial terapéutico de los fármacos moduladores de la actividad de TRPV1, TRPM8 y TRPA1

Numerosos ensayos preclínicos con inhibidores de TRPV1 proporcionan evidencias de que el bloqueo de la actividad de este canal iónico puede ser útil como terapia para el tratamiento del dolor agudo e inflamatorio. Los tratamientos farmacológicos actuales basados en el uso de compuestos antiinflamatorios no esteroideos (AINE), y compuestos opiáceos, producen efectos adversos que limitan la dosis de fármaco empleada, presentan una tolerabilidad reducida y la eficacia disminuye a lo largo del tiempo. La acción de los analgésicos AINE se basa en la inhibición de la actividad de la enzima ciclooxigenasa, lo que reduce la síntesis de prostaglandinas, a su vez la liberación de mediadores de la inflamación, e indirectamente la sensibilización o activación de nociceptores. Los analgésicos opioáceos ejercen sus efectos mediante la estimulación de receptores opiáceos a nivel del sistema nervioso central. A diferencia de los mecanismos de analgesia conocidos, el antagonismo de TRPV1 sucede a nivel de la transducción sensorial de estímulos nocivos, lo que supone un nuevo mecanismo en la supresión de la transmisión del dolor, que podría implicar la aparición de una nueva generación de fármacos más selectivos en la inhibición de las señales nociceptivas (Szallasi et al. 2007).

Con este objetivo, diversas compañías farmacéuticas han identificado nuevos antagonistas de TRPV1, los cuáles se ensayan en estudios clínicos enfocados al tratamiento del dolor agudo e inflamatorio. De este modo, varios compuestos como son AZD1386, GRC6211, MK-2295, NGD8243 y SB-705498 se ensayan

para el tratamiento del dolor dental. Además, SB705498 se ensaya para el tratamiento de migrañas (Khairatkar-Joshi et al. 2009).

En el caso del dolor neuropático, resulta de especial interés el hallazgo de nuevas estrategias terapéuticas debido a que los tratamientos convencionales no son eficaces. Los fármacos AINE no alivian este tipo de dolor, mientras que los compuestos opiáceos solo resultan eficaces a altas dosis, a las cuáles producen efectos adversos. El tratamiento de elección en este caso son los compuestos anticonvulsivos como la gabapentina y pregabalina, compuestos antirritmicos como la mexiletina e incluso antidepresivos como la amitriptilina. En todos los casos su uso se asocia con importantes efectos secundarios (Dray 2008).

Actualmente existen ensayos clínicos para el tratamiento del dolor neuropático basados en la modulación farmacológica de TRPV1 mediante dos estrategias diferentes. Por un lado se ensaya la acción analgésica basada en la desensibilización de TRPV1 mediante la aplicación tópica o inyectable de una alta concentración de análogos de la capsaicina, como NGX4010, y por otro lado se ensayan antagonistas como NGD8243, GRC-6211, AMG 986 y AZD 1386 (Dray 2008).

La implicación de TRPV1 en nocicepción y su validación como una prometedora diana de agentes terapéuticos contra el dolor, han situado en el punto de mira a otros canales iónicos TRP termosensibles e implicados en nocicepción, como son TRPM8 y TRPA1, cuya farmacología, así como su potencial terapéutico son menos conocidos.

La necesidad de búsqueda de nuevos agonistas y antagonistas más selectivos para TRPV1, TRPM8 y TRPA1, que ayuden a un mayor conocimiento de las bases moleculares de la transducción térmica y nocicepción, y a aumentar el potencial terapéutico para el tratamiento clínico del dolor, han motivado el desarrollo de este trabajo de tesis doctoral.

2 OBJETIVOS

UNIVERSITAS
Miguel
Hernández

Los objetivos del presente trabajo son:

OBJETIVO GENERAL

Caracterizar agonistas y antagonistas farmacológicos de la actividad de los canales iónicos TRPV1, TRPA1 y TRPM8.

OBJETIVOS ESPECÍFICOS

- Identificar nuevos agentes químicos con propiedades agonistas y antagonistas de la actividad de los canales iónicos TRP.
- Caracterizar el mecanismo de acción de estos compuestos.
- Estudiar el efecto de estos compuestos sobre la función de neuronas sensoriales primarias que expresan de forma nativa canales iónicos TRP.
- Determinar, mediante estudios conductuales, el posible efecto nociceptor o analgésico producido por estos agentes químicos a través de su efecto sobre los canales iónicos TRP en ratones adultos.

UNIVERSITAS
Miguel
Hernández

3 MATERIALES Y MÉTODOS

UNIVERSITAS
Miguel
Hernández

El estudio farmacológico de los canales iónicos TRPV1, TRPA1 y TRPM8 presentado en esta memoria se realizó mediante el uso de la técnica electrofisiológica conocida como “patch clamp”, en su modalidad de registro de corriente de célula entera (Hamill et al. 1981) y de la técnica de imagen de calcio basada en la fluorimetría de fura-2 (Williams et al. 1985; Moore et al. 1990).

Ambos tipos de estudio se realizaron con líneas celulares de mamífero HEK293, CR#1 y CHO, como sistemas de expresión heteróloga de TRPV1, TRPA1 o TRPM8 al ser expresados de forma transitoria o estable mediante la transfección de las células con ADN plasmídico conteniendo las secuencias de nucleótidos codificantes de los respectivos canales iónicos. Como modelo experimental de expresión nativa de los canales iónicos se usaron neuronas sensoriales primarias de ganglio trigémino en cultivo, obtenidas mediante la extracción de los ganglios trigéminos de ratones o cobayas y la posterior disociación química y mecánica de las neuronas para establecer un cultivo primario sobre el que se realizaron registros de imagen de calcio. Las condiciones ambientales de las células se mantuvieron constantes en un incubador con la temperatura estabilizada a 37 °C y la humedad controlada en una atmósfera de CO_2 del 5%.

Para el estudio de la conducta nociceptiva, se usó el modelo de dolor inducido por la inyección intraplantar de los compuestos y el ensayo en placa caliente para evaluar la inducción de hiperalgesia térmica en ratones adultos.

3.1. Células HEK293

Las células HEK293 se usaron como sistema de expresión transitoria de los canales iónicos TRPV1, TRPM8 y TRPA1 en los experimentos dirigidos a la caracterización del efecto del clotrimazol sobre la actividad de estos canales iónicos. Las células fueron mantenidas en el siguiente medio de cultivo:

- DMEM con suero bovino fetal al 10%
- L-alanil-L-Glutamina a una concentración 4 mM
- Penicilina (100 U/ml)
- Estreptomicina (100 µg/ml)

En los experimentos en los que se estudió el efecto de BCTC sobre la actividad de TRPM8, las células HEK293 utilizadas fueron crecidas en:

- DMEM con suero bovino fetal al 10%
- Penicilina (100 U/ml)
- Estreptomicina (100 µg/ml)

3.1.1. Transfección

Las células HEK293 utilizadas en los experimentos con clotrimazol, se transfectaron transitoriamente con TRPM8 humano o con TRPV1 humano, clonados en el plásmido bicistrónico pCAGGS-IRES-GFP. Para la transfección se usó el reactivo de transfección TransIT-293 (Mirus). Las células transfectadas eran identificadas debido a la emisión de luz fluorescente verde durante la aplicación de luz de excitación a 470 nm de longitud de onda (ver figura 9).

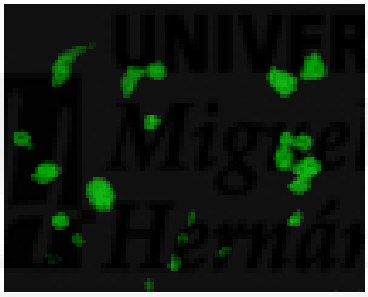

Figura 9. Células Hek293 durante la emisión de luz verde fluorescente.

En los experimentos con BCTC, la transfección transitoria de las células HEK293 se realizó con TRPM8 de rata clonado en el vector bicistrónico pclNeo/IRES-GFP, que al igual que el vector usado para los TRP humanos, porta la proteína verde fluorescente (GFP; Green Fluorescence Protein), la cuál sirve para la identificación de las células transfectadas. Para introducir el DNA plasmídico en las células se usó Lipofectamina 2000 (Invitrogen).

3.2. Células CR#1

Las células CR#1 se usaron como sistema de expresión estable del canal iónico TRPM8 en los experimentos dirigidos al estudio de la dependencia de voltaje de la actividad de este canal iónico. Estas células fueron mantenidas en el siguiente medio de cultivo:

- DMEM con suero bovino fetal al 10%
- Penicilina (100 U/ml)
- Estreptomicina (100 µg/ml)
- Geneticina (450 µg/ml)

3.2.1. Generación de la línea celular CR#1

La línea celular CR#1 fue donada gentilmente a nuestro laboratorio por el Dr. Ramón Latorre, del Centro de Estudios Científicos de Valdivia (Chile). Su generación y caracterización inicial esta descrita en (Brauchi et al. 2004). Brevemente, ser transfectaron, mediante liposomas catiónicos, células HEK293 con el vector plasmídico pCDNA3 conteniendo una secuencia de ADN de TRPM8 de rata. A continuación, las células que expresaron TRPM8 de forma estable fueron seleccionadas mediante la exposición al antibiótico geneticina (G418 sulfato) en una concentración de 800 µg/ml durante dos semanas.

3.3. Células CHO con expresión inducible y estable de TRPA1

Las células CHO-K1/FRT con expresión estable e inducible con tetraciclina de TRPA1 (CHO-TRPA1) se usaron como sistema de expresión heteróloga del canal iónico TRPA1 en los experimentos dirigidos al estudio del efecto del clotrimazol y la nifedipina sobre el canal iónico TRPA1. Estas células fueron mantenidas en el siguiente medio de cultivo:

- DMEM con suero bovino fetal al 10%
- Glutamax® 2%
- Aminoácidos no esenciales 1%
- Penicilina (100 U/ml)
- Estreptomicina (100 µg/ml)
- Higromicina (200 µg/ml)
- Blasticidina (5 µg/ml)

La expresión de TRPA1 se indujo mediante la exposición de las células a 0.25-0.5 µg/ml del antibiótico tetraciclina de 4 a 18 horas antes de los registros.

3.3.1. Generación de células CHO-K1/FRT con expresión inducible de TRPA1

La línea celular CHO con expresión estable e inducible por tetraciclina de TRPA1 fue donada gentilmente a nuestro laboratorio por el Dr. Ardem Patapoutian (The Scripps Research Institute, La Jolla, USA). En primer lugar transfectaron la línea celular CHO Flp-In con el vector pcDNA6/TR para obtener un sistema de expresión inducible con tetraciclina (la línea celular CHO-K1/FRT inducible con tetraciclina), que fue posteriormente co-transfectada con el vector de expresión pcDNA5FRT/TO conteniendo la secuencia de ADN completa de TRPA1 de ratón y el plásmido pOG44 para la expresión de la recombinasa Flp. Las células co-transfectadas se seleccionaron mediante la resistencia a la higromicina (200 µg/ml) (Story et al. 2003).

3.4. Células CHO

La línea celular CHO se usó como control en los experimentos del estudio del efecto del clotrimazol y nifedipina al no tener expresión de TRPA1, a diferencia de las células CHO-TRPA1 que presentaron expresión de TRPA1 incluso al no ser expuestas a tetraciclina (Story et al. 2003). Estas células se mantuvieron en el siguiente medio de cultivo:

- DMEM con suero bovino fetal al 10%
- Glutamax® 2%
- Aminoácidos no esenciales 1%
- Penicilina (100 U/ml)
- Estreptomicina (100 µg/ml)

3.5. Medida de la señal de Ca^{2+} intracelular

Los niveles de Ca^{2+} intracelular se determinaron mediante el análisis fluorimétrico con la sonda fura-2 (Williams et al. 1985; Moore et al. 1990). Para ello, las células se incubaron, a 37 ° C durante 40 minutos en la solución extracelular (ver tabla 1), con la forma permeable Fura-2 acetoximetil ester en una concentración 5 µM. Una vez incubadas, los cristales se lavaron con solución extracelular y se mantuvieron a temperatura ambiente.

Las células cargadas con fura-2 se excitaron de forma alternativa con luz de dos longitudes de onda, 340 y 380 nm, a través del objetivo del microscopio y la fluorescencia emitida fue posteriormente filtrada con un filtro de paso de longitud de onda larga de 510 nm para ser detectada por una cámara CCD (ver figura 10). La razón entre la fluorescencia emitida a las 2 longitudes de excitación (F_{340}/F_{380}) es directamente proporcional a la concentración de Ca^{2+} intracelular (Williams et al. 1985; Moore et al. 1990).

Para la realización de los experimentos se utilizó un sistema de imagen basado en un monocromador, en este caso el modelo Polychrome IV (TILL Photonics, Planegg, Alemania) y una cámara CCD (Roper Scientific, Ottobrunn, Germany) conectada a un microscopio invertido modelo Axiovert 200M (Zeiss). El monocromador y la cámara CCD eran controlados con el programa informático METAFLUOR (Versión 4.65; Universal Imaging, Downingtown, PA, USA), ejecutado desde un PC con un procesador Pentium III.

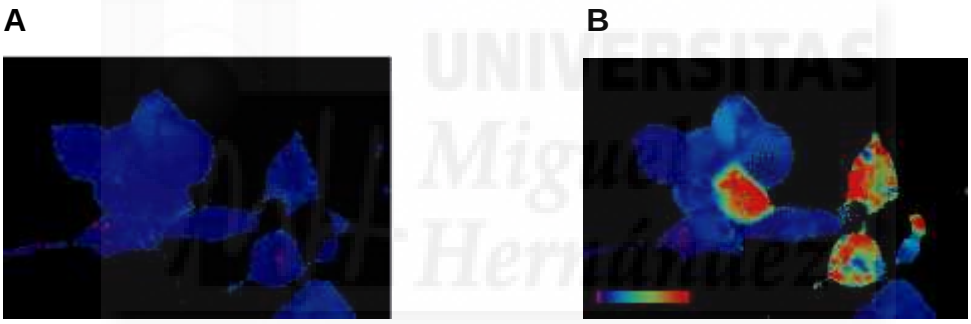

Figura 10. Ejemplo del valor de F_{340}/F_{380}, en una escala de pseudocolores, de células HEK293 cargadas con fura-2, antes (**A**) y después (**B**) del incremento de calcio intracelular. La barra de colores, de rosa a rojo, codifica un rango de $[Ca^{2+}]_i$ de 0 a 880 nM.

3.5.1. Solución extracelular

La solución extracelular empleada en todos los experimentos de la medida de la concentración de calcio intracelular correspondientes al estudio del efecto del clotrimazol sobre los canales iónicos TRPV1, TRPA1 y TRPM8 se detalla en la tabla 1 y en este trabajo se conoce como solución A. Para los experimentos de imagen de calcio del estudio del efecto de la nifedipina sobre el canal iónico TRPA1 y del efecto del BCTC sobre el canal iónico TRPM8 se empleó la solución extracelular conocida en este trabajo como solución B y también es descrita en la tabla 1.

Tabla 1

Solución A		Solución B	
Compuesto	Concentración (mM)	Compuesto	Concentración(mM)
NaCl	140	NaCl	140
KCl	5	KCl	3
$CaCl_2$	2	$CaCl_2$	2.4
$MgCl_2$	1	$MgCl_2$	1.3
Glucosa	5	Glucosa	10
Hepes	10	Hepes	10
pH = 7.4		pH = 7.4	

3.6. Registro electrofisiológico

En los experimentos del estudio del efecto del clotrimazol sobre la actividad de los canales iónicos TRPV1, TRPA1 y TRPM8, las corrientes se midieron con un amplificador EPC-5 (HEKA Electronics, Lambrecht, Germany) entre 16 y 24 horas después de la transfección mediante la fijación de voltaje de la membrana plasmática, usando la técnica “patch-clamp” (ver figura 11), en su configuración de registro de célula entera. La resistencia en el baño de los electrodos, una vez rellenados con la solución intracelular, fue de entre 2 y 4 MΩ. Un cable de cloruro de plata (Ag-AgCl) se usó como electrodo de referencia. Como programa de adquisición se usó el programa informático Clampex 5.0 (Axon Instrumets Inc, Union City, USA). Tanto las corrientes capacitativas como la resistencia en serie fueron compensadas electrónicamente, siendo usados los valores de capacitancia de la membrana para el cálculo de las densidades de corriente, y la compensación entre un 50 y 60% de la resistencia en serie para minimizar los errores de voltaje. Todos los experimentos se realizaron a temperatura ambiente, entre 22 y 24 °C.

En los experimentos en los que se estudió el efecto del clotrimazol sobre los canales iónicos TRPM8 y TRPV1, los protocolos fueron aplicados desde un potencial de reposo de 0 mV, y se alternó un protocolo de rampa con otro de pulsos de voltaje. El protocolo de rampa consistió en la fijación del potencial de membrana desde -50 mV hasta +50 mV, con una duración de 200 ms. El protocolo se aplicó de forma periódica con un intervalo de tiempo entre rampas

igual a 2 s. El protocolo de pulsos de voltaje consistió en la aplicación de pulsos desde -120 mV hasta +160 mV, con una duración de 100 ms en el caso de TRPM8 y 200 ms para TRPV1. El incremento de voltaje entre pulsos fue de 20 mV y a continuación se dió un pulso de +60 mV y 50 ms de duración.

En los experimentos en los que se estudió el efecto del clotrimazol sobre el canal iónico TRPA1 los protocolos fueron aplicados desde un potencial de reposo de 0 mV, y se alternaron un protocolo de rampa con otro de pulsos de voltaje. El protocolo de rampa de fijación de voltaje se aplicó desde -150 mV hasta +150 mV, con una duración de 500 ms. El protocolo de pulsos de voltaje consistió en la aplicación de pulsos desde -150 mV hasta +150 mV, con una duración de 400 ms. El incremento de voltaje entre pulsos fue de 25 mV.

En los experimentos del estudio del efecto de las 1,4 dihidropiridinas y BCTC sobre la actividad del canal iónico TRPA1 y de BCTC sobre la actividad del canal iónico TRPM8, se midieron las corrientes de membrana en configuración de célula entera mediante un amplificador Multiclamp700B (Axon Instruments Inc, Union City, USA). Los electrodos usados tenían una resistencia en el baño de entre 3 y 5 MΩ. Para minimizar errores de voltaje, entre un 50% y 60% de la resistencia en serie fue compensada electrónicamente, así como las corrientes capacitativas para el cálculo de la densidad de corriente. Los datos fueron adquiridos con el programa informático Clampex 9.0 (Axon Instruments, Union City, USA). Los experimentos se realizaron bajo temperatura controlada, entre 30 y 32 °C, mediante un controlador de temperatura modelo CL-100 (Warner Instruments Corp., Hamden, USA).

El efecto de las 1,4 dihidropiridinas sobre el canal iónico TRPA1 se estudió mediante la aplicación de rampas de fijación de voltaje desde un potencial de reposo de -60 mV y precedidas por un prepulso a -150 mV y 100 ms de duración. La rampa lineal de fijación de voltaje estuvo comprendida entre -150 mV y +150 mV, con una duración de 1 s y se aplicó cada 5 s.

En los experimentos en los que se estudió el efecto del BCTC sobre la corriente mediada por los canales iónicos TRPM8 y TRPA1, los protocolos se aplicaron a partir de un potencial de reposo igual a -60 mV, y consistieron en un prepulso desde el potencial de reposo hasta -100 mV, y una duración de 100 ms, seguido de una rampa lineal hasta +100 mV, con una duración igual a

520 ms. La rampa se aplicó repetidamente con un intervalo de tiempo entre las sucesivas aplicaciones de 5 s.

En los experimentos en los que se estudió la dependencia de voltaje de la actividad de TRPM8 en presencia de BCTC el protocolo de rampa usado consistió en una rampa de voltaje lineal comprendida entre -100 mV y +200 mV, con una duración de 525 ms, precedida por un pulso de voltaje de -100 mV y una duración de 100 ms. Esta rampa se aplicó con una frecuencia de 0.2 Hz.

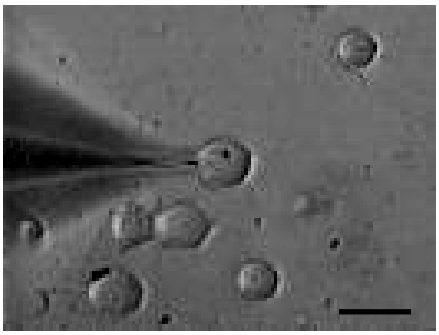

Figura 11. Imagen microscópica del electrodo de "patch-clamp" sobre una célula HEK293. La barra de calibración representa 20 µm.

3.6.1. Soluciones extra e intracelulares

Las soluciones extra e intracelulares empleadas fueron distintas según el tipo de experimento realizado. Para los experimentos electrofisiológicos en los que se ensayó el efecto del clotrimazol sobre la actividad de los canales TRPM8 y TRPV1 se emplearon soluciones extra e intracelulares simétricas (soluciones C) resumidas en la tabla 2. En los experimentos en los que se caracterizó el efecto del clotrimazol sobre la actividad de TRPA1, las soluciones empleadas (soluciones D), aparecen resumidas en la tabla 3. Las condiciones iónicas (soluciones E) para los experimentos en los que se estudia el efecto de las 1,4 dihidropiridinas sobre la actividad de TRPA1 aparecen resumidas en la tabla 4. En el estudio del efecto del BCTC sobre la actividad de TRPM8 y TRPA1 se emplearon las soluciones F descritas en la tabla 5.

Tabla 2

Solución extracelular C		**Solución intracelular C**	
Compuesto	Concentración (mM)	Compuesto	Concentración (mM)
NaCl	150	NaCl	150
$MgCl_2$	5	$MgCl_2$	5
Hepes	10	Hepes	10
EGTA	5	EGTA	5
pH = 7.4		pH = 7.4	

Tabla 3

Solución extracelular D		**Solución intracelular D**	
Compuesto	Concentración (mM)	Compuesto	Concentración (mM)
NaCl	150	NaCl	150
CsCl	5	$MgCl_2$	5
$CaCl_2$	5	Hepes	10
HEPES	10	EGTA	5
Glucosa	10		
pH = 7.4		pH = 7.4	

Tabla 4

Solución extracelular E		**Solución intracelular E**	
Compuesto	Concentración (mM)	Compuesto	Concentración (mM)
NaCl	140	NaCl	140
KCl	3	CsCl	5
$MgCl_2$	1.3	HEPES	10
$CaCl_2$	2.4	EGTA	10
HEPES	10		
Glucosa	10		
pH = 7.4		pH = 7.4	

Nota. A la solución extracelular E empleada en los experimentos con ausencia de calcio extracelular se le añadió 1 mM de EGTA y se retiró el $CaCl_2$ de su composición.

Tabla 5

Solución extracelular F		Solución intracelular F	
Compuesto	Concentración (mM)	Compuesto	Concentración (mM)
NaCl	140	CsCl	140
KCl	3	$MgCl_2$	0.6
$MgCl_2$	1.3	HEPES	10
$CaCl_2$	2.4	EGTA	1
HEPES	10	$ATPNa_2$	1
Glucosa	10	GTPNa	0.1
pH = 7.4		pH = 7.4	

3.7. Análisis de los datos

Los datos electrofisiológicos se analizaron con el programa informático WINASCD, escrito por el Dr. Guy Droogmans (disponible en el sitio web ftp://ftp.cc.kuleuven.ac.be/pub/droogmans/winascd.zip). Para el análisis estadístico de los datos y la presentación de los mismos se usó el programa Origin7.0 (OriginLab Corporation). Los grupos de datos han sido expresados como la media ± error estándar de n experimentos independientes. La significancia estadística entre grupos de datos con distribución normal se determinó mediante la prueba T (prueba *t* de Student) de dos colas, mientras que para análisis no paramétricos se usó la prueba de Smirnov-Kolmogorov. Para la comparación de las medias de diferentes grupos de datos se usó el test de la ANOVA de una vía.

3.7.1. Análisis de la dependencia de voltaje de la actividad de TRPV1 y TRPM8

A partir de la aplicación repetida de rampas de voltaje, se determinaron las curvas corriente-voltaje (I-V) y el curso temporal de la corriente, a un potencial de membrana determinado, así como las curvas dosis-respuesta del efecto producido por el clotrimazol sobre la corriente catiónica mediada por TRPM8 y TRPV1 y por el BCTC y SKF96365 sobre la corriente mediada por TRPM8. Las curvas dosis-respuesta del efecto de estos compuestos se ajustaron a la ecuación de Hill.

Los protocolos de pulsos de voltaje se usaron para el análisis de la dependencia de voltaje de la actividad de TRPM8 y TRPV1. En este caso se determinó la relación corriente en estado estacionario (tramo final de los trazos de corriente) versus al valor de voltaje correspondiente de los pulsos. Las curvas I-V en estado estacionario se ajustaron mediante el método Levenberg-Marquardt, implementado en el programa Origin 7.0, a la curva denominada en esta memoria Boltzmann-lineal, y definida por la siguiente ecuación: $I_{ss} = G_{max} \times ((V-V_{rev}) / (1+\exp((V_{1/2} - V)/K))$.

Mediante este ajuste matemático se estimaron los valores de voltaje al que la probabilidad de apertura de TRPM8 y TRPV1 es del 50% ($V_{1/2}$), la conductancia total en registro de célula entera (G_{max}) y la pendiente de la curva de activación (K). La corriente máxima activada (G_{max} x (V-Vr)) se calculó mediante la división del dato de corriente obtenido, por el valor estimado de la corriente máxima activada, y de este modo se determinó la probabilidad de apertura. Los valores de probabilidad de apertura representados versus el potencial de membrana, se ajustaron matemáticamente a la curva definida por la ecuación de Boltzmann ($I/I_{max} = 1/(1+\exp((V_{1/2} - V)/K))$. En la figura 12 se muestran los pasos descritos para el análisis de la dependencia de voltaje de la actividad de estos canales iónicos.

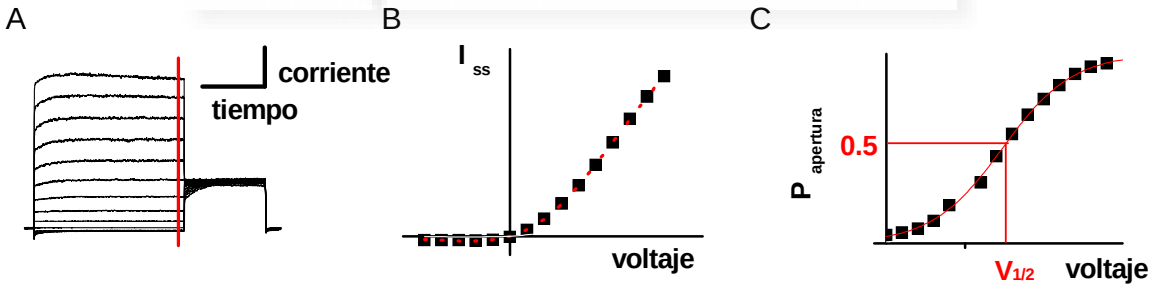

Figura 12. A. Ejemplo de corriente evocada mediante protocolo de pulsos de voltaje. **B.** Curva formada por la corriente en estado estacionario extraída a partir de los puntos de corriente mostrados en **A** y señalados por la línea vertical roja, versus el voltaje. **C.** Curva de activación construida a partir de los valores estimados en **B** mediante el ajuste de la curva Iss-voltaje a la ecuación Boltzmann-lineal.

En los experimentos en los que se estudió el efecto del BCTC, SKF96365 y 1,10-fenantrolina sobre la actividad de TRPM8, los valores de $V_{1/2}$, G_{max} y K se estimaron a partir del ajuste de la ecuación Boltzmann-lineal a los trazos de

corriente correspondientes a la aplicación del protocolo de rampa de voltajes comprendidos entre -100 mV y +200 mV.

3.8. Cultivo de neuronas sensoriales de ganglio trigémino de ratón adulto

Para ensayar el efecto del clotrimazol y la nifedipina en neuronas sensoriales, se aislaron neuronas de ganglio de trigémino de ratones adultos de la cepa C57-B6 (fenotipo silvestre y TRPV1$^{-/-}$) (Caterina et al. 2000) y nulos para el gen *trpa1* (Kwan et al. 2006). Para el estudio del BCTC se usaron cobayas neonatos de la cepa Hartley.

Los ratones fueron anestesiados mediante la inhalación de CO_2 a una concentración del 100% y los cobayas mediante la inyección intraperitoneal de pentobarbital sódico (90 mg/Kg), posteriormente ambos fueron decapitados. A continuación las cabezas se situaron bajo una lupa y se procedió a cortar y separar la piel que cubre la parte superior del cráneo tras lo que se retiró la bóveda craneal mediante el uso de unas tijeras. La masa encefálica fue desplazada tras apoyar unas pinzas en la parte anterior del cerebro y realizar un movimiento lento en dirección a la parte posterior del mismo hasta dejar visibles los ganglios trigéminos, situados en la base del cráneo. Posteriormente se cortaron las ramas periféricas de los ganglios, se cortaron adherencias y extrajeron los cuerpos de los ganglios que fueron depositados en una placa de Petri del tipo P35 con tampón salino (PBS), para a continuación limpiar los restos de tejido conectivo adheridos. Los ganglios fueron trasladados a otra placa P35 que contenía las enzimas colagenasa tipo XI (0.66 mg/ml) y dispasa (3 mg/ml), disueltas en un medio de incubación compuesto por cloruro sódico (NaCl) a concentración 155 mM, fosfato dipotásico (K_2HP0_4) a 1.5 mM, HEPES a 5.6 mM, NaHEPES a 4.8 mM y glucosa a 5 mM. En esta solución enzimática se mantuvieron los ganglios durante 1 hora a 37 °C y a atmósfera de 5% de CO_2 en un incubador para cultivo celular. Tras la disociación enzimática, los ganglios se trasladaron a un tubo de centrífuga junto con el medio de incubación enzimática, y mediante una pipeta pasteur de vidrio se realizó una suave digestión mecánica. A continuación se añadió medio de cultivo al tubo hasta completar un volumen de 5 ml y se centrifugó a 1700 r.p.m. durante 10 minutos. Tras la centrifugación, se desechó el sobrenadante y se añadieron 200 µl de medio de cultivo para la resuspensión del precipitado resultante. La

suspensión fue entonces dividida en volúmenes de 20 µl que se colocaron sobre la superficie de 10 cristales de 6 mm de diámetro, distribuidos en dos placas P35, y que habían sido previamente tratados con poli-L-lisina al 0.01% durante 20 minutos. De este modo se mantuvieron durante 4 horas en el incubador tras lo que se les añadió 1 ml de medio de cultivo a cada placa, que se retiró a continuación y se renovó con el mismo volumen. Las placas se devolvieron al incubador hasta su uso experimental tras 24h aproximadamente.

3.9. Estudio de conducta de dolor

Para este estudio se usaron 33 ratones macho adultos (16 sivestres y 17 TRPV1$^{-/-}$). Todos los procedimientos empleados cumplieron las directrices de la Asociación Internacional para el Estudio del Dolor (IUSP) (Zimmermann 1983). Los animales habían sido estabulados para su cría en jaulas con 6 animales como máximo, en un ciclo 12h luz/oscuridad y alimentados *ad libitum*.

Los animales se colocaron individualmente en cámaras de plástico 1 hora antes del procedimiento experimental para su habituación al entorno. Los reactivos empleados (CLT, BCTC, Nifedipina, aceite de mostaza y Bayk8644) se disolvieron en una solución compuesta por 10% de DMSO, 10% de Tween80 y 80% de PBS. Las drogas se inyectaron en un volumen de 10 µl mediante una inyección intraplantar en la pata izquierda usando una jeringa Hamilton acoplada a una aguja 30 G. Para los experimentos control, a los ratones se les inyectó únicamente el vehículo.

La conducta nociceptiva fue evaluada mediante la cuantificación del tiempo, expresado en segundos, que los animales dedicaron a lamidos, mordiscos y ausencia de apoyo de la pata inyectada durante los 10 minutos posteriores a la inyección.

En los ensayos de placa caliente, la temperatura se mantuvo a 55 ± 0.5 °C y el límite de latencia para evitar daños en los tejidos del ratón fue de 30 s. Los signos de conducta nociceptiva que llevaron a la retirada del ratón de la placa caliente fueron lamidos, mordiscos y saltos. La media de dos pruebas anteriores a la inyección determinó la latencia de retirada basal. Los ensayos de placa caliente se realizaron tras los 10 minutos posteriores a la inyección con 0.5% de clotrimazol, después de la evaluación de la conducta de dolor

espontáneo. Los resultados se expresaron como el porcentaje de la latencia de retirada respecto del valor de retirada basal previo a la inyección.

4 RESULTADOS

UNIVERSITAS
Miguel
Hernández

4.1. Estudio del efecto del clotrimazol sobre los canales iónicos TRPV1, TRPA1 y TRPM8 expresados de forma heteróloga.

El clotrimazol es un compuesto antimitótico imidazólico (ver figura 13) de amplio uso clínico. Previamente, se ha descrito el efecto del clotrimazol sobre distintos canales iónicos entre los que se encuentran los canales de potasio activados por calcio IK(Ca^{2+}) (Jensen et al. 2001), canales de potasio dependientes de voltaje (Hernandez-Benito et al. 2001) y canales de calcio de tipo L (Fearon et al. 2000). También se ha descrito la inhibición irreversible que produce el clotrimazol sobre el canal iónico TRPM2 (Hill et al. 2004). Sin embargo, no existe un conocimiento acerca del efecto de esta substancia sobre los canales iónicos termosensibles pertenecientes a la familia de los canales iónicos TRP, lo que motivó la exploración del efecto del clotrimazol sobre TRPV1, TRPA1 y TRPM8.

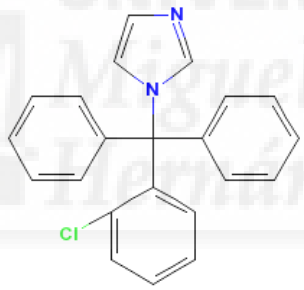

Figura 13. Estructura química del clotrimazol en la que se muestra el característico anillo pentagonal nitrogenado de los compuestos imidazólicos.

4.1.1. Efecto del clotrimazol sobre la $[Ca^{2+}]_i$ en células HEK293 transfectadas con TRPV1 y TRPA1

En primer lugar, se exploró el posible efecto del clotrimazol sobre los canales TRPV1 y TRPA1. Para ello, se expresaron de forma heteróloga en células HEK293 y mediante la técnica fluorimétrica de imagen de calcio intracelular, basada en el uso de la sonda fluorescente fura-2, se midieron los efectos del clotrimazol sobre la concentración de calcio intracelular $[Ca^{2+}]_i$ a temperatura ambiental.

Como se muestra en la figura 14A, la aplicación de 10 µM de clotrimazol produjo un incremento del calcio intracelular en células HEK293 transfectadas con TRPV1 equiparable en amplitud al producido en las mismas células por 100 nM de capsaicina, un agonista selectivo de estos canales, pero no produjo ningún incremento en las células HEK293 que no fueron transfectadas y que se usaron como control.

Al aplicar el clotrimazol en las mismas células HEK293 expresando esta vez el canal iónico TRPA1, se produjo de nuevo un incremento del calcio intracelular (Fig. 14B), pero a diferencia del incremento de la $[Ca^{2+}]_i$ mediado por la activación de TRPV1, que sucedió de forma rápida en todas las células (latencia al pico < 1 minuto), la respuesta mediada por TRPA1 fue más variable y la latencia en alcanzar la máxima amplitud el incremento de la $[Ca^{2+}]_i$ fue mayor (<3 minutos).

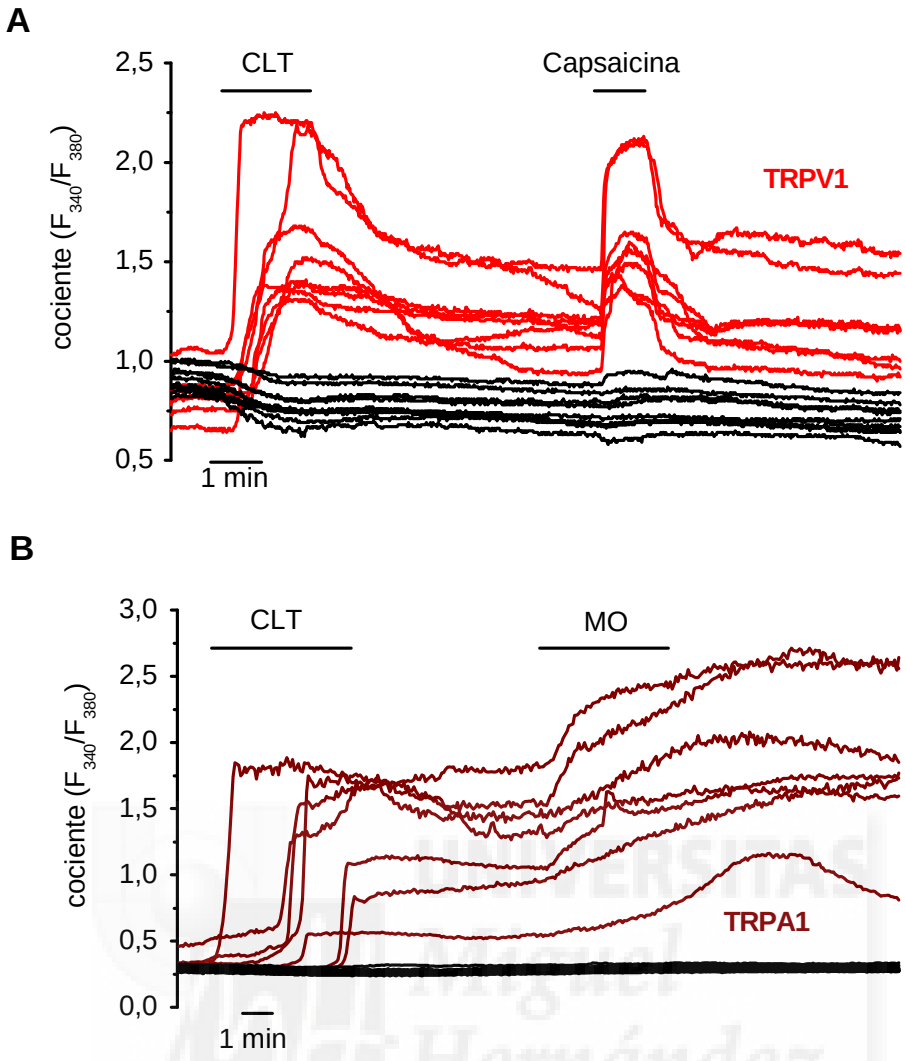

Figura 14. Registro fluorimétrico del calcio intracelular en células HEK293 transfectadas con los canales iónicos TRPV1 y TRPA1 respectivamente. **A.** Cursos temporales de las variaciones de la $[Ca^{2+}]_i$ en respuesta a 10 µM de clotrimazol y 100 nM de capsaicina en células HEK293 transfectadas con TRPV1. Se muestran los registros correspondientes a ocho células individuales (trazos rojos) para ilustrar la variabilidad de las respuestas al clotrimazol. En el mismo campo, las células sin transfectar no respondieron a ambos estímulos (trazos negros). **B.** Cursos temporales de las variaciones de la $[Ca^{2+}]_i$ en respuesta a 5 µM de clotrimazol y 20 µM de MO (aceite de mostaza) en células HEK293 transfectadas con TRPA1. Se muestran los registros correspondientes a siete células individuales (trazos marrones). En el mismo campo, las células sin transfectar no respondieron a ambos estímulos (trazos negros).

4.1.2. Efecto del clotrimazol sobre la $[Ca^{2+}]_i$ en células HEK293 transfectadas con TRPM8.

Posteriormente se estudió el efecto del clotrimazol sobre la $[Ca^{2+}]_i$ en células HEK293 transfectadas con el canal iónico TRPM8 y sobre el incremento de la $[Ca^{2+}]_i$ evocado por la aplicación de 100 µM de mentol en células HEK293 transfectadas con TRPM8. Las células transfectadas presentaron un valor basal de la $[Ca^{2+}]_i$ mayor que las células HEK293 sin transfectar que se usaron como control. Esta elevación se debe a que a temperatura ambiente existe una

flujo neto significativo de entrada de cationes, mediado por TRPM8 (McKemy et al. 2002; Peier et al. 2002; Voets et al. 2004a). La aplicación de 10 µM de clotrimazol redujo la $[Ca^{2+}]_i$ basal además de inhibir de forma total y reversible el incremento de $[Ca^{2+}]_i$ evocado por mentol (Fig.15).

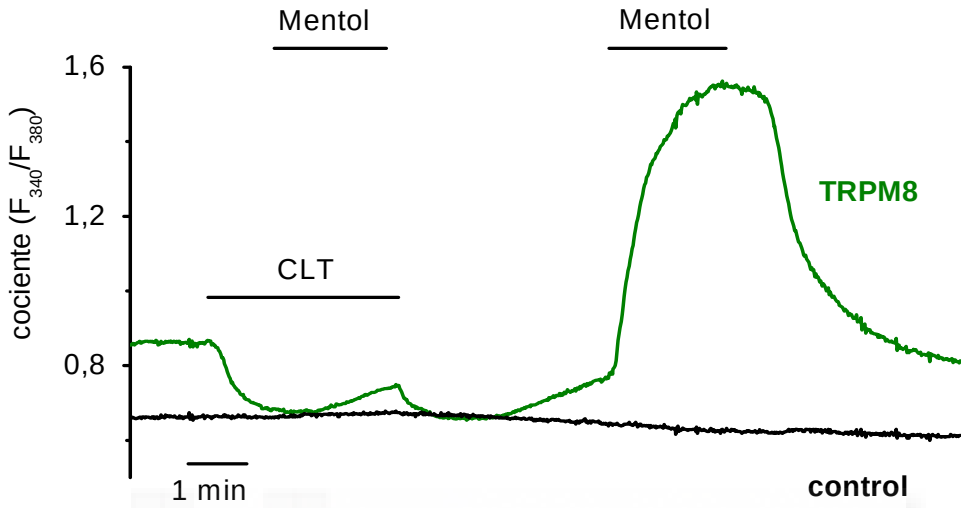

Figura 15. Curso temporal del promedio de las variaciones de la $[Ca^{2+}]_i$ en respuesta a 100 µM de mentol en presencia y ausencia de 10 µM de clotrimazol en células HEK transfectadas con TRPM8 (trazo verde; n=10) y células sin transfectar en el mismo campo (trazo negro; n=5).

4.1.3. Efecto del clotrimazol sobre las corrientes mediadas por TRPV1

Con el objetivo de profundizar en la naturaleza de la respuesta mediada por el canal iónico TRPV1 tras la aplicación del clotrimazol, se usó la técnica de "patch-clamp" en la modalidad de célula entera, en células HEK293 transfectadas con TRPV1. Para seguir los cambios en la amplitud de las corrientes mediadas por TRPV1 durante la aplicación del clotrimazol se aplicaron repetidamente protocolos de rampas de voltaje (Fig. 16B) y la corriente se monitorizó a +50 y – 50 mV. Como se puede observar en las figura 16A, la aplicación de distintas concentraciones de clotrimazol produjo un incremento, dependiente de la dosis (Fig. 16C), de corrientes macroscópicas de salida y de entrada mediadas por TRPV1. Además, en la presencia continua de 5 µM de clotrimazol o concentraciones mayores, la corriente activada mostró una fuerte desensibilización que no ocurrió durante la aplicación de concentraciones menores del clotrimazol. Esta activación no se produjo en las células que no fueron transfectadas (datos no mostrados). La relación

corriente-voltaje de la corriente activada por el clotrimazol mostró rectificación de salida y un potencial de reversión cercano a 0 mV (Fig.16B), características consistentes con las descritas previamente para la corriente mediada por TRPV1 (Voets et al. 2004a; Caterina et al. 1997).

Aunque la actividad de los canales iónicos TRP se describió en un principio como independiente del potencial de membrana, posteriormente se demostró que al menos algunos de ellos muestran una dependencia de voltaje débil, siendo este el caso de los canales iónicos TRP sensibles a temperatura. De este modo, la actividad de TRPV1, TRPV3, TRPM8, TRPM4 y TRPM5 es dependiente de voltaje y esta característica biofísica puede ser modulada por estímulos térmicos y químicos (Hofmann et al. 2003; Brauchi et al. 2004; Voets et al. 2004a; Chung et al. 2005; Talavera et al. 2005).

Al realizar la curva dosis respuesta del efecto del clotrimazol sobre la actividad del canal iónico TRPV1 a dos potenciales de membrana distintos se observó que el efecto potenciador del clotrimazol sobre la corriente mediada por TRPV1 fue mayor a -50 mV que a +50 mV (Fig. 16D). Este dato sugiere un posible cambio en la dependencia de voltaje de la actividad de TRPV1 en presencia del clotrimazol. Para investigar este posible efecto en más profundidad se aplicaron protocolos de pulsos de voltaje en ausencia y presencia de este compuesto (Fig. 16E). Posteriormente, a la curva formada por los valores de corriente en estado estacionario representados frente a los valores correspondientes de potencial de membrana, se le realizó un ajuste matemático a la siguiente función de Boltzmann modificada: I_{ss} (V) = G_{max} x (V-V_{rev}) / (1+exp (($V_{1/2}$ –V)/k)) y de este modo se estimaron los valores de la curva de activación (Fig. 16F). De los datos obtenidos se desprende que el clotrimazol desplaza la curva de activación de TRPV1 hacia valores de potencial de membrana más negativos o fisiológicos, con un cambio de $V_{1/2}$ desde 127± 23 mV en solución control a 41 ± 13 mV en presencia de 3 µM de clotrimazol (n= 4; p< 0,05; prueba T).

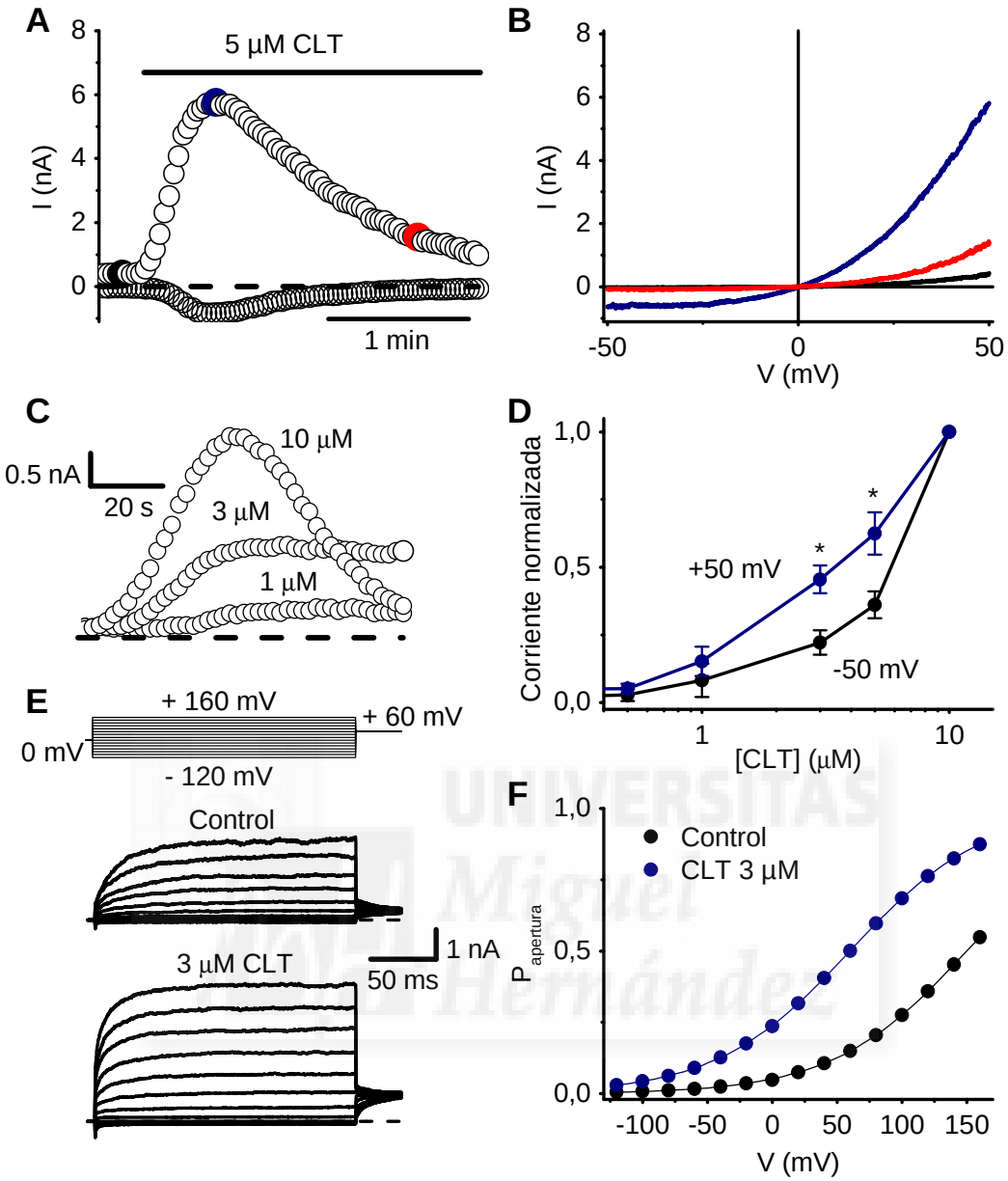

Figura 16. El clotrimazol activa corrientes macroscópicas mediadas por TRPV1 transfectado en células HEK293. **A.** Curso temporal de la corriente de entrada (a -50 mV) y de salida (a + 50 mV) durante la aplicación de 5 µM de clotrimazol. **B.** Curvas corriente-voltaje obtenidas mediante rampas de fijación de voltaje de 200 ms de duración, comprendidas entre -50 y +50 mV y aplicadas en el momento indicado en **A** con el color correspondiente. **C.** Comparación de los cursos temporales de la corriente mediada por TRPV1 durante la aplicación de 1, 3 y 10 µM de clotrimazol. **D.** Curva dosis-respuesta normalizada para la corriente mediada por TRPV1 en presencia de distintas concentraciones del clotrimazol y seguida a los potenciales de membrana indicados (* $p < 0.05$; prueba T). **E.** Corrientes evocadas mediante pulsos de voltaje de 200 ms de duración y comprendidos entre -120 mV y + 160 mV antes (izquierda) y durante (derecha) la aplicación de 3 µM de clotrimazol. **F.** Curvas de activación obtenidas a partir de las corrientes en estado estacionario en ausencia (círculos en negro) y presencia de 3 µM de clotrimazol (círculos en azul).

4.1.4. Efecto del clotrimazol sobre la corriente mediada por TRPA1

Para seguir el curso temporal de los efectos del clotrimazol sobre las corrientes mediadas por TRPA1 se aplicaron repetidamente rampas de voltaje a células CHO transfectadas de forma estable con el canal iónico TRPA1 (ver Materiales y Métodos). En una solución extracelular sin Ca^{2+} y en ausencia del clotrimazol, las rampas de voltaje desde –150 hasta +150 mV evocaron corrientes con una pronunciada rectificación de salida (120 ± 30 pA a +75 mV; -25 ± 5 pA a -75 mV; n=12) lo que indica la existencia de actividad basal del canal iónico (Fig. 17A y B). En las mismas condiciones, la aplicación de 5 µM de clotrimazol evocó un incremento modesto y reversible de la corriente (Fig. 17A y B) que no se observó en células CHO sin transfectar (no se muestran los datos). El efecto del clotrimazol fue dependiente de la dosis empleada y no se saturó con concentraciones de hasta 30 µM, que es la concentración límite a la que es soluble en la solución extracelular (Fig. 17F).

La activación de TRPA1 es dependiente de voltaje (Karashima et al. 2007; Macpherson et al. 2007a; Zurborg et al. 2007). Por ello, intentamos determinar el posible efecto del clotrimazol sobre la dependencia de voltaje de la actividad de TRPA1, midiendo el valor del pico de las corrientes de cola que se generan tras la aplicación de pulsos de voltaje de 400 ms comprendidos entre - 150 y + 150 mV seguidos de un pulso de - 150 mV (Fig. 17C).

En presencia de clotrimazol las corrientes de cola a -150 mV fueron significativamente mayores a partir de valores de potencial de membrana ≥ 25 mV ($p < 0,05$; prueba T), mientras que en ausencia de la droga estas solo se evidenciaron a potenciales de membrana mucho más positivos (Fig. 17D). No fue posible estimar los valores correspondientes a la ecuación de Boltzmann porque la amplitud de la corriente de cola no llegó a ser saturante. Aun así, la amplitud de la corriente de cola para un mismo potencial de membrana fue hasta 10 veces mayor en presencia de clotrimazol. Con todo ello se puede concluir que el clotrimazol produjo un desplazamiento hacia la izquierda de la dependencia de voltaje de la actividad de TRPA1, lo que explica una mayor actividad del canal iónico en presencia de este fármaco a valores de potencial de membrana más negativos o fisiológicos.

Otra característica descrita recientemente en relación a la apertura de TRPA1 ha sido la activación directa que produce el Ca^{2+} intracelular, de modo que la

entrada a la célula de Ca^{2+} extracelular a través de TRPA1 supone un mecanismo de retroalimentación positiva en la activación de este canal iónico (Nagata et al. 2005; Doerner et al. 2007; Zurborg et al. 2007). En este sentido, se estudió el efecto del clotrimazol sobre el canal iónico TRPA1, esta vez en presencia de Ca^{2+} en la solución extracelular y se observó que la respuesta al clotrimazol se potenció. De este modo, en presencia de 5 mM de Ca^{2+}, la corriente de salida durante la aplicación de 5 μM de clotrimazol se incrementó aproximadamente 10 veces y la corriente de entrada 100 veces en comparación con lo observado en ausencia de Ca^{2+} en la solución extracelular (Fig. 17E y F). Los experimentos se desarrollaron en presencia de 5 mM de EGTA en el interior de la pipeta, lo que neutraliza el incremento de Ca^{2+} intracelular como consecuencia de la entrada de Ca^{2+} extracelular. Estos datos en conjunto, indican que la eficiencia del clotrimazol en la activación de TRPA1 depende de la presencia de Ca^{2+} extracelular y la entrada de Ca^{2+} a través del canal iónico.

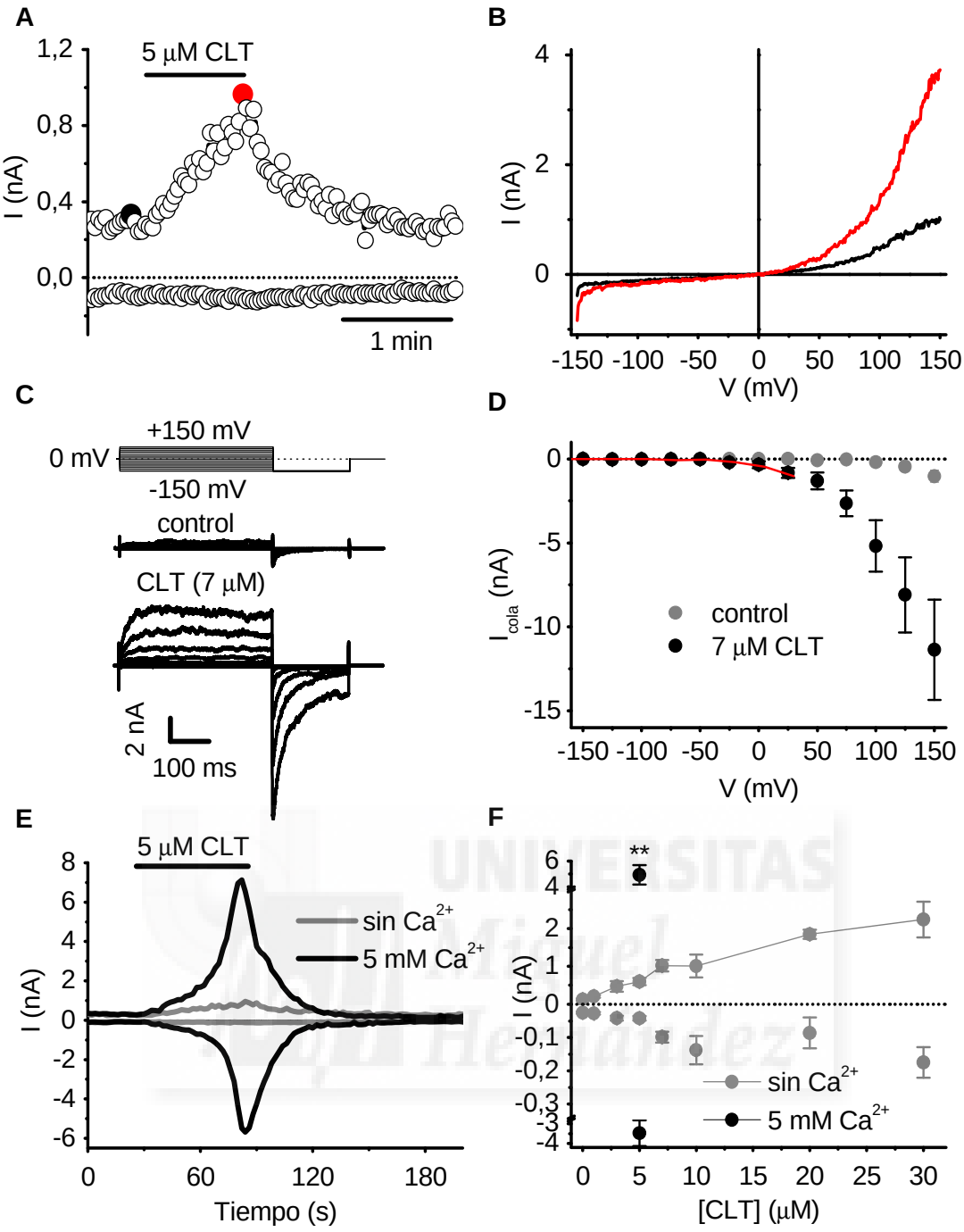

Figura 17. Clotrimazol activa corrientes macroscópicas mediadas por TRPA1 transfectado en células CHO. **A.** Curso temporal de la corriente de entrada (a -75 mV) y de salida (a + 75 mV) mediada por TRPA1 en respuesta a la aplicación de 5 µM de clotrimazol en solución extracelular sin Ca^{2+}. **B.** Curvas corriente-voltaje obtenidas mediante rampas de fijación de voltaje, de 500 ms de duración, comprendidas entre -150 mV y + 150 mV. Los trazos corresponden a los puntos marcados con círculos rellenos en **A** con el color correspondiente. **C.** Corrientes evocadas mediante pulsos de voltaje de 400 ms de duración, comprendidos entre -150 mV y + 150 mV y seguidos por un pulso invariable de -150 mV antes y durante la aplicación de 7 µM de clotrimazol. **D.** Valores del pico de la corriente de cola de entrada a – 150 mV en ausencia (círculos rellenos) y presencia de 7 µM de clotrimazol (círculos abiertos). La línea roja simula los datos obtenidos en ausencia del clotrimazol con un cambio de 110 mV hacia la izquierda. **E.** Curso temporal de la corriente mediada por TRPA1 durante la aplicación de 5 µM de clotrimazol en presencia de 5 mM de Ca^{2+} en la solución extracelular (trazos negros) y en ausencia de Ca^{2+} en la solución extracelular (trazo gris, los mismos datos de la figura 3A) mostrados para ser comparados. **F.** Curva dosis-respuesta para la corriente de entrada (a – 75 mV) y salida (a + 75mV) mediada por TRPA1 en respuesta a distintas concentraciones de clotrimazol, en ausencia de Ca^{2+} extracelular (círculo gris) y en presencia de 5 mM de Ca^{2+} en la solución extracelular (círculo negro) (** $p < 0,01$; prueba T).

4.1.5. Efecto del clotrimazol sobre la corriente mediada por TRPA1 en respuesta a mentol

Recientemente se ha descrito que el mentol activa el canal iónico TRPA1 (Karashima et al. 2007) de manera dependiente de la dosis aplicada, con una respuesta máxima a una concentración igual a 100 µM, y por encima de la cuál ejerce un efecto inhibitorio sobre la actividad de este canal iónico. En este sentido intentamos determinar el posible efecto potenciador del clotrimazol sobre la corriente mediada por TRPA1 en respuesta a mentol.

A tal efecto, se usó el mismo protocolo de rampas de voltaje y condiciones iónicas usadas para los experimentos mostrados en las figuras 17A y B, sobre células HEK293 transfectadas de forma transitoria con el canal iónico TRPA1, y se monitorizó la corriente a +75 mV y -75 mV para seguir el curso temporal de las corrientes de salida y de entrada respectivamente. Como se observa en la figura 18, la aplicación repetida de mentol produjo un incremento de la corriente de salida que no se observó en la corriente de entrada, mientras que la aplicación conjunta del mentol y clotrimazol produjo un mayor incremento de la corriente de salida que la sola aplicación de mentol, y produjo además un incremento de la corriente de entrada. Estos efectos del mentol y clotrimazol sobre la actividad de TRPA1 fueron totalmente reversibles.

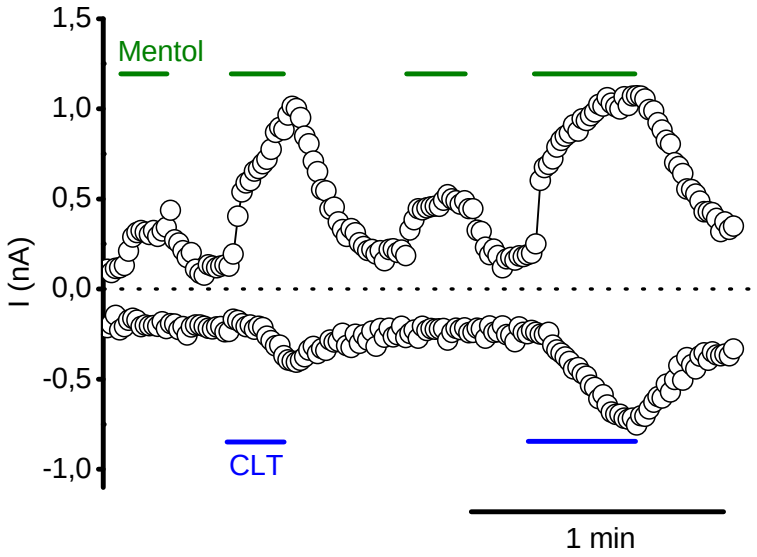

Figura 18. El clotrimazol potencia la corriente macroscópica mediada por TRPA1 en respuesta a mentol en células HEK293. Curso temporal de la corriente de entrada (a -75 mV) y de salida (a + 75 mV) mediada por TRPA1 en respuesta a la aplicación de 50 µM de mentol en ausencia y presencia de 10 µM de clotrimazol.

4.1.6. Efecto del clotrimazol sobre la corriente mediada por TRPM8 en respuesta a mentol

La aplicación de rampas de voltaje en presencia de 100 µM de mentol a 25 °C, en células HEK293 transfectadas de forma transitoria con el canal iónico TRPM8, evocó una corriente con un potencial de reversión cercano a 0 mV y rectificación de salida (Fig. 19B) lo que fue consistente con las características de la corriente mediada por TRPM8 descrita en trabajos anteriores (McKemy et al. 2002; Peier et al. 2002). Para estudiar el curso temporal de los efectos del clotrimazol sobre la corriente TRPM8 activada por mentol se monitorizó la corriente a +50 y –50 mV. Como se puede observar en la figura 19A, la aplicación de 10 µM de clotrimazol inhibió de forma total y reversible las corrientes de entrada y de salida producidas por mentol. El análisis de las curvas dosis-inhibición correspondientes al efecto de distintas concentraciones del clotrimazol sobre las corrientes de salida y de entrada (Fig. 19C) reveló una mayor eficiencia inhibitoria sobre la corriente a –50 mV (IC_{50}= 200 nM) que a +50 mV (IC_{50}= 1.2 µM) lo que indica un posible cambio en la dependencia de voltaje de la actividad de TRPM8 en presencia del clotrimazol. Para investigar el efecto del clotrimazol sobre la dependencia de voltaje de estos canales en más profundidad se aplicaron protocolos de pulsos de voltaje en ausencia y presencia de este compuesto (Fig. 19D). Del análisis de los datos obtenidos (consultar Materiales y Métodos) se desprende que el clotrimazol desplaza la curva de activación de TRPM8 hacia valores de potencial de membrana más positivos, alejándolo del rango fisiológico (Fig. 19E). Además, como se puede observar en la figura 19F, en la que se representan los valores de $V_{1/2}$ (potencial de membrana en el que la probabilidad de apertura es del 50%) correspondientes a la aplicación de distintas concentraciones de clotrimazol, el cambio producido sobre la dependencia de voltaje de la actividad de TRPM8 es dependiente de la dosis de fármaco empleada. Los datos se ajustaron a la ecuación de Hill y de este modo se estimó que la concentración de clotrimazol que produce un 50% de incremento de $V_{1/2}$ fue 3 ± 1 µM (n=5).

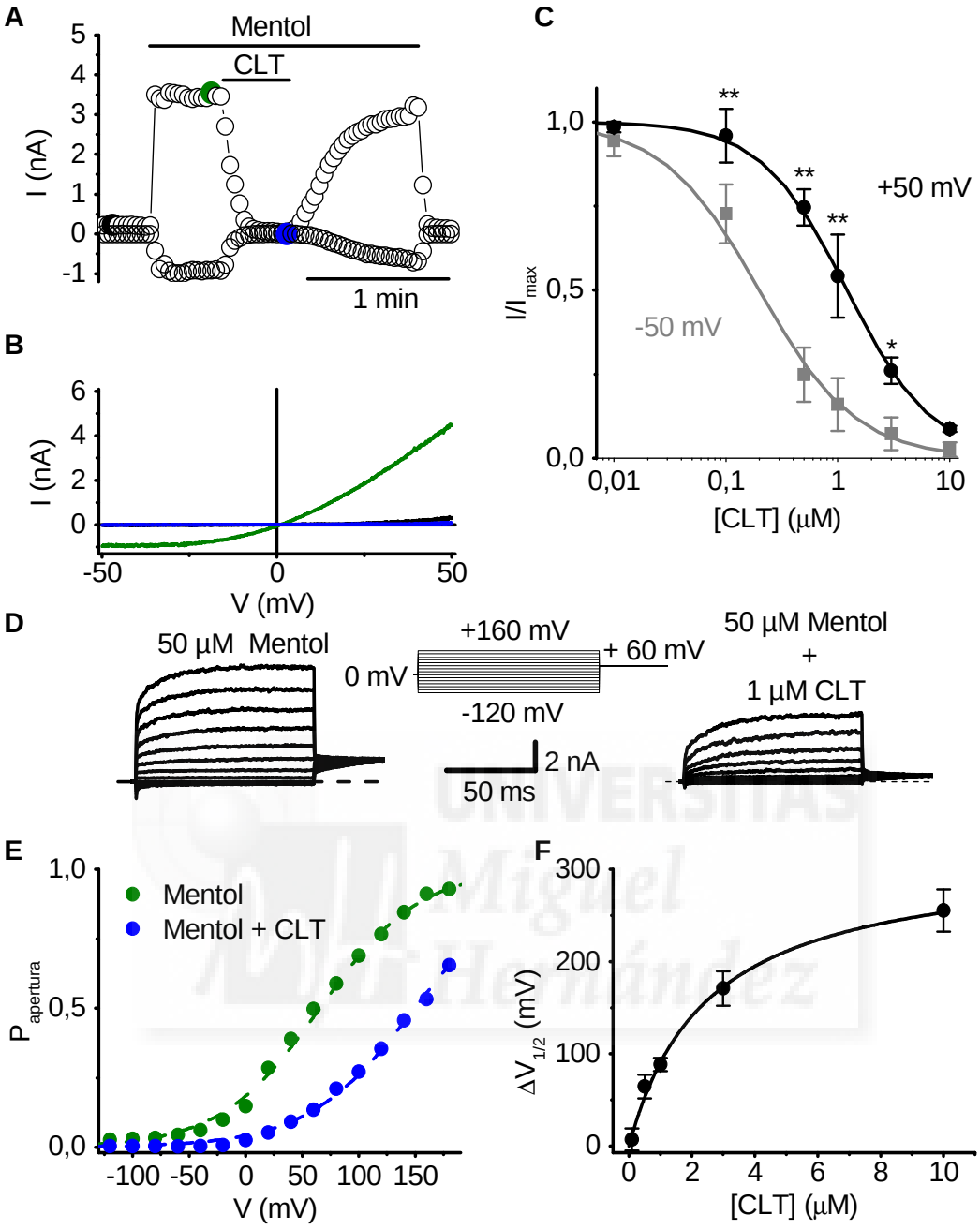

Figura 19. Clotrimazol inhibe la corriente macroscópica mediada por TRPM8 transfectado en células HEK293. **A.** Curso temporal de la corriente de entrada (a -50 mV) y de salida (a +50 mV) evocada por la aplicación de 100 µM de mentol y su inhibición reversible por la aplicación de 10 µM de clotrimazol. **B.** Curvas corriente-voltaje obtenidas mediante rampas de fijación de voltaje de 200 ms de duración, comprendidas entre -50 y +50 mV. Los trazos corresponden a los puntos marcados con círculos rellenos en **A** con el color correspondiente **C.** Curva dosis-respuesta para la inhibición en presencia de distintas concentraciones de clotrimazol de la corriente inducida por mentol y mediada por TRPM8 a -50 mV (cuadrados rellenos) y +50 mV (círculos abiertos) (* p< 0,05, ** p< 0,01; prueba T). **D**. Corrientes evocadas mediante pulsos de voltaje de 100 ms de duración, comprendidos entre -120 y +160 mV en presencia de mentol, antes (izquierda) y después de la adición del clotrimazol (derecha). **E.** Curvas de activación obtenidas a partir de las corrientes inducidas por mentol en estado estacionario en ausencia (círculos rellenos) y presencia (círculos abiertos) de 1 µM de clotrimazol. **F.** Cambio de $V_{1/2}$ en función de la concentración de clotrimazol aplicada.

4.2. Estudio del efecto de la nifedipina sobre la actividad del canal iónico TRPA1 expresado de forma heteróloga

Las 1,4 dihidropiridinas son un grupo de antagonistas de canales de calcio de tipo L (Catterall 2000; Triggle 2003) que tienen gran relevancia en clínica debido a su amplio uso como agentes antihipertensivos para el tratamiento de patologías como la hipertensión y angina de pecho. Debido al escaso conocimiento que existe sobre la interacción de sustancias de uso clínico sobre el canal iónico TRPA1, se exploró el efecto de la nifedipina sobre este canal iónico. Estudios previos en el laboratorio mostraron que las 1,4 dihidropiridinas elevaban el Ca^{2+} intracelular en células CHO transfectadas de forma estable con el canal iónico TRPA1, mientras que no lo hacían en células CHO sin transfectar (Fajardo et al. 2008b).

4.2.1. Efecto de las 1,4 dihidropiridinas sobre la corriente mediada por TRPA1

Mediante el uso de la técnica “patch-clamp” en la configuración de registro de célula entera, se midió la corriente macroscópica mediada por TRPA1 en células CHO-TRPA1 durante la aplicación de 10 μM de nifedipina, la cuál se comparó con la producida por 200 μM de cinamaldehído mediante la aplicación de un protocolo idéntico que consistió en rampas de fijación del potencial de membrana desde -150 a +150 mV aplicadas cada 5 s. Las corrientes evocadas por nifedipina y CM mostraron las características típicas de los canales iónicos TRPA1, que consisten en una corriente catiónica no selectiva con potencial de reversión cercano a 0 mV y una ligera rectificación hacia fuera (Fig. 20B y C).

El curso temporal de la corriente macroscópica se siguió a +100 y -100 mV, y como se observa en la figura 20A, la aplicación de 10 μM de nifedipina y de 200 μM de cinamaldehído mostró en ambos casos una activación transitoria de la corriente que se desensibilizó en la presencia continua de los agonistas. Además, la amplitud de la corriente evocada por ambos agonistas fue similar, a pesar de la menor concentración de nifedipina (Fig. 20A y C), mostrando de este modo la mayor eficiencia de nifedipina en la activación de TRPA1.

El BAYK8644, es un derivado de las 1,4 dihidropiridinas con efecto agonista en lugar de antagonista sobre los canales de calcio de tipo L (Schramm et al.

1983). Por ello, decidimos estudiar también su efecto sobre la corriente mediada por TRPA1. La aplicación de 30 µM de BAYK8644 produjo una activación transitoria de la corriente, similar a lo observado con nifedipina o CM (Fig. 20A, B y C).

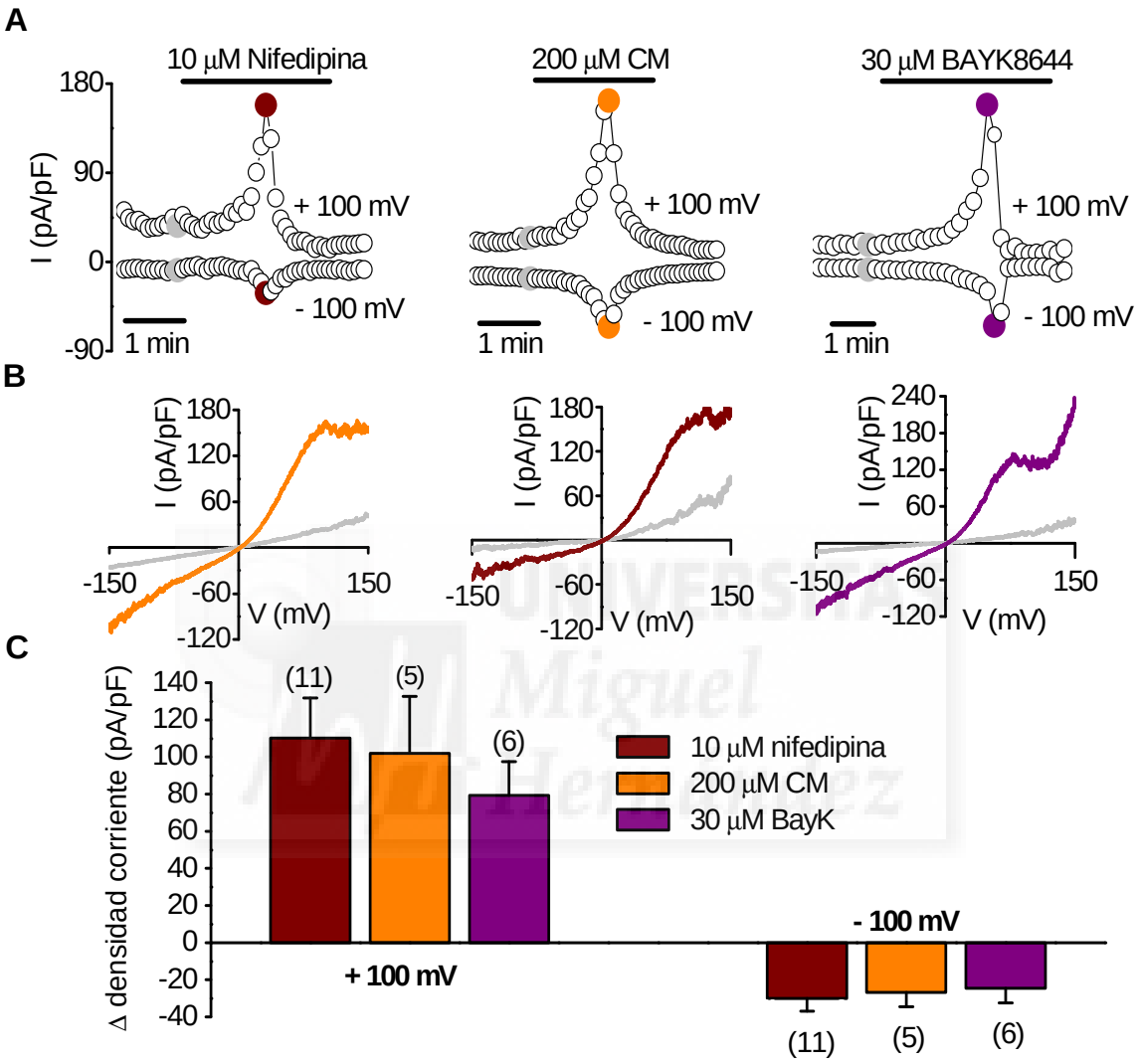

Figura 20. Activación de corrientes similares mediadas por el canal iónico TRPA1 en respuesta a nifedipina, CM y BAYK8644. **A**. Cursos temporales de la corriente macroscópica activada durante la aplicación de 10 µM de nifedipina, 200 µM de CM y 30 µM de BayK8644. Se muestra la desensibilización total de la corriente durante la presencia continua del agonista. **B.** Curvas corriente-voltaje de la corriente total en control (trazo gris) y en presencia de 10 µM de nifedipina (izq.), 200 µM de CM (centro) y 30 µM de BAYK8644 (dcha.). Los trazos corresponden a los puntos marcados con círculos rellenos en **A**. **C.** Densidad de corriente media a +100 y -100 mV evocada por 10 µM de nifedipina, 200 µM de CM y 30 µM de BAYK8644. Cada célula fue expuesta a un único agonista.

Para caracterizar en más detalle el efecto de nifedipina sobre el mecanismo de apertura de TRPA1 se aplicaron pulsos rectangulares de voltaje de entre -150 y +150 mV seguidos de un pulso constante de -150 mV. En la figura 21A, se

muestra como nifedipina activó una corriente sostenida con una pequeña inactivación a valores de potencial de membrana muy positivos. Además, produjo un incremento significativo de la amplitud de las corrientes de cola para todos los potenciales de membrana ($p< 0.01$; prueba T) (Fig. 21B), lo que indica un desplazamiento hacia la izquierda en la dependencia de voltaje de la actividad de TRPA1, similar a lo observado con clotrimazol y otros agonistas como el mentol (Karashima et al. 2007).

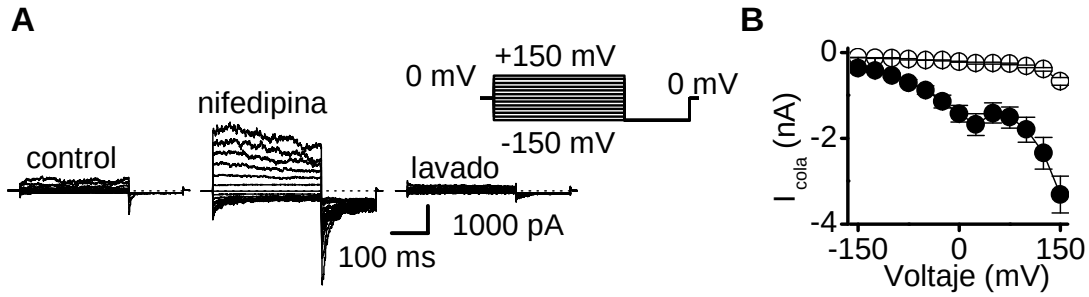

Figura 21. **A.** Corrientes evocadas mediante pulsos de voltaje de 300 ms de duración y comprendidos entre -150 mV y +150 mV, seguidos por un pulso invariable a -150 mV y 150 ms de duración, en presencia y ausencia de 10 µM de nifedipina. **B.** Valores del pico de la corriente de cola de entrada a -150 mV en ausencia (círculos abiertos) y presencia de 10 µM de nifedipina (círculos rellenos).

Estudios recientes han demostrado que la elevación del Ca^{2+} intracelular activa y desensibiliza los canales TRPA1 (Jordt et al. 2004; Nagata et al. 2005; Doerner et al. 2007; Kim et al. 2007; Zurborg et al. 2007; Wang et al. 2008). Para evaluar la posible implicación del Ca^{2+} en la desensibilización de TRPA1 en la respuesta a nifedipina se realizaron experimentos en ausencia de Ca^{2+} extracelular y con 10 mM de EGTA en el interior de la pipeta para tamponar el Ca^{2+} intracelular.

Como se muestra en las figura 22A y B, el curso temporal de la corriente evocada por nifedipina en ausencia y presencia de calcio extracelular fue muy similar (tau de inactivación = 100 ± 36 s frente a 105 ± 27 s; n=4, p=0.9; prueba T). Estos datos indican que el incremento de la $[Ca^{2+}]_i$ no es necesario para que se produzca la desensibilización de TRPA1 en presencia continua de nifedipina.

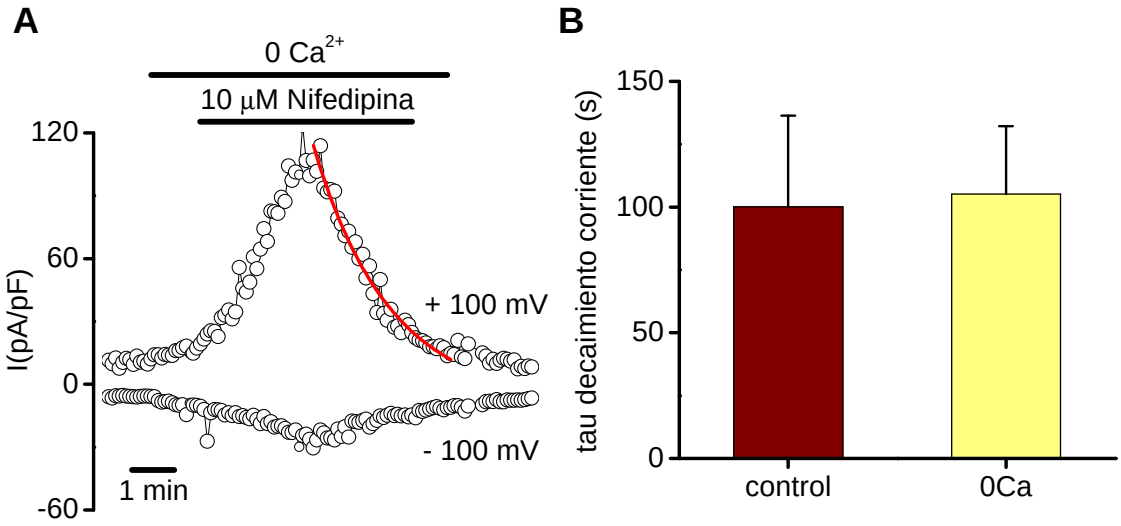

Figura 22. La desensibilización de la corriente activada por nifedipina no depende del aumento del Ca^{2+} intracelular. **A.** Curso temporal de la corriente macroscópica durante la aplicación de 10 μM de nifedipina en ausencia de Ca^{2+} extracelular (10 mM de EGTA en la solución de la pipeta). Se muestra la rápida desensibilización de la corriente durante la presencia continua del agonista. **B.** Constante de tiempo del decaimiento de la corriente en condición control (2.4 mM Ca^{2+}) y en la ausencia de Ca^{2+} externo. Los valores medios no fueron diferentes estadísticamente.

Para estudiar un posible fenómeno de desensibilización cruzada entre nifedipina y CM se aplicaron prepulsos de 10 μM de nifedipina que produjeron la inhibición casi total de la corriente evocada por 200 μM de cinamaldehído (Fig. 23A y B). En ausencia del prepulso la densidad de corriente evocada por CM fue 75.1 ± 28.4 frente a 1.1 ± 0.5 pA/pF tras el prepulso (n=5, $p<0.05$; prueba T).

Estos resultados suponen numerosas evidencias de que la corriente catiónica evocada por nifedipina en células CHO-A1 es mediada por el canal iónico TRPA1.

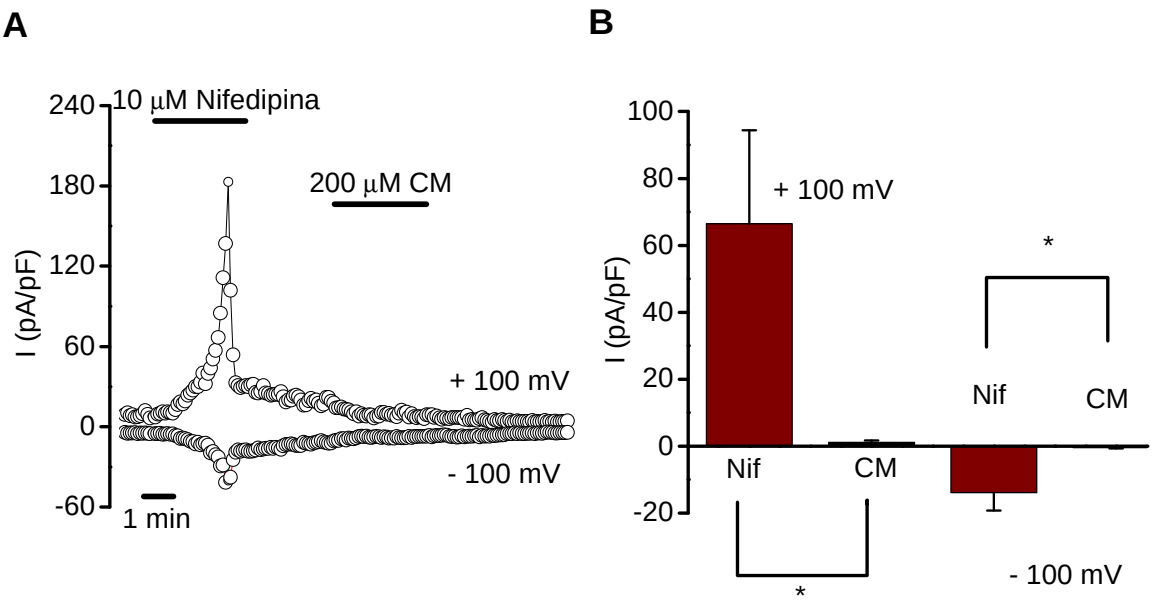

Figura 23. Desensibilización cruzada entre las corrientes mediadas por TRPA1 en respuesta a nifedipina y CM. **A.** Curso temporal de la corriente macroscópica durante aplicaciones consecutivas de 10 μM de nifedipina y 200 μM de CM en la misma célula CHO-TRPA1. Se muestra la ausencia de respuesta a CM después de la activación de la corriente por nifedipina. **B.** Gráfico de barras ilustrando la densidad de corriente media durante las aplicaciones consecutivas de 10 μM de nifedipina y 200 μM de CM (* $p < 0.05$).

4.3. Estudio de los efectos de BCTC, SKF963565 y 1,10-fenantrolina sobre la actividad del canal iónico TRPM8 expresado de forma heteróloga

Los estudios realizados hasta la fecha no han logrado identificar antagonistas selectivos del canal TRPM8. Así, fármacos como el BCTC, con un potente efecto inhibidor sobre TRPV1 (Valenzano et al. 2003), también inhiben las respuestas a mentol mediadas por TRPM8 (Behrendt et al. 2004; Weil et al. 2005) en sistemas de expresión heteróloga.

Otro fármaco, el SKF96365 es un bloqueante inespecífico de canales de calcio operados por receptor y dependientes de voltaje, además de los activados por la liberación de calcio de los depósitos intracelulares (Merritt et al. 1990). SKF96365 también era conocido como un bloqueante de corrientes de potasio con rectificación de entrada en células endoteliales (Schwarz et al. 1994). Recientemente, se demostró un efecto inhibidor del SKF96365 sobre la corriente activada por frío en neuronas de ganglios raquídeos (Reid et al. 2002a).

Finalmente, el complejo Cu-Phe es un agente oxidante capaz de inducir la formación de puentes disulfuro entre grupos tiol, y ha sido empleado en estudios de la apertura de canales operados por voltaje (Liu et al. 1996b).

Recientemente, se ha demostrado que el complejo formado por la fenantrolina y el cobre es un antagonista de TRPV1. En este caso, el complejo actúa como un bloqueante de canal abierto en lugar de inducir la unión de cisteínas (Tousova et al. 2004). De manera similar, la 1,10-fenantrolina libre y el complejo que forma con el cobre son también bloqueantes de canal abierto del canal de Na^+ de músculo esquelético humano (Popa et al. 2006). Con estos antecedentes, creímos conveniente explorar el efecto de estos compuesto sobre el canal iónico TRPM8.

Estudios previos en el laboratorio (Malkia et al. 2007) mostraron que BCTC, SKF96365 y 1,10-fenantrolina inhiben la corriente mediada por TRPM8 en respuesta al frío y además que esta inhibición es dependiente del potencial de membrana. Estos datos sugieren que BCTC, SKF96365 y 1,10-fenantrolina podrían modificar la dependencia de voltaje de la actividad de TRPM8.

4.3.1. Efectos de BCTC, SKF96365 y 1,10-fenantrolina sobre la dependencia de voltaje de la actividad de TRPM8

Como se indicó en la Introducción, el mecanismo de acción de agonistas de TRPM8, como son el frío y el mentol, consiste en desplazar la dependencia de voltaje del canal hacia valores de potencial de membrana más negativos o fisiológicos (Brauchi et al. 2004; Voets et al. 2004a). La dependencia de voltaje de la acción antagonista del BCTC junto con el hecho de presentar carga eléctrica neutra a pH= 7.4, sugirieron la posibilidad de que BCTC podría estar desplazando, de un modo opuesto a mentol y frío, la dependencia de voltaje de la actividad de TRPM8 hacia valores de potencial de membrana más positivos en lugar de actuar como un bloqueante del poro modulado por el potencial transmembrana (Hille 2001). A tal fin, se estudió la actividad de TRPM8 mediante rampas de voltaje de 525 ms de duración en células CR#1 con una expresión estable de TRPM8 (Brauchi et al. 2004) y células HEK293 transfectadas transitoriamente con TRPM8, en la modalidad de registro de célula entera. La figura 24B muestra ejemplos de las trazas de corriente obtenidas bajo las distintas condiciones de temperatura y presencia o ausencia de mentol y BCTC.

La figura 24A muestra el curso temporal de los efectos de 3 μM de BCTC sobre corrientes evocadas por frío y/o mentol a -80, +80 y +160 mV. Como se puede observar, la aplicación de 100 μM de mentol a 33 °C, o la bajada de la temperatura desde 33 °C hasta 20 °C, produjeron un aumento de la corriente de salida que apenas se percibe sobre la corriente de entrada. Además, la aplicación de 100 μM de mentol a 20 °C produjo una clara potenciación de la corriente de entrada. En estas últimas condiciones, la aplicación de 3 μM de BCTC produjo una inhibición incompleta sobre la corriente de salida que sin embargo fue completa sobre la corriente de entrada (Fig.24A y B). Para medir los cambios producidos en la dependencia de voltaje de la actividad de TRPM8, se estimaron los valores de la curva de activación mediante el ajuste matemático de la corriente evocada por las rampas de voltaje a distintas temperaturas, en presencia y ausencia de mentol y BCTC, a la ecuación de Boltzmann-lineal descrita previamente. Como había sido descrito anteriormente, el frío y mentol desplazaron hacia la izquierda la curva de activación, lo que se traduce en un cambio hacia valores más negativos del parámetro $V_{1/2}$ (Voets et al. 2004a). Por el contrario, la aplicación de 3 μM de BCTC produjo un cambio significativo hacia valores más positivos de $V_{1/2}$. La aplicación de 3 μM de BCTC también redujo el valor de G_{max} (conductancia total), pero no modificó K (pendiente de la curva de activación). Los cambios de $V_{1/2}$ producidos por la aplicación de 3 μM de BCTC a 33 °C, 20 °C, 100 uM de mentol a 33 °C, y 100 μM de mentol a 20 °C, fueron respectivamente 34 ± 9 , 67 ± 11, 78 ± 6 y 97 ± 11 mV, lo que indica que el efecto inhibitorio de BCTC sobre la actividad de TRPM8 es mayor en condiciones de más alta probabilidad de apertura de TRPM8.

La figura 24C muestra un resumen de los cambios en $V_{1/2}$ inducidos por la aplicación de BCTC, mentol y temperatura. Se trata de los valores medios de $V_{1/2}$ de varios experimentos y se presentan como los cambios relativos respecto al valor de $V_{1/2}$ a 20 °C ($\Delta V_{1/2}$). Este resumen muestra claramente los cambios bidireccionales producidos por estos agentes químicos y el frío, de modo que se puede observar la cancelación de los efectos de los agonistas y antagonistas respecto al cambio de $V_{1/2}$, como quedó de manifiesto al enfriar la solución hasta 20 °C, lo que produjo un cambio de $V_{1/2}$ hacia valores negativos más pequeño que el producido por la aplicación de 100 μM, que produjo un

cambio de $V_{1/2}$ en el mismo sentido. La aplicación de 3 μM de BCTC en presencia de 100 μM de mentol a 20 °C indujo el cambio de $V_{1/2}$ a un valor similar al medido a 20 °C en ausencia de 100 μM de mentol.

Consecuentemente, se estudió si SKF96365 y 1,10-fenantrolina producían un cambio similar a BCTC sobre la dependencia de voltaje de la actividad de TRPM8. En este caso se estudió el efecto de SKF96365 sobre la corriente evocada a 20 °C. La figura 24D muestra el curso temporal del efecto inhibitorio de SKF96365 sobre la corriente evocada por frío a -80, +80 y +160 mV, mientras que en la figura 24E se muestran los correspondientes trazos originales de la corriente medida al aplicar la rampa de potenciales de membrana en las distintas condiciones. De este modo SKF96365 desplazó $V_{1/2}$ hacia valores de potencial de membrana más positivos ($\Delta V_{1/2}$= 24 ± 3 mV). En el caso de 1,10-fenantrolina también se produjo un cambio hacia valores de potencial de membrana más positivos ($\Delta V_{1/2}$= 35 ± 5 mV).

Estos datos indican que BCTC, SKF96365 y 1,10-fenantrolina producen un cambio en la dependencia de voltaje de la actividad de TRPM8 al desplazar la dependencia de voltaje hacia valores de potencial de membrana más positivos (Fig.24F).

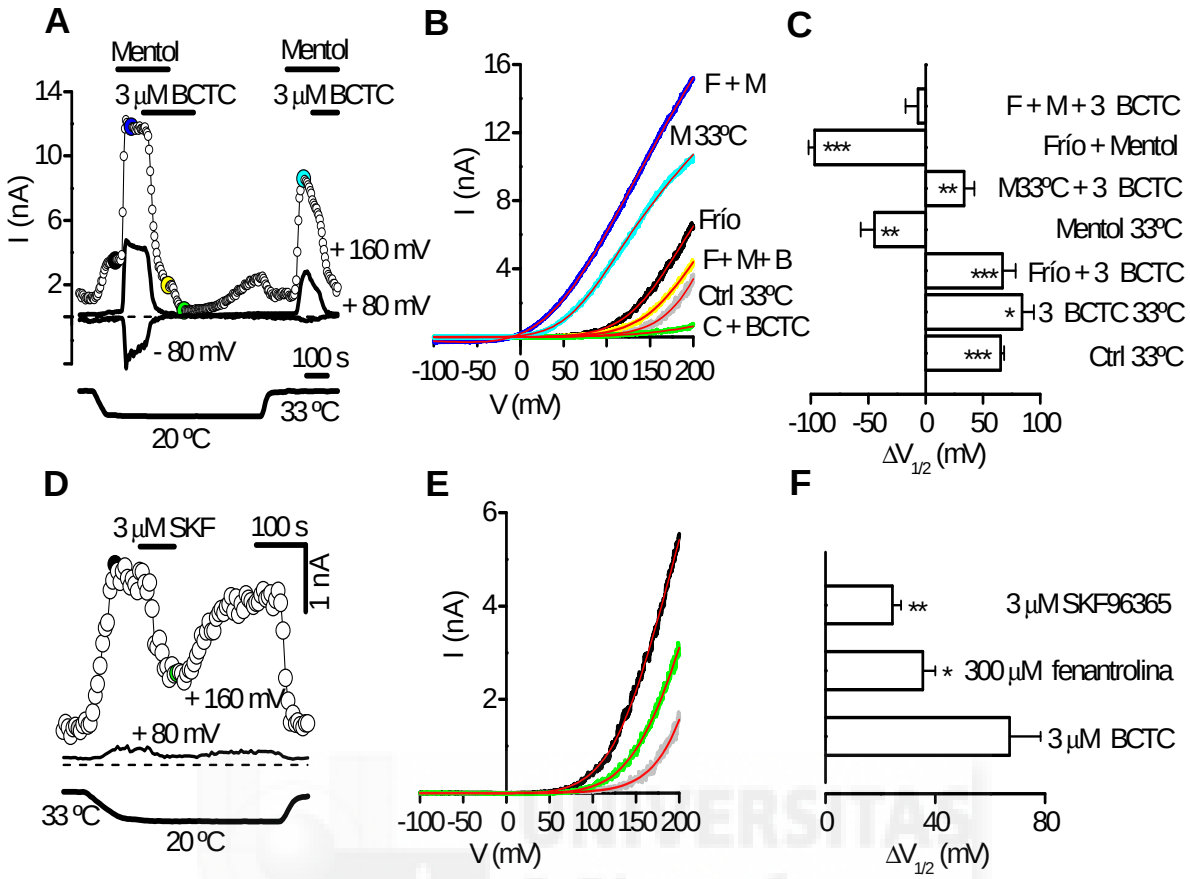

Figura 24. BCTC y SKF96365 desplazan la curva de activación de TRPM8 hacia valores de potencial de membrana más positivos. **A.** Curso temporal de la corriente macroscópica de entrada (-80 mV) y de salida (+80 mV y +160 mV) mediada por TRPM8 en células CR#1 HEK293 en presencia y ausencia de 100 µM de mentol y 3 µM de BCTC a diferentes temperaturas, 33 y 20 ℃. **B.** Curvas corriente-voltaje evocadas mediante rampas de fijación de voltaje de 525 ms de duración, comprendidas entre -100 y + 200 mV y aplicadas en los momentos indicados en **A**. Las líneas rojas superpuestas a cada trazo representan el ajuste de la corriente a la eqn (6). **C.** Histograma de los efectos de BCTC sobre el valor de potencial de membrana correspondiente al 50 % de activación ($V_{1/2}$) de TRPM8 (n= 3-22). Los datos se representaron como los cambios de $V_{1/2}$ respecto al valor obtenido para frío (20 ° C). La significancia estadística se obtuvo mediante el test t no pareado y se indica como *** P<0.001, **P<0.01 y *P<0.05. **D.** Curso temporal de la inhibición causada por SKF96365 sobre la corriente macroscópica de salida (+160 y +80 mV) evocada por frío. Los trazos de corriente correspondientes a los momentos marcados con círculos rellenos se representan en **E**. La línea discontinua indica el nivel cero de corriente; la línea inferior es la temperatura de la solución extracelular. **E.** Curvas corriente-voltaje correspondientes al experimento mostrado en **D**. Las líneas rojas representan los ajustes a la ecuación (6). **F.** Cambios inducidos en $V_{1/2}$ durante la aplicación de 3 µM de BCTC, 3 µM de SKF96365 y 300 µM de 1,10-fenantrolina respecto al valor obtenido a 20 °C. Los valores medios de $V_{1/2}$ durante la aplicación de frío fueron 156 ± 7 mV (BCTC), 158 ± 6 mV (SKF96365) y 146 ± 5 mV (1,10-fenantrolina). La significancia estadística se obtuvo mediante el Análisis de la Varianza (ANOVA) de una vía en combinación con el test Dunnett´s post hoc usando 3µM de BCTC como referencia, y se indica como ** P<0.01 y * P<0.05.

4.4. Estudio del efecto de BCTC sobre la actividad del canal iónico TRPA1 expresado de forma heteróloga

4.4.1. Efecto de BCTC sobre la $[Ca^{2+}]_i$ en células HEK293 transfectadas con el canal iónico TRPA1

Por último se estudió el efecto de BCTC sobre el canal iónico TRPA1. La aplicación de 3 µM de BCTC sobre células HEK293 transfectadas de forma transitoria con TRPA1 de ratón produjo el incremento reversible y significativo ($n=12$, $p< 0.05$; prueba T) de la $[Ca^{2+}]_i$, mientras que no tuvo efecto sobre células sin transfectar (Fig.25A y B).

Además, la aplicación de BCTC sobre el incremento de $[Ca^{2+}]_i$ evocado por cinamaldehído no produjo ningún efecto a diferencia de la aplicación de Rojo de Rutenio, un conocido inhibidor de canales iónicos TRP, que redujo parcialmente la respuesta (Fig. 25C y D).

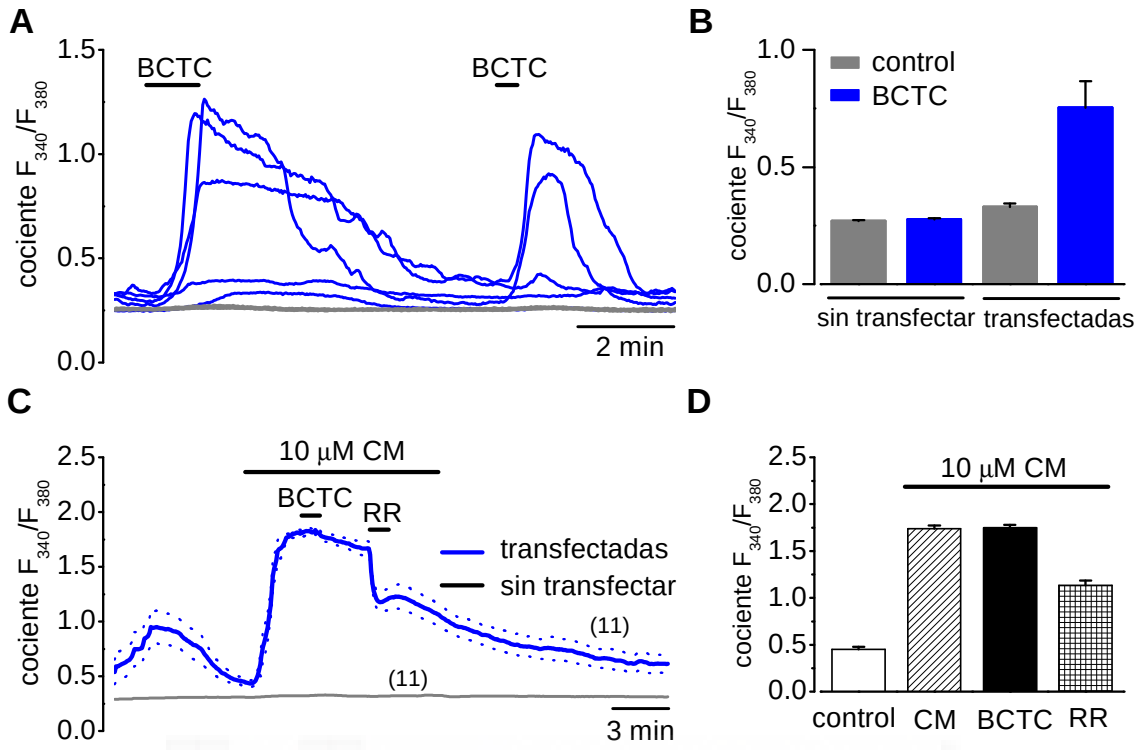

Figura 25. BCTC incrementa la $[Ca^{2+}]_i$ en células HEK293 transfectadas con el canal iónico TRPA1. **A.** Cursos temporales de las variaciones de la $[Ca^{2+}]_i$ en respuesta a dos aplicaciones consecutivas de 3 µM de BCTC. Se muestran los registros correspondientes a cinco células individuales (trazos azules) para ilustrar la variabilidad de las respuestas a BCTC. En el mismo campo, las células sin transfectar no respondieron a ambos estímulos (trazos grises). **B.** Promedio del cociente F_{340}/F_{380} en células sin transfectar y transfectadas con el canal iónico TRPA1 en presencia y ausencia de 3 µM de BCTC. **C.** Curso temporal promedio de las variaciones de la $[Ca^{2+}]_i$ en células HEK293 transfectadas con TRPA1, en condición control, 10 µM de CM, 3 µM de BCTC en presencia de 10 µM de CM y 20 µM de RR en presencia de 10 µM de CM. Es de destacar la ausencia de efecto de la aplicación de BCTC sobre la respuesta a CM y la significativa inhibición parcial (n= 18, $p<0.001$; prueba T) de la respuesta a CM producida por la aplicación de RR. En el mismo campo las células no transfectadas no respondieron a ningún estímulo. **D.** Promedio del cociente F_{340}/F_{380} en células transfectadas con el canal iónico TRPA1 en condición control, 10 µM de CM, 3 µM de BCTC en presencia de 10 µM de CM y 20 µM de RR en presencia de 10 µM de CM.

4.4.2. Efecto de BCTC sobre la corriente mediada por TRPA1

Del mismo modo, la presencia de 3 µM de BCTC incrementó una corriente catiónica no selectiva con potencial de reversión cercano a 0 mV y ligera rectificación de salida tras aplicar rampas de voltaje desde -100 a +100 mV. En las mismas células, la posterior aplicación de cinamaldehído produjo la activación de una corriente de características similares (Fig. 26B). El curso temporal de la corriente seguida a +80 mV mostró un efecto reversible de BCTC sobre la corriente mediada por TRPA1 (Fig. 26A). En las células sin

transfectar no se produjeron cambios en la corriente durante la aplicación de BCTC (Fig. 26C).

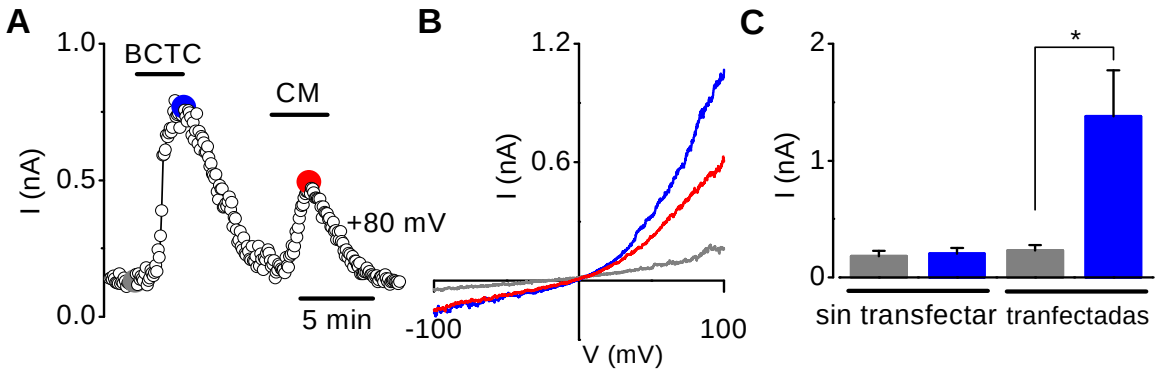

Figura 26. BCTC incrementa la corriente macroscópica mediada por TRPA1 transfectado en células HEK293. **A.** Curso temporal de la corriente macroscópica de salida (a +80 mV) durante la aplicación de 3 µM de BCTC y 100 µM de CM. **B.** Curvas corriente-voltaje obtenidas mediante rampas de fijación de voltaje de 500 ms de duración, comprendidas entre -100 y +100 mV y aplicadas en el momento indicado en **A**. **C.** Promedio de la corriente a +80 mV en células HEK293 sin transfectar y transfectadadas con el canal iónico TRPA1 en ausencia y presencia de 3 µM de BCTC (n=4, * p< 0.05; prueba T).

4.5. Tabla resumen de los efectos de CLT, Nifedipina y BCTC sobre TRPV1, TRPA1 y TRPM8

	Clotrimazol	**Nifedipina**	**BCTC**
TRPV1	activa	desconocido	inhibe
TRPA1	activa	activa	activa
TRPM8	inhibe	sin efecto	inhibe

4.6. Efectos del clotrimazol, nifedipina y BCTC sobre neuronas sensoriales primarias de ganglio trigémino

El siguiente objetivo de nuestro estudio consistió en caracterizar el efecto del clotrimazol, nifedipina y BCTC sobre los canales iónicos TRPV1, TRPA1 y TRPM8 expresados de forma nativa en neuronas sensoriales primarias. Para ello se realizaron disociaciones agudas de neuronas de ganglios trigéminos de ratón y cobaya, en las que se midieron las variaciones de la concentración de calcio intracelular mediante fluorimetría de calcio basada en fura 2-AM.

4.6.1 Efecto del clotrimazol sobre la $[Ca^{2+}]_i$ de una subpoblación de neuronas de ganglio trigémino sensibles a capsaicina y MO

La aplicación del clotrimazol produjo un incremento de la $[Ca^{2+}]_i$ en una subpoblación (21%) de neuronas disociadas de ganglio trigémino de ratón que además respondieron en su totalidad a capsaicina, un agonista específico del canal TRPV1, si bien solo aproximadamente la mitad de las neuronas que respondieron a capsaicina (49%) lo hicieron también al clotrimazol (Fig.27A y C). Posteriormente, se evaluó la contribución relativa de TRPV1 y TRPA1 a los incrementos de $[Ca^{2+}]_i$ inducidos por el clotrimazol. A tal efecto se disociaron neuronas de los ganglios trigéminos de ratones modificados genéticamente para que no expresen el canal iónico TRPV1 ($TRPV1^{-/-}$) (Caterina et al. 2000). La proporción de neuronas que respondieron a la aplicación del clotrimazol (7%) fue más reducida que en el caso de neuronas procedentes de ratones con un genotipo silvestre ($p< 0.001$, test de Kolmogorov-Smirnov) (Fig. 27C y D). Además, la amplitud media de la $[Ca^{2+}]_i$ también fue menor (Δ ratio, 0.72 ± 0.12 para WT frente a 0.31 ± 0.12 para $TRPV1^{-/-}$; $p< 0.05$). Por otro lado, las neuronas de ratones $TRPV1^{-/-}$ no mostraron ninguna respuesta a la aplicación de capsaicina como había sido descrito previamente (Caterina et al. 2000), sin embargo todas respondieron a la aplicación de aceite de mostaza (MO), un agonista específico de TRPA1 (Fig. 27B).

La figura 27D muestra un resumen de las respuestas a clotrimazol y capsaicina de las neuronas de ganglio trigémino de ratones silvestre y $TRPV1^{-/-}$ mediante histogramas de probabilidad acumulada.

En estudios previos sobre la expresión de TRPV1 y TRPA1 en neuronas sensoriales de ganglio trigémino, se observó que el TRPA1 se colocaliza mayoritariamente con neuronas que expresan TRPV1, sensibles a capsaicina (Story et al. 2003; Kobayashi et al. 2005). El conjunto de estas observaciones indican que el clotrimazol excita una subpoblación de neuronas sensoriales de los ganglios trigéminos a través de la activación de TRPV1 y en menor medida de TRPA1.

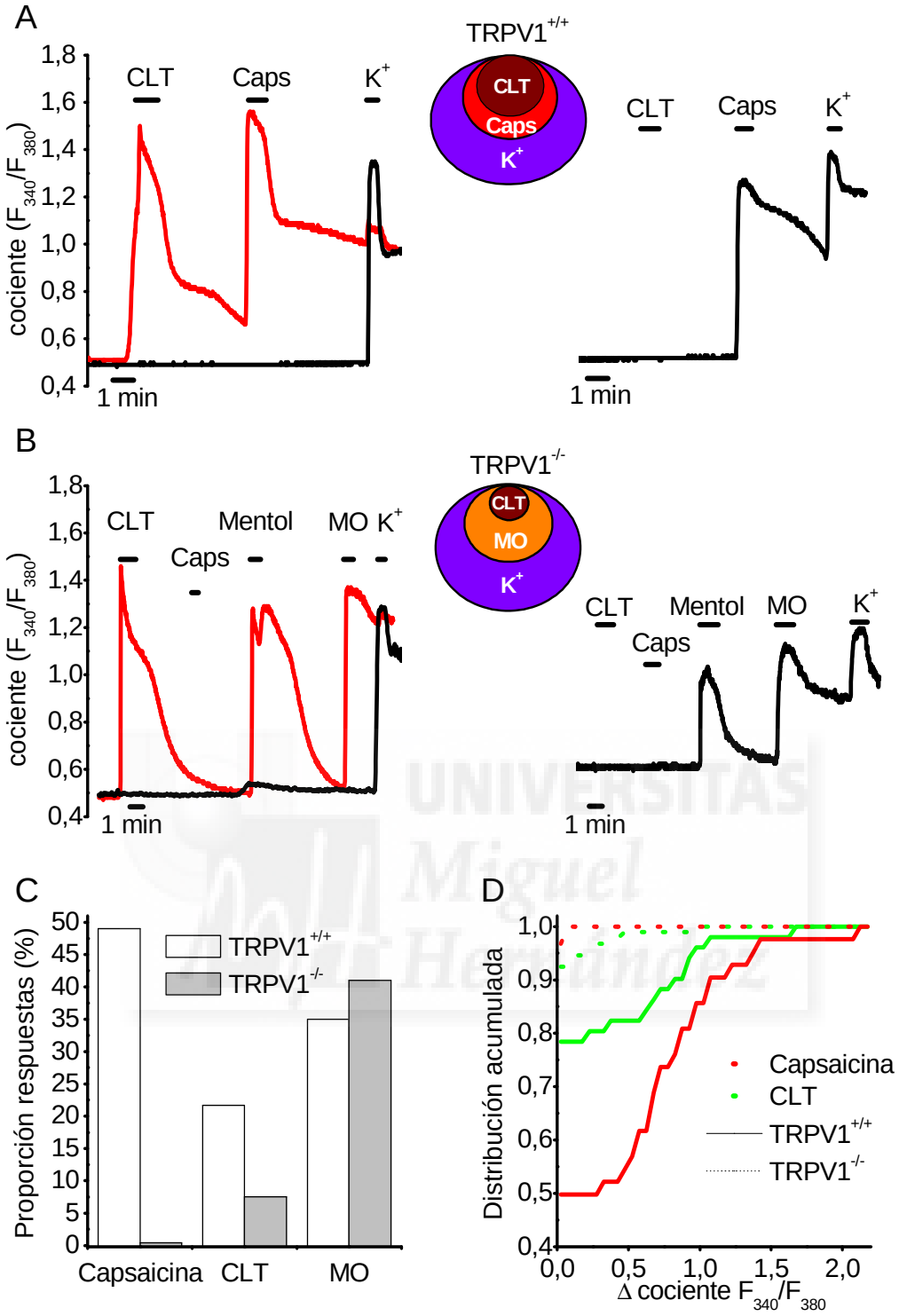

Figura 27. Respuestas a clotrimazol en neuronas trigeminales de ratón. **A.** Ejemplos del curso temporal de las distintas variaciones de la $[Ca^{2+}]_i$ de neuronas de ratones con genotipo silvestre durante la aplicación de 10 µM de clotrimazol, 1 µM de capsaicina, y 60 mM de K^+. Como se ilustra en el diagrama de círculos, las respuestas a clotrimazol solo se observaron en neuronas que también respondieron a la aplicación de capsaicina. **B.** Ejemplos del curso temporal de las distintas variaciones de la $[Ca^{2+}]_i$ en respuesta a 10 µM de clotrimazol, 1 µM de capsaicina, 100 µM de mentol, 100 µM de MO y 60 mM de K^+ en neuronas (n = 83) de ratones TRPV1$^{-/-}$. Como se ilustra en el diagrama de círculos, las respuestas a clotrimazol se observaron solo en neuronas que respondieron a MO. **C.** Porcentaje de neuronas con genotipo silvestre y TRPV1$^{-/-}$ que respondieron a capsaicina, clotrimazol y MO. **D.** Representación de la probabilidad acumulada de respuesta a 1 µM de capsaicina (rojo) y 10 µM de clotrimazol (verde) en neuronas con genotipo silvestre (linea contínua) y TRPV1$^{-/-}$ (líneas discontínuas).

4.6.2. Efectos del clotrimazol sobre el incremento de la $[Ca^{2+}]_i$ en respuesta a mentol en neuronas de ganglio trigémino

Para estudiar el efecto del clotrimazol sobre la actividad de TRPM8 expresado de forma nativa en neuronas sensoriales del ganglio trigémino, se evocó un incremento de $[Ca^{2+}]_i$ en una subpoblación de neuronas mediante la aplicación de mentol, y sobre esta respuesta se evaluó el efecto del clotrimazol. Al igual que en el sistema de expresión heteróloga descrito anteriormente, la aplicación del clotrimazol produjo una inhibición reversible de la respuesta evocada por mentol (Fig. 28A y B).

Con frecuencia, se ha considerado el mentol como un agonista específico de TRPM8, de manera que una respuesta a esta substancia se ha considerado evidencia firme para la expresión de TRPM8 en neuronas sensoriales primarias. Sin embargo, un trabajo reciente (Karashima et al. 2007), refrendado por otros autores (Fajardo et al. 2008a; Xiao et al. 2008), demostró que esta substancia también activa el canal iónico TRPA1. Por tanto, debido a que el clotrimazol activa TRPA1 e inhibe TRPM8, podría resultar útil para distinguir las respuestas a mentol mediadas por TRPM8 y TRPA1.

Se aislaron neuronas sensoriales de los ganglios trigéminos de ratón adulto y se evaluó el efecto del clotrimazol sobre la concentración de calcio intracelular de dos subpoblaciones distintas en función a su sensibilidad a aceite de mostaza (MO), un agonista de TRPA1 usado para evidenciar la expresión de TRPA1 en neuronas sensoriales primarias *in-vitro*. De este modo se determinó que el clotrimazol inhibe de manera reversible y significativa ($n=15$, $p< 0.01$; prueba T) la respuesta a mentol mediada por TRPM8 en neuronas insensibles a la aplicación de MO (Fig. 28A y B), mientras que se produjeron dos tipos de respuestas al aplicar conjuntamente mentol y clotrimazol en neuronas sensibles a MO y obtenidas a partir de ratones TRPV1 $^{-/-}$ con el fin de evaluar solamente los efectos del clotrimazol mediados por TRPA1 y no por TRPV1. Las neuronas en las que la primera aplicación de mentol produjo un incremento de $[Ca^{2+}]_i$ menor (Δ cociente $F_{340}/F_{380} < 0.3$), la segunda aplicación de mentol se potenció significativamente en presencia del clotrimazol ($n=15$, $p< 0.05$; prueba T), pero no fue así en las neuronas en las que la primera aplicación de mentol evocó un incremento de $[Ca^{2+}]_i$ mayor (Δ cociente $F_{340}/F_{380} > 0.3$), ya que no mostraron

una potenciación significativa de la respuesta a mentol en presencia del clotrimazol (Fig 28C y D).

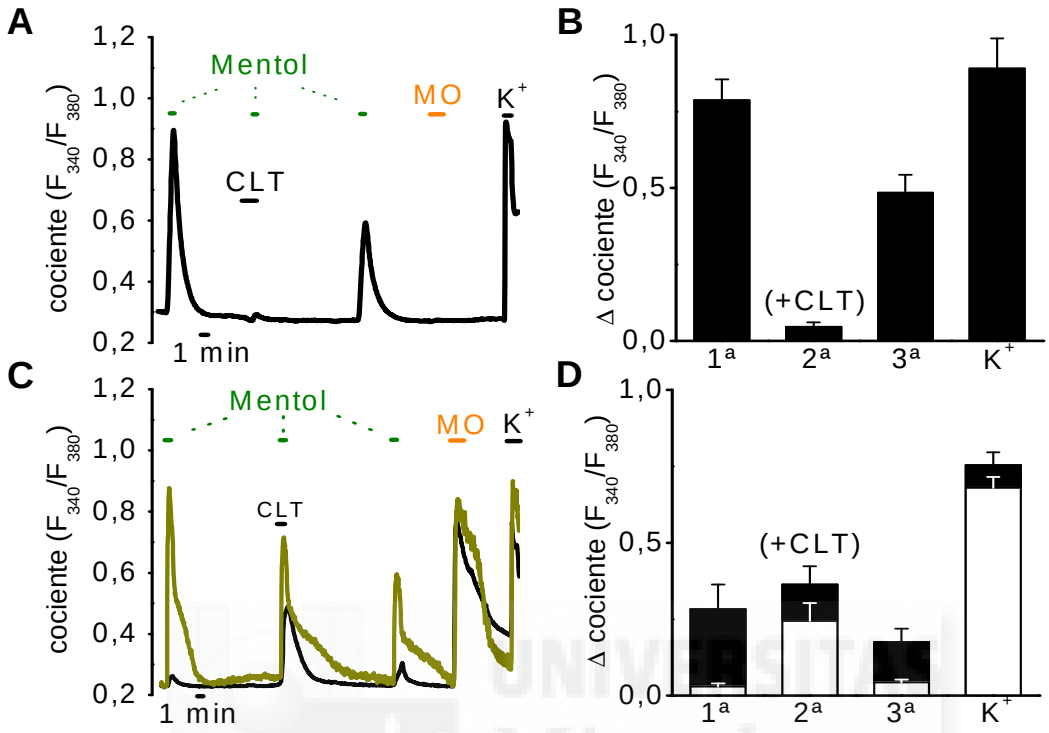

Figura 28. Clotrimazol inhibe la respuesta a mentol mediada por TRPM8 y potencia la mediada por TRPA1 en neuronas de ganglio trigémino. **A.** Ejemplo de la variación de la $[Ca^{2+}]_i$ en respuesta a 100 µM de mentol en neuronas trigeminales que no responden a 100 µM de MO en ausencia y presencia de 10 µM de clotrimazol. **B.** Amplitud media de las respuestas observadas en las neuronas insensibles a la aplicación de MO estudiadas mediante el protocolo mostrado en **A**, ilustrando la inhibición (95 ± 2%) de la respuesta a mentol durante la aplicación del clotrimazol. **C.** El mismo protocolo que en **A**, aplicado sobre neuronas trigeminales de ratones $TRPV1^{-/-}$ sensibles a la aplicación de 100 µM de MO. Se muestran dos trazos, ilustrando dos patrones de respuesta diferentes en estas neuronas. La neurona con una respuesta más pequeña a la primera aplicación de 100 µM de mentol (trazo negro) mostró una respuesta potenciada a la aplicación conjunta de 100 µM de mentol y 10 µM de CLT. Sin embargo, la neurona con una mayor respuesta a la primera aplicación de 100 µM de mentol (trazo gris) no mostró potenciación de la respuesta a la aplicación conjunta de 100 µM de mentol y 10 µM de CLT. **D.** Amplitud media de las respuestas de las neuronas trigeminales de ratones $TRPV1^{-/-}$ sensibles a MO durante la aplicación del protocolo mostrado en **C**.

4.6.3. Efecto de nifedipina sobre la $[Ca^{2+}]_i$ de una subpoblación de neuronas de ganglio trigémino sensibles a MO

La aplicación de 10 μM de nifedipina aumentó la $[Ca^{2+}]_i$ en el 41% de las neuronas ensayadas. Además, la subsiguiente aplicación de 100 μM de MO, un agonista específico de TRPA1, en las mismas neuronas (Fig. 29A), produjo el incremento de la $[Ca^{2+}]_i$ en todas ellas (aunque solo un 77% respondió a ambos agonistas), lo que indica una elevada correlación en la sensibilidad a ambos agonistas.

En una alta proporción (62%) de las neuronas sensibles a nifedipina y MO también se produjo un incremento de la $[Ca^{2+}]_i$ en respuesta a la aplicación de 500 nM de capsaicina, aunque solo un 68% de las neuronas con respuesta a la aplicación de capsaicina respondieron a la aplicación de nifedipina. La co-expresión de TRPV1 y TRPA1 en la misma subpoblación de neuronas sensoriales primarias de ganglios raquídeos y trigéminos había sido descrita en distintos trabajos (Story et al. 2003; Akopian et al. 2007). En la figura 29D se muestra un resumen de las relaciones entre las respuestas a los distintos agonistas mediante la representación de un diagrama de Venn-Euler.

Para comprobar que el incremento de la $[Ca^{2+}]_i$ producido por nifedipina estaba mediado por la activación de TRPA1, se aplicó el mismo protocolo sobre neuronas disociadas a partir de ganglios trigéminos de ratones nulos para TRPA1 (Kwan et al. 2006). Como se muestra en la figura 29C, la aplicación de 10 μM de nifedipina o 100 μM de MO no produjo el incremento de la $[Ca^{2+}]_i$ en ninguna de las neuronas procedentes de los animales $TRPA1^{-/-}$, sin embargo la aplicación de 500 nM de capsaicina evocó un incremento de la $[Ca^{2+}]_i$ con una amplitud (Fig. 29B) y en un porcentaje similar al observado en animales con genotipo silvestre. En las figuras 29 E-G se muestra un resumen de las respuestas a los tres agonistas (nifedipina, MO y capsaicina) mediante histogramas de probabilidad acumulada y en la figura 29H se representan los porcentajes de respuesta.

Estos resultados demuestran que el incremento de la $[Ca^{2+}]_i$ en neuronas sensoriales de los ganglios trigéminos de ratones adultos está mediada exclusivamente por la activación del canal iónico TRPA1.

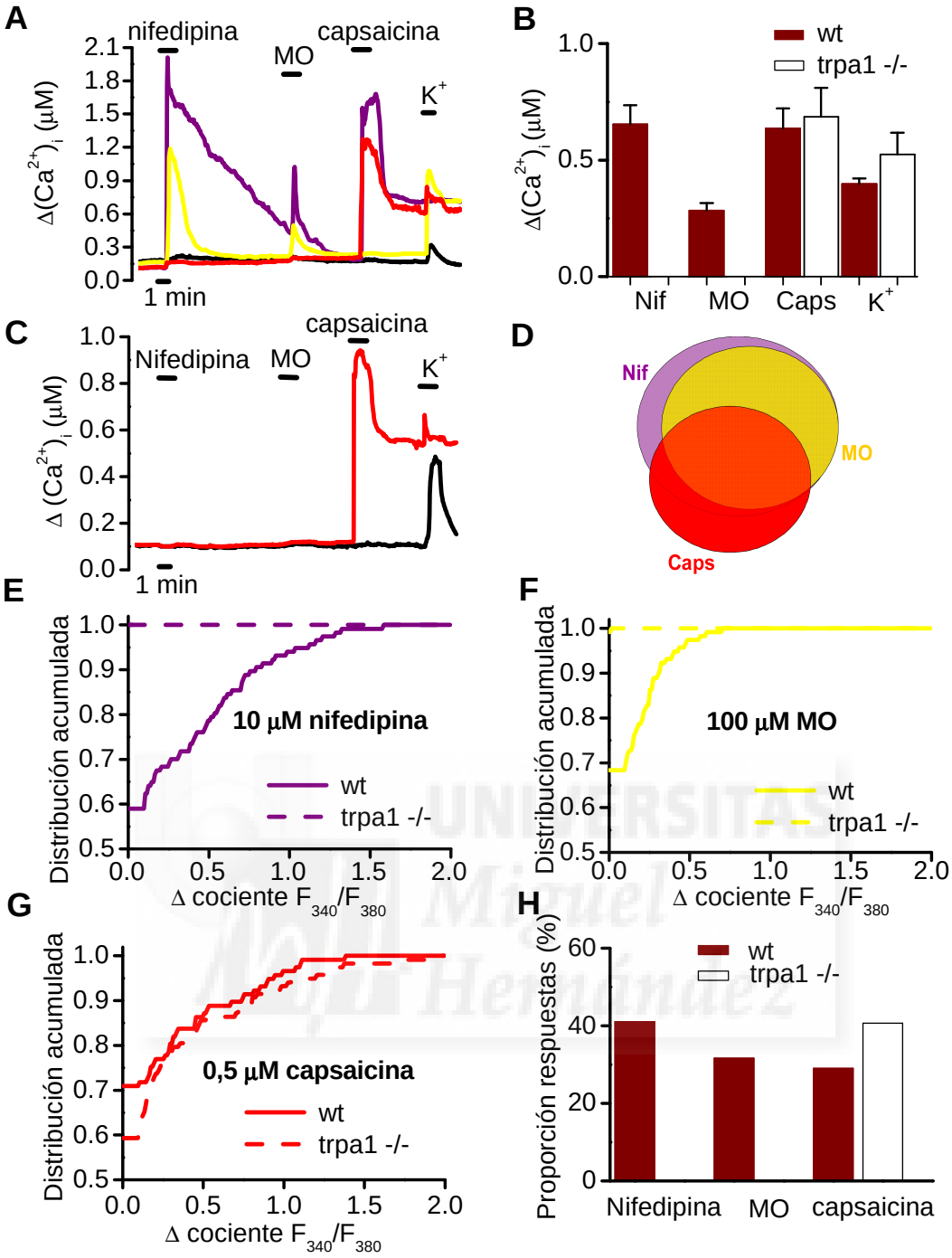

Figura 29. Nifedipina activa canales iónicos TRPA1 en neuronas sensoriales de gánglio trigémino de ratón. **A.** Ejemplo de las variaciones de la $[Ca^{2+}]_i$ en respuesta a la aplicación de 10 μM de nifedipina, 100 μM de aceite de mostaza (MO), 0.5 μM de capsaicina (Caps) y 60 mM de K^+ en neuronas sensoriales de ganglio trigémino (TG) de ratones con genotipo silvestre. Es de destacar que todas las neuronas sensibles a nifedipina también lo fueron a MO. **B.** Incremento medio de la $[Ca^{2+}]_i$ producido por la aplicación de 10 μM de nifedipina, 100 μM de alilisotiocianato (MO), 0.5 μM de capsaicina (Caps) y 60 mM de K^+ en neuronas sensoriales TG. **C.** Variaciones de la $[Ca^{2+}]_i$ en respuesta a la aplicación de 10 μM de nifedipina, 100 μM de alilisotiocianato (MO), 0.5 μM de capsaicina (Caps) y 60 mM de K^+ en neuronas sensoriales de ganglio trigémino (TG) de ratones TRPA1$^{-/-}$. Es de destacar la ausencia de respuestas a nifedipina y MO. **D.** Diagrama de Venn ilustrando el solapamiento en las respuestas a los tres agonistas. **E,F,G.** Distribución acumulada de los incrementos de la $[Ca^{2+}]_i$ en respuesta a la aplicación de 10 μM de nifedipina, 100 μM de MO y 0.5 μM de capsaicina en ratones con genotipo silvestre (líneas continuas) y TRPA1 $^{-/-}$ (líneas discontinuas). **H.** Porcentaje de las neuronas TG que respondieron a la aplicación de nifedipina, MO y capsaicina en ratones con genotipo silvestre y TRPA1 $^{-/-}$.

4.6.4. Efecto del BCTC sobre la $[Ca^{2+}]_i$ evocada por mentol o frío en neuronas sensoriales primarias de ganglio trigémino sensibles a mentol

El canal iónico TRPM8 tiene un patrón de expresión muy limitado en el sistema nervioso, restringiéndose a una subpoblación de neuronas sensoriales primarias de los ganglios trigéminos y raquídeos (McKemy et al. 2002; Peier et al. 2002). La mayor parte de las neuronas que son sensibles a la aplicación de frío también lo son al mentol (Reid et al. 2001; McKemy et al. 2002; Viana et al. 2002; Thut et al. 2003), y además expresan ARN mensajero para la transcripción de TRPM8 (Nealen et al. 2003).

Se estudió el efecto del BCTC sobre el incremento de la $[Ca^{2+}]_i$ en respuesta a la aplicación de 100 µM de mentol o el enfriamiento de la temperatura de la solución externa desde 33-35 °C hasta ~ 18 °C en neuronas de trigémino de cobaya neonato. Como se puede observar en la figura 30, la aplicación de BCTC inhibió completamente ($n=7$, $p<0.001$; prueba T) la señal de calcio inducida por mentol en neuronas sensoriales sensibles al frío (Fig. 30A y B). Además, la aplicación de BCTC inhibió de forma variable el incremento de la $[Ca^{2+}]_i$ evocada por el enfriamiento de la solución extracelular de neuronas sensibles a mentol. De este modo, describimos tres tipos de respuestas. De un total de 20 neuronas, en un 25%, la respuesta a frío fue total y reversiblemente inhibida por BCTC a una concentración de 3 µM, y además, en tres de tres de estas neuronas, la aplicación de mentol a una concentración de 100 µM potenció la respuesta a frío (Fig. 30D). Estos datos sugieren que la respuesta a frío observada en estas neuronas es mediada por TRPM8. En un 20% de las neuronas, la aplicación de la misma concentración de BCTC no inhibió la respuesta a frío, y el mentol no produjo *per se* un incremento de la $[Ca^{2+}]_i$, ni potenció la respuesta a frío (Fig. 30E), lo que sugiere que en estas neuronas la respuesta a frío no es mediada por TRPM8. Por último, en un 55% de las neuronas, la respuesta a frío fue inhibida parcialmente por la aplicación de BCTC, y en cinco de seis de estas neuronas, la aplicación de mentol incrementó la señal de calcio intracelular. En la figura 30C se muestra un resumen de los incrementos medios de la $[Ca^{2+}]_i$ y de la inhibición media que BCTC produce sobre las respuestas a frío ($n=20$, $p<0.01$; prueba T).

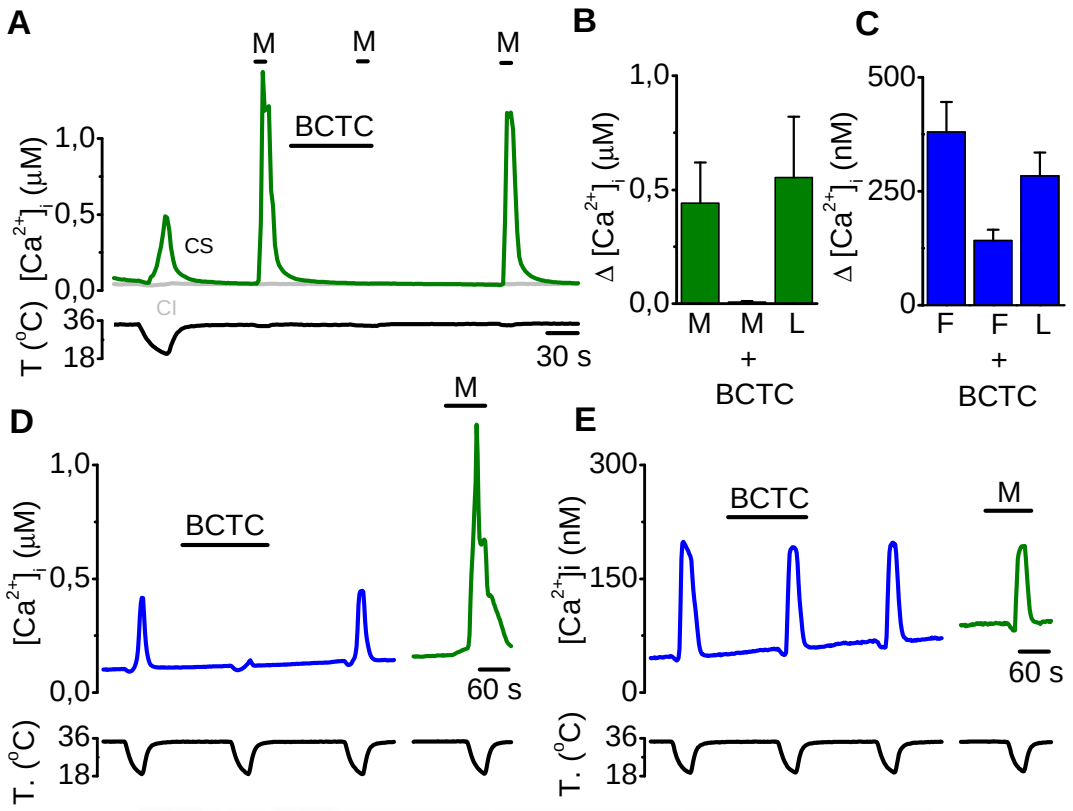

Figura 30. BCTC inhibe el incremento de la $[Ca^{2+}]_i$ inducido por mentol y frío exclusivamente en la subpoblación de neuronas sensibles a mentol de ganglio trigémino de cobaya neonato. **A.** Ejemplos de las variaciones de la $[Ca^{2+}]_i$ en respuesta a la aplicación de 100 µM de mentol (M) en ausencia y presencia de 3 µM de BCTC, y del enfriamiento (F) de la solución extracelular desde 36 ℃ hasta ~18 ℃ (CS: sensible al enfriamie nto; CI: insensible al enfriamiento) **B.** Histograma resumen de los efectos de 3 µM de BCTC en el experimento mostrado en **A**. **D** y **E.** Ejemplos de las variaciones de la $[Ca^{2+}]_i$ en respuesta al enfriamiento de la solución extracelular desde 36 ℃ hasta ~ 18 ℃ en ausencia y presencia de 3 µM de BCTC, y la aplicación de 100 µM de mentol. **C.** Histograma resumen de los efectos de 3 µM de BCTC en los experimentos mostrados en **D** y **E**.

4.7. Efectos del clotrimazol y nifedipina sobre la nocicepción de ratones adultos

Por último, se estudió el posible efecto del clotrimazol, la nifedipina y el BCTC sobre las respuestas nociceptivas, mediante la inyección intraplantar de los compuestos en la pata del tren posterior de ratones adultos. De los resultados anteriores, cabría esperar un efecto proalgésico del clotrimazol y la nifedipina. Para ello se cuantificó el tiempo durante el que los ratones mostraron signos conductuales que se relacionan con la percepción del dolor. Estos signos consistieron en lamidos, batimiento, y retraimiento de la pata inyectada.

La inyección de una solución 0.5% de clotrimazol produjo signos claros de conductas algésicas al generar un mayor tiempo de lamido y batimiento de la pata inyectada frente al producido por la inyección del vehículo. Además, esta

conducta de dolor fue atenuada significativamente al añadir 1 μM de BCTC en la solución de 0.5 % de clotrimazol. En claro contraste, la inyección de 0.5% de clotrimazol en ratones TRPV1$^{-/-}$ no produjo cambios en la conducta respecto a la inyección con vehículo (Fig. 31A).

Estudios previos demostraron que el canal iónico TRPV1 está implicado en la transducción sensorial del calor intenso, y los agentes químicos tanto endógenos como exógenos pueden sensibilizar a TRPV1 en su respuesta al calor, lo que implicaría hiperalgesia térmica *in vivo*. Para investigar si el clotrimazol afecta la sensibilidad de las patas de los ratones al calor intenso, se usó el ensayo de placa caliente (55 ° C) y se midió el tiempo de latencia anterior a la exhibición de signos de huída, como fueron el retraimiento alternativo de las patas o saltos. Las latencias para animales sin inyectar, o inyectados con vehículo, no fueron significativamente diferentes entre los animales con genotipo silvestre (15.4 ± 2.2 s) y los animales TRPV1$^{-/-}$ (13.7 ± 1.1 s; p= 0.50). Estos datos son consistentes con estudios previos (Caterina et al. 2000; Davis et al. 2000). Sin embargo, la inyección de la solución de 0.5% de clotrimazol redujo de forma significativa la latencia de ratones con genotipo silvestre y no tuvo ningún efecto sobre la latencia de ratones TRPV1$^{-/-}$ (Fig. 31B).

Estos datos indican que la inyección del clotrimazol en la pata del ratón produce una conducta de dolor e hiperalgesia térmica que implica la activación de TRPV1.

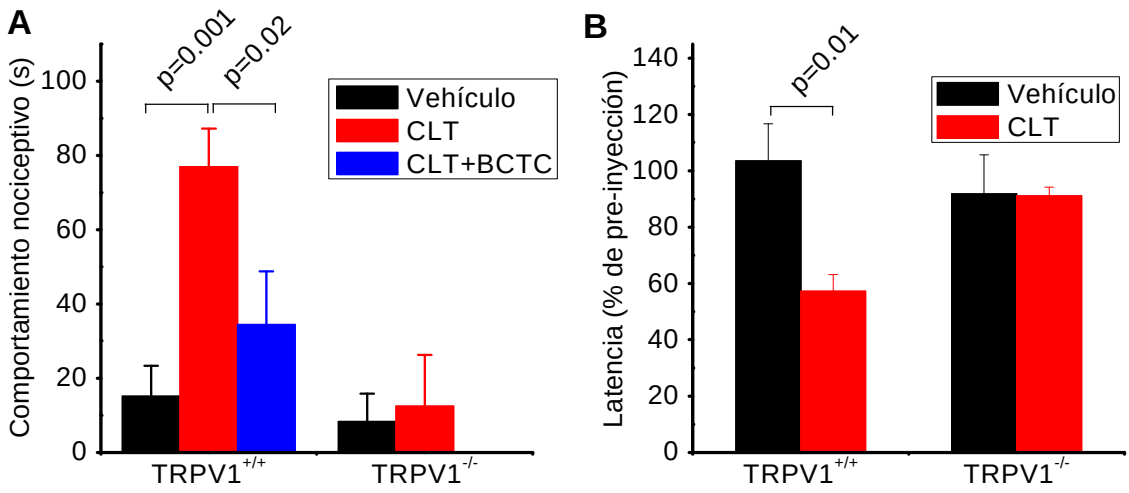

Figura 31. La inyección intraplantar del clotrimazol induce comportamiento nociceptivo e hiperalgesia térmica en ratones. **A.** Duración del comportamiento nociceptivo en los primeros 10 minutos tras la inyección intraplantar del vehículo, CLT, o CLT más BCTC (en ratones con genotipo silvestre y TRPV1$^{-/-}$). **B.** Cambio de la latencia de retirada en el test de la placa caliente (55 ℃), examinado 10-15 minutos después de la inyección intraplantar del vehículo o CLT en ratones con genotipo silvestre y TRPV1$^{-/-}$.

Por último se ensayó el efecto de la nifedipina sobre la conducta del dolor en ratones adultos con genotipo silvestre. En este caso, la inyección de distintas soluciones con 0.1, 1, 10 y 50 mM de nifedipina no se acompañaron de un comportamiento diferente al de la inyección con vehículo. Tampoco se observó un comportamiento diferente respecto del vehículo con la inyección de 100 μM de MO, sin embargo la inyección de 1 mM de MO si que se acompañó de una conducta nociceptiva clara, al mostrar una mayor y significativa duración de los signos de dolor respecto del vehículo. Debido al conocido efecto antagonista de la nifedipina sobre los canales de calcio de tipo L, esta propiedad podría disminuir la excitabilidad periférica e impedir el posible efecto doloroso de la nifedipina a través de la activación de TRPA1. Para contrastar esta hipótesis, se inyectó BAYK8644, un agonista de los canales de calcio de tipo L, además de agonista de TRPA1. En este caso, sí que se produjo un significativo incremento de la duración de los signos de dolor respecto a lo observado con la inyección del vehículo (Fig. 32).

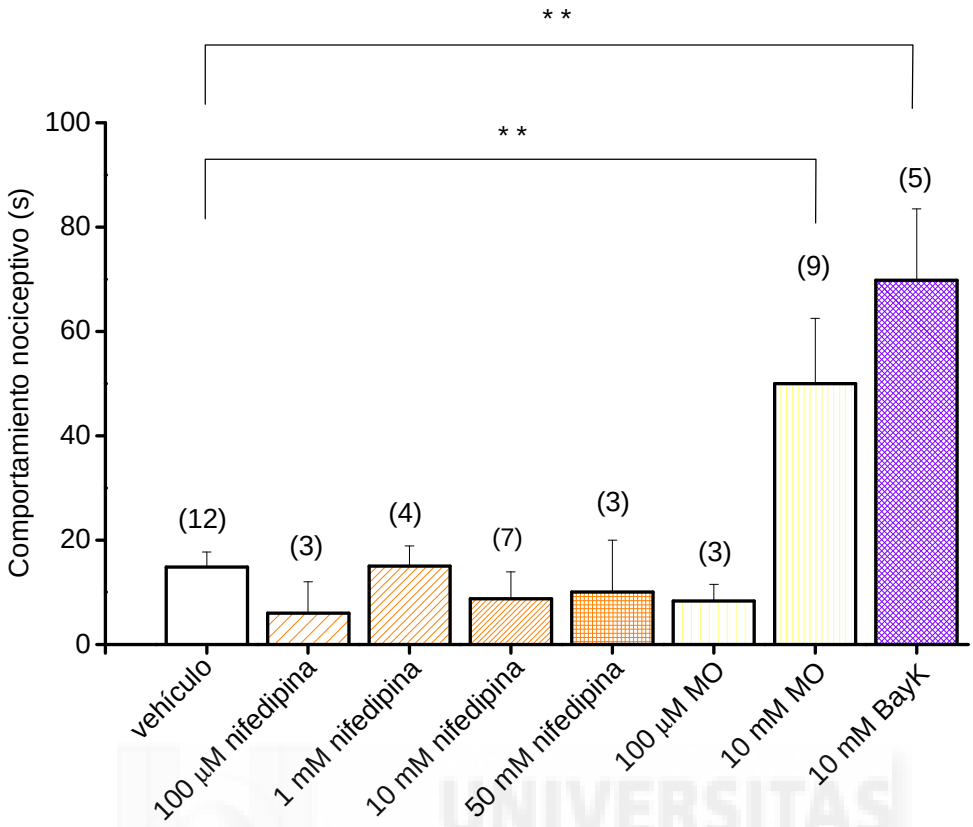

Figura 32. Efecto de la inyección intraplantar de distintos agonistas de TRPA1 sobre conductas nociceptivas. Duración del comportamiento asociado al dolor en los primeros 10 minutos tras la inyección intraplantar del vehículo, diferentes concentraciones de nifedipina (100 μM, 1 mM, 10 mM y 50 mM), dos concentraciones distintas de MO (100 μM y 10 mM) y BayK8644 (10 mM) en ratones con genotipo silvestre. Es de destacar que las inyecciones intraplantares de 10 mM de MO o 10 mM BayK8644 indujeron un claro comportamiento de dolor (** $p<0.01$; prueba T).

UNIVERSITAS
Miguel
Hernández

5 DISCUSIÓN

UNIVERSITAS
Miguel
Hernández

Dado el escaso conocimiento que existe en la actualidad acerca de la farmacología y función de los canales iónicos TRPV1, TRPA1 y TRPM8, resultan de especial relevancia los estudios enfocados a la caracterización de nuevos agonistas y antagonistas farmacológicos. Además de su potencial uso como agentes terapéuticos, pueden tener interés como nuevas herramientas que permitan un mejor conocimiento de su función en el organismo. Además, el análisis detallado de su mecanismo de acción, permite un conocimiento más profundo de las características biofísicas y estructurales de estos tres canales iónicos.

5.1. Efectos de clotrimazol, nifedipina y BCTC sobre la actividad de los canales iónicos termosensibles TRPV1, TRPA1 y TRPM8 expresados de forma heterologa

En este trabajo se describe por primera vez el efecto agonista del compuesto antifúngico clotrimazol sobre los canales iónicos TRPV1 y TRPA1, así como su efecto inhibidor sobre la actividad del canal iónico TRPM8. También se muestra por primera vez el efecto agonista de la nifedipina y del BCTC sobre la actividad del canal iónico TRPA1. Además, se confirma el efecto inhibidor de BCTC sobre la corriente mediada por TRPM8 en respuesta a mentol y frío.

5.1.1. Mecanismo de acción

También se analizó el mecanismo de acción de los fármacos, a través de la caracterización de su efecto sobre la dependencia de voltaje de la apertura de los tres canales iónicos mencionados. Diferentes estudios han mostrado que los estímulos térmicos, además de diversos agentes químicos con capacidad agonista o antagonista, modulan la actividad de determinados canales iónicos de la familia de los TRP, entre ellos TRPV1, TRPM8 y TRPA1 mediante el cambio que producen en la dependencia de voltaje de su actividad (Brauchi et al. 2004; Karashima et al. 2007; Talavera et al. 2005; Voets et al. 2004a; Zurborg et al. 2007). En dos de estos trabajos (Brauchi et al. 2004; Voets et al. 2004a) se muestra como el incremento de la corriente catiónica mediada por TRPM8 en respuesta a frío o a la aplicación de mentol, se debe a que ambos estímulos producen un desplazamiento en la curva de activación de este canal

iónico hacia valores de potencial de membrana más negativos. También se muestra que el incremento de la temperatura o la aplicación de capsaicina en el caso de TRPV1 (Voets et al. 2004a), y del mentol o del Ca^{2+} intracelular, en el caso de TRPA1, desplazan la curva de activación hacia valores de potencial de membrana más negativos o fisiológicos.

En este trabajo, hemos observado que la aplicación de clotrimazol sobre TRPV1 modificó la dependencia de voltaje de este canal iónico, desplazando su curva de activación hacia valores de potencial de membrana más negativos. Esto implica una mayor probabilidad de que TRPV1 esté abierto a potenciales de membrana fisiológicos en presencia del clotrimazol, y explicaría el incremento que produce este compuesto sobre la corriente catiónica mediada por TRPV1. Igualmente, el análisis de las corrientes mediadas por TRPA1 en respuesta a la aplicación de clotrimazol y de nifedipina sobre TRPA1, sugiere un desplazamiento de la curva de activación hacia valores de potencial de membrana más negativos, lo que explicaría el incremento de corriente observado al aplicarlos. Por otro lado, también hemos observado que la aplicación de clotrimazol o BCTC modificó la dependencia de voltaje de TRPM8, desplazando su curva de activación hacia valores de potencial de membrana más positivos. Esto implica una menor probabilidad de que TRPM8 esté abierto a potenciales de membrana fisiológicos en presencia del clotrimazol y del BCTC, y explicaría la inhibición que producen estos compuestos sobre la corriente catiónica mediada por TRPM8.

La idea de que los efectos del clotrimazol, nifedipina y BCTC sobre los canales iónicos termosensibles TRPV1, TRM8 y TRPA1 se acompañen de un cambio de la dependencia de voltaje de activación, es coherente con un mecanismo de apertura dependiente de voltaje y sujeto a modificación por agonistas o antagonistas químicos (Brauchi et al. 2004; Voets et al. 2004a; Karashima et al. 2007; Zurborg et al. 2007).

Se ha descrito que el calcio intracelular es esencial para el efecto agonista de la icilina y el frío sobre el canal iónico TRPA1 (Doerner et al. 2007; Zurborg et al. 2007; Karashima et al. 2009). A diferencia de estos agonistas, la activación de TRPA1 por nifedipina ocurre en ausencia de Ca^{2+} intracelular, al igual que ocurre durante la activación de TRPA1 por mentol (Karashima et al. 2007). Determinados compuestos electrofílicos como son el cinamaldehído, alil

isotiocianato y acroleína activan TRPA1 a través de la modificación covalente de los residuos de cisteína localizados en el extremo N terminal intracelular de esta proteína (Hinman et al. 2006; Macpherson et al. 2007a). En el caso de las 1,4 dihidropiridinas es improbable que el mecanismo de activación implique una unión covalente debido a que no presenta en su estructura grupos reactivos electrófilos, y al igual que la activación de TRPA1 por mentol (Karashima et al. 2007), nuestros datos son consistentes con una modificación de la energía de apertura o cierre del canal, que conlleva el desplazamiento de la curva de activación de TRPA1 en presencia de nifedipina hacia valores de potencial de membrana más negativos.

5.2. Efectos del clotrimazol, nifedipina y BCTC sobre neuronas sensoriales primarias de ganglio trigémino

En neuronas sensoriales primarias el canal iónico TRPA1 co-localiza con TRPV1 en una subpoblación de neuronas peptidérgicas nociceptivas (Story et al. 2003; Jordt et al. 2004; Obata et al. 2005). La aplicación de clotrimazol produjo el incremento de la $[Ca^{2+}]_i$ en una fracción de las neuronas sensibles a capsaicina y/o MO, mientras que el 100% de las células HEK293 que expresaron TRPV1 o TRPA1 respondieron a la misma dosis de clotrimazol en experimentos de imagen de calcio o “patch-clamp”. Estos datos indican que la activación de TRPA1 inducida por el clotrimazol en neuronas de los ganglios trigéminos no siempre es suficiente para generar una señal de calcio detectable, lo cuál podría ser atribuido a una menor eficiencia agonista del clotrimazol comparada con la de capsaicina para activar TRPV1 o MO para activar TRPA1. Además, ambos canales iónicos tienen una activación dependiente de voltaje, por lo que su sensibilidad a estímulos agonistas como el clotrimazol varía en función del potencial de membrana de la neurona. Otro factor que podría determinar la mayor eficiencia del clotrimazol en la generación de una señal de calcio mediada por TRPV1 o TRPA1 en sistemas de expresión heteróloga, comparada con la respuesta observada en neuronas *en cultivo*, sería el hecho de que la excitabilidad de las neuronas sensibles a temperatura está determinada por la contribución relativa de la actividad excitadora o inhibidora de los diferentes canales iónicos presentes en su

membrana (Viana et al. 2002; Madrid et al. 2009). Además, no se puede descartar que las neuronas tengan mecanismos de expulsión del clotrimazol al exterior celular que eviten una activación detectable de TRPV1 y/o TRPA1. Por ejemplo, se ha demostrado que las levaduras que sobreexpresan la proteína MDR1 (Multidrug Resistance 1), que codifica un sistema activo de transporte para compuestos antimicóticos, desarrollan resistencia al clotrimazol (White et al. 2002; Looi et al. 2005).

Existe un alto grado de solapamiento entre los estímulos que activan TRPM8 y TRPA1, como es el caso de los agonistas icilina, frío y mentol (McKemy et al. 2002; Peier et al. 2002; Story et al. 2003; Karashima et al. 2007). Diversos trabajos han usado agonistas específicos de TRPA1, como por ejemplo el MO para identificar funcionalmente la presencia de este canal iónico en las neuronas sensoriales. Desafortunadamente, el efecto de estos compuestos es poco reversible debido a que forman enlaces covalentes durante la activación de TRPA1. Por tanto, el clotrimazol se muestra como una herramienta útil para discernir entre las respuestas mediadas por TRPM8 o TRPA1 ante un mismo estímulo en neuronas sensoriales primarias, dado que como se demuestra en este trabajo, el clotrimazol inhibe la respuesta a mentol mediada por TRPM8 y no modifica o incluso potencia la respuesta a mentol mediada por TRPA1 en neuronas de los ganglios trigéminos. Además los efectos del clotrimazol son rápidos y reversibles.

La aplicación de nifedipina incrementó la concentración de calcio intracelular en una subpoblación de neuronas sensoriales de ganglio trigémino de ratón sensibles a AITC, un agonista específico de TRPA1. Además, no se observó ninguna respuesta a nifedipina en las neuronas de ratones nulos para el gen *trpa1*, lo que indica que el efecto excitador de nifedipina se explica a través de la activación de TRPA1.

En este trabajo se muestra como BCTC activa TRPA1 expresado de forma heteróloga, sin embargo no se observó ninguna respuesta excitadora a BCTC en neuronas sensoriales de ganglio trigémino de ratones neonatos (datos no mostrados). Estos datos son consistentes con un trabajo reciente que muestra que TRPA1 no se expresa de forma funcional hasta aproximadamente el séptimo día postnatal, a diferencia de TRPM8 y TRPV1 que lo hacen desde la fase embrionaria (Hjerling-Leffler et al. 2007).

El mentol se ha usado en los últimos años como agonista específico de TRPM8. Este punto de vista ha cambiado, al demostrarse recientemente que también posee acción agonista sobre TRPA1 (Karashima et al. 2007; Xiao et al. 2008). En este trabajo mostramos como la aplicación de BCTC inhibe completamente la respuesta a mentol de neuronas de trigémino cobaya neonato, y de forma parcial la respuesta a frío en esta población de neuronas sensibles a la aplicación de mentol. Estos resultados son consistentes con los observados en neuronas trigeminales de ratón neonato al aplicar protocolos idénticos (Madrid et al. 2006). Dado que los cobayas y ratones usados fueron menores a siete días postnatales, y a esta edad TRPA1 no se expresa de forma funcional (Hjerling-Leffler et al. 2007) se puede concluir que todas las respuestas a mentol y a frío inhibidas mediante la aplicación de BCTC sobre estas neuronas trigeminales son mediadas por TRPM8. Además, nuestros datos sugieren que la respuesta a frío que no se inhibe en presencia de BCTC estaría mediada por otro u otros mecanismos moleculares adicionales (Maingret et al. 2000; Reid et al. 2001; Viana et al. 2002; Kang et al. 2005; Madrid et al. 2006; Madrid et al. 2009) a la activación de TRPM8 y/o TRPA1.

5.3. Efectos del clotrimazol y nifedipina sobre la nocicepción de ratones adultos

5.3.1. Clotrimazol

La inyección intraplantar del clotrimazol se acompañó de una conducta de dolor en los ratones y además incrementó la sensibilidad de los mismos a la aplicación de estímulos de calor intenso. Estos resultados son consistentes con los que han sido observados tras la inyección de agonistas específicos del canal iónico TRPV1 como por ejemplo la capsaicina y resiniferatoxina (Caterina et al. 2000). Al igual que para capsaicina y resiniferatoxina (Caterina et al. 2000), en este trabajo la administración local de la solución con clotrimazol no se acompañó de conducta de dolor o de hiperalgesia térmica en ratones TRPV1$^{-/-}$. La ausencia de signos visibles de dolor en los ratones TRPV1$^{-/-}$ indica que la iniciación del dolor inducido por la administración del clotrimazol no depende de la activación de TRPA1.

En cuanto a la relevancia clínica de estos compuestos, el clotrimazol tiene un uso muy extendido como medicamento de aplicación tópica, pero aún existe un conocimiento limitado de las bases moleculares de las acciones biológicas de este fármaco. El clotrimazol es un compuesto antimicótico que se usa en un gran número de preparaciones para el tratamiento de infecciones por hongos en la piel, vagina y boca (Sawyer et al. 1975). Generalmente es una sustancia que es bien tolerada por los pacientes, pero en muchos casos la aplicación de preparaciones que contienen el clotrimazol se acompaña de efectos secundarios indeseables tales como irritación y sensación de quemazón en la piel y mucosas (Binet et al. 1994; Del Palacio et al. 2001). El mecanismo molecular que explica el efecto antimicótico del clotrimazol se conoce desde hace años (Hitchcock et al. 1990) y consiste en la inhibición de la actividad de un tipo específico de enzima citocromo P450 presente en hongos e imprescindible para la síntesis de ergosterol, un componente esencial de la membrana plasmática de estos organismos. Por el contrario, no se conocen los mecanismos moleculares que operan bajo los efectos secundarios de la aplicación tópica del clotrimazol. Es bien conocido que los canales iónicos TRPV1 y TRPA1 presentes en neuronas sensoriales primarias están implicados en la detección de estímulos térmicos y de compuestos químicos que conducen a la generación de dolor e irritación (Julius et al. 2001; Clapham 2003; Nilius 2007; Tominaga 2007), lo que conjuntamente con nuestros datos sugiere que la activación de TRPV1 y TRPA1 median los efectos indeseables de la aplicación tópica del clotrimazol. En este trabajo se muestra además que la aplicación conjunta de clotrimazol con BCTC, un antagonista potente de TRPV1, se acompaña de una menor respuesta nociceptora que la observada durante la administración de clotrimazol solo. Estos datos sugieren que el uso de antagonistas específicos de TRPV1, podrían ser útiles en la formulación de nuevas cremas con efectos secundarios más reducidos.

Además, los efectos agonistas del clotrimazol sobre TRPA1 en expresión heteróloga o nativa se producen a concentraciones más altas y al ser aplicado conjuntamente con mentol, lo que ocurre en muchas cremas que contienen el clotrimazol.

Por otro lado, el efecto antagonista del clotrimazol y BCTC sobre TRPM8 tanto en expresión heteróloga como nativa en neuronas de los ganglios trigéminos,

sugiere la posibilidad de su uso en condiciones patológicas como la alodinia por frío y determinados procesos tumorales (Bidaux et al. 2007; Colburn et al. 2007).

5.3.2. Nifedipina

Estudios psicofísicos en humanos indican que los compuestos agonistas de TRPA1 provocan sensación de quemazón y pinchazos que se correlacionan con la activación de nociceptores (Handwerker et al. 1991; Simons et al. 2003), lo que sugiere que este canal iónico está implicado en la transducción del dolor. Sin embargo, a pesar de que la nifedipina activó eficientemente el canal iónico TRPA1, no se observaron signos de conducta nociceptora al ser inyectada en la pata de los ratones. Este resultado es consistente con el menor efecto irritador de la nifedipina en humanos (Schramm et al. 1983) en comparación con el cinamaldehído. Debido a que la nifedipina bloquea corrientes de Ca^{2+} dependientes de voltaje en neuronas sensoriales periféricas (Gover et al. 2003) es posible que el efecto inhibidor de la nifedipina sobre los canales de calcio de tipo L impida la propagación de impulsos eléctricos a pesar de la activación de TRPA1. Por otro lado, el calcio intracelular activa directamente TRPA1 (Doerner et al. 2007; Zurborg et al. 2007), por lo que la inhibición de canales de calcio dependientes de voltaje podría estar restringiendo el flujo de calcio al interior celular y de este modo atenuando la potenciación de la actividad de TRPA1 debida a un ciclo de retroalimentación positiva por la entrada de calcio (Nagata et al. 2005; Doerner et al. 2007; Zurborg et al. 2007; Karashima et al. 2009).

5.4. Posibles implicaciones clínicas de la activación de TRPA1 por 1,4 dihidropiridinas.

Las 1,4 dihidropiridinas son la base estructural de la que derivan numerosos medicamentos usados en clínica para el tratamiento de diferentes afecciones cardiovasculares como la hipertensión y la angina de pecho (Catterall 2000; Triggle 2003) debido a su efecto vasodilatador. Los resultados de este trabajo sugieren que la activación de TRPA1 por 1,4 dihidropiridinas podría ser un mecanismo adicional al conocido efecto inhibidor sobre los canales de calcio de

tipo L. Al respecto, existe el precedente de que otros agonistas de TRPA1 como son el Δ9-tetrahidrocanabiol, la alicina y AITC inducen vasodilatación arterial a través de un mecanismo que implica la activación de TRPA1 (Jordt et al. 2004; Bautista et al. 2005). Además, el tratamiento prolongado con 1,4 dihidropiridinas tiene como efecto adverso la aparición de hiperplasia gingival en un número significativo de pacientes (Ellis et al. 1999). Hasta ahora se desconoce la etiología de este efecto secundario, aunque se sugiere que la inducción mediante agonistas de canales catiónicos no selectivos de una entrada de Ca^{2+} en fibroblastos de las encías podría estar implicada en el desarrollo de esta patología (Hattori et al. 2006). De este modo, la activación de TRPA1 por dihidropiridinas descrita en este trabajo sugiere la posibilidad de su implicación en este crecimiento gingival anormal.

6 CONCLUSIONES

UNIVERSITAS
Miguel
Hernández

Las conclusiones del presente trabajo son:

1. El agente antifúngico clotrimazol produce un incremento de la concentración de calcio intracelular y de las corrientes catiónicas mediadas por los canales iónicos TRPV1 y TRPA1 en sistemas de expresión heteróloga. Además, este efecto agonista se acompaña de un desplazamiento de la curva de activación hacia valores de potencial de membrana más negativos, dentro del rango fisiológico.
2. El clotrimazol incrementa la concentración de calcio intracelular de una subpoblación de neuronas en cultivo procedentes de ganglio trigémino de ratón, a través de la activación de los canales iónicos TRPV1 y TRPA1 expresados de forma nativa.
3. El clotrimazol produce comportamiento de dolor e induce hiperalgesia térmica en el test de dolor por inyección intraplantar y de placa caliente respectivamente, en ratones con genotipo silvestre. La aplicación conjunta del clotrimazol y de BCTC atenúa esta conducta de dolor en estos mismos ratones. Además, la inyección del clotrimazol no produce conducta de dolor ni hiperalgesia térmica en ratones nulos para el gen *trpv1.* Todo ello indica que la activación del canal iónico TRPV1 es responsable de la conducta observada.
4. El clotrimazol inhibe la señal de calcio intracelular e inhibe la corriente catiónica mediada por TRPM8 en respuesta a mentol en sistemas de expresión heteróloga. Este efecto antagonista se acompaña de un desplazamiento de la dependencia de voltaje de activación hacia valores de potencial de membrana más positivos, alejados del rango fisiológico.
5. El clotrimazol inhibe la señal de calcio intracelular en respuesta a mentol y mediada por TRPM8, mientras que no inhibe o potencia la señal de calcio intracelular en respuesta a mentol y mediada por TRPA1 en neuronas en cultivo de ganglio trigémino de ratón adulto.
6. El compuesto químico BCTC inhibe la corriente catiónica mediada por TRPM8 en respuesta a frío y mentol en sistemas de expresión heteróloga. Este efecto antagonista se explicaría por un desplazamiento de la dependencia de voltaje hacia valores de potencial de membrana

más positivos, impidiendo su apertura a valores fisiológicos del potencial de membrana.

7. El BCTC inhibe completamente la señal de calcio intracelular mediada por TRPM8 en respuesta a mentol, y parcialmente a frío, en una subpoblación de neuronas en cultivo sensibles a la aplicación de mentol y procedentes de ganglio trigémino de cobaya neonato.
8. El BCTC produce un incremento de la concentración de calcio intracelular y de la corriente catiónica mediada por el canal iónico TRPA1 en sistemas de expresión heteróloga.
9. Los compuestos químicos SKF963565 y 1,10 fenantrolina inhiben la corriente catiónica mediada por TRPM8 en respuesta a frío en sistemas de expresión heteróloga. Este efecto antagonista se acompaña de un desplazamiento de la dependencia de voltaje hacia valores de potencial de membrana más positivos.
10. Los compuestos químicos nifedipina y BAYK8644, dos conocidas 1,4 dihidropiridinas, incrementan la corriente catiónica mediada por TRPA1 en sistemas de expresión heteróloga.
11. La nifedipina incrementa la concentración de calcio intracelular de una subpoblación de neuronas en cultivo procedentes de ganglio trigémino de ratón adulto, a través del canal iónico TRPA1 expresado de forma nativa.
12. La nifedipina no produce comportamiento de dolor en el ensayo de inyección intraplantar, pero el BAYK8644 si, lo que sugiere que el efecto inhibidor de la nifedipina sobre las corrientes de Ca^{2+} dependientes de voltaje en neuronas sensoriales periféricas, neutraliza el posible efecto excitador mediado por la activación de TRPA1 en las mismas neuronas.

7 BIBLIOGRAFÍA

UNIVERSITAS
Miguel
Hernández

1. Abe J, Hosokawa H, Sawada Y, Matsumura K, Kobayashi S (2006) Ca2+-dependent PKC activation mediates menthol-induced desensitization of transient receptor potential M8. Neurosci Lett 397:140-144.

2. Akopian AN, Ruparel NB, Jeske NA, Hargreaves KM (2007) Transient receptor potential TRPA1 channel desensitization in sensory neurons is agonist dependent and regulated by TRPV1-directed internalization. J Physiol 583:175-193.

3. Andersson DA, Chase HW, Bevan S (2004) TRPM8 activation by menthol, icilin, and cold is differentially modulated by intracellular pH. J Neurosci 24:5364-5369.

4. Andersson DA, Nash M, Bevan S (2007) Modulation of the cold-activated channel TRPM8 by lysophospholipids and polyunsaturated fatty acids. J Neurosci 27:3347-3355.

5. Bandell M, Dubin AE, Petrus MJ, Orth A, Mathur J, Hwang SW, Patapoutian A (2006) High-throughput random mutagenesis screen reveals TRPM8 residues specifically required for activation by menthol. Nat Neurosci 9:493-500.

6. Bandell M, Story GM, Hwang SW, Viswanath V, Eid SR, Petrus MJ, Earley TJ, Patapoutian A (2004) Noxious cold ion channel TRPA1 is activated by pungent compounds and bradykinin. Neuron 41:849-857.

7. Bang S, Kim KY, Yoo S, Kim YG, Hwang SW (2007) Transient receptor potential A1 mediates acetaldehyde-evoked pain sensation. Eur J Neurosci 26:2516-2523.

8. Basbaum AI, Jessell T (2004) The Perception of Pain. En: Principles of Neural Sciences 4/e (Kandel E, Schwartz J, Jessell T, eds), pp 372-392. New York: McGraw-Hill.

9. Bautista DM, Jordt SE, Nikai T, Tsuruda PR, Read AJ, Poblete J, Yamoah EN, Basbaum AI, Julius D (2006) TRPA1 mediates the inflammatory actions of environmental irritants and proalgesic agents. Cell 124:1269-1282.

10. Bautista DM, Movahed P, Hinman A, Axelsson HE, Sterner O, Hogestatt ED, Julius D, Jordt SE, Zygmunt PM (2005) Pungent products from garlic activate the sensory ion channel TRPA1. Proc Natl Acad Sci U S A 102:12248-12252.

11. Bautista DM, Siemens J, Glazer JM, Tsuruda PR, Basbaum AI, Stucky CL, Jordt SE, Julius D (2007) The menthol receptor TRPM8 is the principal detector of environmental cold. Nature 448:204-208.

12. Behrendt HJ, Germann T, Gillen C, Hatt H, Jostock R (2004) Characterization of the mouse cold-menthol receptor TRPM8 and

vanilloid receptor type-1 VR1 using a fluorometric imaging plate reader (FLIPR) assay. Br J Pharmacol 141:737-745.

13. Belmonte C, Viana F (2008) Molecular and cellular limits to somatosensory specificity. Mol Pain 4:14.

14. Bhave G, Hu HJ, Glauner KS, Zhu W, Wang H, Brasier DJ, Oxford GS, Gereau RW (2003) Protein kinase C phosphorylation sensitizes but does not activate the capsaicin receptor transient receptor potential vanilloid 1 (TRPV1). Proc Natl Acad Sci U S A 100:12480-12485.

15. Bhave G, Zhu W, Wang H, Brasier DJ, Oxford GS, Gereau RW (2002) cAMP-dependent protein kinase regulates desensitization of the capsaicin receptor (VR1) by direct phosphorylation. Neuron 35:721-731.

16. Bidaux G, Flourakis M, Thebault S, Zholos A, Beck B, Gkika D, Roudbaraki M, Bonnal JL, Mauroy B, Shuba Y, Skryma R, Prevarskaya N (2007) Prostate cell differentiation status determines transient receptor potential melastatin member 8 channel subcellular localization and function. J Clin Invest 117:1647-1657.

17. Bilmen JG, Michelangeli F (2002) Inhibition of the type 1 inositol 1,4,5-trisphosphate receptor by 2-aminoethoxydiphenylborate. Cell Signal 14:955-960.

18. Binet O, Soto-Melo J, Delgadillo J, Videla S, Izquierdo I, Forn J (1994) Flutrimazole 1% dermal cream in the treatment of dermatomycoses: a randomized, multicentre, double-blind, comparative clinical trial with 1% clotrimazole cream. Flutrimazole Study Group. Mycoses 37:455-459.

19. Bodding M, Wissenbach U, Flockerzi V (2007) Characterisation of TRPM8 as a pharmacophore receptor. Cell Calcium 42:618-628.

20. Brauchi S, Orio P, Latorre R (2004) Clues to understanding cold sensation: thermodynamics and electrophysiological analysis of the cold receptor TRPM8. Proc Natl Acad Sci U S A 101:15494-15499.

21. Brauchi S, Orta G, Salazar M, Rosenmann E, Latorre R (2006) A hot-sensing cold receptor: C-terminal domain determines thermosensation in transient receptor potential channels. J Neurosci 26:4835-4840.

22. Caterina MJ, Julius D (2001) The vanilloid receptor: a molecular gateway to the pain pathway. Annu Rev Neurosci 24:487-517.

23. Caterina MJ, Leffler A, Malmberg AB, Martin WJ, Trafton J, Petersen-Zeitz KR, Koltzenburg M, Basbaum AI, Julius D (2000) Impaired nociception and pain sensation in mice lacking the capsaicin receptor. Science 288:306-313.

24. Caterina MJ, Rosen TA, Tominaga M, Brake AJ, Julius D (1999) A capsaicin-receptor homologue with a high threshold for noxious heat. Nature 398:436-441.

25. Caterina MJ, Schumacher MA, Tominaga M, Rosen TA, Levine JD, Julius D (1997) The capsaicin receptor: a heat-activated ion channel in the pain pathway. Nature 389:816-824.

26. Catterall WA (2000) Structure and regulation of voltage-gated Ca2+ channels. Annu Rev Cell Dev Biol 16:521-555.

27. Cesare P, McNaughton P (1996) A novel heat-activated current in nociceptive neurons and its sensitization by bradykinin. Proc Natl Acad Sci U S A 93:15435-15439.

28. Cesare P, Moriondo A, Vellani V, McNaughton PA (1999) Ion channels gated by heat. Proc Natl Acad Sci U S A 96:7658-7663.

29. Chuang HH, Neuhausser WM, Julius D (2004) The super-cooling agent icilin reveals a mechanism of coincidence detection by a temperature-sensitive TRP channel. Neuron 43:859-869.

30. Chuang HH, Prescott ED, Kong H, Shields S, Jordt SE, Basbaum AI, Chao MV, Julius D (2001) Bradykinin and nerve growth factor release the capsaicin receptor from PtdIns(4,5)P2-mediated inhibition. Nature 411:957-962.

31. Chung MK, Guler AD, Caterina MJ (2005) Biphasic currents evoked by chemical or thermal activation of the heat-gated ion channel, TRPV3. J Biol Chem 280:15928-15941.

32. Chung MK, Lee H, Mizuno A, Suzuki M, Caterina MJ (2004) 2-aminoethoxydiphenyl borate activates and sensitizes the heat-gated ion channel TRPV3. J Neurosci 24:5177-5182.

33. Clapham DE (2003) TRP channels as cellular sensors. Nature 426:517-524.

34. Clapham DE (2009) Transient Receptor Potential (TRP) Channels. En: Encyclopedia of Neuroscience (Squire LR, ed), pp 1109-1131. Oxford: Academic Press.

35. Colburn RW, Lubin ML, Stone DJ, Jr., Wang Y, Lawrence D, D'Andrea MR, Brandt MR, Liu Y, Flores CM, Qin N (2007) Attenuated cold sensitivity in TRPM8 null mice. Neuron 54:379-386.

36. Corey DP, Garcia-Anoveros J, Holt JR, Kwan KY, Lin SY, Vollrath MA, Amalfitano A, Cheung EL, Derfler BH, Duggan A, Geleoc GS, Gray PA, Hoffman MP, Rehm HL, Tamasauskas D, Zhang DS (2004) TRPA1 is a candidate for the mechanosensitive transduction channel of vertebrate hair cells. Nature 432:723-730.

37. Cosens DJ, Manning A (1969) Abnormal electroretinogram from a Drosophila mutant. Nature 224:285-287.

38. Craib SJ, Ellington HC, Pertwee RG, Ross RA (2001) A possible role of lipoxygenase in the activation of vanilloid receptors by anandamide in the guinea-pig bronchus. Br J Pharmacol 134:30-37.

39. Dai Y, Moriyama T, Higashi T, Togashi K, Kobayashi K, Yamanaka H, Tominaga M, Noguchi K (2004) Proteinase-activated receptor 2-mediated potentiation of transient receptor potential vanilloid subfamily 1 activity reveals a mechanism for proteinase-induced inflammatory pain. J Neurosci 24:4293-4299.

40. Dai Y, Wang S, Tominaga M, Yamamoto S, Fukuoka T, Higashi T, Kobayashi K, Obata K, Yamanaka H, Noguchi K (2007) Sensitization of TRPA1 by PAR2 contributes to the sensation of inflammatory pain. J Clin Invest 117:1979-1987.

41. Davis JB, Gray J, Gunthorpe MJ, Hatcher JP, Davey PT, Overend P, Harries MH, Latcham J, Clapham C, Atkinson K, Hughes SA, Rance K, Grau E, Harper AJ, Pugh PL, Rogers DC, Bingham S, Randall A, Sheardown SA (2000) Vanilloid receptor-1 is essential for inflammatory thermal hyperalgesia. Nature 405:183-187.

42. De Petrocellis L., Harrison S, Bisogno T, Tognetto M, Brandi I, Smith GD, Creminon C, Davis JB, Geppetti P, Di M, V (2001) The vanilloid receptor (VR1)-mediated effects of anandamide are potently enhanced by the cAMP-dependent protein kinase. J Neurochem 77:1660-1663.

43. Del PA, Ortiz FJ, Perez A, Pazos C, Garau M, Font E (2001) A double-blind randomized comparative trial: eberconazole 1% cream versus clotrimazole 1% cream twice daily in Candida and dermatophyte skin infections. Mycoses 44:173-180.

44. Dhaka A, Murray AN, Mathur J, Earley TJ, Petrus MJ, Patapoutian A (2007) TRPM8 is required for cold sensation in mice. Neuron 54:371-378.

45. Doerner JF, Gisselmann G, Hatt H, Wetzel CH (2007) Transient receptor potential channel A1 is directly gated by calcium ions. J Biol Chem 282:13180-13189.

46. Dray A (2008) Neuropathic pain: emerging treatments. Br J Anaesth 101:48-58.

47. Ellis JS, Seymour RA, Steele JG, Robertson P, Butler TJ, Thomason JM (1999) Prevalence of gingival overgrowth induced by calcium channel blockers: a community-based study. J Periodontol 70:63-67.

48. Fajardo O, Meseguer V, Belmonte C, Viana F (2008a) TRPA1 channels mediate cold temperature sensing in mammalian vagal sensory neurons: pharmacological and genetic evidence. J Neurosci 28:7863-7875.

49. Fajardo O, Meseguer V, Belmonte C, Viana F (2008b) TRPA1 channels: novel targets of 1,4-dihydropyridines. Channels (Austin) 2:429-438.

50. Fearon IM, Ball SG, Peers C (2000) Clotrimazole inhibits the recombinant human cardiac L-type Ca2+ channel alpha 1C subunit. Br J Pharmacol 129:547-554.

51. Fields HL (1987) Pain. pp 354. New York: McGraw-Hill.

52. Fujita F, Moriyama T, Higashi T, Shima A, Tominaga M (2007) Methyl p-hydroxybenzoate causes pain sensation through activation of TRPA1 channels. Br J Pharmacol 151:153-160.

53. Garcia-Anoveros J, Nagata K (2007) TRPA1. Handb Exp Pharmacol 347-362.

54. Gavva NR, Klionsky L, Qu Y, Shi L, Tamir R, Edenson S, Zhang TJ, Viswanadhan VN, Toth A, Pearce LV, Vanderah TW, Porreca F, Blumberg PM, Lile J, Sun Y, Wild K, Louis JC, Treanor JJ (2004) Molecular determinants of vanilloid sensitivity in TRPV1. J Biol Chem 279:20283-20295.

55. Gover TD, Kao JP, Weinreich D (2003) Calcium signaling in single peripheral sensory nerve terminals. J Neurosci 23:4793-4797.

56. Green BG, Schoen KL (2007) Thermal and nociceptive sensations from menthol and their suppression by dynamic contact. Behav Brain Res 176:284-291.

57. Guimaraes M, Jordt SE (2007) TRPA1: A Sensory Channel of Many Talents. En: TRPA1 Ion Channel Function in Sensory Transduction and Cellular Signalling Cascades (Liedtke W, Heller S, eds), pp 151-163. London: CRC Press.

58. Gunthorpe MJ, Harries MH, Prinjha RK, Davis JB, Randall A (2000) Voltage- and time-dependent properties of the recombinant rat vanilloid receptor (rVR1). J Physiol 525 Pt 3:747-759.

59. Hamill OP, Marty A, Neher E, Sakmann B, Sigworth FJ (1981) Improved patch-clamp techniques for high-resolution current recording from cells and cell-free membrane patches. Pflugers Arch 391:85-100.

60. Handwerker HO, Forster C, Kirchhoff C (1991) Discharge patterns of human C-fibers induced by itching and burning stimuli. J Neurophysiol 66:307-315.

61. Hardie RC, Minke B (1992) The trp gene is essential for a light-activated Ca2+ channel in Drosophila photoreceptors. Neuron 8:643-651.

62. Hattori T, Wang PL (2006) Calcium antagonist isradipine-induced calcium influx through nonselective cation channels in human gingival fibroblasts. Eur J Med Res 11:93-96.

63. Henshall SM, Afar DE, Hiller J, Horvath LG, Quinn DI, Rasiah KK, Gish K, Willhite D, Kench JG, Gardiner-Garden M, Stricker PD, Scher HI,

Grygiel JJ, Agus DB, Mack DH, Sutherland RL (2003) Survival analysis of genome-wide gene expression profiles of prostate cancers identifies new prognostic targets of disease relapse. Cancer Res 63:4196-4203.

64. Hernandez-Benito MJ, Macianskiene R, Sipido KR, Flameng W, Mubagwa K (2001) Suppression of transient outward potassium currents in mouse ventricular myocytes by imidazole antimycotics and by glybenclamide. J Pharmacol Exp Ther 298:598-606.

65. Hill K, McNulty S, Randall AD (2004) Inhibition of TRPM2 channels by the antifungal agents clotrimazole and econazole. Naunyn Schmiedebergs Arch Pharmacol 370:227-237.

66. Hill K, Schaefer M (2007) TRPA1 is differentially modulated by the amphipathic molecules trinitrophenol and chlorpromazine. J Biol Chem 282:7145-7153.

67. Hille B (2001) Ion Channels of Excitable Membranes. Sinauer Associates.

68. Hinman A, Chuang HH, Bautista DM, Julius D (2006) TRP channel activation by reversible covalent modification. Proc Natl Acad Sci U S A 103:19564-19568.

69. Hitchcock CA, Dickinson K, Brown SB, Evans EG, Adams DJ (1990) Interaction of azole antifungal antibiotics with cytochrome P-450-dependent 14 alpha-sterol demethylase purified from Candida albicans. Biochem J 266:475-480.

70. Hjerling-Leffler J, Alqatari M, Ernfors P, Koltzenburg M (2007) Emergence of functional sensory subtypes as defined by transient receptor potential channel expression. J Neurosci 27:2435-2443.

71. Hofmann T, Chubanov V, Gudermann T, Montell C (2003) TRPM5 is a voltage-modulated and Ca(2+)-activated monovalent selective cation channel. Curr Biol 13:1153-1158.

72. Howard J, Bechstedt S (2004) Hypothesis: a helix of ankyrin repeats of the NOMPC-TRP ion channel is the gating spring of mechanoreceptors. Curr Biol 14:R224-R226.

73. Hu HZ, Gu Q, Wang C, Colton CK, Tang J, Kinoshita-Kawada M, Lee LY, Wood JD, Zhu MX (2004) 2-aminoethoxydiphenyl borate is a common activator of TRPV1, TRPV2, and TRPV3. J Biol Chem 279:35741-35748.

74. Hwang SW, Cho H, Kwak J, Lee SY, Kang CJ, Jung J, Cho S, Min KH, Suh YG, Kim D, Oh U (2000) Direct activation of capsaicin receptors by products of lipoxygenases: endogenous capsaicin-like substances. Proc Natl Acad Sci U S A 97:6155-6160.

75. Jaquemar D, Schenker T, Trueb B (1999) An ankyrin-like protein with transmembrane domains is specifically lost after oncogenic transformation of human fibroblasts. J Biol Chem 274:7325-7333.

76. Jensen BS, Strobaek D, Olesen SP, Christophersen P (2001) The Ca2+-activated K+ channel of intermediate conductance: a molecular target for novel treatments? Curr Drug Targets 2:401-422.

77. Jin X, Morsy N, Winston J, Pasricha PJ, Garrett K, Akbarali HI (2004) Modulation of TRPV1 by nonreceptor tyrosine kinase, c-Src kinase. Am J Physiol Cell Physiol 287:C558-C563.

78. Jordt SE, Bautista DM, Chuang HH, McKemy DD, Zygmunt PM, Hogestatt ED, Meng ID, Julius D (2004) Mustard oils and cannabinoids excite sensory nerve fibres through the TRP channel ANKTM1. Nature 427:260-265.

79. Jordt SE, Julius D (2002) Molecular basis for species-specific sensitivity to "hot" chili peppers. Cell 108:421-430.

80. Jordt SE, McKemy DD, Julius D (2003) Lessons from peppers and peppermint: the molecular logic of thermosensation. Curr Opin Neurobiol 13:487-492.

81. Julius D, Basbaum AI (2001) Molecular mechanisms of nociception. Nature 413:203-210.

82. Jung J, Shin JS, Lee SY, Hwang SW, Koo J, Cho H, Oh U (2004) Phosphorylation of vanilloid receptor 1 by Ca2+/calmodulin-dependent kinase II regulates its vanilloid binding. J Biol Chem 279:7048-7054.

83. Kang D, Choe C, Kim D (2005) Thermosensitivity of the two-pore domain K+ channels TREK-2 and TRAAK. J Physiol 564:103-116.

84. Karashima Y, Damann N, Prenen J, Talavera K, Segal A, Voets T, Nilius B (2007) Bimodal action of menthol on the transient receptor potential channel TRPA1. J Neurosci 27:9874-9884.

85. Karashima Y, Prenen J, Meseguer V, Owsianik G, Voets T, Nilius B (2008) Modulation of the transient receptor potential channel TRPA1 by phosphatidylinositol 4,5-biphosphate manipulators. Pflugers Arch 457:77-89.

86. Karashima Y, Talavera K, Everaerts W, Janssens A, Kwan KY, Vennekens R, Nilius B, Voets T (2009) TRPA1 acts as a cold sensor in vitro and in vivo. Proc Natl Acad Sci U S A 106:1273-1278.

87. Katsura H, Obata K, Mizushima T, Yamanaka H, Kobayashi K, Dai Y, Fukuoka T, Tokunaga A, Sakagami M, Noguchi K (2006) Antisense knock down of TRPA1, but not TRPM8, alleviates cold hyperalgesia after spinal nerve ligation in rats. Exp Neurol 200:112-123.

88. Khairatkar-Joshi N, Szallasi A (2009) TRPV1 antagonists: the challenges for therapeutic targeting. Trends Mol Med 15:14-22.

89. Kim D, Cavanaugh EJ (2007) Requirement of a soluble intracellular factor for activation of transient receptor potential A1 by pungent chemicals: role of inorganic polyphosphates. J Neurosci 27:6500-6509.

90. Kim D, Cavanaugh EJ, Simkin D (2008) Inhibition of transient receptor potential A1 channel by phosphatidylinositol-4,5-bisphosphate. Am J Physiol Cell Physiol 295:C92-C99.

91. Kwan KY, Allchorne AJ, Vollrath MA, Christensen AP, Zhang DS, Woolf CJ, Corey DP (2006) TRPA1 contributes to cold, mechanical, and chemical nociception but is not essential for hair-cell transduction. Neuron 50:277-289.

92. LaMotte RH, Campbell JN (1978) Comparison of responses of warm and nociceptive C-fiber afferents in monkey with human judgments of thermal pain. J Neurophysiol 41:509-528.

93. Lee G, Abdi K, Jiang Y, Michaely P, Bennett V, Marszalek PE (2006) Nanospring behaviour of ankyrin repeats. Nature 440:246-249.

94. Liman ER (2006) Thermal gating of TRP ion channels: food for thought? Sci STKE 2006:e12.

95. Lishko PV, Procko E, Jin X, Phelps CB, Gaudet R (2007) The ankyrin repeats of TRPV1 bind multiple ligands and modulate channel sensitivity. Neuron 54:905-918.

96. Liu B, Qin F (2005) Functional control of cold- and menthol-sensitive TRPM8 ion channels by phosphatidylinositol 4,5-bisphosphate. J Neurosci 25:1674-1681.

97. Liu L, Lo Y, Chen I, Simon SA (1997) The responses of rat trigeminal ganglion neurons to capsaicin and two nonpungent vanilloid receptor agonists, olvanil and glyceryl nonamide. J Neurosci 17:4101-4111.

98. Liu L, Simon SA (1996a) Similarities and differences in the currents activated by capsaicin, piperine, and zingerone in rat trigeminal ganglion cells. J Neurophysiol 76:1858-1869.

99. Liu Y, Jurman ME, Yellen G (1996b) Dynamic rearrangement of the outer mouth of a K+ channel during gating. Neuron 16:859-867.

100. Looi CY, D' Silva EC, Seow HF, Rosli R, Ng KP, Chong PP (2005) Increased expression and hotspot mutations of the multidrug efflux transporter, CDR1 in azole-resistant Candida albicans isolates from vaginitis patients. FEMS Microbiol Lett 249:283-289.

101. Louis SM, Jamieson A, Russell NJ, Dockray GJ (1989) The role of substance P and calcitonin gene-related peptide in neurogenic plasma extravasation and vasodilatation in the rat. Neuroscience 32:581-586.

102. Lukacs V, Thyagarajan B, Varnai P, Balla A, Balla T, Rohacs T (2007) Dual regulation of TRPV1 by phosphoinositides. J Neurosci 27:7070-7080.

103. Macpherson LJ, Dubin AE, Evans MJ, Marr F, Schultz PG, Cravatt BF, Patapoutian A (2007a) Noxious compounds activate TRPA1 ion channels through covalent modification of cysteines. Nature 445:541-545.

104. Macpherson LJ, Geierstanger BH, Viswanath V, Bandell M, Eid SR, Hwang S, Patapoutian A (2005) The pungency of garlic: activation of TRPA1 and TRPV1 in response to allicin. Curr Biol 15:929-934.

105. Macpherson LJ, Xiao B, Kwan KY, Petrus MJ, Dubin AE, Hwang S, Cravatt B, Corey DP, Patapoutian A (2007b) An ion channel essential for sensing chemical damage. J Neurosci 27:11412-11415.

106. Madrid R, de la PE, Donovan-Rodriguez T, Belmonte C, Viana F (2009) Variable threshold of trigeminal cold-thermosensitive neurons is determined by a balance between TRPM8 and Kv1 potassium channels. J Neurosci 29:3120-3131.

107. Madrid R, Donovan-Rodriguez T, Meseguer V, Acosta MC, Belmonte C, Viana F (2006) Contribution of TRPM8 channels to cold transduction in primary sensory neurons and peripheral nerve terminals. J Neurosci 26:12512-12525.

108. Maingret F, Lauritzen I, Patel AJ, Heurteaux C, Reyes R, Lesage F, Lazdunski M, Honore E (2000) TREK-1 is a heat-activated background K(+) channel. EMBO J 19:2483-2491.

109. Malkia A, Madrid R, Meseguer V, de la PE, Valero M, Belmonte C, Viana F (2007) Bidirectional shifts of TRPM8 channel gating by temperature and chemical agents modulate the cold sensitivity of mammalian thermoreceptors. J Physiol 581:155-174.

110. Maruyama T, Kanaji T, Nakade S, Kanno T, Mikoshiba K (1997) 2APB, 2-aminoethoxydiphenyl borate, a membrane-penetrable modulator of Ins(1,4,5)P3-induced Ca2+ release. J Biochem 122:498-505.

111. McKemy DD, Neuhausser WM, Julius D (2002) Identification of a cold receptor reveals a general role for TRP channels in thermosensation. Nature 416:52-58.

112. McNamara CR, Mandel-Brehm J, Bautista DM, Siemens J, Deranian KL, Zhao M, Hayward NJ, Chong JA, Julius D, Moran MM, Fanger CM (2007) TRPA1 mediates formalin-induced pain. Proc Natl Acad Sci U S A 104:13525-13530.

113. McNamara FN, Randall A, Gunthorpe MJ (2005) Effects of piperine, the pungent component of black pepper, at the human vanilloid receptor (TRPV1). Br J Pharmacol 144:781-790.

114. Merritt JE, Armstrong WP, Benham CD, Hallam TJ, Jacob R, Jaxa-Chamiec A, Leigh BK, McCarthy SA, Moores KE, Rink TJ (1990) SK&F 96365, a novel inhibitor of receptor-mediated calcium entry. Biochem J 271:515-522.

115. Messeguer A, Planells-Cases R, Ferrer-Montiel A (2006) Physiology and pharmacology of the vanilloid receptor. Curr Neuropharmacol 4:1-15.

116. Montell C, Birnbaumer L, Flockerzi V, Bindels RJ, Bruford EA, Caterina MJ, Clapham DE, Harteneck C, Heller S, Julius D, Kojima I, Mori Y, Penner R, Prawitt D, Scharenberg AM, Schultz G, Shimizu N, Zhu MX (2002) A unified nomenclature for the superfamily of TRP cation channels. Mol Cell 9:229-231.

117. Montell C, Rubin GM (1989) Molecular characterization of the Drosophila trp locus: a putative integral membrane protein required for phototransduction. Neuron 2:1313-1323.

118. Moore ED, Becker PL, Fogarty KE, Williams DA, Fay FS (1990) Ca2+ imaging in single living cells: theoretical and practical issues. Cell Calcium 11:157-179.

119. Mosavi LK, Cammett TJ, Desrosiers DC, Peng ZY (2004) The ankyrin repeat as molecular architecture for protein recognition. Protein Sci 13:1435-1448.

120. Mustafa S, Oriowo M (2005) Cooling-induced contraction of the rat gastric fundus: mediation via transient receptor potential (TRP) cation channel TRPM8 receptor and Rho-kinase activation. Clin Exp Pharmacol Physiol 32:832-838.

121. Nagata K, Duggan A, Kumar G, Garcia-Anoveros J (2005) Nociceptor and hair cell transducer properties of TRPA1, a channel for pain and hearing. J Neurosci 25:4052-4061.

122. Nealen ML, Gold MS, Thut PD, Caterina MJ (2003) TRPM8 mRNA is expressed in a subset of cold-responsive trigeminal neurons from rat. J Neurophysiol 90:515-520.

123. Nilius B (2007) TRP channels in disease. Biochim Biophys Acta 1772:805-812.

124. Nilius B, Talavera K, Owsianik G, Prenen J, Droogmans G, Voets T (2005a) Gating of TRP channels: a voltage connection? J Physiol 567:35-44.

125. Nilius B, Voets T (2005b) TRP channels: a TR(I)P through a world of multifunctional cation channels. Pflugers Arch 451:1-10.

126. Numazaki M, Tominaga T, Takeuchi K, Murayama N, Toyooka H, Tominaga M (2003b) Structural determinant of TRPV1 desensitization interacts with calmodulin. Proc Natl Acad Sci U S A 100:8002-8006.

127. Numazaki M, Tominaga T, Takeuchi K, Murayama N, Toyooka H, Tominaga M (2003a) Structural determinant of TRPV1 desensitization interacts with calmodulin. Proc Natl Acad Sci U S A 100:8002-8006.

128. Obata K, Katsura H, Mizushima T, Yamanaka H, Kobayashi K, Dai Y, Fukuoka T, Tokunaga A, Tominaga M, Noguchi K (2005) TRPA1 induced in sensory neurons contributes to cold hyperalgesia after inflammation and nerve injury. J Clin Invest 115:2393-2401.

129. Okazawa M, Takao K, Hori A, Shiraki T, Matsumura K, Kobayashi S (2002) Ionic basis of cold receptors acting as thermostats. J Neurosci 22:3994-4001.

130. Owsianik G, D'hoedt D, Voets T, Nilius B (2006a) Structure-function relationship of the TRP channel superfamily. Rev Physiol Biochem Pharmacol 156:61-90.

131. Owsianik G, Talavera K, Voets T, Nilius B (2006b) Permeation and selectivity of TRP channels. Annu Rev Physiol 68:685-717.

132. Peier AM, Moqrich A, Hergarden AC, Reeve AJ, Andersson DA, Story GM, Earley TJ, Dragoni I, McIntyre P, Bevan S, Patapoutian A (2002) A TRP channel that senses cold stimuli and menthol. Cell 108:705-715.

133. Peterlin Z, Chesler A, Firestein S (2007) A painful trp can be a bonding experience. Neuron 53:635-638.

134. Petrus M, Peier AM, Bandell M, Hwang SW, Huynh T, Olney N, Jegla T, Patapoutian A (2007) A role of TRPA1 in mechanical hyperalgesia is revealed by pharmacological inhibition. Mol Pain 3:40.

135. Phelps CB, Gaudet R (2007) The role of the N terminus and transmembrane domain of TRPM8 in channel localization and tetramerization. J Biol Chem 282:36474-36480.

136. Popa MO, Lerche H (2006) Cu2+ (1,10 phenanthroline)3 is an open-channel blocker of the human skeletal muscle sodium channel. Br J Pharmacol 147:808-814.

137. Premkumar LS, Ahern GP (2000) Induction of vanilloid receptor channel activity by protein kinase C. Nature 408:985-990.

138. Premkumar LS, Qi ZH, Van BJ, Raisinghani M (2004) Enhancement of potency and efficacy of NADA by PKC-mediated phosphorylation of vanilloid receptor. J Neurophysiol 91:1442-1449.

139. Premkumar LS, Raisinghani M, Pingle SC, Long C, Pimentel F (2005) Downregulation of transient receptor potential melastatin 8 by protein kinase C-mediated dephosphorylation. J Neurosci 25:11322-11329.

140. Prescott ED, Julius D (2003) A modular PIP2 binding site as a determinant of capsaicin receptor sensitivity. Science 300:1284-1288.

141. Prevarskaya N, Zhang L, Barritt G (2007) TRP channels in cancer. Biochim Biophys Acta 1772:937-946.

142. Rathee PK, Distler C, Obreja O, Neuhuber W, Wang GK, Wang SY, Nau C, Kress M (2002) PKA/AKAP/VR-1 module: A common link of Gs-mediated signaling to thermal hyperalgesia. J Neurosci 22:4740-4745.

143. Reichling DB, Levine JD (1997) Heat transduction in rat sensory neurons by calcium-dependent activation of a cation channel. Proc Natl Acad Sci U S A 94:7006-7011.

144. Reid G, Babes A, Pluteanu F (2002a) A cold- and menthol-activated current in rat dorsal root ganglion neurones: properties and role in cold transduction. J Physiol 545:595-614.

145. Reid G, Flonta M (2001) Cold transduction by inhibition of a background potassium conductance in rat primary sensory neurones. Neurosci Lett 297:171-174.

146. Reid G, Flonta ML (2002b) Ion channels activated by cold and menthol in cultured rat dorsal root ganglion neurones. Neurosci Lett 324:164-168.

147. Rohacs T, Lopes CM, Michailidis I, Logothetis DE (2005) PI(4,5)P2 regulates the activation and desensitization of TRPM8 channels through the TRP domain. Nat Neurosci 8:626-634.

148. Rosenbaum T, Gordon-Shaag A, Munari M, Gordon SE (2004) Ca2+/calmodulin modulates TRPV1 activation by capsaicin. J Gen Physiol 123:53-62.

149. Salazar H, Llorente I, Jara-Oseguera A, Garcia-Villegas R, Munari M, Gordon SE, Islas LD, Rosenbaum T (2008) A single N-terminal cysteine in TRPV1 determines activation by pungent compounds from onion and garlic. Nat Neurosci 11:255-261.

150. Sawyer PR, Brogden RN, Pinder RM, Speight TM, Avery (1975) Clotrimazole: a review of its antifungal activity and therapeutic efficacy. Drugs 9:424-447.

151. Schramm M, Thomas G, Towart R, Franckowiak G (1983) Novel dihydropyridines with positive inotropic action through activation of Ca2+ channels. Nature 303:535-537.

152. Schwarz G, Droogmans G, Nilius B (1994) Multiple effects of SK&F 96365 on ionic currents and intracellular calcium in human endothelial cells. Cell Calcium 15:45-54.

153. Simons CT, Carstens MI, Carstens E (2003) Oral irritation by mustard oil: self-desensitization and cross-desensitization with capsaicin. Chem Senses 28:459-465.

154. Stein AT, Ufret-Vincenty CA, Hua L, Santana LF, Gordon SE (2006) Phosphoinositide 3-kinase binds to TRPV1 and mediates NGF-stimulated TRPV1 trafficking to the plasma membrane. J Gen Physiol 128:509-522.

155. Stein RJ, Santos S, Nagatomi J, Hayashi Y, Minnery BS, Xavier M, Patel AS, Nelson JB, Futrell WJ, Yoshimura N, Chancellor MB, De MF (2004) Cool (TRPM8) and hot (TRPV1) receptors in the bladder and male genital tract. J Urol 172:1175-1178.

156. Story GM, Peier AM, Reeve AJ, Eid SR, Mosbacher J, Hricik TR, Earley TJ, Hergarden AC, Andersson DA, Hwang SW, McIntyre P, Jegla T, Bevan S, Patapoutian A (2003) ANKTM1, a TRP-like channel expressed in nociceptive neurons, is activated by cold temperatures. Cell 112:819-829.

157. Szallasi A, Cortright DN, Blum CA, Eid SR (2007) The vanilloid receptor TRPV1: 10 years from channel cloning to antagonist proof-of-concept. Nat Rev Drug Discov 6:357-372.

158. Szolcsanyi J (2004) Forty years in capsaicin research for sensory pharmacology and physiology. Neuropeptides 38:377-384.

159. Szolcsanyi J (1977) A pharmacological approach to elucidation of the role of different nerve fibres and receptor endings in mediation of pain. J Physiol (Paris) 73:251-259.

160. Szolcsanyi J, Szallasi A, Szallasi Z, Joo F, Blumberg PM (1990) Resiniferatoxin: an ultrapotent selective modulator of capsaicin-sensitive primary afferent neurons. J Pharmacol Exp Ther 255:923-928.

161. Takashima Y, Daniels RL, Knowlton W, Teng J, Liman ER, McKemy DD (2007) Diversity in the neural circuitry of cold sensing revealed by genetic axonal labeling of transient receptor potential melastatin 8 neurons. J Neurosci 27:14147-14157.

162. Talavera K, Yasumatsu K, Voets T, Droogmans G, Shigemura N, Ninomiya Y, Margolskee RF, Nilius B (2005) Heat activation of TRPM5 underlies thermal sensitivity of sweet taste. Nature 438:1022-1025.

163. Thut PD, Wrigley D, Gold MS (2003) Cold transduction in rat trigeminal ganglia neurons in vitro. Neuroscience 119:1071-1083.

164. Tominaga M (2007) Nociception and TRP channels. Handb Exp Pharmacol489-505.

165. Tominaga M, Caterina MJ, Malmberg AB, Rosen TA, Gilbert H, Skinner K, Raumann BE, Basbaum AI, Julius D (1998) The cloned capsaicin receptor integrates multiple pain-producing stimuli. Neuron 21:531-543.

166. Toth A, Boczan J, Kedei N, Lizanecz E, Bagi Z, Papp Z, Edes I, Csiba L, Blumberg PM (2005) Expression and distribution of vanilloid receptor 1 (TRPV1) in the adult rat brain. Brain Res Mol Brain Res 135:162-168.

167. Tousova K, Susankova K, Teisinger J, Vyklicky L, Vlachova V (2004) Oxidizing reagent copper-o-phenanthroline is an open channel blocker of the vanilloid receptor TRPV1. Neuropharmacology 47:273-285.

168. Triggle DJ (2003) 1,4-Dihydropyridines as calcium channel ligands and privileged structures. Cell Mol Neurobiol 23:293-303.

169. Tsavaler L, Shapero MH, Morkowski S, Laus R (2001) Trp-p8, a novel prostate-specific gene, is up-regulated in prostate cancer and other malignancies and shares high homology with transient receptor potential calcium channel proteins. Cancer Res 61:3760-3769.

170. Tsuruda PR, Julius D, Minor DL, Jr. (2006) Coiled coils direct assembly of a cold-activated TRP channel. Neuron 51:201-212.

171. Valenzano KJ, Grant ER, Wu G, Hachicha M, Schmid L, Tafesse L, Sun Q, Rotshteyn Y, Francis J, Limberis J, Malik S, Whittemore ER, Hodges D (2003) N-(4-tertiarybutylphenyl)-4-(3-chloropyridin-2-yl)tetrahydropyrazine -1(2H)-carbox-amide (BCTC), a novel, orally effective vanilloid receptor 1 antagonist with analgesic properties: I. in vitro characterization and pharmacokinetic properties. J Pharmacol Exp Ther 306:377-386.

172. Varga A, Bolcskei K, Szoke E, Almasi R, Czeh G, Szolcsanyi J, Petho G (2006) Relative roles of protein kinase A and protein kinase C in modulation of transient receptor potential vanilloid type 1 receptor responsiveness in rat sensory neurons in vitro and peripheral nociceptors in vivo. Neuroscience 140:645-657.

173. Vellani V, Mapplebeck S, Moriondo A, Davis JB, McNaughton PA (2001) Protein kinase C activation potentiates gating of the vanilloid receptor VR1 by capsaicin, protons, heat and anandamide. J Physiol 534:813-825.

174. Venkatachalam K, Montell C (2007) TRP channels. Annu Rev Biochem 76:387-417.

175. Viana F, de la PE, Belmonte C (2002) Specificity of cold thermotransduction is determined by differential ionic channel expression. Nat Neurosci 5:254-260.

176. Vlachova V, Teisinger J, Susankova K, Lyfenko A, Ettrich R, Vyklicky L (2003) Functional role of C-terminal cytoplasmic tail of rat vanilloid receptor 1. J Neurosci 23:1340-1350.

177. Voets T, Droogmans G, Wissenbach U, Janssens A, Flockerzi V, Nilius B (2004a) The principle of temperature-dependent gating in cold- and heat-sensitive TRP channels. Nature 430:748-754.

178. Voets T, Janssens A, Droogmans G, Nilius B (2004b) Outer pore architecture of a Ca2+-selective TRP channel. J Biol Chem 279:15223-15230.

179. Voets T, Nilius B (2003) TRPs make sense. J Membr Biol 192:1-8.

180. Voets T, Owsianik G, Janssens A, Talavera K, Nilius B (2007) TRPM8 voltage sensor mutants reveal a mechanism for integrating thermal and chemical stimuli. Nat Chem Biol 3:174-182.

181. Voets T, Prenen J, Fleig A, Vennekens R, Watanabe H, Hoenderop JG, Bindels RJ, Droogmans G, Penner R, Nilius B (2001) CaT1 and the calcium release-activated calcium channel manifest distinct pore properties. J Biol Chem 276:47767-47770.

182. Vriens J, Watanabe H, Janssens A, Droogmans G, Voets T, Nilius B (2004) Cell swelling, heat, and chemical agonists use distinct pathways for the activation of the cation channel TRPV4. Proc Natl Acad Sci U S A 101:396-401.

183. Wang YY, Chang RB, Waters HN, McKemy DD, Liman ER (2008) The nociceptor ion channel TRPA1 is potentiated and inactivated by permeating calcium ions. J Biol Chem 283:32691-32703.

184. Watanabe H, Vriens J, Suh SH, Benham CD, Droogmans G, Nilius B (2002) Heat-evoked activation of TRPV4 channels in a HEK293 cell expression system and in native mouse aorta endothelial cells. J Biol Chem 277:47044-47051.

185. Weil A, Moore SE, Waite NJ, Randall A, Gunthorpe MJ (2005) Conservation of functional and pharmacological properties in the distantly related temperature sensors TRVP1 and TRPM8. Mol Pharmacol 68:518-527.

186. White TC, Holleman S, Dy F, Mirels LF, Stevens DA (2002) Resistance mechanisms in clinical isolates of Candida albicans. Antimicrob Agents Chemother 46:1704-1713.

187. Williams DA, Fogarty KE, Tsien RY, Fay FS (1985) Calcium gradients in single smooth muscle cells revealed by the digital imaging microscope using Fura-2. Nature 318:558-561.

188. Wissenbach U, Niemeyer BA, Flockerzi V (2004) TRP channels as potential drug targets. Biol Cell 96:47-54.

189. Xiao B, Dubin AE, Bursulaya B, Viswanath V, Jegla TJ, Patapoutian A (2008) Identification of transmembrane domain 5 as a critical molecular determinant of menthol sensitivity in mammalian TRPA1 channels. J Neurosci 28:9640-9651.

190. Xu H, Blair NT, Clapham DE (2005) Camphor activates and strongly desensitizes the transient receptor potential vanilloid subtype 1 channel in a vanilloid-independent mechanism. J Neurosci 25:8924-8937.

191. Xu H, Ramsey IS, Kotecha SA, Moran MM, Chong JA, Lawson D, Ge P, Lilly J, Silos-Santiago I, Xie Y, DiStefano PS, Curtis R, Clapham DE (2002) TRPV3 is a calcium-permeable temperature-sensitive cation channel. Nature 418:181-186.

192. Yang XR, Lin MJ, McIntosh LS, Sham JS (2006) Functional expression of transient receptor potential melastatin- and vanilloid-related channels in pulmonary arterial and aortic smooth muscle. Am J Physiol Lung Cell Mol Physiol 290:L1267-L1276.

193. Zhang L, Jones S, Brody K, Costa M, Brookes SJ (2004) Thermosensitive transient receptor potential channels in vagal afferent neurons of the mouse. Am J Physiol Gastrointest Liver Physiol 286:G983-G991.

194. Zhang X, Huang J, McNaughton PA (2005) NGF rapidly increases membrane expression of TRPV1 heat-gated ion channels. EMBO J 24:4211-4223.

195. Zhang X, Li L, McNaughton PA (2008) Proinflammatory mediators modulate the heat-activated ion channel TRPV1 via the scaffolding protein AKAP79/150. Neuron 59:450-461.

196. Zimmermann M (1983) Ethical guidelines for investigations of experimental pain in conscious animals. Pain 16:109-110.

197. Zurborg S, Yurgionas B, Jira JA, Caspani O, Heppenstall PA (2007) Direct activation of the ion channel TRPA1 by Ca2+. Nat Neurosci 10:277-279.

198. Zygmunt PM, Petersson J, Andersson DA, Chuang H, Sorgard M, Di M, V, Julius D, Hogestatt ED (1999) Vanilloid receptors on sensory nerves mediate the vasodilator action of anandamide. Nature 400:452-457.

8 ANEXO: PUBLICACIONES

UNIVERSITAS
Miguel
Hernández

Cellular/Molecular

Transient Receptor Potential Channels in Sensory Neurons Are Targets of the Antimycotic Agent Clotrimazole

Victor Meseguer,[1,2] Yuji Karashima,[1] Karel Talavera,[1] Dieter D'Hoedt,[1] Tansy Donovan-Rodríguez,[2] Felix Viana,[2] Bernd Nilius,[1] and Thomas Voets[1]

[1]Laboratory of Ion Channel Research, Division of Physiology, Department of Molecular Cell Biology, Campus Gasthuisberg O&N1, KU Leuven, B-3000 Leuven, Belgium, and [2]Instituto de Neurociencias de Alicante, Universidad Miguel Hernández-Consejo Superior de Investigaciones Científicas, 03550 San Juan de Alicante, Spain

Clotrimazole (CLT) is a widely used drug for the topical treatment of yeast infections of skin, vagina, and mouth. Common side effects of topical CLT application include irritation and burning pain of the skin and mucous membranes. Here, we provide evidence that transient receptor potential (TRP) channels in primary sensory neurons underlie these unwanted effects of CLT. We found that clinically relevant CLT concentrations activate heterologously expressed TRPV1 and TRPA1, two TRP channels that act as receptors of irritant chemical and/or thermal stimuli in nociceptive neurons. In line herewith, CLT stimulated a subset of capsaicin-sensitive and mustard oil-sensitive trigeminal neurons, and evoked nocifensive behavior and thermal hypersensitivity with intraplantar injection in mice. Notably, CLT-induced pain behavior was suppressed by the TRPV1-antagonist BCTC [(*N*-(-4-tertiarybutylphenyl)-4-(3-cholorpyridin-2-yl)tetrahydropyrazine-1(2*H*)-carboxamide)] and absent in TRPV1-deficient mice. In addition, CLT inhibited the cold and menthol receptor TRPM8, and blocked menthol-induced responses in capsaicin- and mustard oil-insensitive trigeminal neurons. The concentration for 50% inhibition (IC_{50}) of inward TRPM8 current was ~200 nM, making CLT the most potent known TRPM8 antagonist and a useful tool to discriminate between TRPM8- and TRPA1-mediated responses. Together, our results identify TRP channels in sensory neurons as molecular targets of CLT, and offer means to develop novel CLT preparations with fewer unwanted sensory side effects.

Key words: **TRP channels; sensory neurons; clotrimazole; temperature sensing; pain; chemoreceptor**

Introduction

Clotrimazole (CLT) is an antifungal compound commonly used in over-the-counter medications for the topical treatment of fungal infections of the skin, vagina, and mouth (Sawyer et al., 1975). CLT exerts its antifungal actions by inhibiting P450-dependent enzymes (Hitchcock et al., 1990). Other well known molecular targets of CLT are intermediate conductance Ca^{2+}-activated potassium (IK_{Ca}) channels, including the erythrocyte Gardos channel (KCNN4) (Alvarez et al., 1992); CLT-induced inhibition of the Gardos channel, leading to reduced erythrocyte dehydratation, is a promising therapy in sickle cell disease (Brugnara et al., 1996). In addition, CLT can inhibit cell proliferation *in vitro* and *in vivo*, which has been ascribed to a CLT-induced depletion of intracellular Ca^{2+} stores and blockade of store-dependent Ca^{2+} influx (Benzaquen et al., 1995). As such, CLT and related substances have potential as antiproliferative and antimetastatic agents for the treatment of various human diseases.

Received March 20, 2007; revised Nov. 23, 2007; accepted Nov. 26, 2007.

This work was supported by grants from the Human Frontiers Science Program (RGP32/2004), the Belgian Federal Government (IUAP P5/05), the Research Foundation-Flanders (G.0172.03; G.0565.07), the Research Council of the KU Leuven (GOA 2004/07; EF/95/010), the Spanish Minsitry of Education (SAF2004-01011), the Generalitat Valenciana Predoctoral Fellowship Program (CTBPRB/2003/151), and the Fundación Marcelino Botín. We thank the members of our laboratories for helpful discussions, and J. Prenen and A. Janssens for technical assistance.

Correspondence should be addressed to Thomas Voets at the above address. E-mail: thomas.voets@med.kuleuven.be.

DOI:10.1523/JNEUROSCI.4772-07.2008

 0270-6474/08/280576-11$15.00/0

Although mostly well tolerated, a significant fraction of patients using topical CLT experience side effects such as irritation and burning of the skin and mucous membranes (Binet et al., 1994; del Palacio et al., 2001). Moreover, oral CLT has been reported to induce nausea, gastrointestinal disturbances, and altered taste sensations in some patients (Sawyer et al., 1975; Koletar et al., 1990). The mechanisms underlying these unwanted side effects of CLT are still not well understood.

The transient receptor potential (TRP) superfamily is a large group of cation channels that play a general role as cellular sensors (Clapham, 2003; Voets et al., 2005; Nilius et al., 2007). Several TRP channels members are involved in the detection of thermal, mechanical and chemical stimuli, and in the initiation of irritation and pain caused by such stimuli (Julius and Basbaum, 2001; Voets et al., 2005; Tominaga, 2007). In this study, we identify TRP channels in sensory neurons as novel sensitive targets of CLT. We demonstrate that CLT is an agonist of TRPV1 and TRPA1, two TRP channels involved in the detection of noxious physical and chemical stimuli by nociceptors (Caterina et al., 1997; Caterina et al., 2000; Davis et al., 2000; Story et al., 2003; Bautista et al., 2005; Nagata et al., 2005; Bautista et al., 2006; Kwan et al., 2006), a potent antagonist of TRPM8, an important sensor of environmental cold and of cooling substances such as menthol (McKemy et al., 2002; Peier et al., 2002a; Bautista et al., 2007; Colburn et al., 2007; Dhaka et al., 2007; Voets et al., 2007b). Moreover, we show that intraplantar injection of CLT evokes

nocifensive behavior and thermal hyperalgesia in mice, which can be attenuated by pharmacological inhibition or genetic ablation of TRPV1.

Materials and Methods

Cell cultures and gene expression. Human embryonic kidney 293 (HEK293) cells were grown in DMEM containing 10% (v/v) fetal calf serum, 4 mM L-alanyl-L-glutamine, 100 U ml^{-1} penicillin and 100 μg ml^{-1} streptomycin at 37°C in a humidity-controlled incubator with 10% CO_2. Cells were transiently transfected with human TRPM8, human TRPV1 or mouse TRPA1 cloned in the bicistronic pCAGGS-IRES-GFP vector using TransIT-293 transfection reagent (Mirus, Madison, WI). In some experiments, we also used a tetracycline-inducible system for expression of mouse TRPA1 in Chinese hamster ovary (CHO) cells, as described previously (Story et al., 2003).

Trigeminal ganglion neurons from adult mice (postnatal months 1–3) were cultured as described previously (Madrid et al., 2006). In brief, mice were killed by inhalation of 100% CO_2 followed by rapid decapitation. After removal, ganglia were cut in small pieces and incubated for 45 min at 37°C in a dissociation solution containing (in mM) 155 NaCl, 1.5 K_2HPO_4, 5.6 HEPES, 4.8 Na-HEPES, and 5 glucose. The solution also contained 0.07% collagenase type XI (Sigma, St. Louis, MO) and 0.3% dispase (Invitrogen, Carlsbad, CA). After incubation, tissue fragments were gently triturated with a fire-polished glass pipette, and the resultant suspension was centrifuged at 1700 rpm for 10 min. The pellet obtained was resuspended and cultured in a medium containing: 89% minimum essential medium (MEM), 10% fetal calf serum supplemented with 1% MEM vitamins (Invitrogen), 100 μg/ml penicillin/streptomycin, and nerve growth factor (NGF; mouse 7S, 100 ng/ml; Sigma). Cells were plated on poly-L-Lysine-coated glass coverslips and used after 1 d in culture. *TRPV1* $^{-/-}$ mice (stock number 003770) (see Caterina et al., 2000) were purchased from The Jackson Laboratory (Bar Harbor, ME).

Measurement of the intracellular $[Ca^{2+}]_i$. Cells were incubated with 2 μM Fura-2 AM ester for 30 min at 37°C. Intracellular Ca^{2+} concentration ($[Ca^{2+}]_i$) was measured on a monochromator-based imaging system consisting of a Polychome IV monochromator (Till Photonics, Martinsried, Germany) and a Roper Scientific (Tucson, AZ) CCD camera connected to a Zeiss (Oberkochen, Germany) Axiovert 200M inverted microscope, or on an Olympus (Tokyo, Japan) CellM system. Fluorescence was measured during excitation at 340 and 380 nm, and after correction for the individual background fluorescence signals, the ratio of the fluorescence at both excitation wavelengths (F_{340}/F_{380}) was monitored. The extracellular solution used in $[Ca^{2+}]_i$ measurements contained (in mM) 140 NaCl, 4 KCl, 2 $CaCl_2$, 1 $MgCl_2$, 5 glucose, and 10 HEPES, pH 7.4.

Electrophysiological recordings. Currents were recorded in the whole-cell configuration of the patch-clamp technique using an EPC-7 or EPC-9 amplifier and Pulse (HEKA Elektronik, Lambrecht/Pfalz, Germany) or pClamp 9 (Molecular Devices, Sunnyvale, CA) software. Data were sampled at 5–20 kHz and filtered off-line at 1–5 kHz. Between 40 and 60% of the series resistance was compensated to minimize voltage errors. Most experiments were performed using identical intracellular and extracellular Ca^{2+}-free solutions containing (in mM) 150 NaCl, 5 $MgCl_2$, 5 EGTA, and 10 HEPES, pH 7.4. Indicated experiments were performed using a Ca^{2+}-containing extracellular solution with (in mM) 150 NaCl, 5 CsCl, 5 $CaCl_2$, 10 glucose, and 10 HEPES, pH 7.4.

Reagents. Clotrimazole [1-(chloro-α, α-diphenylbenzyl)-imidazole], capsaicin, and mustard oil (allyl isothiocyanate; MO) were purchased from Sigma. Menthol (DL-menthol) was from Merck (Darmstadt, Germany). *N*-(-4-tertiarybutylphenyl)-4-(3-cholorpyridin-2-yl)tetrahydropyrazine-1(2*H*)-carboxamide (BCTC) was a kind gift from Grünenthal (Aachen, Germany). Clotrimazole and mustard oil were dissolved in DMSO, and menthol and capsaicin in ethanol.

Behavioral analysis. Thirty-three adult mice were used in the behavioral experiments [16 wild-type (WT) and 17 *TRPV1* $^{-/-}$]. All procedures described were approved by the local ethics committee and followed guidelines of the International Association for the Study of Pain (Zimmermann, 1983). Animals were housed maximum six per cage on a 12 h light/dark cycle with food and water *ad libitum*.

Mice were placed in individual transparent plastic chambers and allowed to acclimatize for at least 1 h before testing. CLT (0.5%) and CLT plus BCTC (0.5% + 1 μM) were prepared in a solution of the following composition: 10% DMSO, 10% Tween 80, and 80% PBS. Drugs were delivered in a volume of 10 μl via intraplantar injection to the left hind paw using a 30-gauge needle coupled to a Hamilton syringe. In control experiments, mice were injected with vehicle alone.

Nocifensive behavior (licking, biting, flinching, lifting, or guarding of the injected hind paw) was monitored for 10 min after injection and expressed as the total number of seconds during which these behaviors were exhibited over the 10 min period.

The hot plate (Letica Scientific Instruments, Barcelona, Spain) was maintained at 55 ± 0.5°C with a cutoff latency of 30 s to avoid tissue damage. Endpoints for withdrawal were licking, biting, and flinching of the hind paws, and jumping. The mean of two baseline tests determined the preinjection withdrawal latency. Postinjection hot plate tests were performed immediately after the evaluation of nocifensive behavior and the results were expressed as a percentage of preinjection withdrawal latency.

Data analysis. Data analysis was performed using Origin 7.0 (OriginLab, Northampton, MA). Group data are expressed as mean ± SEM from *n* independent experiments. Significance between groups was tested using the unpaired or paired Student's *t* tests or the Kolmogorov–Smirnov test for comparison of non-normally distributed data sets.

Plots of steady-state currents (I_{ss}) in function of *V* were fitted using a modified Boltzmann function as follows:

$$I_{SS}(V) = G(V) \times V = \frac{G_{max} \times V}{1 + exp(-\frac{z}{kT}(V - V_{1/2}))} \quad (1)$$

where G_{max} is the maximal conductance (kept constant for a given cell), *z* the gating charge (in elementary charge units: $e_o = 1.6 \times 10^{-19}$ C), $V_{1/2}$ the voltage for half-maximal activation, *k* the Boltzmann constant (1.38×10^{-23} JK^{-1}), and *T* the absolute temperature. Apparent P_{open} was determined as G/G_{max}, where *G* was obtained from steady-state currents as I_{ss}/V. At 0 mV, *G* was taken as the value obtained from the fit using Equation 1. As an alternative approach, voltage-dependent activation curves were also estimated from peak tail currents measured at a fixed potential (+60 mV for TRPM8 and TRPV1; −150 mV for TRPA1) following steps to different test voltages. Outward tail currents (at +60 mV) were used in the case of TRPM8 and TRPV1, because inward currents at negative voltages inactivate too fast (time constant <1 ms) to be reliably measured (Voets et al., 2004). In general, both approaches yielded $V_{1/2}$ estimates that differed by <10 mV.

Results

Screening the effects of clotrimazole on sensory TRP channels

To evaluate the possible role of TRP channels in mediating the sensory effects of CLT, we performed intracellular Ca^{2+} imaging experiments on HEK293 cells expressing TRP channels present in sensory neurons and skin keratinocytes, namely TRPV1–4, TRPM8, and TRPA1 (Voets et al., 2005). Note that a previous report already described irreversible inhibition by CLT of TRPM2 (Hill et al., 2004), an ADP-ribose-gated, heat-activated channel expressed in brain and blood cells but not in sensory neurons (Perraud et al., 2001; Togashi et al., 2006).

Application of 10 μM CLT to HEK293 cells expressing the heat-activated TRPV1 produced a robust $[Ca^{2+}]_i$ increase, which was of comparable magnitude to the response to 100 nM capsaicin (Fig. 1*A*). In contrast, CLT (10 μM) did not evoke a Ca^{2+} increase in control HEK293 cells or cells expressing the closely related heat-activated TRPV2, TRPV3, and TRPV4 channels (Caterina et al., 1999; Peier et al., 2002b; Smith et al., 2002; Xu et al., 2002; Nilius et al., 2004) (supplemental Fig. 1, available at www.jneurosci.org as supplemental material). Application of CLT led to a reduction of the basal $[Ca^{2+}]_i$ in cells expressing TRPV4,

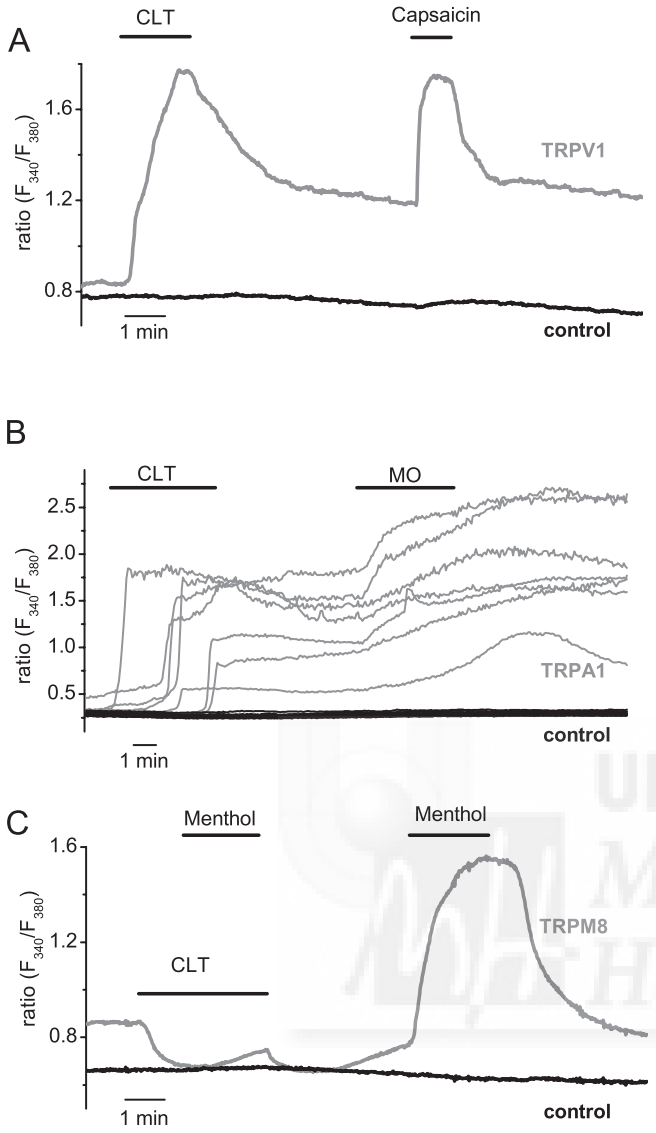

Figure 1. Effects of clotrimazole on calcium responses mediated by heterologously expressed TRPV1, TRPA1 and TRPM8. ***A***, Average ratiometric $[Ca^{2+}]_i$ responses to 5 μM CLT and 100 nM capsaicin in TRPV1-transfected HEK cells loaded with Fura-2 AM (red trace; $n = 8$). In the same field, nontransfected cells did not respond to either stimuli (black trace; $n = 10$). ***B***, Ratiometric $[Ca^{2+}]_i$ responses to 5 μM CLT and 20 μM MO in TRPA1-transfected HEK cells. Recordings from seven individual cells (red traces) are shown to illustrate the variability in the time course of the CLT responses. In the same field, nontransfected cells did not respond to either stimuli (black traces). ***C***, Average ratiometric $[Ca^{2+}]_i$ responses to 100 μM menthol in the presence and absence of 10 μM CLT in TRPM8-transfected HEK cells (red trace; $n = 10$) and nontransfected cells in the same field (black trace; $n = 5$).

suggesting a partial inhibition of basal channel activity (supplemental Fig. 1*C*, available at www.jneurosci.org as supplemental material), which is in line with previous studies showing an indirect inhibition of TRPV4 activity by cytochrome P450 inhibitors (Watanabe et al., 2003).

HEK293 cells expressing TRPA1, a sensor of various irritant chemicals, also displayed a clear $[Ca^{2+}]_i$ increase in response to 10 μM CLT (Fig. 1*B*). However, whereas $[Ca^{2+}]_i$ responses to CLT in TRPV1-expressing cells were fast, reaching maximal amplitude in <1 min (Fig. 1*A*), TRPA1-expressing cells responded significantly slower, with variable delays of up to 3 min (Fig. 1*B*).

HEK293 cells expressing the cold-activated TRPM8 exhibit an increased basal intracellular Ca^{2+} concentration ($[Ca^{2+}]_i$) caused by significant inward TRPM8 current at room temperature (McKemy et al., 2002; Peier et al., 2002a; Voets et al., 2004). In these cells, application of 10 μM CLT rapidly decreased the basal $[Ca^{2+}]_i$ and strongly impaired the response to 100 μM menthol (Fig. 1*C*).

With respect to the unwanted sensory side effects of CLT, activation of TRPV1 and TRPA1 appears most relevant. Moreover, because activation of TRPM8 in sensory neurons by cooling or menthol elicits analgesia, inhibition of this channel may also contribute to the irritation evoked by CLT. We therefore set out to evaluate the effects of CLT on these three channels in more detail.

Clotrimazole activates TRPV1

In whole-cell patch-clamp experiments, application of 5 μM CLT activated robust inward and outward whole-cell currents in HEK293 cells expressing TRPV1 (Fig. 2*A*). This activation was never observed in nontransfected cells (data not shown). The current–voltage relationship of the CLT-activated current showed outward rectification and a reversal potential close to 0 mV, in line with the previously described properties of TRPV1 (Caterina et al., 1997; Voets et al., 2004) (Fig. 2*B*). CLT also activated outwardly rectifying cation currents when applied to the intracellular face of inside-out patches from TRPV1-expressing cells (supplemental Fig. 2, available at www.jneurosci.org as supplemental material), indicating that CLT activates the channel in a membrane-delimited manner. As shown in Figure 2, *A* and *C*, currents evoked in the continuous presence of CLT at concentrations 5 μM or higher exhibited desensitization, which was not evident at lower concentrations. The effect of CLT was voltage dependent (Fig. 2*D*), suggesting that this drug affects the mechanism of TRPV1 activation rather than then number of active TRPV1 channels. Previous studies have shown that several temperature-sensitive TRP channels (TRPV1, TRPV3, TRPM8, TRPM4, and TRPM5) are voltage-gated, and that thermal and chemical stimuli act on these channels by shifting the voltage dependence of activation (Voets et al., 2004, 2007a; Chung et al., 2005; Talavera et al., 2005; Malkia et al., 2007). To investigate the voltage dependence of the effect of CLT on TRPV1 in more detail, we applied voltage steps ranging from −120 to +160 mV (Fig. 2*D*,*E*), which allows determining the voltage-dependent activation curves from the steady-state current–voltage relationships (see Materials and Methods). Analysis of steady-state currents measured during voltage steps at 25°C revealed a strong leftward shift of the activation curve, with a change in the voltage for half-maximal activation ($V_{1/2}$) from 127 ± 23 mV in control to 41 ± 13 mV in the presence of 3 μM CLT ($n = 4$) (Fig. 2*E*,*F*). Even larger shifts of the activation curves were evident at higher concentrations, but these were difficult to quantify because of the rapid current desensitization (Fig. 2*C*). From these data we can conclude that CLT activates TRPV1 by shifting the voltage dependence of activation, highly similar to the effects of capsaicin (Voets et al., 2004).

Clotrimazole activates TRPA1

Next, we investigated the effects of CLT on heterologously expressed TRPA1 channels. Note that most initial experiments were performed using tetracycline-inducible expression of TRPA1 in CHO cells; highly similar results were later obtained in transiently expressed HEK293 cells (see Figs. 1, 6) (and data not shown). In control (Ca^{2+}-free) extracellular solution and in the absence of agonist, voltage ramps from −150 to +150 mV elicited sizable, strongly outwardly rectifying currents (0.12 ± 0.03

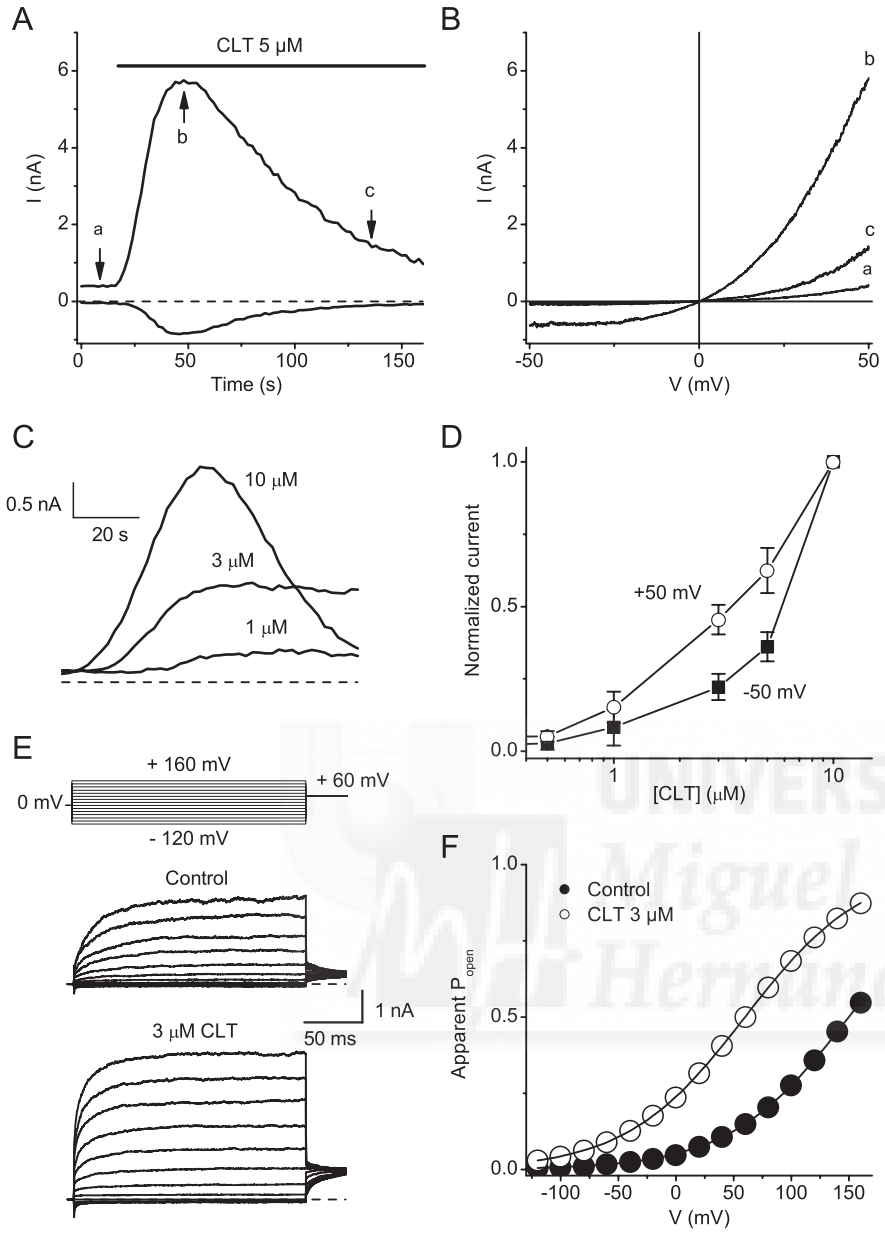

Figure 2. Clotrimazole activates TRPV1-mediated whole-cell currents in HEK cells. ***A***, Time course of the development of inward (at −50 mV) and outward (at +50 mV) TRPV1 current after application of 5 μM CLT. ***B***, Current–voltage relations obtained during 200-ms voltage ramps from −50 to +50 mV applied at the time points indicated in (***A***). ***C***, Comparison of the time course of TRPV1 current development after application of 1, 3, and 10 μM clotrimazole. ***D***, Normalized dose–response curve for the CLT-induced TRPV1 current development at the indicated voltages. ***E***, Currents elicited by 200 ms voltage steps ranging from −120 to +160 mV before (left) and during (right) addition of 3 μM CLT. ***F***, Activation curves obtained from steady-state currents in the absence (filled circles) and presence of 3 μM CLT (open circles).

nA at +75 mV; −0.025 ± 0.005 nA at −75 mV; $n = 12$), indicative of some basal TRPA1 channel activity (Fig. 3*A*,*B*). Application of CLT at a concentration of 5 μM evoked a modest and reversible increase of this outwardly rectifying current (Fig. 3*A*,*B*). CLT had no measurable effect on whole-cell currents in naive CHO cells (data not shown). The effect of CLT on TRPA1 current was dose-dependent, and did not saturate at concentrations up to 30 μM, which is close to the solubility limit of CLT in extracellular solution (Fig. 3*F*).

As TRPA1 shows voltage dependence (Karashima et al., 2007; Macpherson et al., 2007; Zurborg et al., 2007), we analyzed the effects of CLT using a voltage step protocol consisting of 400-ms voltage steps to test potentials ranging from −150 to +150 mV followed by an invariant step to −150 mV (Fig. 3*C*). In the absence of CLT, significant inward tail currents at −150 mV were only measured following test potentials ≥ +100 mV (Fig. 3*C*,*D*). After application of 7 μM CLT, inward tail currents were already significant at test potentials ≥0 mV, and the peak amplitude of the tail current following a test potential of +150 mV increased 10-fold (Fig. 3*C*,*D*). Even in the presence of CLT, tail current amplitudes did not show saturation for test potentials up to +150 mV (Fig. 3*D*). As a result, reliable estimation of G_{max} and determination of $V_{1/2}$ from Boltzmann was not feasible. Yet, a comparison of the voltage dependence of tail current amplitudes indicates that 7 μM CLT causes a leftward shift of the voltage-dependent activation curve of >100 mV (Fig. 3*D*).

Intracellular Ca^{2+} directly activates TRPA1, and permeating Ca^{2+} exerts a strong positive feedback on TRPA1 activity (Nagata et al., 2005; Doerner et al., 2007; Zurborg et al., 2007). Moreover, entering Ca^{2+} can induce rapid desensitization of TRPA1 currents activated by agonists such as mustard oil (Nagata et al., 2005; Doerner et al., 2007). Therefore, we tested the effects of CLT on TRPA1 in Ca^{2+}-containing extracellular solution and found a striking potentiation of the agonist effect of CLT. In the presence of 5 mM Ca^{2+}, outward TRPA1 currents activated by 5 μM CLT were increased ~10-fold and inward currents ~100-fold in comparison with Ca^{2+} free conditions (Fig. 3*E*,*F*). Moreover, current activation in the presence of extracellular Ca^{2+} was followed by pronounced desensitization, despite the continued presence of CLT (Fig. 3*E*, data not shown). Thus, the efficacy of CLT to activate TRPA1 is strongly dependent on extracellular Ca^{2+} and Ca^{2+} influx through the channel. It should also be noted that the maximal CLT-induced inward current amplitude in Ca^{2+}-containing solution (−3.47 ± 0.65 nA; $n = 10$) was only half of that induced by 20 μM MO (−6.45 ± 0.7 nA; $n = 8$; $p < 0.01$), indicating that CLT is a partial TRPA1 agonist.

Clotrimazole inhibits TRPM8

Application of 100 μM menthol at 25°C activates a current in TRPM8 transfected HEK293 cells that reverses near 0 mV and exhibits outward rectification (Fig. 2*B*), in line with previous reports (McKemy et al., 2002; Peier et al., 2002a; Voets et al., 2004). CLT (10 μM) produced a pronounced suppression of the menthol-induced current, which recovered to a large extent after washout (Fig. 4*A*). Detailed analysis of the dose dependence revealed that CLT is a more potent inhibitor of inward current

(IC_{50} = 200 nM at −50 mV) than outward current (IC_{50} = 1.2 μM at +50 mV). Analysis of the voltage dependence of TRPM8 using voltage steps revealed that application of 1 μM CLT induced a significant rightward shift of the voltage-dependent activation curve of TRPM8. $V_{1/2}$ increased by 89 ± 7 mV (n = 5), resulting in an almost complete inhibition of channel activity at negative voltages. The change in $V_{1/2}$ ($\Delta V_{1/2}$) produced by CLT was dose-dependent (Fig. 4*F*); fitting a Hill function to the data yielded a concentration for half-maximal effect of 3.0 ± 1.6 μM, a maximal shift of 340 ± 70 mV and a Hill coefficient of 0.9 ± 0.2 (n = 5). Together, these results indicate that CLT inhibits TRPM8 currents by causing a positive shift of the voltage dependence of channel activation.

CLT excites a subset of capsaicin- and mustard oil-sensitive sensory neurons

Next, we tested the effects of CLT on cultured mouse trigeminal sensory neurons. TRPV1, TRPA1 and TRPM8 are expressed in subsets of primary sensory neurons where they function as thermosensors and/or chemosensors. Although the exact distribution and colocalization of these channels in these neurons is somewhat controversial, the consensus is that TRPA1 and TRPV1 have a partially overlapping expression pattern in capsaicin-sensitive nociceptive neurons, whereas TRPM8 is expressed in a clearly distinct subpopulation of sensory neurons (Story et al., 2003; Kobayashi et al., 2005).

Application of 10 μM CLT evoked an increase in $[Ca^{2+}]_i$ in a subset of cells that corresponded to 21% of viable neurons (Fig. 5*A*,*C*). Importantly, all CLT-activated neurons were also sensitive to 1 μM capsaicin, indicating that CLT-induced activation is restricted to TRPV1-expressing neurons (Fig. 5*A*, inset). It should be noted, however, that only approximately half of the capsaicin-sensitive neurons, which corresponded to 49% of the total cell population, responded to 10 μM CLT (Fig. 5*A*).

To evaluate the relative contribution of TRPV1 and TRPA1 channels to the CLT-induced responses, we tested the effects of CLT on trigeminal neurons from *TRPV1*$^{-/-}$ mice. As expected from previous work (Caterina et al., 2000), all TRPV1-deficient neurons were fully unresponsive to capsaicin (Fig. 5*B*,*C*). Notably, the responsiveness to CLT was significantly reduced compared with wild type (p < 0.001, Kolmogorov–Smirnov test): only 7% of the cells showed a detectable response to 10 μM CLT (Fig. 5*C*,*D*), and the average amplitude of the $[Ca^{2+}]_i$ increase in responsive cells was lower than in wild-type cells (Δratio, 0.72 ± 0.12 for WT vs 0.31 ± 0.12 for *TRPV1*$^{-/-}$ neurons; p < 0.05). Importantly, all CLT-responsive TRPV1-deficient neurons were also stimulated by MO (100 μM), indicating that CLT sensitivity in the *TRPV1*$^{-/-}$ neurons is restricted to TRPA1-expressing neurons (Fig. 5*B*). Together, these data indicate that CLT excites nociceptive neurons through activation of TRPV1 and to a lesser extent TRPA1 channels.

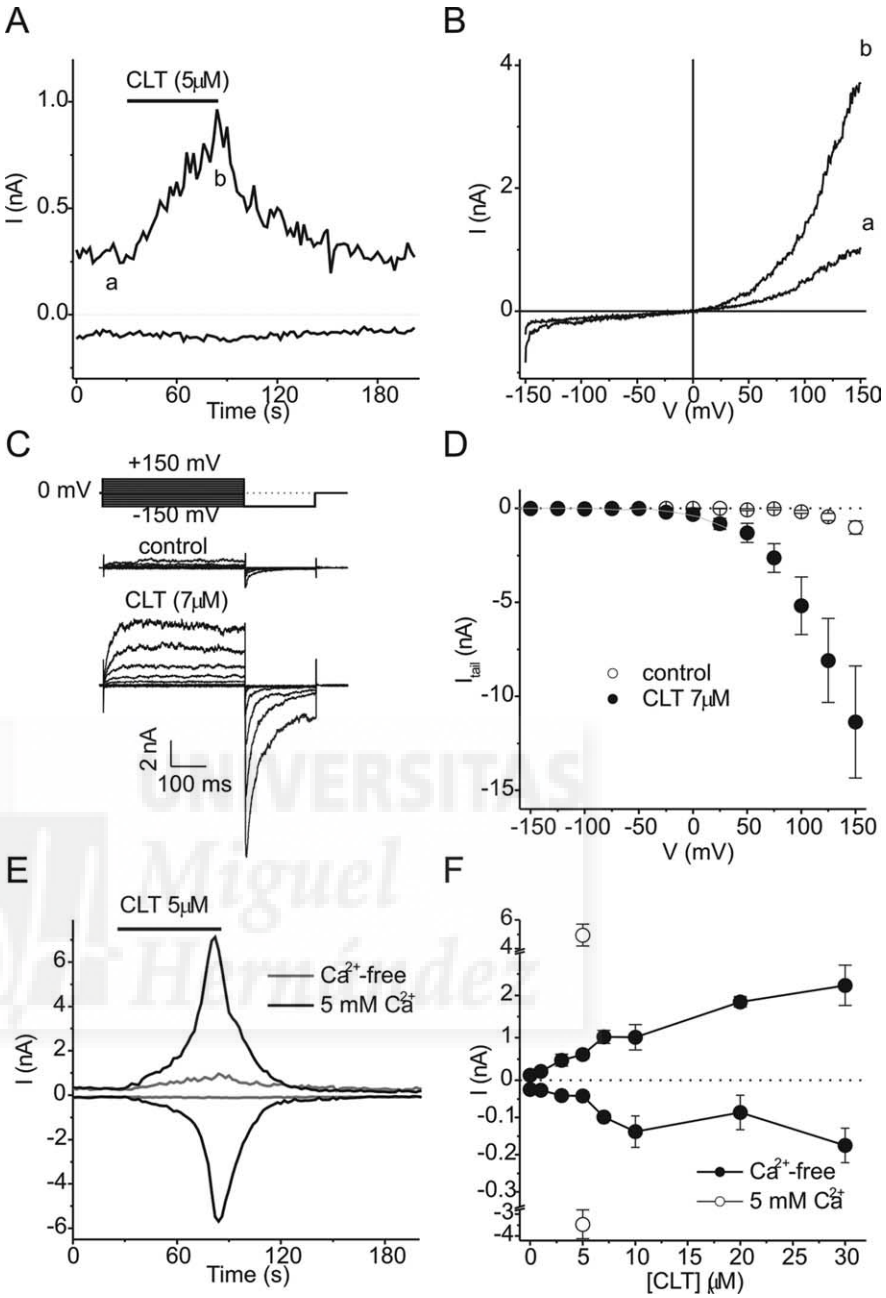

Figure 3. Clotrimazole activates TRPA1-mediated whole-cell currents in CHO cells. ***A***, Time course of the development of inward (at −75 mV) and outward (at +75 mV) TRPA1 currents after application of 5 μM CLT in control (Ca^{2+}-free) extracellular solution. ***B***, Current–voltage relations obtained during 500 ms voltage ramps from −150 to +150 mV at the time points indicated in ***A***. ***C***, Currents evoked in response to 400 ms voltage steps ranging from −150 to 150 mV followed by an invariant step to −150 mV before and during application of 7 μM CLT. ***D***, Peak inward tail currents at −150 mV in the absence (filled circles) and presence of 7 μM CLT (open circles). The gray line represents the data obtained in the absence of CLT, shifted to the left by 110 mV. ***E***, Time course of TRPA1 current development and desensitization after application of 5 μM clotrimazole in the presence of extracellular Ca^{2+} (5 mM; black line). A time course obtained in Ca^{2+}-free solution (gray; same data as in Fig. 3*A*) is shown for comparison. ***F***, Dose–response curve for the CLT-induced inward and outward TRPA1 current.

CLT differentiates TRPM8- and TRPA1-mediated responses to menthol

Previously, menthol-induced responses in sensory neurons were considered strong evidence for the expression of TRPM8. How-

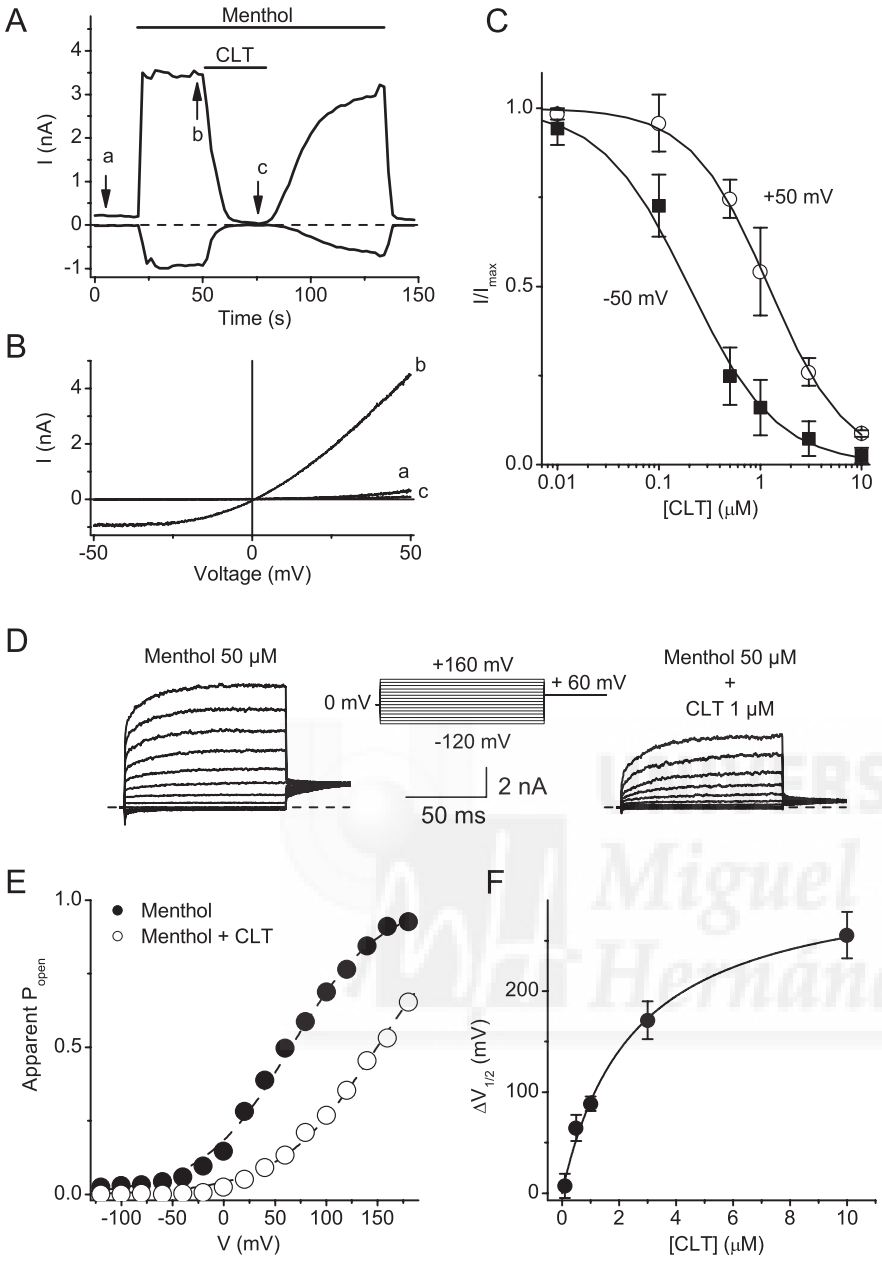

Figure 4. Clotrimazole inhibits TRPM8-mediated whole-cell current in transfected HEK cells. ***A***, Time course of inward (at −50 mV) and outward (at +50 mV) TRPM8 current activation by 100 μM menthol and its reversible inhibition by 10 μM CLT. ***B***, Current–voltage relations obtained during 200 ms voltage ramps from −50 to + 50 mV at the time points indicated in ***A***. ***C***, Dose–response curve for the inhibition of menthol induced TRPM8 current by CLT at −50 mV (filled square) and +50 mV (open circles). ***D***, Currents elicited in response to 100 ms voltage steps ranging from −120 to +160 mV in presence of 100 μM menthol, before (left) and during (right) addition of CLT. ***E***, Activation curves obtained from steady-state currents for menthol-induced currents in the absence (filled circles) and presence (open circles) of 1 μM clotrimazole. ***F***, Change in $V_{1/2}$ as a function of CLT concentration.

ever, this vision needs to be revised after our recent findings that menthol also has an agonistic effect on TRPA1 channels (Karashima et al., 2007). Given its opposite effects on TRPA1 and TRPM8, we investigated whether CLT could be used to distinguish between TRPA1- and TRPM8-mediated menthol responses. As illustrated in Figure 6, *A* and *D*, repeated application of 50 μM menthol leads to rapid and reversible activation of TRPM8 and TRPA1 heterologously expressed in HEK cells. Coapplication of 10 μM CLT leads to a strong inhibition of the menthol-response in TRPM8-expressing cells, whereas the menthol response in TRPA1-expressing cells is clearly potentiated by CLT (Fig. 6*A*,*D*).

To isolate the effects of CLT on TRPM8-mediated menthol responses in sensory neurons, we studied its effects in mustard oil-insensitive, menthol-sensitive trigeminal neurons (Karashima et al., 2007). In this subpopulation, which corresponds to ~10% of viable neurons (Karashima et al., 2007), 10 μM CLT caused a decrease of basal $[Ca^{2+}]_i$ and produced a strong and reversible inhibition of the $[Ca^{2+}]_i$ rise evoked by applying 100 μM menthol (Fig. 6*B*,*C*). These results indicate that the inhibitory effect of CLT on basal and menthol-induced TRPM8 activity is preserved in sensory neurons. Then, to dissect the effects of CLT on TRPA1-mediated menthol responses in sensory neurons, we examined the effect of coapplication of menthol and CLT in MO-sensitive trigeminal neurons from *TRPV1*$^{-/-}$ mice (Karashima et al., 2007). We observed two types of responses in this subset of neurons. Neurons that showed only a small response to a first menthol application (Δratio, <0.3) displayed a significantly enhanced response to a subsequent application of menthol in the presence of CLT (Fig. 6*E*,*F*). In contrast, neurons that showed a more robust response to a first menthol application (Δratio, >0.3) did not show significant CLT-induced enhancement (Fig. 6*E*,*F*). Possibly, CLT-induced TRPA1 potentiation in these cells is masked by Ca^{2+}-induced desensitization.

Together, these properties demonstrate that CLT can be used as pharmacological tool to discriminate between TRPM8- and TRPA1-mediated chemosensory responses.

CLT causes TRPV1-mediated nocifensive behavior and thermal hyperalgesia

Finally, we tested to what extent the effects of CLT on TRP channels in sensory neurons results in pain-related behavior in mice. Intra-plantar injection of CLT evoked clear nocifensive behavior in wild type mice, as evidenced by strongly increased flinching and licking behavior compared with vehicle-injected mice (Fig. 7*A*). Coinjection of BCTC, a potent TRPV1 antagonist, significantly attenuated CLT-induced pain behavior (Fig. 7*A*). Moreover, *TRPV1*$^{-/-}$ mice did not exhibit significant nocifensive behavior in response to CLT injection (Fig. 7*A*).

TRPV1 is involved in detecting noxious heat, and previous studies have shown that several endogenous and exogenous chemicals can sensitize TRPV1 to heat resulting in thermal hyperalgesia *in vivo*. To investigate whether CLT affects the sensitivity to heat, we assayed the effect of the intraplantar CLT injection on the thermoresponsive behavior using a hot plate assay at 55°C. These experiments were performed 10 min after CLT in-

jection, at which time the acute CLT-induced nocifensive behavior had fully ceased. In line with a previous study (Davis et al., 2000; but see Caterina et al., 2000), hot plate latencies in noninjected or vehicle-injected mice were not significantly different between WT (15.4 ± 2.2 s) and *TRPV1*$^{-/-}$ mice (13.7 ± 1.1 s; $p = 0.50$). Importantly, intraplantar injection of CLT caused a significant reduction in hot plate latency in WT but not in the *TRPV1*$^{-/-}$ mice (Fig. 7*B*). Together, these behavioral experiments demonstrate that CLT evokes nocifensive behavior and thermal hyperalgesia in mice in a TRPV1-dependent manner.

Discussion

Despite its wide use in various over-the-counter medications, the biological actions of CLT are only partly understood. In particular, the origin of the sensory side effects of oral or topical CLT were not known. Our present results identify TRP channels involved in thermosensation and chemosensation in sensory neurons as novel CLT targets. We demonstrate that CLT is an agonist of TRPV1 and TRPA1, two excitatory TRP channels expressed in nociceptors (Caterina et al., 1997; Caterina et al., 2000; Davis et al., 2000; Story et al., 2003; Jordt et al., 2004; Bautista et al., 2005; Nagata et al., 2005; Bautista et al., 2006; Kwan et al., 2006), and a potent antagonist of TRPM8, a cold- and menthol sensor in cold-sensitive sensory neurons (McKemy et al., 2002; Peier et al., 2002a; Bautista et al., 2007; Colburn et al., 2007; Dhaka et al., 2007; Voets et al., 2007b). Moreover, we show that intraplantar injection of CLT evokes nocifensive behavior and induces hypersensitivity to heat in mice, which can be attenuated by pharmacological inhibition or genetic ablation of TRPV1. These results point at TRPV1 as a major culprit for the irritation and burning that can be experienced after topical application of CLT.

Previous studies have shown that thermal stimuli as well as a variety of chemical agonists and antagonists can modulate activity of certain TRP channels, including TRPV1, TRPM8, and TRPA1, by shifting the voltage dependence of activation (Piper et al., 1999; Brauchi et al., 2004; Voets et al., 2004; Chung et al., 2005; Talavera et al., 2005; Karashima et al., 2007; Malkia et al., 2007; Voets et al., 2007a). Our present results show that CLT also changes the voltage dependence of TRPV1, TRPA1, and TRPM8. In the case of TRPV1 and TRPA1, CLT shifts the voltage dependence toward more negative voltages, which promotes channel opening in the physiological voltage range. In contrast, CLT shifts the voltage dependence of TRPM8 toward more positive voltages, thereby counteracting the effects of menthol and cold on the channel. As such, CLT can also be considered as a gating modifier rather than as an (ant)agonist of these channels.

Two previous reports have provided compelling evidence that activation of TRPA1 by several of its agonists occurs through covalent modification of cysteine residues on the channel (Hin-

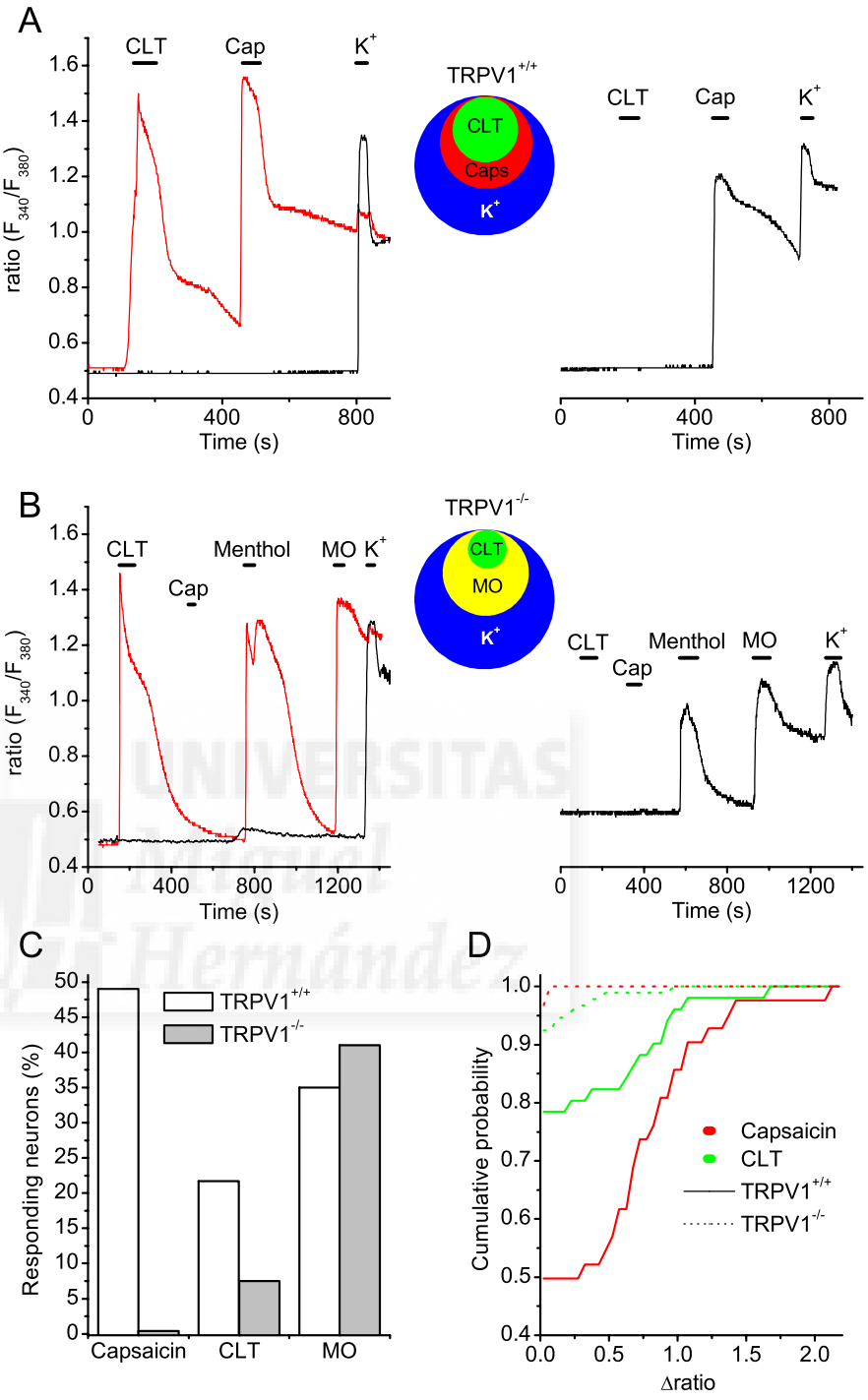

Figure 5. Clotrimazole responses in mouse trigeminal neurons. ***A***, Ratiometric $[Ca^{2+}]_i$ measurements from Fura-2 AM-loaded neurons from wild type mice showing different types of responses to 10 μM CLT, 1 μM capsaicin (Caps) and 60 mM K^+. As depicted by circles (inset), CLT responses were only observed in capsaicin-sensitive neurons. ***B***, Representative ratiometric $[Ca^{2+}]_i$ responses to 10 μM CLT, 100 μM capsaicin, 100 μM menthol (Men), 100 μM MO, and 60 mM K^+ in neurons ($n = 83$) from *TRPV1*$^{-/-}$ mice. As depicted by circles (inset), CLT responses were only observed in mustard oil sensitive neurons. ***C***, Percentage of wild-type and *TRPV1*$^{-/-}$ neurons responding to capsaicin, CLT, and mustard oil. ***D***, Cumulative probability plot of the responses to 1 μM capsaicin (red) and 10 μM CLT (green) in wild-type (solid lines) and *TRPV1*$^{-/-}$ (dashed lines) neurons.

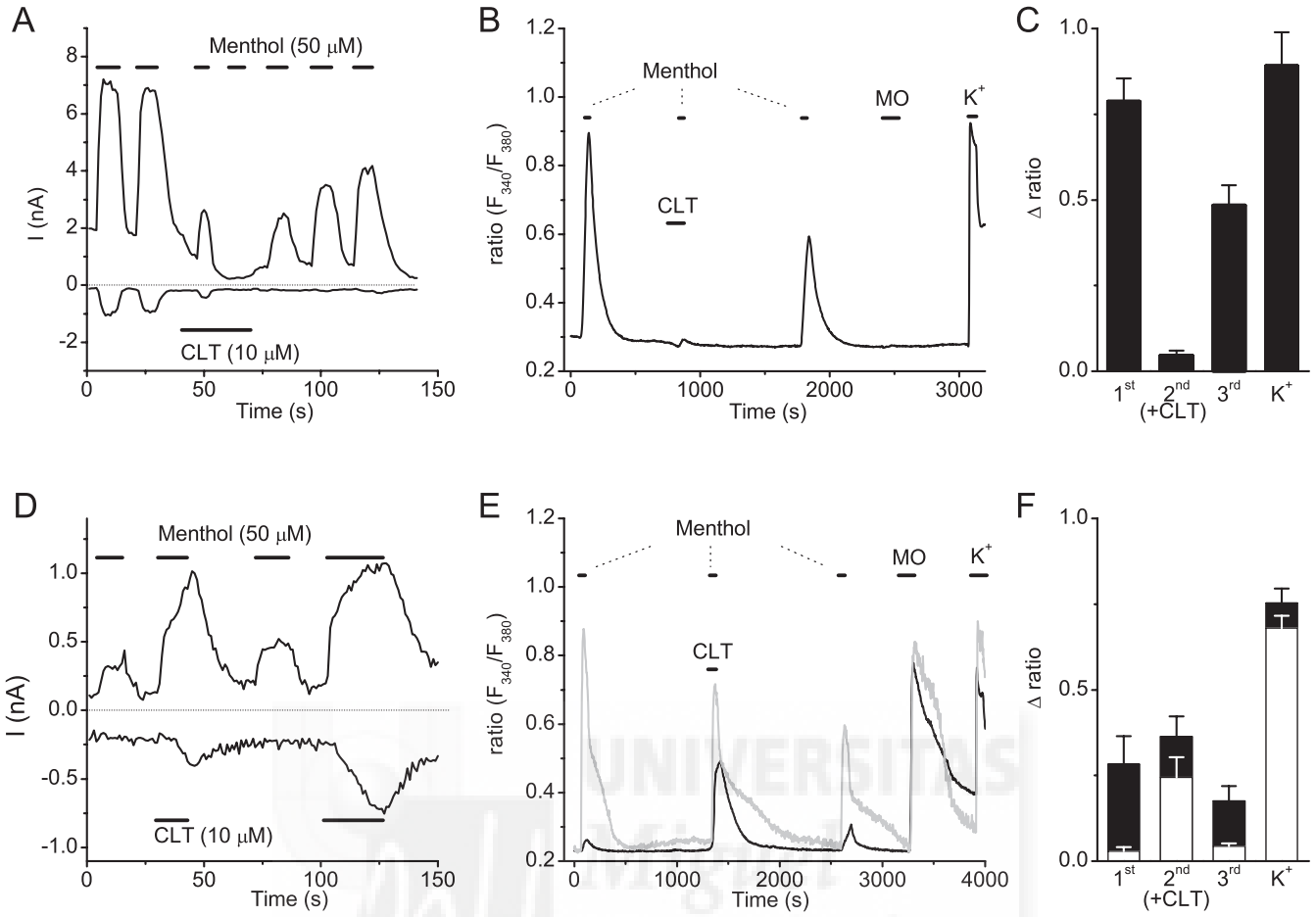

Figure 6. Clotrimazole distinguishes between TRPM8- and TRPA1-mediated menthol-responses. ***A***, Whole-cell currents in HEK cells transfected with TRPM8 illustrating the reversible inhibition of responses to menthol (100 μM) by CLT(10 μM). ***B***, Ratiometric $[Ca^{2+}]_i$ responses to menthol (100 μM) in an MO-insensitive sensory neuron in the absence and presence of CLT (10 μM). ***C***, Mean responses in menthol-sensitive, MO-insensitive sensory neurons ($n = 15$) to a stimulation protocol as in ***B***, illustrating the strong inhibition (95 $\pm$ 2% block) of the menthol response by CLT. ***D***, Same as in ***A***, but for HEK cells transfected with TRPA1, illustrating the reversible potentiation of menthol responses by 10 CLT. ***E***, Same as in ***B***, but in MO-sensitive *TRPV1* $^{-/-}$ sensory neurons. Two traces are shown, illustrating two distinct patterns of responses in these cells. A cell with a small response to a first menthol application (black trace; Δratio, 0.05) exhibited a strongly potentiated response to the combination menthol plus CLT. In contrast, CLT-induced potentiation of the menthol response was not observed in a cell with a robust response to a first menthol application (gray trace; Δratio, 0.65). ***F***, Mean responses in MO-sensitive *TRPV1* $^{-/-}$ sensory neurons ($n = 15$) to a stimulation protocol as in ***E***.

man et al., 2006; Macpherson et al., 2007). The authors of these studies realized that known TRPA1 agonists such as mustard oil, cinnamaldehyde or acrolein are electrophiles that can react with the thiol group of cysteine residues on proteins. One study also provided direct evidence for a covalent modification of TRPA1 by these agonists (Macpherson et al., 2007). Moreover, mutation of specific cysteine residues in the N terminus strongly reduced its sensitivity to cysteine-reactive agonists, but not to icilin, an agonist that exhibits no obvious reactivity to cysteines (Hinman et al., 2006; Macpherson et al., 2007). It is unlikely that CLT activation of TRPA1 involves covalent binding to the channel. First, CLT is neither electrophilic nor known to react with cysteine or other amino acids. Second, the effect of CLT on TRPA1 was readily reversible on washout and could be repeated several times in the same cell. In contrast, covalent modification of cysteine residues can persist for minutes to hours (Macpherson et al., 2007). Thus, we consider it most likely that CLT acts on TRPA1 through a "classical," noncovalent interaction with the channel, similar to the effects of menthol on TRPA1 (Karashima et al., 2007).

In previous studies it has proven difficult to unambiguously separate TRPM8 and TRPA1 responses in sensory neurons. This is mainly because of the substantial overlap in stimuli that activate TRPM8 and TRPA1: both channels were shown to be activated by icilin, cold and menthol (McKemy et al., 2002; Peier et al., 2002a; Story et al., 2003; Karashima et al., 2007). It should be noted that whether TRPA1 plays a role as a cold sensor *in vivo* remains a matter of strong debate (Story et al., 2003; Jordt et al., 2004; Bautista et al., 2006; Kwan et al., 2006; Sawada et al., 2007; Zurborg et al., 2007). Previous studies have often used TRPA1-selective agonists such as MO to discriminate between TRPA1- and TRPM8-mediated responses. However, because of their covalent binding to TRPA1 (and possibly other cellular targets) the effects of these agonists are only poorly reversible. Our present findings identify CLT as probably a more useful tool to distinguish between TRPM8- and TRPA1-mediated responses in sensory neurons. CLT can be used as a potent inhibitor of TRPM8, while activating TRPA1 and potentiating TRPA1-mediated responses to agonists such as menthol. Importantly, these effects of CLT are rapidly and almost completely reversible.

Only a subset of capsaicin-sensitive and/or MO-sensitive trigeminal neurons showed a Ca^{2+} response to 10 μM CLT, whereas 100% of TRPV1- or TRPA1-expressing HEK293 cells responded to the same dose of CLT in Ca^{2+} imaging or patch-clamp exper-

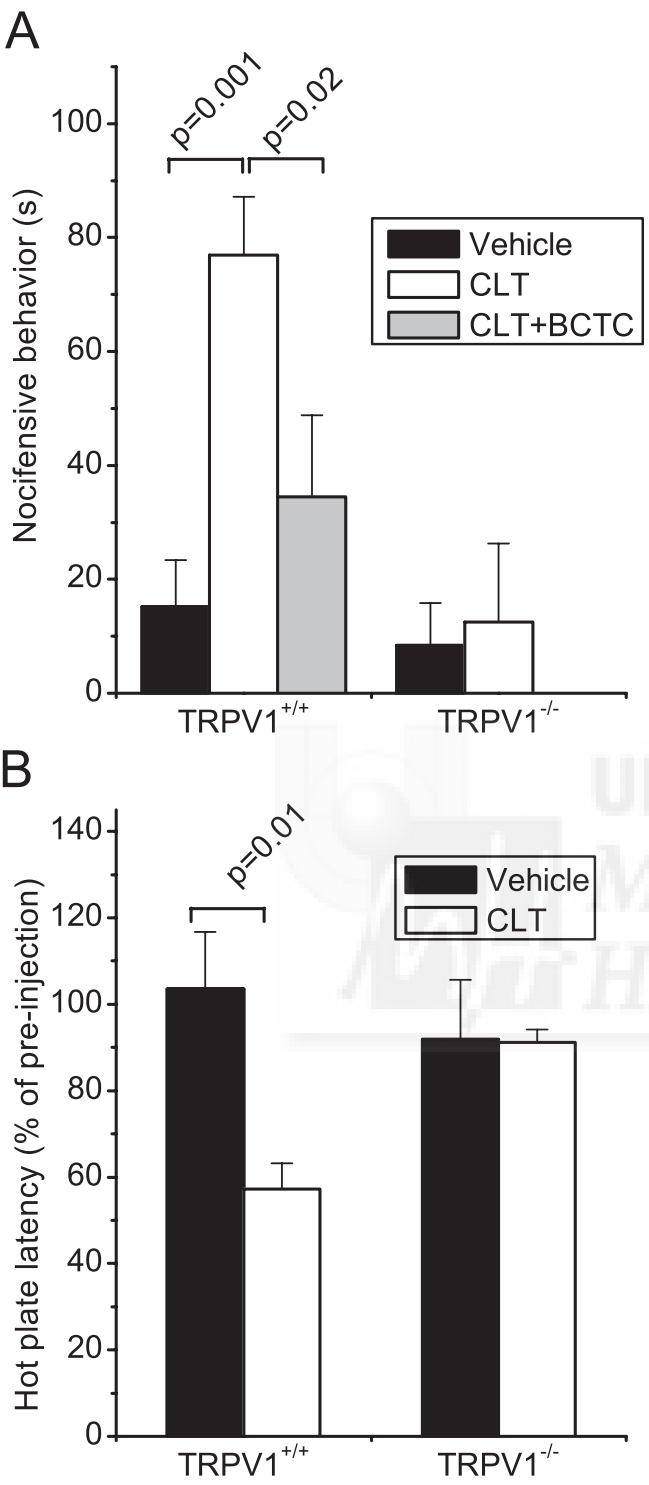

Figure 7. Intraplantar injection of Clotrimazole evokes pain and thermal hyperalgesia in mice. ***A***, Duration of nocifensive behavior in the first 10 min after intraplantar injection of vehicle, CLT or CLT plus BCTC in wild-type and *TRPV1* $^{-/-}$ mice. ***B***, Change in response latency on a hot plate (55°C) 10–15 min after intraplantar injection of vehicle or CLT wild-type and *TRPV1* $^{-/-}$ mice.

iments. This indicates that CLT-induced activation of TRPA1 and/or TRPV1 is not always sufficient to provoke a detectable Ca^{2+} signal in trigeminal neurons, which can be attributed to the lower agonist potency of CLT compared with capsaicin (TRPV1) or MO (TRPA1). Moreover, both TRPV1 and TRPA1 are voltage-dependent, and their sensitivity to activating stimuli such as CLT varies depending on the membrane potential of the neuron. In general, it is well known that the excitability of thermosensory neurons is determined by the relative activity of excitatory and inhibitory ionic channels (Viana et al., 2002). Finally, it cannot be excluded that the some neurons have mechanisms that mediate rapid extrusion or breakdown of CLT and thereby prevent it from significantly activating TRPV1/TRPA1. For example, it has been shown in yeast that high expression of drug extrusion pumps such as multidrug resistance 1 (MDR1) can lead to resistance to CLT (White et al., 2002; Looi et al., 2005). Independent of the mechanism, the lower cellular sensitivity to CLT compared with capsaicin or MO matches with the milder perceived sensory effects of CLT when applied to the tongue or mucous membranes.

It is known that topical application of CLT preparations in humans can evoke unwanted side effects such as irritation and burning of the skin and mucous membranes (Binet et al., 1994; del Palacio et al., 2001). Our present results provide a straightforward explanation for such sensory side-effects, namely activation of TRPV1- and TRPA1-containing nociceptive neurons. Most importantly, we found that intraplantar injection of CLT evoked robust nocifensive behavior in mice and increased the sensitivity to noxious heat, similar to what has been observed after intraplantar injection of selective TRPV1 agonists such as capsaicin or resiniferatoxin (Caterina et al., 2000). As for capsaicin and resiniferatoxin (Caterina et al., 2000), we found that both the acute nocifensive behavior and the thermal hyperalgesia evoked by CLT were completely absent in *TRPV1* $^{-/-}$ mice. The absence of obvious signs of pain-related behavior in the *TRPV1* $^{-/-}$ mice could indicate that TRPA1 plays only a minor role in the initiation of CLT-induced pain. Our results obtained in heterologous systems and isolated sensory neurons suggest, however, that activation of TRPA1 may become more relevant to nociception at higher CLT concentrations or when CLT is coapplied with other TRPA1-agonists such as menthol, as is the case in many CLT-containing creams.

In conclusion, we have identified thermosensory and chemosensory TRP channels in sensory neurons as novel targets of the widely used drug CLT. CLT is, to our knowledge, the most sensitive known inhibitor of TRPM8, and as such CLT may have therapeutic potential for the treatment of TRPM8-related conditions such as cold allodynia or even certain types of malignancies (Bidaux et al., 2007; Colburn et al., 2007; Voets et al., 2007b). In addition, we demonstrated that CLT represents a useful tool to discriminate between TRPM8- and TRPA1-mediated responses. Finally, knowledge of the agonist effect of CLT on TRP channels in nociceptors may form the basis for the development of new CLT preparations with reduced sensory side effects.

References

Alvarez J, Montero M, Garcia-Sancho J (1992) High affinity inhibition of Ca^{2+}-dependent K^+ channels by cytochrome P-450 inhibitors. J Biol Chem 267:11789–11793.

Bautista DM, Movahed P, Hinman A, Axelsson HE, Sterner O, Hogestatt ED, Julius D, Jordt SE, Zygmunt PM (2005) Pungent products from garlic activate the sensory ion channel TRPA1. Proc Natl Acad Sci USA 102:12248–12252.

Bautista DM, Jordt SE, Nikai T, Tsuruda PR, Read AJ, Poblete J, Yamoah EN, Basbaum AI, Julius D (2006) TRPA1 mediates the inflammatory actions of environmental irritants and proalgesic agents. Cell 124:1269–1282.

Bautista DM, Siemens J, Glazer JM, Tsuruda PR, Basbaum AI, Stucky CL, Jordt SE, Julius D (2007) The menthol receptor TRPM8 is the principal detector of environmental cold. Nature 448:204–208.

Benzaquen LR, Brugnara C, Byers HR, Gatton-Celli S, Halperin JA (1995)

Clotrimazole inhibits cell proliferation *in vitro* and *in vivo*. Nat Med 1:534–540.

Bidaux G, Flourakis M, Thebault S, Zholos A, Beck B, Gkika D, Roudbaraki M, Bonnal JL, Mauroy B, Shuba Y, Skryma R, Prevarskaya N (2007) Prostate cell differentiation status determines transient receptor potential melastatin member 8 channel subcellular localization and function. J Clin Invest 117:1647–1657.

Binet O, Soto-Melo J, Delgadillo J, Videla S, Izquierdo I, Forn J (1994) Flutrimazole 1% dermal cream in the treatment of dermatomycoses: a randomized, multicentre, double-blind, comparative clinical trial with 1% clotrimazole cream. Flutrimazole Study Group. Mycoses 37:455–459.

Brauchi S, Orio P, Latorre R (2004) Clues to understanding cold sensation: thermodynamics and electrophysiological analysis of the cold receptor TRPM8. Proc Natl Acad Sci USA 101:15494–15499.

Brugnara C, Gee B, Armsby CC, Kurth S, Sakamoto M, Rifai N, Alper SL, Platt OS (1996) Therapy with oral clotrimazole induces inhibition of the Gardos channel and reduction of erythrocyte dehydration in patients with sickle cell disease. J Clin Invest 97:1227–1234.

Caterina MJ, Schumacher MA, Tominaga M, Rosen TA, Levine JD, Julius D (1997) The capsaicin receptor: a heat-activated ion channel in the pain pathway. Nature 389:816–824.

Caterina MJ, Rosen TA, Tominaga M, Brake AJ, Julius D (1999) A capsaicin-receptor homologue with a high threshold for noxious heat. Nature 398:436–441.

Caterina MJ, Leffler A, Malmberg AB, Martin WJ, Trafton J, Petersen-Zeitz KR, Koltzenburg M, Basbaum AI, Julius D (2000) Impaired nociception and pain sensation in mice lacking the capsaicin receptor. Science 288:306–313.

Chung MK, Guler AD, Caterina MJ (2005) Biphasic currents evoked by chemical or thermal activation of the heat-gated ion channel, TRPV3. J Biol Chem 280:15928–15941.

Clapham DE (2003) TRP channels as cellular sensors. Nature 426:517–524.

Colburn RW, Lubin ML, Stone Jr DJ, Wang Y, Lawrence D, D'Andrea MR, Brandt MR, Liu Y, Flores CM, Qin N (2007) Attenuated cold sensitivity in TRPM8 null mice. Neuron 54:379–386.

Davis JB, Gray J, Gunthorpe MJ, Hatcher JP, Davey PT, Overend P, Harries MH, Latcham J, Clapham C, Atkinson K, Hughes SA, Rance K, Grau E, Harper AJ, Pugh PL, Rogers DC, Bingham S, Randall A, Sheardown SA (2000) Vanilloid receptor-1 is essential for inflammatory thermal hyperalgesia. Nature 405:183–187.

del Palacio A, Ortiz FJ, Perez A, Pazos C, Garau M, Font E (2001) A double-blind randomized comparative trial: eberconazole 1% cream versus clotrimazole 1% cream twice daily in *Candida* and dermatophyte skin infections. Mycoses 44:173–180.

Dhaka A, Murray AN, Mathur J, Earley TJ, Petrus MJ, Patapoutian A (2007) TRPM8 is required for cold sensation in mice. Neuron 54:371–378.

Doerner JF, Gisselmann G, Hatt H, Wetzel CH (2007) Transient receptor potential channel A1 is directly gated by calcium ions. J Biol Chem 282:13180–13189.

Hill K, McNulty S, Randall AD (2004) Inhibition of TRPM2 channels by the antifungal agents clotrimazole and econazole. Naunyn Schmiedebergs Arch Pharmacol 370:227–237.

Hinman A, Chuang HH, Bautista DM, Julius D (2006) TRP channel activation by reversible covalent modification. Proc Natl Acad Sci USA 103:19564–19568.

Hitchcock CA, Dickinson K, Brown SB, Evans EG, Adams DJ (1990) Interaction of azole antifungal antibiotics with cytochrome P-450-dependent 14 alpha-sterol demethylase purified from *Candida albicans*. Biochem J 266:475–480.

Jordt SE, Bautista DM, Chuang HH, McKemy DD, Zygmunt PM, Hogestatt ED, Meng ID, Julius D (2004) Mustard oils and cannabinoids excite sensory nerve fibres through the TRP channel ANKTM1. Nature 427:260–265.

Julius D, Basbaum AI (2001) Molecular mechanisms of nociception. Nature 413:203–210.

Karashima Y, Damann N, Prenen J, Talavera K, Segal A, Voets T, Nilius B (2007) Bimodal action of menthol on the transient receptor potential channel TRPA1. J Neurosci 27:9874–9884.

Kobayashi K, Fukuoka T, Obata K, Yamanaka H, Dai Y, Tokunaga A, Noguchi K (2005) Distinct expression of TRPM8, TRPA1, and TRPV1 mRNAs in rat primary afferent neurons with aδ/c-fibers and colocalization with trk receptors. J Comp Neurol 493:596–606.

Koletar SL, Russell JA, Fass RJ, Plouffe JF (1990) Comparison of oral fluconazole and clotrimazole troches as treatment for oral candidiasis in patients infected with human immunodeficiency virus. Antimicrob Agents Chemother 34:2267–2268.

Kwan KY, Allchorne AJ, Vollrath MA, Christensen AP, Zhang DS, Woolf CJ, Corey DP (2006) TRPA1 contributes to cold, mechanical, and chemical nociception but is not essential for hair-cell transduction. Neuron 50:277–289.

Looi CY, EC DS, Seow HF, Rosli R, Ng KP, Chong PP (2005) Increased expression and hotspot mutations of the multidrug efflux transporter, CDR1 in azole-resistant *Candida albicans* isolates from vaginitis patients. FEMS Microbiol Lett 249:283–289.

Macpherson LJ, Dubin AE, Evans MJ, Marr F, Schultz PG, Cravatt BF, Patapoutian A (2007) Noxious compounds activate TRPA1 ion channels through covalent modification of cysteines. Nature 445:541–545.

Madrid R, Donovan-Rodriguez T, Meseguer V, Acosta MC, Belmonte C, Viana F (2006) Contribution of TRPM8 channels to cold transduction in primary sensory neurons and peripheral nerve terminals. J Neurosci 26:12512–12525.

Malkia A, Madrid R, Meseguer V, de la Pena E, Valero M, Belmonte C, Viana F (2007) Bidirectional shifts of TRPM8 channel gating by temperature and chemical agents modulate the cold sensitivity of mammalian thermoreceptors. J Physiol (Lond) 581:155–174.

McKemy DD, Neuhausser WM, Julius D (2002) Identification of a cold receptor reveals a general role for TRP channels in thermosensation. Nature 416:52–58.

Nagata K, Duggan A, Kumar G, Garcia-Anoveros J (2005) Nociceptor and hair cell transducer properties of TRPA1, a channel for pain and hearing. J Neurosci 25:4052–4061.

Nilius B, Owsianik G, Voets T, Peters JA (2007) Transient receptor potential cation channels in disease. Physiol Rev 87:165–217.

Nilius B, Vriens J, Prenen J, Droogmans G, Voets T (2004) TRPV4 calcium entry channel: a paradigm for gating diversity. Am J Physiol Cell Physiol 286:C195–C205.

Peier AM, Moqrich A, Hergarden AC, Reeve AJ, Andersson DA, Story GM, Earley TJ, Dragoni I, McIntyre P, Bevan S, Patapoutian A (2002a) A TRP channel that senses cold stimuli and menthol. Cell 108:705–715.

Peier AM, Reeve AJ, Andersson DA, Moqrich A, Earley TJ, Hergarden AC, Story GM, Colley S, Hogenesch JB, McIntyre P, Bevan S, Patapoutian A (2002b) A heat-sensitive TRP channel expressed in keratinocytes. Science 296:2046–2049.

Perraud AL, Fleig A, Dunn CA, Bagley LA, Launay P, Schmitz C, Stokes AJ, Zhu Q, Bessman MJ, Penner R, Kinet JP, Scharenberg AM (2001) ADP-ribose gating of the calcium-permeable LTRPC2 channel revealed by Nudix motif homology. Nature 411:595–599.

Piper AS, Yeats JC, Bevan S, Docherty RJ (1999) A study of the voltage dependence of capsaicin-activated membrane currents in rat sensory neurones before and after acute desensitization. J Physiol (Lond) 518:721–733.

Sawada Y, Hosokawa H, Hori A, Matsumura K, Kobayashi S (2007) Cold sensitivity of recombinant TRPA1 channels. Brain Res 1160:39–46.

Sawyer PR, Brogden RN, Pinder RM, Speight TM, Avery (1975) Clotrimazole: a review of its antifungal activity and therapeutic efficacy. Drugs 9:424–447.

Smith GD, Gunthorpe MJ, Kelsell RE, Hayes PD, Reilly P, Facer P, Wright JE, Jerman JC, Walhin JP, Ooi L, Egerton J, Charles KJ, Smart D, Randall AD, Anand P, Davis JB (2002) TRPV3 is a temperature-sensitive vanilloid receptor-like protein. Nature 418:186–190.

Story GM, Peier AM, Reeve AJ, Eid SR, Mosbacher J, Hricik TR, Earley TJ, Hergarden AC, Andersson DA, Hwang SW, McIntyre P, Jegla T, Bevan S, Patapoutian A (2003) ANKTM1, a TRP-like channel expressed in nociceptive neurons, is activated by cold temperatures. Cell 112:819–829.

Talavera K, Yasumatsu K, Voets T, Droogmans G, Shigemura N, Ninomiya Y, Margolskee RF, Nilius B (2005) Heat activation of TRPM5 underlies thermal sensitivity of sweet taste. Nature 438:1022–1025.

Togashi K, Hara Y, Tominaga T, Higashi T, Konishi Y, Mori Y, Tominaga M (2006) TRPM2 activation by cyclic ADP-ribose at body temperature is involved in insulin secretion. EMBO J 25:1804–1815.

Tominaga M (2007) Nociception and TRP channels. Handb Exp Pharmacol 179:489–505.

Viana F, de la Pena E, Belmonte C (2002) Specificity of cold thermotransduction is determined by differential ionic channel expression. Nat Neurosci 5:254–260.

Voets T, Droogmans G, Wissenbach U, Janssens A, Flockerzi V, Nilius B (2004) The principle of temperature-dependent gating in cold- and heat-sensitive TRP channels. Nature 430:748–754.

Voets T, Talavera K, Owsianik G, Nilius B (2005) Sensing with TRP channels. Nat Chem Biol 1:85–92.

Voets T, Owsianik G, Janssens A, Talavera K, Nilius B (2007a) TRPM8 voltage sensor mutants reveal a mechanism for integrating thermal and chemical stimuli. Nat Chem Biol 3:174–182.

Voets T, Owsianik G, Nilius B (2007b) Trpm8. Handb Exp Pharmacol 179:329–344.

Watanabe H, Vriens J, Prenen J, Droogmans G, Voets T, Nilius B (2003) Anandamide and arachidonic acid use epoxyeicosatrienoic acids to activate TRPV4 channels. Nature 424:434–438.

White TC, Holleman S, Dy F, Mirels LF, Stevens DA (2002) Resistance mechanisms in clinical isolates of *Candida albicans*. Antimicrob Agents Chemother 46:1704–1713.

Xu H, Ramsey IS, Kotecha SA, Moran MM, Chong JA, Lawson D, Ge P, Lilly J, Silos-Santiago I, Xie Y, DiStefano PS, Curtis R, Clapham DE (2002) TRPV3 is a calcium-permeable temperature-sensitive cation channel. Nature 418:181–186.

Zimmermann M (1983) Ethical guidelines for investigations of experimental pain in conscious animals. Pain 16:109–110.

Zurborg S, Yurgionas B, Jira JA, Caspani O, Heppenstall PA (2007) Direct activation of the ion channel TRPA1 by Ca^{2+}. Nat Neurosci 10:277–279.

UNIVERSITAS
Miguel
Hernández

[Channels 2:6, 429-438; November/December 2008]; ©2008 Landes Bioscience

Research Paper

TRPA1 channels

Novel targets of 1,4-dihydropyridines

Otto Fajardo,† Victor Meseguer,† Carlos Belmonte and Félix Viana*

Instituto de Neurociencias de Alicante; Universidad Miguel Hernández-CSIC; Alicante Spain

†These authors contributed equally to this work.

Abbreviations: 2-APB, 2-Aminoethoxydiphenyl borate; AITC, allyl-isothiocyanate; CAPS, capsaicin; CGRP, calcitonin gene related peptide; CHO, chinese hamster ovary; CHO-TRPA1, CHO cells stably expressing TRPA1; CM, cinnamaldehyde; EGTA, ethylene glycol tetraacetic acid; KO, knock out; MO, mustard oil; NGF, nerve growth factor; NIF, nifedipine; PIP_2, phosphatidylinositol (4,5)-bisphosphate; TG, trigeminal ganglion; TRP, transient receptor potential; TRPA1, transient receptor potential type A1; TRPV1, transient receptor potential type V1; WT, wild-type

Key words: pain, Ca^{2+} channel antagonist, nociceptor, sensory transduction, nifedipine, BayK8644

Transient receptor potential type A1 (TRPA1) channels are cation permeable channels activated by irritant chemicals and pungent natural compounds. Their location in peptidergic sensory terminals innervating the skin and blood vessels makes them important effectors of vasodilator responses of neural origin. 1,4-dihydropyridines are a class of L-type calcium channel antagonists commonly used in the treatment of hypertension and ischemic heart disease. Here we show that four different 1,4-dihydropyridines (nifedipine, nimodipine, nicardipine and nitrendipine), and the structurally related L-type calcium channel agonist BayK8644, exert powerful excitatory effects on TRPA1 channels. The activation does not depend on elevated Ca^{2+} levels and cross-desensitizes with that produced by other TRPA1 agonists. The activation produced by nifedipine was reduced by camphor and the selective TRPA1 antagonist HC03001. In a subclass of mouse nociceptors expressing TRPA1 channels, assessed by responses to the TRPA1 agonist mustard oil, nifedipine also produced large elevations in $[Ca^{2+}]_i$. These responses were fully abrogated in TRPA1(-/-) mice. These findings identify TRPA1 channels as a new molecular target for the 1,4-dihydropyridine class of calcium channel modulators.

Introduction

Transient receptor potential (TRP) channels comprise an extensive family of cation permeable channels found in animals and fungi. Close to 30 members have been identified in mammals, with a wide expression profile.[1-3] Many TRP channels are involved in sensory signaling cascades, detecting physicochemical signals in the environment.[4,5] TRPA1, a TRP channel phylogenetically separate from the rest, is a remarkable example of a broad-band chemodetector, responding to many natural and synthetic irritants.[6,7] In sensory ganglia, TRPA1 co-localizes with TRPV1 in a subset of nociceptor peptidergic neurons.[8-10] Furthermore, psychophysical studies in humans indicate that activators of TRPA1 induce a burning or pricking sensation,[11-13] suggesting that the channel is involved in nociceptor signaling.

TRPA1 is also unique in the molecular mechanism of activation. Unlike traditional chemoreceptors (e.g., odorant and olfactory receptors) that can discriminate between closely related chemical structures, TRPA1 is activated by structurally different molecules with high chemical reactivity. These highly electrophilic compounds interact with thiol groups in side chains of intracellular cysteines in the TRPA1 molecule, forming covalent bonds.[14,15] These interactions give rise to long lasting channel openings that can be reversed by reducing agents such as dithiothreitol. The growing list of TRPA1 activators includes allyl isothiocyanate (AITC) (mustard oil), cinnamaldehyde (cinnamon oil), methyl salicilate (wintergreen oil), allicin (present in garlic extract), eugenol (cloves), gingerol (ginger), N-ethylmaleimide, 2-APB, trinitrophenol, and a number of volatile irritants, such as 2-propenal (acrolein) and 2-pentenal.[16-18]

Other, nonelectrophilic substances, such as icilin and Δ9-tetrahydrocannabinol also activate TRPA1.[8,9,19] Mutational studies have established that the activation by icilin is not dependent on covalent interactions and probably relies on a more traditional binding pocket.[14,19] Menthol and structurally related compounds have a dual action on TRPA1, activation at low concentrations and channel block at higher doses.[20,21] Calcium ions and other divalents (e.g., Mn^{2+}) activate directly TRPA1.[22,23] This interaction depends on an EF-hand motif in the N terminus of TRPA1. A soluble cytosolic factor appears to be essential for normal TRPA1 function.[24] A notable study on TRPA1 knockout mice has clarified the unique chemical sensitivity of this ion channel.[17] These animals were completely insensitive to mustard oil and allicin. In addition, these animals had pronounced deficits in bradykinin-evoked nociceptor

*Correspondence to: Félix Viana; Instituto de Neurociencias de Alicante; Universidad Miguel Hernández-CSIC; Apartado 18; San Juan de Alicante 03550 Spain; Tel.: +34.96.591.9211; Fax: +34.96.591.9561; Email: felix.viana@umh.es

Submitted: 07/04/08; Revised: 10/03/08; Accepted: 10/03/08

Previously published online as a *Channels* E-publication:
http://www.landesbioscience.com/journals/channels/article/7126

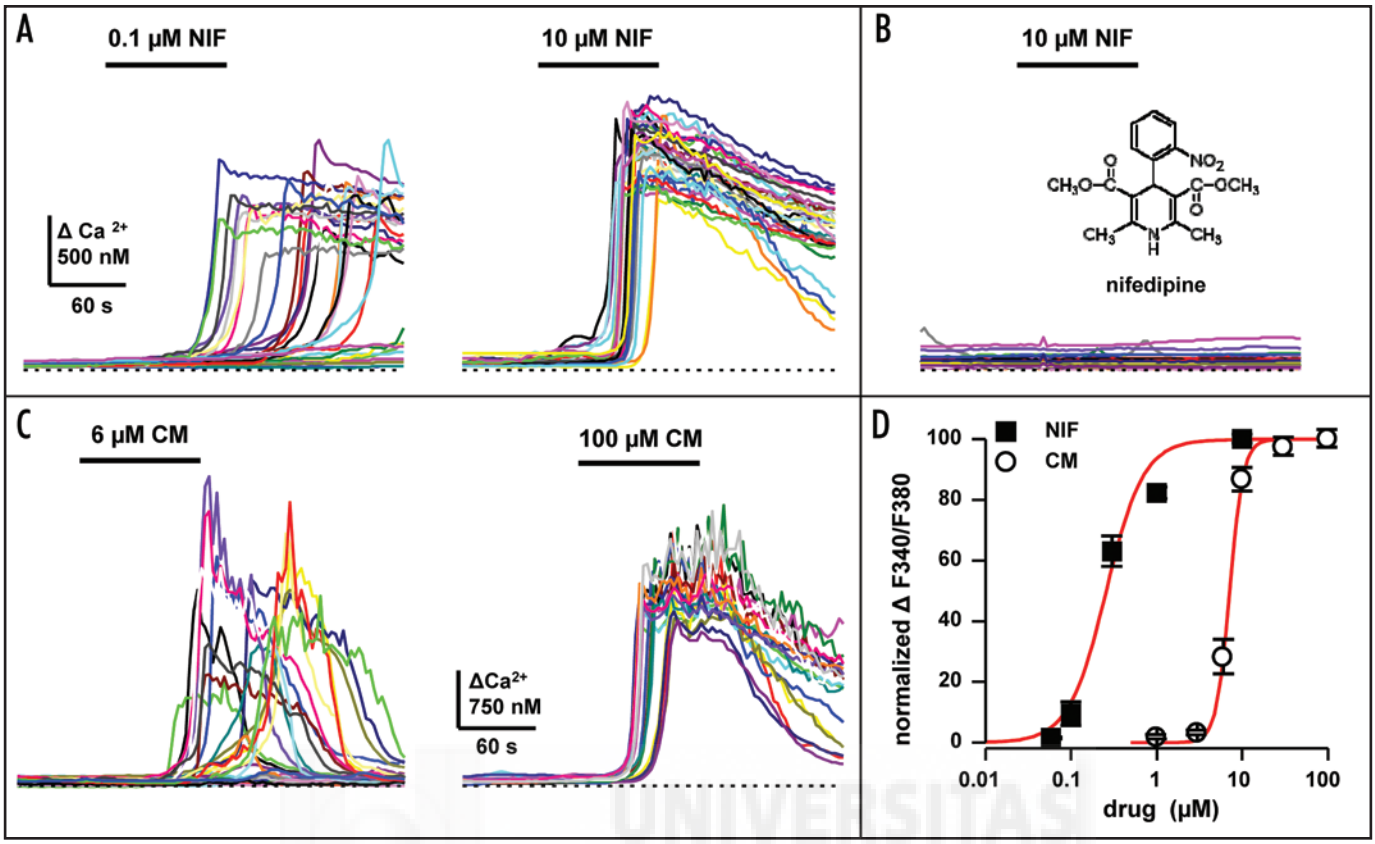

Figure 1. Nifedipine activates a calcium influx pathway in TRPA1-expressing cells. (A) Experimental recordings of the effects of 0.1 and 10 M nifedipine (NIF) on $[Ca^{2+}]_i$ levels in TRPA1-CHO cells. (B) Lack of responses to 10 mM nifedipine in standard CHO cells. Same calibration bars as in (A). (C) Effects of 6 and 100 M cinnamaldehyde (CM) on $[Ca^{2+}]_i$ levels in TRPA1-CHO cells. (D) Dose-response curves for nifedipine and CM. Each data point corresponds to the average of >25 cells. The solid lines represent the fit to the Hill equation. In the case of nifedipine, the fit to the data yielded an EC_{50} = 0.40 ± 0.02 M and a Hill slope of 2.1 ± 0.1. In the case of CM, the fit to the data yielded an EC_{50} = 6.50 ± 0.35 M and a Hill slope of 4.4 ± 0.4.

excitation, highlighting a fundamental role for TRPA1 in neurogenic inflammatory pain.[17,18,25]

Allicin, AITC and Δ9-tetrahydrocannabinol, three structurally unrelated agonists of TRPA1 channels, are known to induce arterial vasorelaxation.[9,26] The mechanism involves release of CGRP from peptidergic terminals innervating peripheral vessels.[27-29]

We asked whether other clinically relevant hypotensive agents might activate TRPA1 channels as well. Here we show that 1,4-dihydropyridines, a broad class of L-type calcium channel antagonists,[30,31] extensively used in the treatment of hypertension and angina pectoris, exert powerful excitatory effects on recombinant and native TRPA1 channels. These findings expand the spectrum of molecular targets for 1,4-dihydropyridines.

Results

Nifedipine evokes $[Ca^{2+}]_i$ responses in CHO-TRPA1 cells. Using CHO cells expressing the mouse variant of TRPA1, we tested the effects of nifedipine on $[Ca^{2+}]_i$ levels. As shown in Figure 1A, nifedipine produced a dose-dependent $[Ca^{2+}]_i$ elevation from a baseline temperature of 34°C. At low doses of agonist (e.g., 100 nM) only a fraction of cells responded with a variable latency. These responses were characterized by an initial slow rise and, upon reaching a certain $[Ca^{2+}]_i$ level, a fast fully reversible Ca^{2+} transient. At higher concentrations of nifedipine (e.g., 10 μM) all cells responded with a nearly identical time course: a rapid phase at nearly constant latency and a more sustained plateau. The elevation in $[Ca^{2+}]_i$ produced by 10 μM nifedipine averaged 2227 ± 86 nM (n = 83). In contrast, application of 10 μM nifedipine to standard CHO cells had no measurable effect on $[Ca^{2+}]_i$ levels (Fig. 1B). The mean elevation for each concentration of nifedipine was fitted to the Hill equation and had an ED_{50} of 0.4 ± 0.02 μM (Fig. 1D).

For comparison, we tested the effects of cinnamaldehyde (CM), a specific activator of TRPA1 channels. During identical protocols, CM also produced a dose-dependent elevation in $[Ca^{2+}]_i$ (Fig. 1C), with detectable effects requiring a concentration >1 μM. In the case of CM, the ED_{50} was 6.5 ± 0.35 μM (Fig. 1D), demonstrating that nifedipine is a more potent activator of TRPA1 channels than CM. The mean $[Ca^{2+}]_i$ elevation produced by 100 μM CM averaged 2940 ± 198 nM (n = 53).

In the absence of extracellular Ca^{2+}, the elevation in $[Ca^{2+}]_i$ produced by nifedipine was fully abrogated, indicating that it depends on activation of a Ca^{2+} influx pathway (Fig. 2A). Moreover, readdition of Ca^{2+} in the absence of agonist triggered a response (not shown), suggesting that activation of the channel is very sustained.

Camphor is a blocker of TRPA1 channels.[32,33] As shown in Figure 2B, application of 2 mM camphor in the continuous presence of 1 μM nifedipine produced a notable inhibition of the $[Ca^{2+}]_i$ elevations triggered by the agonist. The mean inhibition was 29.6 ± 1.3%

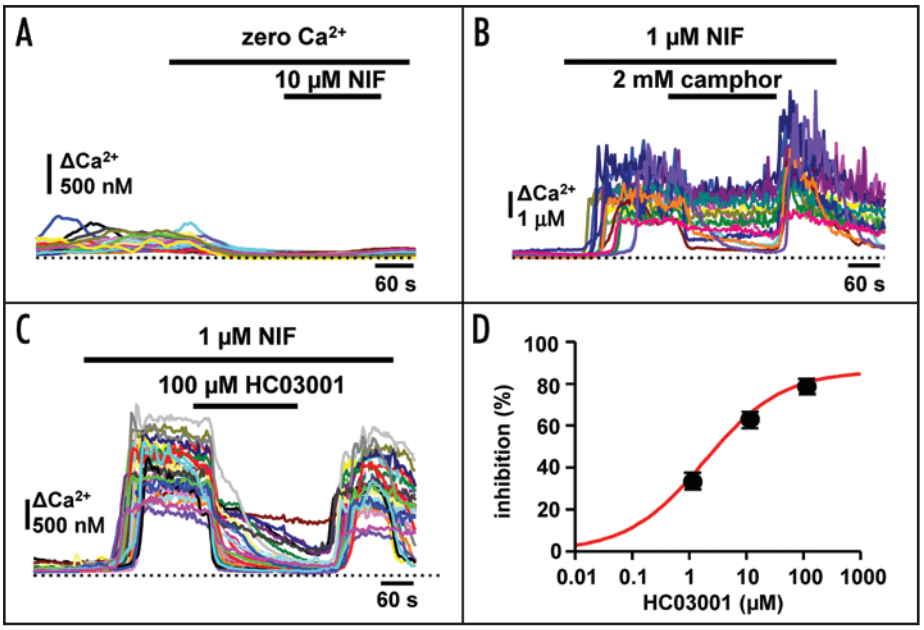

Figure 2. Dependence of nifedipine responses on extracellular Ca^{2+} and block by TRPA1 antagonists. (A) Application of 10 μM nifedipine in the absence of external Ca^{2+} produced no measurable $[Ca^{2+}]_i$ elevation. (B) During prolonged applications of 1 μM nifedipine, addition of 2 mM camphor produced a reversible reduction in $[Ca^{2+}]_i$ levels. (C) Inhibition of $[Ca^{2+}]_i$ responses to 1 μM nifedipine by 100 μM HC03001. (D) Dose-response curve of inhibitory effects of HC03001 on nifedipine-evoked $[Ca^{2+}]_i$ responses. Each data point corresponds to the average of >25 cells. The solid lines represent the fit to the Hill equation. The IC_{50} was 1.80 ± 0.00 μM.

(n = 89) and was fully reversible upon wash. Recently, a novel, highly selective antagonist of TRPA1 channels has been identified, with blocking actions on recombinant and native TRPA1 channels.[33,34] This compound, HC03001, produced a potent (IC_{50} 1.8 μM) and fully reversible inhibition of nifedipine-evoked $[Ca^{2+}]_i$ elevations (Fig. 2C and D).

These results indicate that nifedipine potently activates a Ca^{2+} influx pathway in TRPA1 expressing cells that can be inhibited by selective TRPA1 antagonists.

Activation of TRPA1 by other 1,4-dihydropyridines. We used fluorescence Ca^{2+} imaging to screen the effects of other clinically relevant 1,4-dihydropyridines on TRPA1 activity. All compounds tested, which included nimodipine (ED_{50} = 0.8 ± 1.3 μM), nicardipine (ED_{50} = 0.5 ± 0.07 μM) and nitrendipine (ED_{50} = 3.8 ± 0.3 μM) produced a dose-dependent $[Ca^{2+}]_i$ elevation from a baseline temperature of 34°C. Representative responses at 10 μM are shown in Figure 3. Their characteristics are virtually identical to those described for nifedipine. (±)BayK8644, a dihydropyridine derivative that functions as a calcium channel agonist rather than an antagonist,[35] also activated TRPA1 dose-dependently (ED_{50} = 32.7 ± 0.2 μM), suggesting that the agonist effect of dihydropyridines on TRPA1 is independent of its action on L-type calcium channels (Fig. 4A and B). None of these drugs had an effect on naive CHO cells (not shown).

The *R*-(+) and *S*-(-) enantiomers of BayK8644 function as antagonist and agonist of L-type Ca^{2+} channels respectively.[36] Thus, we investigated their action on TRPA1. As shown in Figure 4 both enantiomers displayed dose-dependent activating effects upon TRPA1, with similar potency: ED_{50} = 20.8 ± 1.5 μM for R-BayK8644 and 41.5.8 ± 1.1 μM for R-BayK8644.

We also tested the effects of pyridine, a compound with a related chemical core. Pyridine at 1 mM produced no effects in CHO-TRPA1 cells. Diltiazem, a structurally unrelated Ca^{2+}-channel antagonist belonging to the phenylalkylamine class, had non-specific actions, evoking calcium rises only at very high concentrations (ED_{50} = 1.6 mM) in both CHO-TRPA1 and naive CHO cells (not shown).

Activation of TRPA1 currents by nifedipine. We used whole-cell patch-clamp recordings to investigate the effects of 10 μM nifedipine on TRPA1-mediated currents in CHO cells. Currents were evoked by voltage ramps from -150 to +150 mV, delivered every 5 s, and the current evoked at +/-100 mV was plotted vs. time (Fig. 5A). Application of nifedipine activated a non selective, modestly outwardly rectifying current, with characteristics typical of TRPA1 channels (Fig. 5B). The nifedipine-sensitive current had a slow rise time, reversed at 2.3 ± 0.5 mV (n = 8) and showed a decreased conductance at more positive potentials.[37] In contrast to results obtained with $[Ca^{2+}]_i$ imaging, the current evoked by nifedipine showed marked desensitization during continuous application of the drug.

For comparison, CHO-TRPA1 cells were probed with the reference TRPA1 agonist cinnamaldehyde (CM). As shown in Figure 5A and B, 200 μM CM activated a current with characteristics identical to the nifedipine-sensitive current, suggesting that the former is mediated by activation of TRPA1 channels. Furthermore, BayK8644 also activated a similar current (Fig. 5A and B). Mean current densities activated by 10 μM nifedipine, 200 μM CM and 30 μM BayK8644 were similar (Fig. 5E), consistent with a more potent agonist effect of nifedipine observed in the $[Ca^{2+}]_i$ imaging data.

To characterize the effects of nifedipine on TRPA1 channel gating in more detail, we used a protocol of rectangular voltage pulses (300 ms duration) to potentials varying between -150 and +150 mV, followed by a constant step to -150 mV for 150 ms. As shown in Figure 5C, nifedipine activated a sustained current with modest time-dependent inactivation at very positive potentials. The slowly deactivating inward tail current at -150 mV increased non-monotonically with depolarization, displaying a dent at depolarized potentials, consistent with a partial inactivation of the current at positive voltages. Analysis of tail currents indicates that nifedipine produces a strong leftward shift of the activation curve, which results in significant channel activity at more physiological voltages (Fig. 5D). Taken together, these results suggest that nifedipine modulates the voltage-dependent activation of TRPA1.[20]

Further evidence for the identity between nifedipine- and CM-activated currents was obtained during cross-desensitization experiments. As shown in Figure 6A, application of a nifedipine prepulse for 180 s produced an almost full inhibition of CM-evoked currents. The density of CM-evoked current, measured at +100 mV, was 75.1 ± 28.4 pA/pF (n = 5) in the absence of a nifedipine prepulse and 1.1 ± 0.5 pA/pF following nifedipine ($p < 0.05$, n = 5) (Fig. 5B).

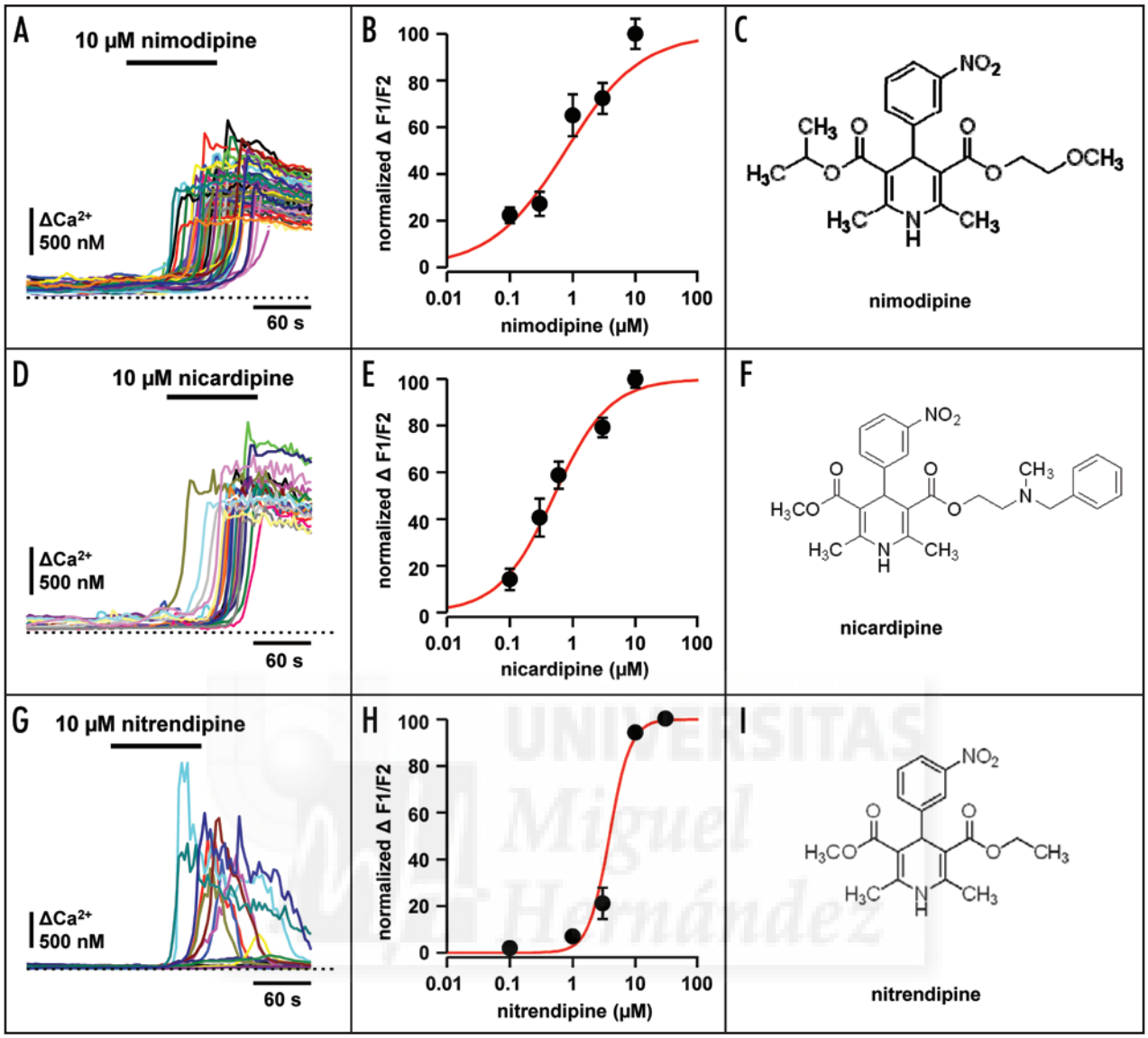

Figure 3. Activation of TRPA1 by different 1,4-dihydropyridines. (A, D and G) Elevations in $[Ca^{2+}]_i$ produced by applications of 10 μM nimodipine, 10 μM nicardipine, 10 μM nitrendipine. Note the variable effectiveness of the different dihydropyridines. (B, E and H) Dose-response curves for nimodipine, nicardipine, nitrendipine. Each data point corresponds to the average of >25 cells. The solid lines represent the fit to the Hill equation. The ED_{50} was 0.8 ± 1.3 μM for nimodipine; 0.5 ± 0.07 μM for nicardipine, 3.8 ± 0.3 μM for nitrendipine. (C, F and I) Chemical structure of nimodipine, nicardipine and nitrendipine.

Desensitization of nifedipine-sensitive current is not mediated by intracellular Ca^{2+}. TRPA1 channels are calcium permeable and intracellular calcium ions have dual effects on their gating: They produce a direct activation and also desensitization.[9,22-24,38] To test for the possible involvement of elevated $[Ca^{2+}]_i$ ions in the desensitization of the current evoked by nifedipine, we performed recordings in the absence of external Ca^{2+} plus 1 mM EGTA, and with 10 mM EGTA in the pipette. As shown in Figure 7A, activation of the current by nifedipine was still observed under buffered Ca^{2+} conditions. Furthermore, as shown in Figure 7B the time course or current desensitization in the absence of external Ca^{2+} was similar to results obtained in control records (τ = 100 ± 73 s in control vs 105 ± 27 s in zero Ca^{2+}, n = 4; p = 0.9), suggesting that elevation in $[Ca^{2+}]_i$ is not necessary for current activation, neither to trigger the desensitization.

Nifedipine activates TRPA1 channels in trigeminal sensory neurons. TRPA1 is strongly expressed in a subset of nociceptor sensory neurons.[9,39] Thus, we tested the effects of nifedipine in cultured adult mouse trigeminal sensory neurons. As shown in Figure 8A, nifedipine (10 μM) produced a robust $[Ca^{2+}]_i$ elevation in a fraction of TG neurons. Out of 117 neurons tested, 10 μM nifedipine elevated $[Ca^{2+}]_i$ in 48 of them (41%). Average $[Ca^{2+}]_i$ elevation by nifedipine was 654 ± 82 nM (Fig. 8B). The same neurons were probed with 100 μM mustard oil (MO), a specific TRPA1 agonist.[17] There was a strong correlation in sensitivity to both compounds. All nifedipine-sensitive neurons were activated by MO and 77% responded to both agonists. A large fraction (62%) of nifedipine- and MO-sensitive neurons were also activated by the TRPV1 agonist capsaicin (500 nM), but only 68% of all capsaicin-sensitive neurons were responsive to nifedipine. A colocalization between TRPA1 and TRPV1 in DRG and trigeminal

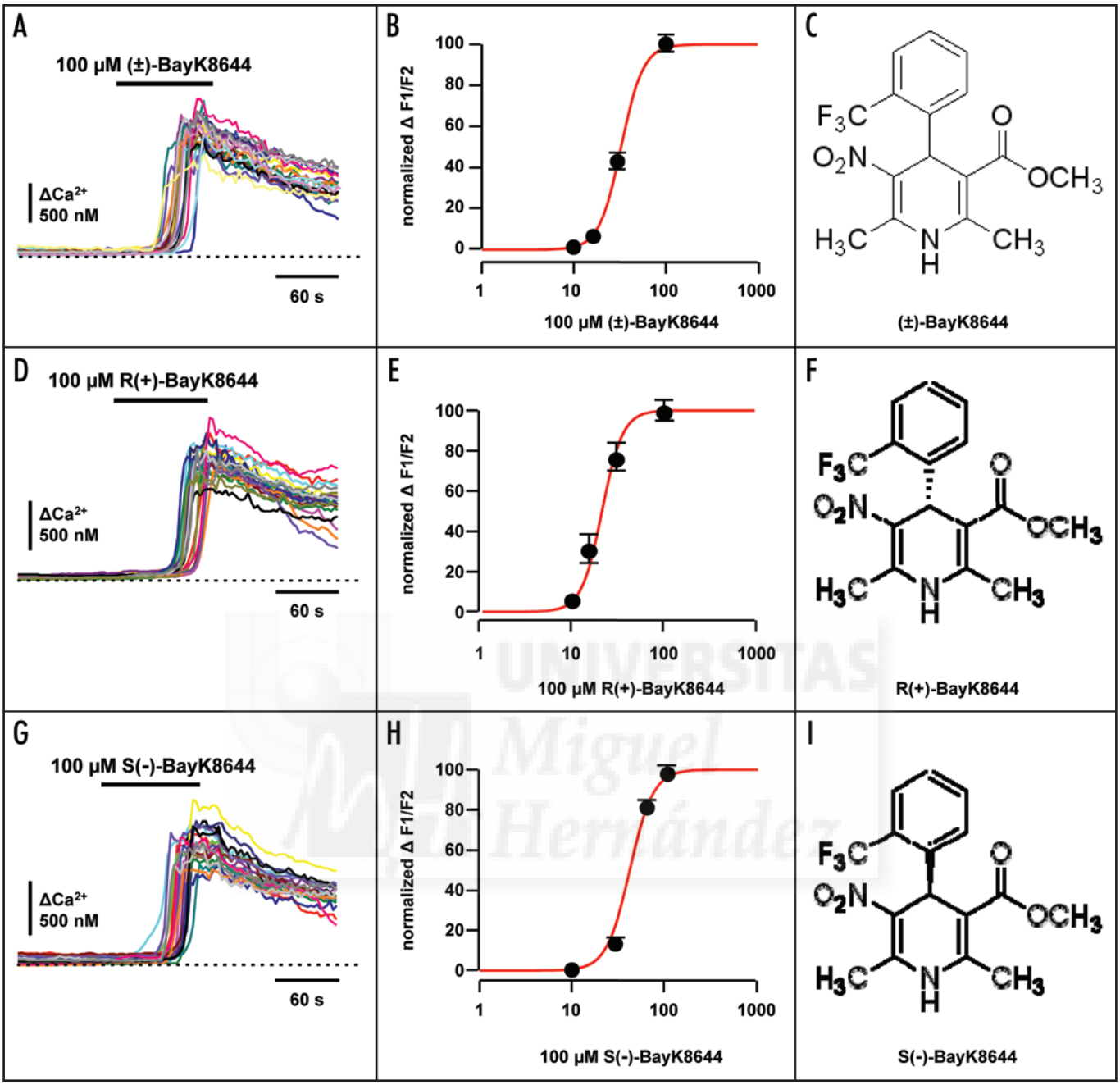

Figure 4. Activation of TRPA1 by BayK8644 lacks stereoselectivity. (A, D and G) Elevations in $[Ca^{2+}]_i$ produced by applications of 100 μM (±)BayK8644, 100 μM R-(+) BayK8644 and 100 μM S-(-) BayK8644 in TRPA1 expressing CHO cells. (B, E and H) Dose-response curves for (±)BayK8644, R-(+) BayK8644 and S-(-) BayK8644. Each data point corresponds to the average of >25 cells. The solid lines represent the fit to the Hill equation. The ED_{50} was and 32.7 ± 0.2 μM for (±)BayK8644, 20.8 ± 1.5 μM for R-(+) BayK8644 and 41.5 ± 1.1 μM for S-(-) BayK8644. (C, F and I) Chemical structure of (±)BayK8644, R-(+) BayK8644 and S-(-) BayK8644 respectively.

sensory neurons has been noted previously.[8,40] Figure 8D summarizes these relationships in a Venn diagram.

To verify that nifedipine responses were mediated by activation of TRPA1 channels, we repeated the same protocol in TG sensory neurons obtained from TRPA1 knock out mice.[25] As shown in Figure 8C, in TRPA1(-/-) animals the responses of sensory neurons to nifedipine and/or mustard oil were abolished. In contrast, the amplitude of responses and the percentage of capsaicin-sensitive neurons were unchanged. Figures 8E–H shows a summary of responses to the three agonists (nifedipine, MO and capsaicin), represented as cumulative probability histograms and percentage of responsive neurons histogram.

These results demonstrate that nifedipine-evoked $[Ca^{2+}]_i$ signals in nociceptive trigeminal sensory neurons are mediated exclusively by activation of native TRPA1 channels.

Discussion

Here we show that several clinically relevant 1,4-dihydropyridines can act as potent agonists of recombinant and native TRPA1 channels. Three of them, nifedipine, nimodipine and nicardidipine, had

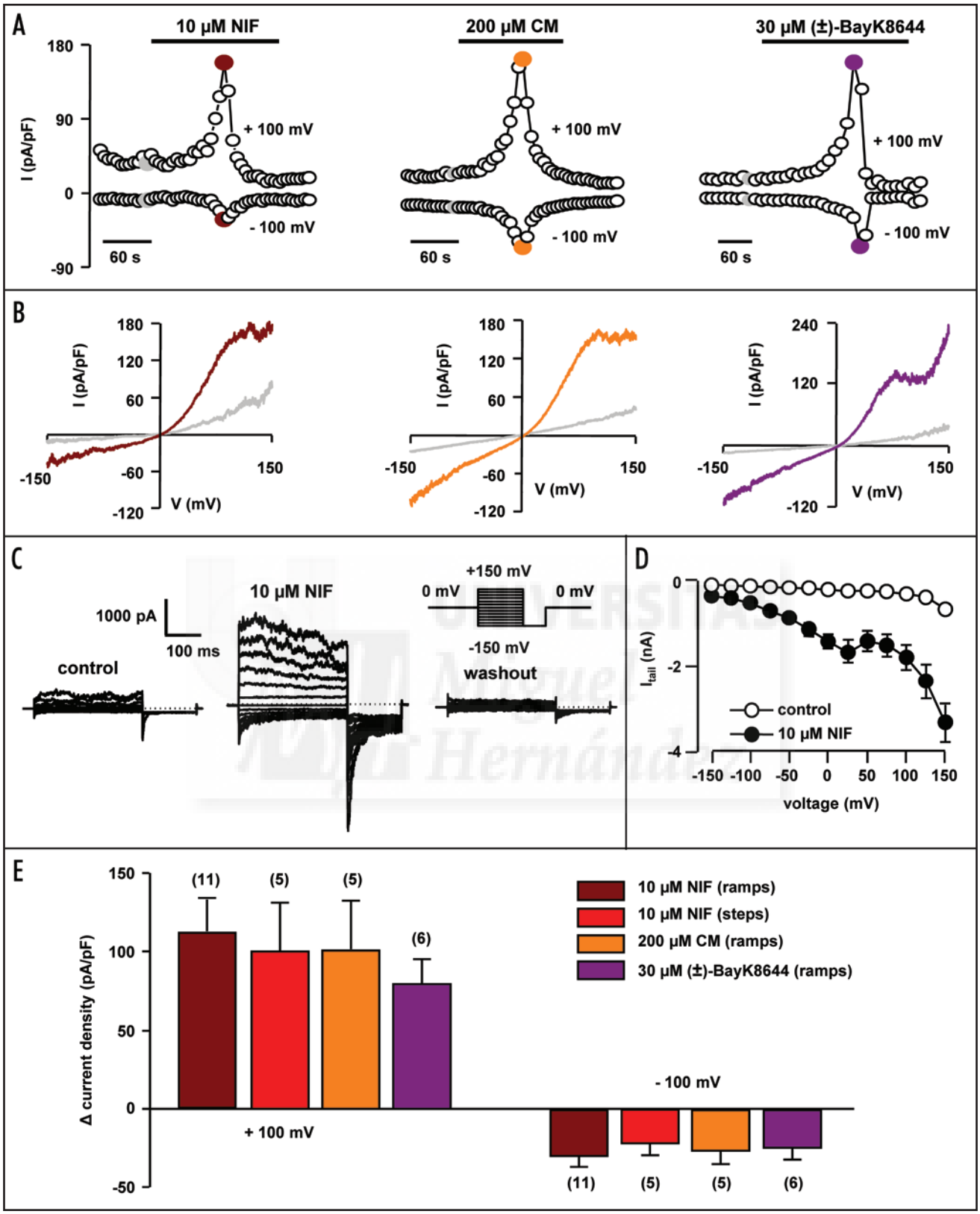

Figure 5. Activation of similar TRPA1-dependent currents by 1,4-dihydropyridines and CM. (A) Time course of whole-cell current during application of 10 μM nifedipine, 200 μM cinnamaldehyde (CM) and 30 μM (±) BayK8644. Note the full desensitization of the current in the continuous presence of agonist. (B) Current-voltage relationships of whole-cell currents in control solution (grey traces) and in the presence of 10 μM nifedipine, 200 μM CM and 30 μM (±) BayK8644. The traces correspond to the points marked with filled circles in (A). (C) Currents in response to 300-ms voltage steps ranging from -150 to +150 mV before (left), during (center) and after (right) addition of 10 μM nifedipine. (D) Tail currents at -150 mV in control solution and in the presence of 10 μM nifedipine. Data represent the average of five cells using the step protocol shown in (C). (E) Average current density at +100 and -100 mV evoked by 10 μM nifedipine, 200 μM CM and 30 μM (±) BayK8644. Each cell was exposed to only one agonist.

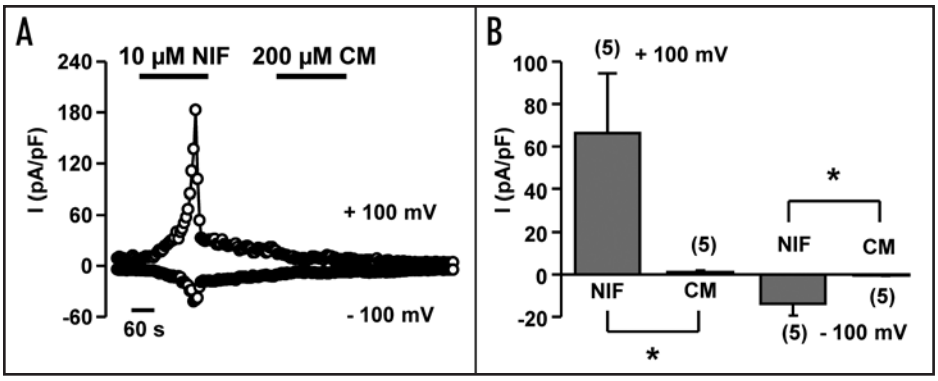

Figure 6. Cross desensitization between nifedipine and CM activation of TRPA1 currents. (A) Time course of whole-cell current during consecutive applications of 10 μM nifedipine (NIF) and 200 μM CM to the same CHO-TRPA1 cell. Note the lack of response to CM following activation of the current by nifedipine. (B) Summary bar graph of mean current density during consecutive applications of 10 μM nifedipine and 200 μM CM.

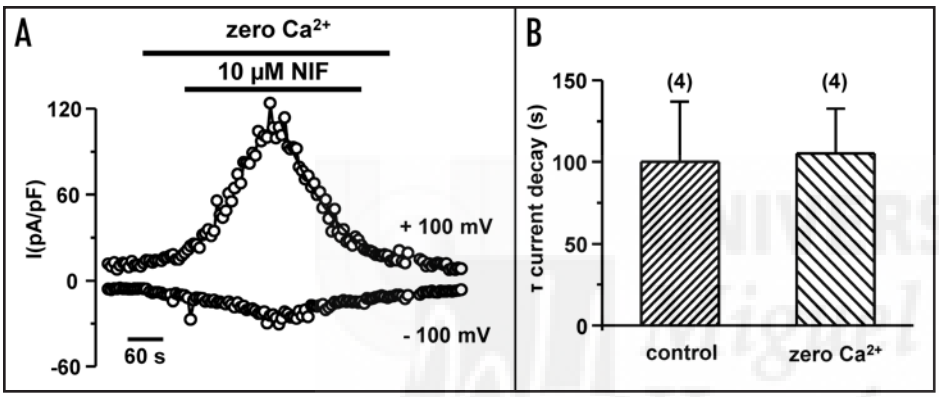

Figure 7. Desensitization of nifedipine-sensitive current is not mediated by intracellular Ca^{2+}. (A) Time course of whole-cell current during application of 10 μM nifedipine in the absence of external Ca^{2+} and 10 mM intracellular EGTA. Note the fast desensitization of the current in the continuous presence of agonist. (B) Time constant of current decay in control conditions (2.4 mM Ca^{2+}) and in the absence of external Ca^{2+}. The mean values were not statistically different (p = 0.9).

ED_{50} values below 1 μM, indicating that 1,4-dihydropyridines are one of the most potent class of TRPA1 agonists reported so far,[7] surpassing the potency of cinnamaldehyde and mustard oil, two reference agonists for TRPA1 channels. The absence of responses to nifedipine in sensory neurons obtained from TRPA1(-/-) mice indicates that these excitatory effects of dihydropyridines are fully explained by actions on TRPA1 channels.

The relevance of our finding derives from the widespread clinical use of 1,4-dihydropyridines as L-type calcium channel antagonists. Indeed, the 1,4-dihydropyridine nucleus serves as the scaffold for many important cardiovascular agents,[30,31] used in the treatment of hypertension and angina pectoris. Our work suggests that some of these actions may also involve the activation of TRPA1 channels in addition to the known actions on L-type calcium channels. In this context, it is relevant that other TRPA1 agonists, including Δ9-tetrahydrocannabinol, allicin and AITC, have been shown to induce arterial vasorelaxation by a TRPA1-dependent mechanism.[9,26] A common, adverse side effect of 1,4-dihydropyridines treatment is the appearance of peripheral leg edema caused by fluid extravasation.[41] Besides the direct vasodilatory actions of 1,4-dihydropyridines on vascular smooth muscle, it is possible that activation by dihydropyridines of TRPA1 channels in peptidergic sensory terminals cause release of vasoactive substances and alterations in vascular permeability and contribute to this unwanted effect of 1,4-dihydropyridine treatment.

Despite the powerful activation of TRPA1 by all dihydropyridines tested, no signs of behavioral pain have been observed following local application of nifedipine to the hind paw of mice (unpublished observations).[42] This data agree with the low pungency and irritation profile of dihydropyridines in humans,[35] when compared to cinnamaldehyde. Because nifedipine blocks electrically evoked Ca^{2+} transients in peripheral sensory nerves,[43] it is possible that these potent inhibitory actions on L-type Ca^{2+} channels prevent the propagation of electrical impulses at nerve terminals, despite a powerful TRPA1 activation. In sensory neurons stimulated with TRP channel openers, action potential-dependent calcium influx, through voltage-gated Ca^{2+} channels, is much more significant than direct flux through open TRP channels.[44] In addition, dihydropyridines block activity-dependent substance P release.[45] This effect would minimize the axonal reflex and the release of vasoactive substances (e.g., substance P) from nociceptors which are known to occur after TRPA1 activation.[46] These, so called, neurogenic inflammation recruits immunocompetent cells and upregulates growth factors exacerbating the pain. Finally, because elevated intracellular Ca^{2+} activates TRPA1 channels directly,[22,23] by blocking calcium influx, dihydropyridines may prevent the potentiating feedback loop of calcium on TRPA1 activity.

The molecular mechanism of action of nifedipine on TRPA1 channels needs to be worked out. The relatively high Hill slopes for dihydropyridines activation of TRPA1 don't necessarily reflect a cooperative interaction between drug and receptor and may be due to the calcium-dependent activation of TRPA1.[22,23] All dihydropyridines tested exerted an activating effect, albeit with different potency. Many electrophilic substances, such as cinnameldehyde, AITC and acrolein activate TRPA1 by covalent modification of cysteines located in the intracellular N-terminus of the protein.[14,15] Because of their physicochemical profile, it is unlikely that 1,4-dihydropyridines act by covalent binding. Other nonreactive substances also activate TRPA1, including menthol,[20] icilin,[19] trinitrophenol[47] and clotrimazole.[48] Recently, it was shown that residues in transmembrane domain 5 determine the sensitivity of TRPA1 to menthol.[49]

In contrast to the actions of icilin,[19,22] calcium is not essential for the excitatory actions of dihydropyridines. Nifedipine showed strong cross-desensitization with CM and MO, both in recombinant and native channels. CM also desensitizes the stimulatory effects

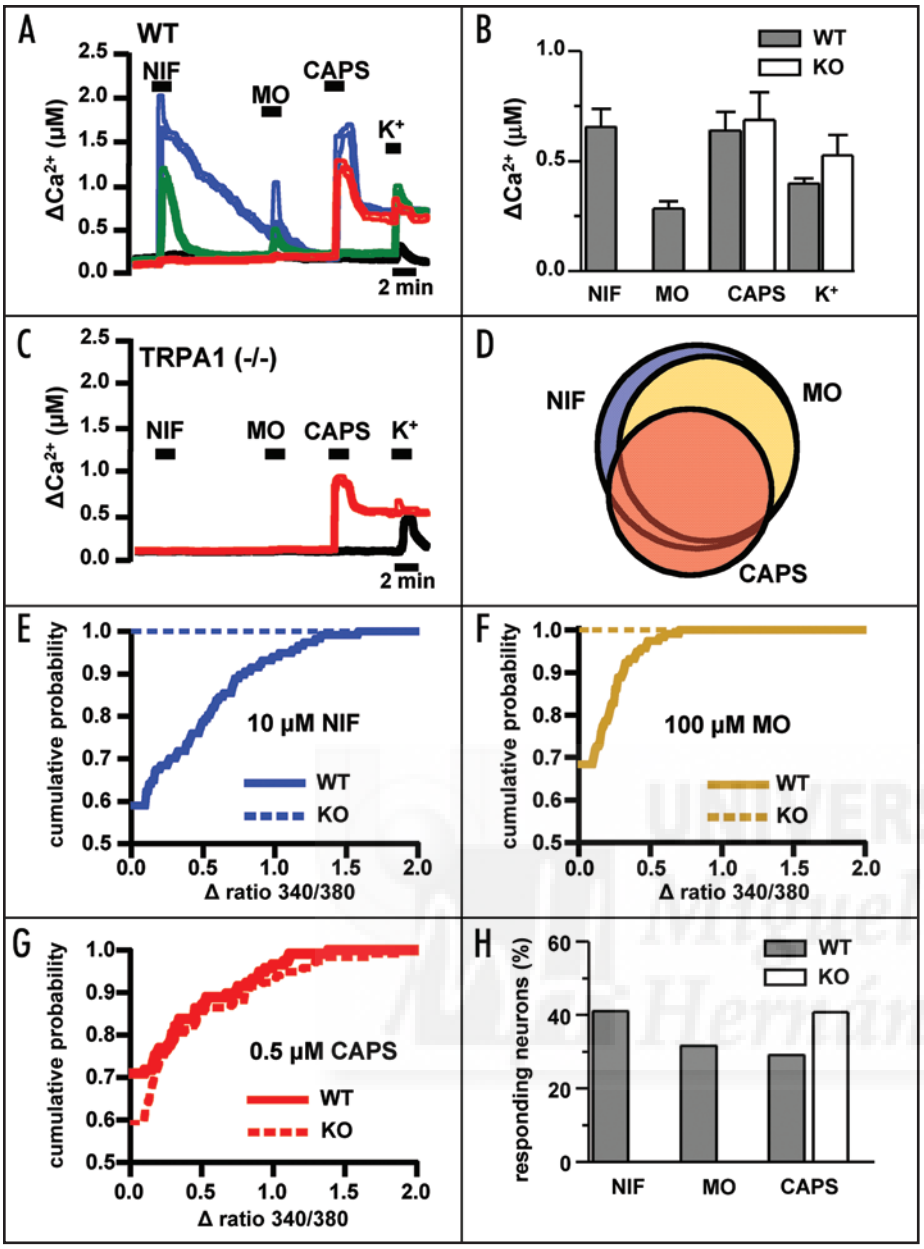

Figure 8. Nifedipine activates TRPA1 channels in trigeminal sensory neurons. (A) Representative ratiometric $[Ca^{2+}]_i$ responses to 10 μM nifedipine (NIF), 100 μM mustard oil (MO), 0.5 μM capsaicin (CAPS) and 60 mM K^+ in trigeminal (TG) sensory neurons from wild-type mice. Note that the two nifedipine-sensitive neurons were also MO sensitive. (B) Average $[Ca^{2+}]_i$ elevations produced by 10 μM nifedipine, 100 μM mustard oil, 0.5 μM capsaicin and 60 mM K^+ in WT and TRPA1(-/-) mice TG sensory neurons. (C) Ratiometric $[Ca^{2+}]_i$ responses to 10 μM nifedipine, 100 μM mustard oil, 0.5 μM capsaicin and 60 mM K^+ in TG sensory neurons from TRPA1 knockout mice. Note the absence of responses to nifedipine and mustard oil. (D) Venn diagram illustrating the overlap in the responses to the three agonists in wildtype mice. (E–G) Cumulative distribution of ratiometric $[Ca^{2+}]_i$ responses to 10 μM nifedipine, 100 μM mustard oil and 0.5 μM capsaicin in wild-type (solid lines) and TRPA1(-/-) mice (dashed lines). (H) Percentage of TG neurons responsive to nifedipine, MO and capsaicin in wild-type and TRPA1(-/-) mice.

of menthol.[20] The extent and time course of acute desensitization of TRPA1 channels by chemical agonists is surprisingly variable in the literature.[14,38,40] These differences have been ascribed to various mechanisms, including $[Ca^{2+}]_i$ levels, differences between recombinant and native channels and changes in cellular PIP_2 levels. The Ca^{2+}-independent desensitization of TRPA1 by nifedipine we observed is similar to the one observed by Akopian et al., during application of mustard oil.[40] In our hands, responses in intact cells (evaluated with Ca^{2+} imaging) desensitized much less than during whole-cell recordings, suggesting that, under physiological conditions, activation of TRPA1 by dihydropyridines may lead to persistent Ca^{2+} influx. The difference in the time course of responses may be explained by the dependence of TRPA1 activation on intracellular polyamines that would wash away during whole cell dialysis.[24]

Besides their potential clinical interest as TRPA1 modulators, 1,4-dihydropyridines may also become useful tools in dissecting out the molecular determinants of mechanoelectrical transduction by inner ear hair cells, an unsettled topic.[50] There is conflicting experimental evidence for the role of TRPA1 or TRPA1-like channels in this process.[38,51] In view of our findings, it would be interesting to investigate the effects of 1,4-dihydropyridines on hair cell transducer currents.

In summary, we identified TRPA1 as a novel molecular target of 1,4-dihydropyridines. Given the wide clinical use of 1,4-dihydropyridines and the key role of TRPA1 channels in nociceptor signaling and pain, further investigations on the interaction between both molecules should be fruitful and may lead to new findings with therapeutic benefits in the future.

Materials and Methods

Neuronal culture. All experimental procedures concerning animals were carried out according to the Spanish Royal Decree 223/1988 and the European Community Council directive 86/609/EEC.

Neuronal culturing methods were similar to those used previously.[52] Trigeminal ganglia were isolated from young adult (postnatal months 1–3) OF1 wild-type (WT) and TRPA1 knockout (KO) mice[25] and incubated for one hour with 0.07% collagenase XI + 0.3% Dispase at 37°C. Thereafter, ganglia were mechanically dissociated and cultured in MEM with Earle's BSS and L-Glutamine (Invitrogen) supplemented with 10% fetal bovine serum (Invitrogen), 1% MEM vitamin solution (Invitrogen), 100 μg/ml penicillin/streptomycin and 100 ng/ml NGF. Cells were plated on poly-l-lysine-coated glass cover slips and used after one day in culture.

Cell culture. Chinese hamster ovary cells (CHO) were cultured in DMEM containing 10% of fetal bovine serum, 2% glutamax (Invitrogen), 1% non-essential amino acids (Invitrogen) and 200 μg/ml penicillin/streptomycin. An inducible CHO cell line stably expressing mouse TRPA1 channels was kindly provided by Ardem

Patapoutian (The Scripps Research Institute, USA). These cells were cultured as described in Story et al.[8] Expression of TRPA1 was induced by application of 0.25–0.5 μg/ml tetracycline 4–18 hours prior to recording.

Calcium imaging. Calcium imaging experiments were conducted with the fluorescent indicator Fura-2. Cells were incubated with 5 μM Fura-2-acetoxymethylester (Molecular Probes Europe, Netherlands) for 60 min at 37°C. Fluorescence measurements were made with a Zeiss Axioskop FS (Germany) upright microscope fitted with an ORCA ER CCD camera (Hamamatsu, Japan). Fura-2 was excited at 340 nm and 380 nm (excitation time 200 or 300 ms) with a rapid switching monochromator (TILL Photonics, Germany). Mean fluorescence intensity ratios (F340/F380) were displayed online with Metafluor software (Molecular Devices, PA). The bath solution, from here on referred to as "control solution", contained (in mM): 140 NaCl, 3 KCl, 2.4 $CaCl_2$, 1.3 $MgCl_2$, 10 HEPES and 10 glucose, and was adjusted to a pH of 7.4 with NaOH. Bath temperature was maintained at 34–36°C by a custom-built Peltier device.

Electrophysiology. Whole-cell voltage-clamp recordings were performed with standard patch-pipettes (3–5 MΩ) made of borosilicate glass capillaries (Harvard Apparatus Ltd., UK) and contained (in mM): 140 NaCl, 5 CsCl, 10 EGTA, 10 HEPES, (305 mOsm/kg; pH 7.4, adjusted with NaOH). The control bath solution (30 ± 1°C) was the same as for calcium imaging experiments. During calcium-free experiments the bath solution was as follows: 140 NaCl, 3 KCl, 1.3 $MgCl_2$,10 HEPES, 1 EGTA, 10 Glucose. Current signals were recorded with a Multiclamp 700B patch-clamp amplifier (Molecular Devices). Stimulus delivery and data acquisition were performed using pClamp 9 software (Molecular Devices). Current development was monitored with repetitive (0.2 Hz) injections of 1-s-duration voltage ramps from -150 to +150 mV.

Electrophysiological data were analyzed with WinASCD software written by Dr. Guy Droogmans (ftp://ftp.cc.kuleuven.ac.be/pub/droogmans/winascd.zip) and Origin 7.0 (OriginLab Corporation).

Chemical modulators. Nifedipine (RBI), nicardipine (Sigma), nitrendipine (Miles Pharmaceutical), nimodipine (Sigma), (±) BayK8644 (methyl 1,4-dihydro-2,6-dimethyl-3-nitro-4-(2-trifluoromethylphenyl)-pyridine-5-carboxylate) and the optical enantiomers, (+)BayK8644 and (-)BayK8644 (Tocris), diltiazem (Sigma), Pyridine (Sigma), allyl isothiocyanate (Sigma) and cinnamaldehyde (Sigma) were stored as stock solutions and diluted immediately before the experiments. HC03001 was supplied by Hydra Biosciences (Cambridge, USA). All experiments were performed under very low ambient light levels, to minimize the potential degradation of dihydropyridines.

Data analysis. Data are reported as mean ± standard error of the mean. Dose-response data were normalized to the maximum response of the drug in each case and then were fitted with the Hill equation using the Levenberg-Marquardt method implemented in Origin 7.0 software. The standard errors of the mean were used as weights in fitting where applicable. When comparing two means, statistical significance ($p < 0.05$) was assessed by Student's two-tailed t-test.

Acknowledgements

The authors thank E. Quintero, S. Sarret, A. Miralles and A. Pérez Vegara for excellent technical assistance. The CHO cell line expressing murine TRPA1 was supplied Dr. A. Patapoutian (The Scripps Research Institute). The mouse TRPA1(-/-) line was generously donated by Drs. K. Kwan and D. Corey (Harvard Medical School). We are also thankful to M. Moran and D. del Camino (Hydra Biosciences) for the kind gift of HC03001. Otto Fajardo and Victor Meseguer were supported by predoctoral fellowships from the Spanish Consejo Superior de Investigaciones Científicas (CSIC) and the Generalitat Valenciana respectively. The work was supported by funds from the Spanish Ministry of Education and Science: projects BFU2007-61855 to Felix Viana and BFU2005-08741 and CONSOLIDER-INGENIO 2010 CSD2007-00023 to Carlos Belmonte, and the Spanish Fundación Marcelino Botín.

References

1. Venkatachalam K, Montell C. TRP channels. Annu Rev Biochem 2007; 76:387-417.
2. Montell C, Birnbaumer L, Flockerzi V. The TRP channels, a remarkably functional family. Cell 2002; 108:595-8.
3. Pedersen SF, Owsianik G, Nilius B. TRP channels: An overview. Cell Calcium 2005; 38:233-52.
4. Clapham DE. TRP channels as cellular sensors. Nature 2003; 426:517-24.
5. Nilius B, Voets T. Diversity of TRP channel activation. Novartis Found Symp 2004; 258:140-9.
6. Peterlin Z, Chesler A, Firestein S. A painful trp can be a bonding experience. Neuron 2007; 53:635-8.
7. Garcia-Anoveros J, Nagata K. TRPA1. Handb Exp Pharmacol 2007; 347-62.
8. Story GM, Peier AM, Reeve AJ, Eid SR, Mosbacher J, Hricik TR, Earley TJ, Hergarden AC, Andersson DA, Hwang SW, McIntyre P, Jegla T, Bevan S, Patapoutian A. ANKTM1, a TRP-like channel expressed in nociceptive neurons, is activated by cold temperatures. Cell 2003; 112:819-29.
9. Jordt SE, Bautista DM, Chuang HH, McKemy DD, Zygmunt PM, Hogestatt ED, Meng ID, Julius D. Mustard oils and cannabinoids excite sensory nerve fibres through the TRP channel ANKTM1. Nature 2004; 427:260-5.
10. Obata K, Katsura H, Mizushima T, Yamanaka H, Kobayashi K, Dai Y, Fukuoka T, Tokunaga A, Tominaga M, Noguchi K. TRPA1 induced in sensory neurons contributes to cold hyperalgesia after inflammation and nerve injury. J Clin Invest 2005; 115:2393-401
11. Simons CT, Carstens MI, Carstens E. Oral irritation by mustard oil: self-desensitization and cross-desensitization with capsaicin. Chem Senses 2003; 28:459-65.
12. Handwerker HO, Forster C, Kirchhoff C. Discharge patterns of human C-fibers induced by itching and burning stimuli. J Neurophysiol 1991; 66:307-15.
13. Albin KC, Carstens MI, Carstens E. Modulation of oral heat and cold pain by irritant chemicals. Chem Senses 2008; 33:3-15.
14. Macpherson LJ, Dubin AE, Evans MJ, Marr F, Schultz PG, Cravatt BF, Patapoutian A. Noxious compounds activate TRPA1 ion channels through covalent modification of cysteines. Nature 2007; 445:541-5.
15. Hinman A, Chuang HH, Bautista DM, Julius D. TRP channel activation by reversible covalent modification. Proc Natl Acad Sci USA 2006; 103:19564-8.
16. Macpherson LJ, Geierstanger BH, Viswanath V, Bandell M, Eid SR, Hwang S, Patapoutian A. The pungency of garlic: Activation of TRPA1 and TRPV1 in response to allicin. Curr Biol 2005; 15:929-34.
17. Bautista DM, Jordt SE, Nikai T, Tsuruda PR, Read AJ, Poblete J, Yamoah EN, Basbaum AI, Julius D. TRPA1 mediates the inflammatory actions of environmental irritants and proalgesic agents. Cell 2006; 124:1269-82.
18. Bandell M, Story GM, Hwang SW, Viswanath V, Eid SR, Petrus MJ, Earley TJ, Patapoutian A. Noxious cold ion channel TRPA1 is activated by pungent compounds and bradykinin. Neuron 2004; 41:849-57.
19. Chuang HH, Neuhausser WM, Julius D. The super-cooling agent icilin reveals a mechanism of coincidence detection by a temperature-sensitive TRP channel. Neuron 2004; 43:859-69.
20. Karashima Y, Damann N, Prenen J, Talavera K, Segal A, Voets T, Nilius B. Bimodal action of menthol on the transient receptor potential channel TRPA1. J Neurosci 2007; 27:9874-84.
21. Macpherson LJ, Hwang SW, Miyamoto T, Dubin AE, Patapoutian A, Story GM. More than cool: Promiscuous relationships of menthol and other sensory compounds. Mol Cell Neurosci 2006; 32:335-43
22. Doerner JF, Gisselmann G, Hatt H, Wetzel CH. Transient receptor potential channel A1 is directly gated by calcium ions. J Biol Chem 2007; 282:13180-9.
23. Zurborg S, Yurgionas B, Jira JA, Caspani O, Heppenstall PA. Direct activation of the ion channel TRPA1 by Ca^{2+}. Nat Neurosci 2007; 10:277-9.
24. Kim D, Cavanaugh EJ. Requirement of a soluble intracellular factor for activation of transient receptor potential A1 by pungent chemicals: role of inorganic polyphosphates. J Neurosci 2007; 27:6500-9.
25. Kwan KY, Allchorne AJ, Vollrath MA, Christensen AP, Zhang DS, Woolf CJ, Corey DP. TRPA1 Contributes to cold, mechanical, and chemical nociception but is not essential for hair-cell transduction. Neuron 2006; 50:277-89.

26. Bautista DM, Movahed P, Hinman A, Axelsson HE, Sterner O, Hogestatt ED, Julius D, Jordt SE, Zygmunt PM. Pungent products from garlic activate the sensory ion channel TRPA1. Proc Natl Acad Sci USA 2005; 102:12248-52.
27. Zygmunt PM, Andersson DA, Hogestatt ED. Delta 9-tetrahydrocannabinol and cannabinol activate capsaicin-sensitive sensory nerves via a CB1 and CB2 cannabinoid receptor-independent mechanism. J Neurosci 2002; 22:4720-7.
28. Zygmunt PM, Petersson J, Andersson DA, Chuang H, Sorgard M, Di MV, Julius D, Hogestatt ED. Vanilloid receptors on sensory nerves mediate the vasodilator action of anandamide. Nature 1999; 400:452-7.
29. Kawasaki H, Takasaki K, Saito A, Goto K. Calcitonin gene-related peptide acts as a novel vasodilator neurotransmitter in mesenteric resistance vessels of the rat. Nature 1988; 335:164-7.
30. Triggle DJ. 1,4-Dihydropyridines as calcium channel ligands and privileged structures. Cell Mol Neurobiol 2003; 23:293-303.
31. Catterall WA. Structure and regulation of voltage-gated Ca^{2+} channels. Annu Rev Cell Dev Biol 2000; 16:521-55.
32. Xu H, Blair NT, Clapham DE. Camphor activates and strongly desensitizes the transient receptor potential vanilloid subtype 1 channel in a vanilloid-independent mechanism. J Neurosci 2005; 25:8924-37.
33. Fajardo O, Meseguer V, Belmonte C, Viana F. TRPA1 channels mediate cold temperature sensing in mammalian vagal sensory neurons: pharmacological and genetic evidence. J Neurosci 2008; 28:7863-75.
34. McNamara CR, Mandel-Brehm J, Bautista DM, Siemens J, Deranian KL, Zhao M, Hayward NJ, Chong JA, Julius D, Moran MM, Fanger CM. TRPA1 mediates formalin-induced pain. Proc Natl Acad Sci USA 2007; 104:13525-30.
35. Schramm M, Thomas G, Towart R, Franckowiak G. Novel dihydropyridines with positive inotropic action through activation of Ca^{2+} channels. Nature 1983; 303:535-7.
36. Franckowiak G, Bechem M, Schramm M, Thomas G. The optical isomers of the 1,4-dihydropyridine BAY K 8644 show opposite effects on Ca channels. Eur J Pharmacol 1985; 114:223-6.
37. Andersson DA, Gentry C, Moss S, Bevan S. Transient receptor potential A1 is a sensory receptor for multiple products of oxidative stress. J Neurosci 2008; 28:2485-94.
38. Nagata K, Duggan A, Kumar G, Garcia-Anoveros J. Nociceptor and hair cell transducer properties of TRPA1, a channel for pain and hearing. J Neurosci 2005; 25:4052-61.
39. Peier AM, Moqrich A, Hergarden AC, Reeve AJ, Andersson DA, Story GM, Earley TJ, Dragoni I, McIntyre P, Bevan S, Patapoutian A. A TRP channel that senses cold stimuli and menthol. Cell 2002; 108:705-15.
40. Akopian AN, Ruparel NB, Jeske NA, Hargreaves KM. Transient receptor potential TRPA1 channel desensitization in sensory neurons is agonist dependent and regulated by TRPV1-directed internalization. J Physiol 2007; 583:175-93.
41. Messerli FH. Vasodilatory edema: A common side effect of antihypertensive therapy. Curr Cardiol Rep 2002; 4:479-82.
42. Smith FL, Davis RW, Carter R. Influence of Voltage-sensitive Ca^{2+} channel drugs on bupivacaine infiltration anesthesia in mice. Anesthesiology 2001; 95:1189-97.
43. Gover TD, Kao JP, Weinreich D. Calcium signaling in single peripheral sensory nerve terminals. J Neurosci 2003; 23:4793-7.
44. Viana F, de la Pena E, Belmonte C. Specificity of cold thermotransduction is determined by differential ionic channel expression. Nat Neurosci 2002; 5:254-60.
45. Holz GG, Dunlap K, Kream RM. Characterization of the electrically evoked release of substance P from dorsal root ganglion neurons: Methods and dihydropyridine sensitivity. J Neurosci 1988; 8:463-71.
46. Trevisani M, Siemens J, Materazzi S, Bautista DM, Nassini R, Campi B, Imamachi N, Andre E, Patacchini R, Cottrell GS, Gatti R, Basbaum AI, Bunnett NW, Julius D, Geppetti P. 4-Hydroxynonenal, an endogenous aldehyde, causes pain and neurogenic inflammation through activation of the irritant receptor TRPA1. Proc Natl Acad Sci USA 2007; 104:13519-24.
47. Hill K, Schaefer M. TRPA1 is differentially modulated by the amphipathic molecules trinitrophenol and chlorpromazine. J Biol Chem 2007; 282:7145-53.
48. Meseguer V, Karashima Y, Talavera K, D'Hoedt D, Donovan-Rodriguez T, Viana F, Nilius B, Voets T. Transient receptor potential channels in sensory neurons are targets of the antimycotic agent clotrimazole. J Neurosci 2008; 28:576-86.
49. Xiao B, Dubin AE, Bursulaya B, Viswanath V, Jegla TJ, Patapoutian A. Identification of transmembrane domain 5 as a critical molecular determinant of menthol sensitivity in mammalian TRPA1 channels. J Neurosci 2008; 28:9640-51.
50. Christensen AP, Corey DP. TRP channels in mechanosensation: direct or indirect activation? Nat Rev Neurosci 2007; 8:510-21.
51. Corey DP, Garcia-Anoveros J, Holt JR, Kwan KY, Lin SY, Vollrath MA, Amalfitano A, Cheung EL, Derfler BH, Duggan A, Geleoc GS, Gray PA, Hoffman MP, Rehm HL, Tamasauskas D, Zhang DS. TRPA1 is a candidate for the mechanosensitive transduction channel of vertebrate hair cells. Nature 2004; 432:723-30.
52. Madrid R, Donovan-Rodriguez T, Meseguer V, Acosta MC, Belmonte C, Viana F. Contribution of TRPM8 channels to cold transduction in primary sensory neurons and peripheral nerve terminals. J Neurosci 2006; 26:12512-25.

Bidirectional shifts of TRPM8 channel gating by temperature and chemical agents modulate the cold sensitivity of mammalian thermoreceptors

Annika Mälkiä, Rodolfo Madrid, Victor Meseguer, Elvira de la Peña, María Valero, Carlos Belmonte and Félix Viana

Alicante Institute of Neuroscience, University Miguel Hernández-CSIC

TRPM8, a member of the melastatin subfamily of transient receptor potential (TRP) cation channels, is activated by voltage, low temperatures and cooling compounds. These properties and its restricted expression to small sensory neurons have made it the ion channel with the most advocated role in cold transduction. Recent work suggests that activation of TRPM8 by cold and menthol takes place through shifts in its voltage-activation curve, which cause the channel to open at physiological membrane potentials. By contrast, little is known about the actions of inhibitors on the function of TRPM8. We investigated the chemical and thermal modulation of TRPM8 in transfected HEK293 cells and in cold-sensitive primary sensory neurons. We show that cold-evoked TRPM8 responses are effectively suppressed by inhibitor compounds SKF96365, 4-(3-chloro-pyridin-2-yl)-piperazine-1-carboxylic acid (4-tert-butyl-phenyl)-amide (BCTC) and 1,10-phenanthroline. These antagonists exert their effect by shifting the voltage dependence of TRPM8 activation towards more positive potentials. An opposite shift towards more negative potentials is achieved by the agonist menthol. Functionally, the bidirectional shift in channel gating translates into a change in the apparent temperature threshold of TRPM8-expressing cells. Accordingly, in the presence of the antagonist compounds, the apparent response-threshold temperature of TRPM8 is displaced towards colder temperatures, whereas menthol sensitizes the response, shifting the threshold in the opposite direction. Co-application of agonists and antagonists produces predictable cancellation of these effects, suggesting the convergence on a common molecular process. The potential for half maximal activation of TRPM8 activation by cold was ∼140 mV more negative in native channels compared to recombinant channels, with a much higher open probability at negative membrane potentials in the former. In functional terms, this difference translates into a shift in the apparent temperature threshold for activation towards higher temperatures for native currents. This difference in voltage-dependence readily explains the high threshold temperatures characteristic of many cold thermoreceptors. The modulation of TRPM8 activity by different chemical agents unveils an important flexibility in the temperature–response curve of TRPM8 channels and cold thermoreceptors.

(Received 22 November 2006; accepted after revision 16 February 2007; first published online 22 February 2007)
Corresponding author A. Mälkiä: Instituto de Neurociencias de Alicante, Universidad Miguel Hernández-Consejo Superior de Investigaciones Cientificas (CSIC), Apartado 18, San Juan de Alicante 03550, Spain.
Email: annika.malkia@ umh.es

Transient receptor potential (TRP) channels comprise an extensive family of cation-permeable channels found in animals and fungi. More than 30 members have been identified in mammals, with a wide expression profile (Montell *et al.* 2002; Clapham, 2003). Targeted gene deletions of several TRP channels have revealed some of their key physiological functions, which include pheromone sensory signalling (TRPC2), innocuous heat sensation (TRPV3), osmoregulatory responses (TRPV4), taste transduction (TRPM5) and nociception (TRPV1 and TRPA1) (for references, see original publications by Caterina *et al.* 2000; Bautista *et al.* 2006; Kwan *et al.* 2006; and reviews by Fleig & Penner, 2004; Wissenbach *et al.* 2004; Desai & Clapham, 2005; Pedersen *et al.* 2005; Nilius *et al.* 2007). Many TRP channels have polymodal activation and several are thought to play important roles in somatosensory thermal transduction (reviewed by Jordt *et al.* 2003; McKemy, 2005; Dhaka *et al.* 2006).

 DOI: 10.1113/jphysiol.2006.123059

TRPM8 is a non-selective calcium-permeable TRP channel that is activated by cold and menthol, and is postulated to play a critical role in the transduction of moderate cold stimuli that give rise to cool sensations (McKemy *et al.* 2002; Peier *et al.* 2002; Reid, 2005; Voets *et al.* 2007). TRPM8 has a limited expression profile in the nervous system, restricted to a subpopulation of primary sensory neurons of small diameter in dorsal root and trigeminal ganglia (McKemy *et al.* 2002; Peier *et al.* 2002). Most cold-sensitive neurons are excited by both cooling and menthol (Reid & Flonta, 2001; McKemy *et al.* 2002; Viana *et al.* 2002; Thut *et al.* 2003), and also express TRPM8 mRNA transcripts (Nealen *et al.* 2003). Moreover, many cold-sensitive neurons express a non-selective cation current (I_{cold}) with biophysical and pharmacological properties consistent with the properties of TRPM8-dependent currents in transfected cells (Okazawa *et al.* 2002; Reid *et al.* 2002). In addition, TRPM8 has been found in prostate tissue, where its physiological function remains uncertain (Tsavaler *et al.* 2001; Zhang & Barritt, 2006).

Although TRP channels were originally thought to be voltage independent, it now seems that several of them exhibit weak voltage dependence (Hofmann *et al.* 2003; Nilius *et al.* 2003, 2005; Brauchi *et al.* 2004; Voets *et al.* 2004). In the case of TRPM8, the voltage dependence manifests as activation upon depolarization to positive transmembrane potentials, and a rapid and voltage-dependent closure at negative potentials (Brauchi *et al.* 2004; Voets *et al.* 2004). Cooling shifts the activation curve of TRPM8 towards more negative potentials, and thus increases the probability of channel openings at physiological membrane potentials. A similar shift is induced by the cooling agent menthol, causing the channel to activate at temperatures above 30°C (Voets *et al.* 2004).

Despite the important physiological functions of TRP channels, knowledge about their biophysical properties is still modest compared to that of other ion channels (Owsianik *et al.* 2006) and pharmacological tools to study or modulate them are very limited (Desai & Clapham, 2005; Dhaka *et al.* 2006). A notable exception is the pharmacology of the heat- and vanilloid-activated channel TRPV1, which has expanded significantly in the past few years (Garcia-Martinez *et al.* 2002; Valenzano *et al.* 2003; Krause *et al.* 2005). By contrast, reports on means to regulate TRPM8 activity are scarce and incomplete. Recent studies show that ethanol inhibits TRPM8 function at concentrations of the order of 0.5–3% (Weil *et al.* 2005; Benedikt *et al.* 2007). In addition, a number of known TRPV1 antagonists have been tested on heterologously expressed TRPM8 channels, such as the complex between the divalent copper ion and 1,10-phenanthroline (Cu–Phe), capsazepine, 4-(3-chloro-pyridin-2-yl)-piperazine-1-carboxylic acid (4-tert-butyl-phenyl)-amide (BCTC) and the related thio-BCTC and (*2R*)-4-C3-chloro-2-pyridinyl)-2-methyl-*N*-[4-(trifluoromethyl)phenyl]-1-piperazinecarboxamide (CTPC), the urea derivative SB-452533 and the cinnamide derivative SB-366791 (Behrendt *et al.* 2004; Weil *et al.* 2005; Madrid *et al.* 2006). With the exception of BCTC and ethanol, studies with these antagonists have been limited to responses evoked by application of menthol at constant room temperature – a mixture of chemical and physiological stimuli – thereby revealing little information about the nature and mechanism of the inhibition. Furthermore, almost nothing is known about the actions of these or other TRPM8 blockers on native thermoreceptors.

In many cases, the lack of specific blockers prevents or impairs a proper functional characterization of the channel in physiological systems. The availability of selective and potent TRPM8 channel antagonists is an essential tool in clarifying the role of different ion channels in thermal responses of intact cold receptors. In addition, modulators of TRPM8 activity have significant therapeutic potential in the treatment of prostate cancer (Zhang & Barritt, 2006). Here, we studied SKF96365, BCTC and 1,10-phenanthroline for their blocking effects on cold-activated TRPM8 responses. BCTC and SKF96365, which exhibited high antagonist potency, were subsequently characterized with respect to their mechanism of inhibition; results suggest a similar but opposite mode of action to that of menthol. The results obtained on recombinant channels were verified on native cold thermoreceptors.

Methods

Cloning of TRPM8 in pcINeo/IRES–GFP

Transfection of HEK293 cells with TRPM8 was carried out using the recombinant bicistronic expression plasmid pcINeo–TRPM8–IRES–GFP, which carries the protein-coding region of rat TRPM8 (accession number, AY072788) and the green fluorescent protein (GFP) coupled by an internal ribosomal entry site (IRES) sequence. GFP fluorescence could thus be used to identify TRPM8-expressing cells. The bicistronic vector pcINeo–IRES–GFP was provided by Jan Eggermont (Katholieke Universiteit Leuven, Belgium) and pcDNA3–TRPM8 was made available by David Julius (University of California, San Francisco, CA, USA). The new construct was verified by automatic sequencing.

Cell culture

HEK293 cells were obtained from the European Collection of Cell Cultures (Salisbury, UK). Cells were cultured in Dulbecco's modified Eagle's medium (DMEM) containing 10% fetal bovine serum and antibiotics, and plated in 2 cm × 2 cm wells at 4–5 × 10^5 cells $well^{-1}$. Next,

20–24 h after plating, the cells were transfected with the TRPM8–IRES–GFP construct by incubating them with a solution containing the plasmid DNA ($2\,\mu g\,well^{-1}$) and Lipofectamine 2000 (Invitrogen; $3\,\mu l\,well^{-1}$) for 4–6 h. Subsequently, the cells were trypsinized and replated on laminin-coated round coverslips (12 mm diameter) at $8–10 \times 10^4$ cells coverslip^{-1}. GFP-positive cells were selected for calcium-imaging or electrophysiology experiments 20–72 h after transfection.

HEK293 cells stably expressing rat TRPM8 channels (CR#1 cells) were kindly provided by Ramón Latorre (Center for Scientific Studies, Valdivia, Chile). They were cultured as described in by Brauchi *et al.* (2004).

All experimental procedures concerning animals were carried out according to the Spanish Royal Decree 223/1988 and the European Community Council directive 86/609/EEC. Trigeminal ganglion neurons from neonatal mice were cultured as previously described (de la Pena *et al.* 2005). In brief, newborn Swiss OF1 mice (postnatal day 1–5) were anaesthetized with ether and decapitated. The trigeminal ganglia were isolated and incubated with 1 mg ml^{-1} collagenase type IA, and cultured in a medium containing 45% DMEM, 45% F-12 and 10% fetal calf serum (Invitrogen), supplemented with 4 mM L-glutamine (Invitrogen), $200\,\mu g\,ml^{-1}$ streptomycin, $125\,\mu g\,ml^{-1}$ penicillin, 17 mM glucose and nerve growth factor (NGF, mouse 7S, 100 ng ml^{-1}, Sigma-Aldrich, Madrid, Spain). Cells were plated on poly-L-lysine-coated glass coverslips and used after 1–3 days in culture.

Calcium imaging

The calcium imaging experiments were conducted with the fluorescent indicator Fura-2. Prior to each experiment, the cells were incubated with $5\,\mu M$ acetoxymethylester form of Fura-2 (Molecular Probes Europe, the Netherlands) for 45 min at 37°C. Fluorescence measurements were made with a Zeiss Axioskop FS (Germany) upright microscope fitted with an ORCA ER CCD camera (Hamamatsu, Japan). Fura-2 was excited at 340 and 380 nm (excitation time, 200 or 300 ms) with a rapid switching monochromator (TILL Photonics, Germany), and the emitted fluorescence was filtered with a 510 nm long-pass filter. Mean fluorescence intensity ratios (F_{340}/F_{380}) were displayed on-line with Axon Imaging Workbench or Metafluor software (Molecular Devices, PA, USA). The calcium imaging experiments were performed simultaneously with temperature recordings. The bath solution, referred to as 'control solution', contained (mM): NaCl 140, KCl 3, $CaCl_2$ 2.4, $MgCl_2$ 1.3, Hepes 10 and glucose 10, and was adjusted to pH 7.4 with NaOH.

Electrophysiology

Whole-cell voltage-clamp recordings were performed simultaneously with temperature recordings. Standard patch pipettes (3–5 MΩ) were made of borosilicate glass capillaries (Harvard Apparatus Ltd, UK) and contained (mM): CsCl 140, $MgCl_2$ 0.6, EGTA 1 and Hepes 10; 278 mosmol kg^{-1}, pH adjusted to 7.4 with CsOH. In I_{cold} threshold experiments, the internal solution contained (mM): KCl 140, NaCl 6, $MgCl_2$ 0.6, EGTA 1, NaATP 1, NaGTP 0.1 and Hepes 10; 282 mosmol kg^{-1}, pH adjusted to 7.4 with KOH). The bath solution used was the same as in the calcium imaging experiments. For whole-cell recordings in trigeminal neurons, patch pipettes had a resisitance of 7–8 MΩ. To measure the activation of I_{cold} in neurons, the bath solution contained (mM): NaCl 140, KCl 3, $MgCl_2$ 1.3, $CaCl_2$ 0.1, Hepes 10, glucose 10 and TTX 0.5×10^{-3}; pH was adjusted to 7.4 with NaOH. The pipette solution contained (mM): CsCl 140, $MgCl_2$ 0.6, EGTA 1, Hepes 10, $ATPNa_2$ 1 and GTPNa 0.1; pH was adjusted to 7.4 with CsOH. These modifications were necessary to minimize large voltage-dependent currents. Current signals were recorded with an Axopatch 200B patch-clamp amplifier (Molecular Devices). Stimulus delivery and data acquisition were performed using pCLAMP9 software (Molecular Devices).

Chemical modulators

The chemical substances studied for their modulatory effect on TRPM8 were the cooling agent L-menthol (Scharlau, Spain), and the antagonists 1,10-phenanthroline (Sigma), SKF96365 (Tocris Bioscience, Bristol, UK) and BCTC which was a kind gift from Grünenthal GmbH Aachen (Germany).

Temperature stimulation

Coverslips with cultured cells were placed in a microchamber and continuously perfused with solutions warmed to 32–34°C. The temperature was adjusted with a water-cooled Peltier device placed at the inlet of the chamber, and controlled by a feedback device. Cold sensitivity was investigated with a temperature drop to 15–18°C (see Fig. 1*E*).

Experimental protocols and interpretation of results

During calcium-imaging experiments, the effects of the antagonist compounds were investigated with a protocol, wherein a first cooling stimulus in control solution was followed by a second one in the presence of a blocking agent (see Fig. 2*A* and *B*). To account for possible desensitization of the response during subsequent cooling stimuli, the same protocol was carried out in the absence of antagonists (see Fig. 1*H*). The observed reduction of the second response peak in control solution was taken into account when quantifying the blocking effects of the antagonists by defining an expected maximum response (Max Response)

for the second application:

$$\text{MaxResponse}_{2\text{nd}} = \text{DS} \times \text{MaxResponse}_{1\text{st}} \quad (1)$$

where DS is the desensitization coefficient obtained with the double-pulse protocol. For the dose–inhibition curves, the block was thus obtained from:

$$\text{Block} = 1 - \text{Response}_{\text{blocker}}/\text{MaxResponse}_{2\text{nd}} \quad (2)$$

where $\text{Response}_{\text{blocker}}$ is the response in the presence of antagonist, and fitted to the Hill equation:

$$\text{Block} = \text{Block}_{\text{max}}/(1 + (\text{IC}_{50}/c)^n) \quad (3)$$

where $\text{Block}_{\text{max}}$ is the maximum block, IC_{50} is the concentration of half-maximal inhibition, c is the blocker concentration and n is the Hill coefficient. The protocol employed to study the effect of menthol on the cold sensitivity of TRPM8 was similar to above except that the baseline temperature of the experiments was adjusted to 39–45°C to reveal information about shifts in the response threshold.

We also used whole-cell recordings of cold-induced currents to investigate the action of the different antagonists on TRPM8 channel activity. For dose–inhibition correlations, blocker compounds were briefly applied during an extended cold stimulus (see Fig. 2*D* and *E*). Current development was monitored with repetitive (0.2 Hz) injections of 1 s duration voltage ramps from −100 to +100 mV. The current block for the dose–inhibition curves was measured at +80 mV. To compare the effects of blockers on cold-evoked currents in individual cells, data were normalized to the response in control solution using the following equation:

$$\text{Block} = 1 - \text{Response}_{\text{blocker}}/\text{Response}_{\text{control}} \quad (4)$$

where $\text{Response}_{\text{control}}$ is the response in the absence of blocker. Dose–inhibition data were fitted to the Hill equation presented in eqn (3). All current responses were corrected for leak currents, which were measured at 34°C to avoid interference from TRPM8, and temperature-corrected by a factor $Q_{\Delta T}$ according to the following expression (Hille, 2001):

$$Q_{\Delta_T} = (Q_{10})^{\Delta T/10} \quad (5)$$

where ΔT is the difference between the baseline temperature (34°C) and the temperature of the cold stimulus. On the basis of control experiments in non-transfected HEK293 cells, the value of Q_{10} was fixed at 1.5, which is a reasonable value for the conductance of voltage-gated channels (Hille, 2001).

To provide information on shifts in the threshold temperatures, a protocol similar to that used for calcium imaging was used, where responses to cold in the presence and absence of antagonists were recorded at a holding potential of −60 mV. To estimate the shifts in the voltage dependence of activation of TRPM8 in HEK293 cells, current–voltage (I–V) relationships obtained from repetitive (0.2 Hz) voltage ramps (−100 to +200 mV, 525 ms duration) were fitted with a function that combines a linear conductance multiplied by a Boltzmann activation term (Nilius *et al.* 2006):

$$I = g \times (V - E_{\text{rev}})/(1 + \exp[(V_{1/2} - V)/s]) \quad (6)$$

where g is the whole-cell conductance, E_{rev} is the reversal potential, $V_{1/2}$ is the potential for half maximal activation and s is the slope factor. The assumption of a linear conductance is based on the observation by Voets *et al.* (2004) that open TRPM8 channels exhibit an ohmic I–V dependence. For each cell, fitting was started by analysing a condition with strong channel activation; typically 100 μM menthol at 20°C. The value obtained for the parameter g at this condition was defined as g_{max} and used as a limit in the fitting of the remaining experimental conditions: $g < g_{\text{max}}$. E_{rev} was fixed at a value close to the measured reversal potential of the current evoked by menthol and cooling. For trigeminal ganglion neurons, I–V relationships were obtained from voltage ramps (−100 to +200 mV) of 1.5 s duration.

Using voltage ramps instead of steps involves the possibility of not working under steady-state conditions. The benefit of the ramp protocol is, nevertheless, that it is more rapid, thus minimizing the time-dependent rundown of the current. We performed control experiments where we applied voltage ramps at two different speeds (525 ms and 5 s duration) in the same cells. No statistically significant difference was observed between the fitting parameters at the two speeds. However, we do not rule out the possibilty that the absolute values of the parameters may be slightly affected by non-stationary conditions.

Data analysis

Data are reported as mean ± standard error of the mean. The apparent threshold temperatures were estimated as the first point at which the measured signal (F_{340}/F_{380} or current) deviated by at least four times the standard deviation of its baseline. Data were analysed with WinASCD written by Dr Guy Droogmans (ftp://ftp.cc.kuleuven.ac.be/pub/droogmans/winascd.zip) and Origin 7.0 (OriginLab Corporation). Fitting was carried out with the Levenberg–Marquardt method implemented in Origin 7.0 software. In dose–response fits, the standard errors of the mean were used as weights. When comparing two means, statistical significance ($P < 0.05$) was assessed by Student's two-tailed t test. For multiple comparison of means obtained in the same subjects, one-way repeated-measures ANOVA was performed using GraphPad Prism version 4.00 for Windows (San Diego, CA, USA, www.graphpad.com).

Results

Co-transfection with TRPM8 and GFP

Analysis of 25 separate calcium-imaging experiments, with a total of 107 GFP-expressing HEK293 cells, revealed that 88% of these responded to a cold stimulus (Fig. 1*A–D*). As non-transfected HEK293 cells (Fig. 1*B* and *D*) or cells transfected with the empty vector pcINeo/IRES–GFP (data not shown) do not respond to cooling, this was taken as proof of the presence of functional TRPM8 channels in the cells. The time that the cells spent in culture between transfection and experiment seemed to influence the correlation between GFP fluorescence and TRPM8 expression. Cells that were used during days 1

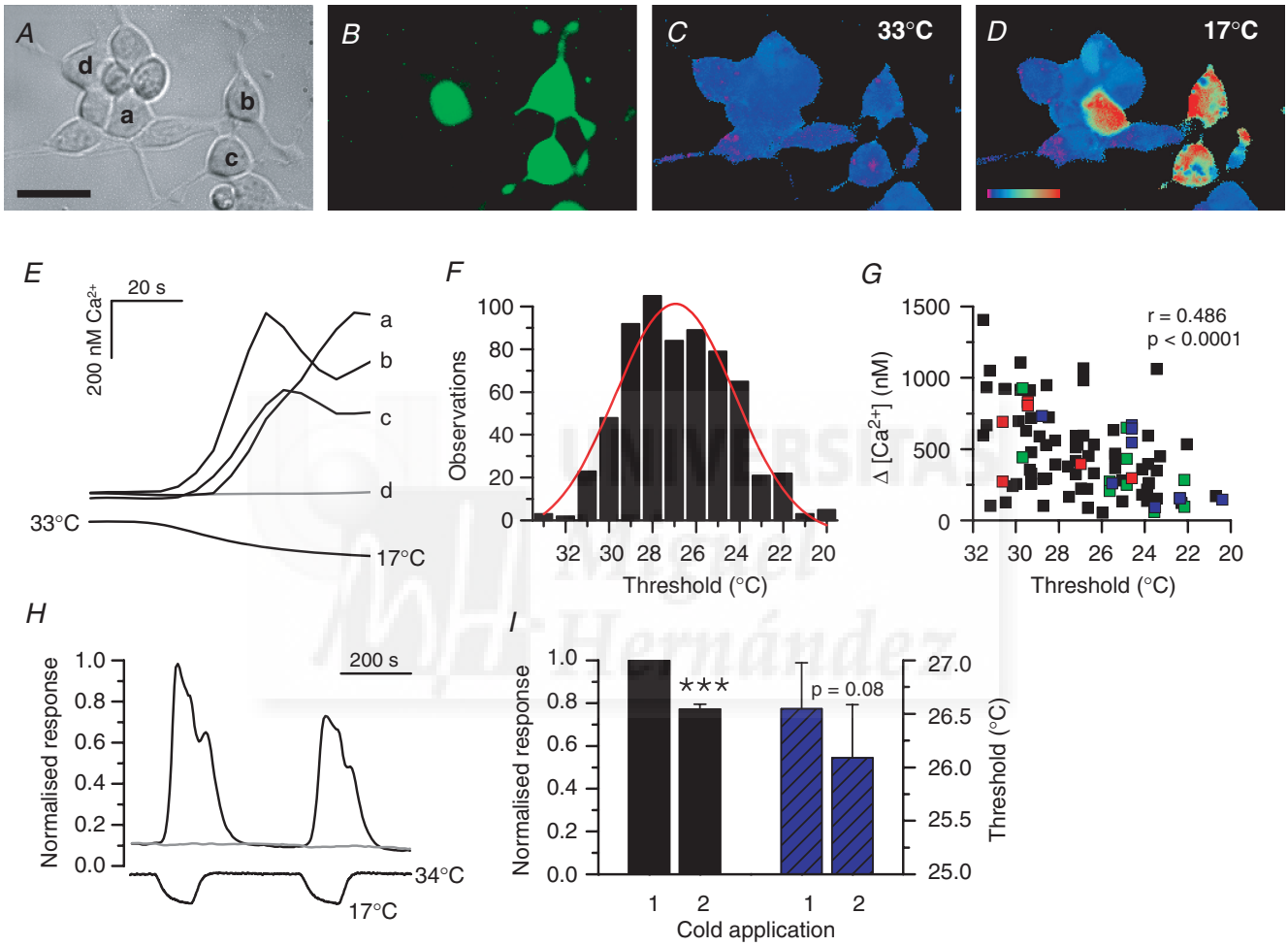

Figure 1. Properties of cold responses in TRPM8-expressing HEK293 cells
Microscope images of optical field viewed with transmitted light (*A*), GFP fluorescence (excitation at 470 nm) (*B*), and Fura-2 fluorescence (ratiometric image from excitation at 340 and 380 nm) at 33°C (*C*) and 17°C (*D*). The calibration bar, 30 μm; colour coding, pink to red:, 0–880 nM Ca^{2+}. *E,* calcium-imaging recording of cold-evoked responses in the three GFP-positive cells visualized above (a, b and c), exhibiting different apparent threshold temperatures. The GFP-negative cell (d) did not respond to cooling. *F,* histogram of apparent temperature thresholds in individual TRPM8-transfected HEK293 cells in control solution, when the temperature was lowered from 32—33°C: mean, 26.8 ± 0.1°C; *n*, 641; median, 27.0°C; range, 13°C. The red curve represents the Gaussian fit of the histogram. *G,* correlation between threshold temperature and calcium increase in 95 cells. The coloured squares indicate data from individual experiments. The statistical significance of the correlation coefficient is indicated with its two-tailed *P* value. *H,* calcium-imaging experiment of two subsequent cold applications in control solution. The intracellular Ca^{2+} response (upper trace) was normalized to the peak value obtained during the first cold application. The response in the GFP-negative cell, which did not respond to cooling, was normalized to the peak value of the GFP-positive cell. *I,* left: the desensitization of the second cold response averaged 23 ± 2% ($n = 39$, $P < 0.001$, Student's paired *t* test) compared to the first one. Right: the threshold temperature of the second cold response (26.1 ± 0.5°C) was not statistically different from the first one (26.5 ± 0.4°C; $n = 35$, $P = 0.08$, Student's paired *t* test).

and 2 (i.e. 20–58 h after transfection) exhibited the highest co-expression values: 94% of the GFP-positive cells were also TRPM8-positive at day 1 ($n = 34$) and 96% at day 2 ($n = 55$). The lowest percentage (72%, $n = 18$) was found in cells studied during day 3 (64–82 h) post transfection. A plausible explanation for this finding may be that by day 3, the amount of GFP in the cells reaches a toxic level (Liu *et al.* 1999).

Cold-evoked responses in TRPM8-transfected HEK293 cells

From electrophysiology experiments, we determined a mean apparent threshold temperature of TRPM8 in HEK293 cells in control solution of 27.6 ± 0.5°C ($n = 19$), when the temperature was lowered from a base value of 32–33°C at a holding potential of −60 mV. In the calcium-imaging experiments, the apparent threshold temperature was 26.8 ± 0.1°C ($n = 641$). The threshold distribution in the calcium-imaging experiments exhibited a range of 13°C and a median value of 27.0°C (see Fig. 1*F*). The wide range of observed thresholds cannot be attributed to experimental error, as cells in the same field exhibited largely different threshold temperatures (see Fig. 1*E*). The mean Ca^{2+} elevation was 480 ± 40 nM ($n = 95$). As seen in Fig. 1*G*, a low but statistically significant correlation could be established between response threshold and amplitude of Ca^{2+} increase, the trend being that large calcium responses are more likely to occur in cells with high threshold temperatures.

When two subsequent cooling stimuli were carried out, as shown in Fig. 1*H*, the amplitude of the second response was found to be 23 ± 2% smaller than the first one ($n = 39$, $P < 0.001$, Student's paired t test; Fig. 1*I*). This mean desensitization of the response was taken into consideration when estimating the blocking effects of drugs, by assigning a desensitization correction (DS, 0.77) to the expected response in eqn (1). Whereas DS affected the response amplitude, it did not affect the threshold temperatures of subsequent cold-evoked responses (Fig. 1*I*).

SKF96365, BCTC and 1,10-phenanthroline block cold-evoked responses in TRPM8-expressing HEK293 cells

SKF96365 is a non-specific blocker of various calcium-permeable channels, including both receptor-operated and voltage-gated types, as well as those activated by internal calcium store depletion (Merritt *et al.* 1990). At higher concentrations (IC_{50}, ∼40 μM), SKF96365 has also been reported to block an inwardly rectifying K^+ current in endothelial cells (Schwarz *et al.* 1994). In dorsal root ganglion neurons, a cold-activated current was reduced by almost 70% in the presence of 100 μM SKF96365 (Reid *et al.* 2002).

We tested the effects of SKF96365 on cold-evoked responses in TRPM8-transfected HEK293 cells. As shown in Fig. 2*A*, 20 μM SKF96365 produced a robust and reversible inhibition of cold-evoked $[Ca^{2+}]_i$ elevation in transfected cells. To quantify the potency of SKF96365 as a TRPM8 channel antagonist, we constructed dose–inhibition curves (Fig. 2*C*) from the responses at 17.5°C: a temperature at which the average response in control solution had reached its maximum value. Hill fits to these data yielded an IC_{50} of 1.0 ± 0.2 μM. At the end of each experiment, the cells were left in control solution for 15 min to remove the accumulated antagonist. Washing out the effects of SKF96365 was concentration dependent and amounted to 56–85% of the initial signal, for decreasing concentration of the blocker.

In the whole-cell electrophysiology experiments, various concentrations of SKF96365 (0.1–20 μM) were applied during an extended cooling stimulus (Fig. 2*D*). Currents were evoked by consecutive voltage ramps from −100 to +100 mV, delivered every 5 s, and I_{cold} at +80 mV was plotted *versus* time. SKF96365 produced a concentration-dependent, but incomplete inhibition of this current, as seen in Fig. 2*D*. This effect was highly reversible upon washing: the initial signal recovered by > 80% for concentrations below 10 μM, and > 70% for 10 and 20 μM SKF96365. Figure 2*F* shows the complete dose–response curve of block of cold-evoked currents by SKF96365 at +80 mV and 17–18°C. The solid line represents the fit to the Hill equation, which yielded an IC_{50} of 0.8 ± 0.1 μM.

BCTC was recently introduced as an orally bioavailable antagonist agent of the TRPV1 channel, with a high selectivity in an extensive radioligand screen against other ion channels (Valenzano *et al.* 2003). More recent studies demonstrate that BCTC also readily blocks menthol-evoked (Behrendt *et al.* 2004; Weil *et al.* 2005) and cold-evoked responses of TRPM8 (Madrid *et al.* 2006). We tried to establish BCTC as a reference compound of TRPM8 block, comparing its effects on TRPM8 with those of other drugs. A typical calcium-imaging recording is shown in Fig. 2*B*. The Hill fit (Fig. 2*C*) of the blockade at 17.5°C yielded an IC_{50} of 0.68 ± 0.06 μM and full block at high concentrations. The recovery of the initial signal after a 5 min washing period depended on the BCTC concentration used, varying between 21% and 63% for the highest and lowest concentrations tested. Whole-cell electrophysiology experiments (Fig. 2*E*), confirmed that BCTC potently blocks TRPM8-mediated cold responses at +80 mV with an IC_{50} of 0.54 ± 0.04 μM and $Block_{max}$ of 1.00 ± 0.01 (Fig. 2*F*).

Cu–Phe is an oxidizing agent capable of inducing formation of disulphide bridges between appropriately

located thiol groups, and has been widely employed in studies of the gating motion of voltage-gated channels (Liu *et al.* 1996). The Cu–Phe complex is also an antagonist of the TRPV1 channel; however, in this case it acts as an open-channel blocker instead of inducing cysteine cross-linking (Tousova *et al.* 2004). Meanwhile, both the free 1,10-phenanthroline and its Cu–Phe complex are equally potent open-channel blockers of the human skeletal muscle Na^+ channel (Popa & Lerche, 2006).

In our studies, the free 1,10-phenanthroline acted as an antagonist of the TRPM8-mediated cold-evoked responses in HEK293 cells. The dose–response data of 1,10-phenanthroline block from calcium-imaging and whole-cell electrophysiology experiments were fitted to the Hill equation (Fig. 2*C* and *F*), and yielded IC_{50} values of 100 ± 20 and $180 \pm 20\ \mu$M, respectively. We subsequently investigated the inhibitory capacity of the Cu–Phe complex on cold-evoked TRPM8 responses. In the presence of $100\ \mu$M Cu^{2+} and $400\ \mu$M 1,10-phenanthroline, $78 \pm 4\%$ ($n = 24$) of the calcium response was blocked at 17.5°C (Fig. 2*C*, grey square), a value almost identical to that observed in the presence of $400\ \mu$M free 1,10-phenanthroline alone ($77 \pm 4\%$, $n = 26$, $P = 0.83$, Student's unpaired *t* test). Thus, in the case of TRPM8, complex formation with the divalent copper ion does not seem to be necessary for 1,10-phenanthroline antagonism. The inhibition in response to free and complexed 1,10-phenanthroline was reversible which

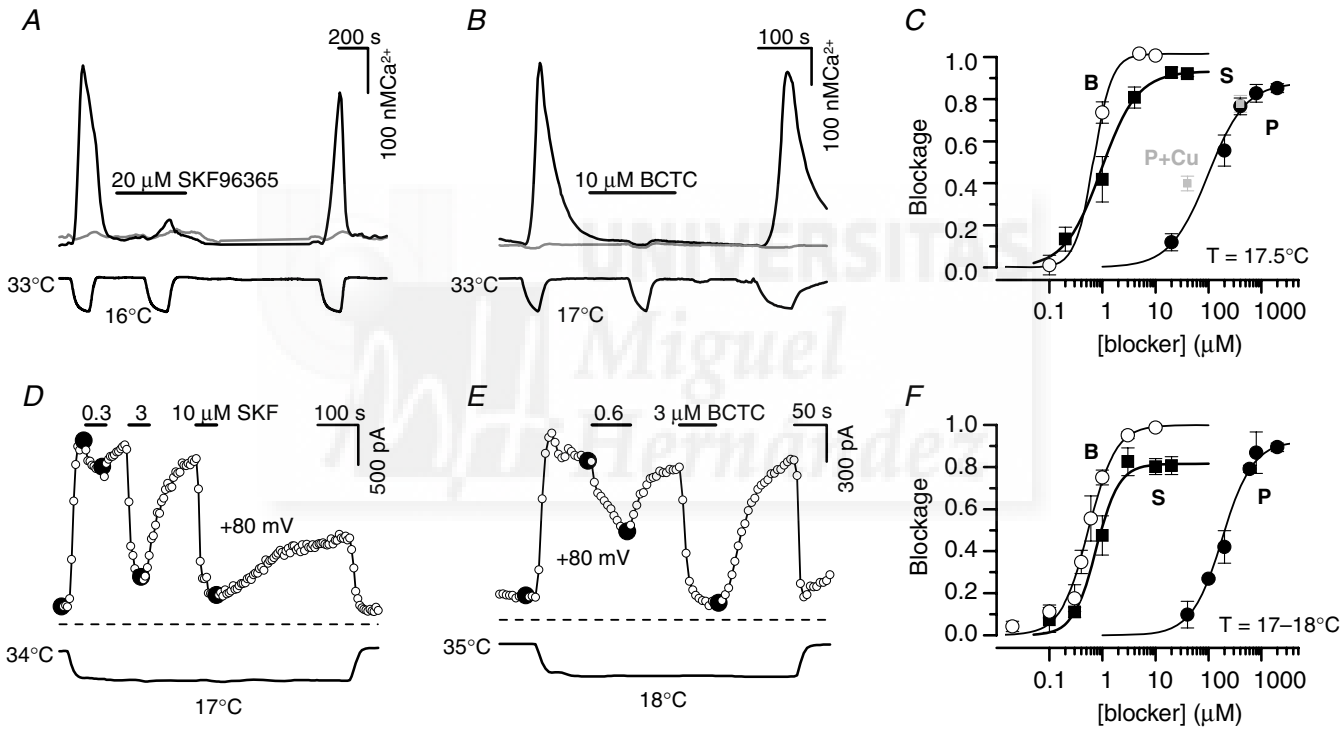

Figure 2. BCTC, SKF96365 and 1,10-phenanthroline block cold-evoked responses in TRPM8-expressing HEK293 cells

A and *B*, experimental recordings of the effects of 20 μM SKF96365 and 10 μM BCTC on cold-evoked $[Ca^{2+}]_i$ responses in TRPM8-transfected HEK293 cells. Upper trace shows intracellular Ca^{2+} and lower trace represents bath temperature. The unresponsive cells (grey traces) did not express GFP. *C*, dose–inhibition curves from calcium-imaging experiments of BCTC (B), SKF96365 (S) and 1,10-phenanthroline (P) at 17.5°C. The solid lines represent the fits to the Hill equation. The fits to the data yielded an IC_{50} of $0.68 \pm 0.06\ \mu$M, $Block_{max}$ of 1.015 ± 0.009, and a Hill slope *n* of 2.5 ± 0.6 for BCTC ($n = 4$–18 cells); IC_{50} of $1.0 \pm 0.2\ \mu$M, $Block_{max}$ of 0.93 ± 0.02, Hill slope *n* of 1.3 ± 0.3 for SKF96365 ($n = 9$–20 cells); IC_{50} of $100 \pm 20\ \mu$M, $Block_{max}$ of 0.88 ± 0.03, Hill slope *n* of 1.2 ± 0.2 for 1,10-phenanthroline ($n = 8$–26 cells). For comparison, blockade obtained with 1,10-phenanthroline in the presence of Cu^{2+} are shown in grey (P:Cu^{2+} concentration ratio, 4 : 1). *D–E*, time course of the block caused by various concentrations of SKF96365 and BCTC on cold-evoked whole-cell currents at +80 mV. The dashed lines indicate the zero current level; lower trace is bath temperature. *F*, dose–inhibition curves of BCTC (B), SKF96365 (S) and 1,10-phenanthroline (P) at temperature (*T*) of 17–18°C and holding potential of +80 mV. The solid lines represent the fits to the Hill equation, which yielded the parameters IC_{50} of $0.54 \pm 0.04\ \mu$M, $Block_{max}$ of 1.00 ± 0.01, Hill slope *n* of 1.7 ± 0.2 ($n = 2$–8 cells) for BCTC; IC_{50} of $0.8 \pm 0.1\ \mu$M, $Block_{max}$ of 0.82 ± 0.03, Hill slope *n* of 2.0 ± 0.4 ($n = 2$–5 cells) for SKF96365; IC_{50} of $180 \pm 20\ \mu$M; $Block_{max}$ of 0.92 ± 0.03, Hill slope *n* of 1.5 ± 0.1 ($n = 2$–5 cells) for 1,10-phenanthroline (see text for definitions).

strongly indicates that the mechanism of inhibition does not involve cross-linking of cysteines (Liu *et al.* 1996; Aziz *et al.* 2002).

Blockade of I_{cold} by BCTC and SKF96365 is voltage dependent

The nature of the antagonism of cold-evoked currents of TRPM8 by BCTC and SKF96365 was studied in more detail with whole-cell electrophysiology. As seen in Fig. 3*A* and *D*, cooling of the control bath solution from around 35°C to 18°C activated a current characterized by a reversal potential near 0 mV and strong outward rectification, as reported before for TRPM8 currents (McKemy *et al.* 2002; Voets *et al.* 2004). The concentration-dependent inhibition of this current by SKF96365 and BCTC is clearly seen in the *I–V* plots. More detailed analysis of the *I–V* curves revealed that blockade of I_{cold} by the two antagonists is voltage dependent. Figure 3*B* and *E* shows the blockade induced by concentrations around the IC_{50} of BCTC and SKF96365 over a wide range of potentials, demonstrating that I_{cold} is strongly blocked at negative potentials by these submaximal concentrations of antagonist, while a significant fraction of the current remains at more positive potentials. The statistical significance of the observed differences in degree of block with potential was assessed using a one-way repeated-measures ANOVA test combined with a post test for a linear trend. The results (BCTC, $P < 0.01$ for one-way repeated-measures ANOVA and $P < 0.001$ for linear regression; SKF96365, $P < 0.001$ for both) indicate that the mean blockade at different potentials is statistically different, and that the voltage dependence of the block is not an artefact caused by random error.

The *I–V* data were further employed to construct dose–inhibition curves at different potentials. As the

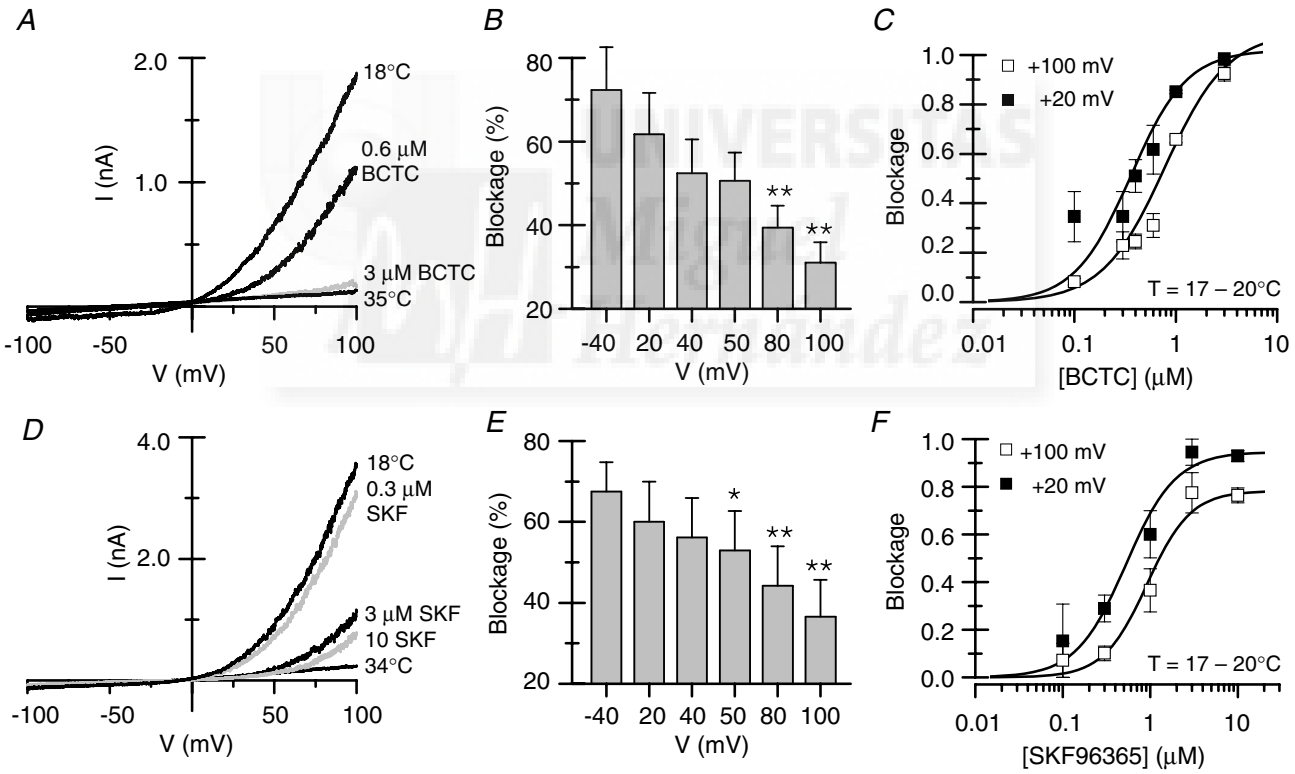

Figure 3. Inhibition of TRPM8 by BCTC and SKF96365 is voltage dependent
A and *D,* current–voltage relationships of cold-evoked currents and the effects of various concentrations of BCTC and SKF96365. The antagonists were applied at a temperature of 18°C. The locations of the voltage ramps are marked with large, filled circles in Fig. 2*D* and *E*. *B,* the blockade by 0.6 μM BCTC analysed over various potentials. Dunnett's *post hoc* test in combination with one-way repeated-measures ANOVA ($P < 0.01$) was employed to assess statistical significance between the blockade at each of the studied potentials and at –40 mV (**$P < 0.01$). *C,* dose–inhibition curves of 0.6 μM BCTC at +20 and +100 mV. Whereas the maximum blockade was unaffected, the IC_{50} was increased with increasing depolarization. *E,* the blockade by 1 μM SKF96365 analysed over various potentials. Statistical significance was assessed with Dunnett's *post hoc* test in combination with one-way repeated-measures ANOVA ($P < 0.001$) between the blockade at each of the studied potentials and at –40 mV. *F,* dose–inhibition curves of SKF96365 at +20 and +100 mV. Note that both maximum blockade and IC_{50} varied as a function of potential.

cold-evoked inward current was often very small, analysis at negative potentials was less accurate, and thus the potentials +20 and +100 mV were chosen for illustrative purposes. For BCTC, shown in Fig. 3*C*, the effect of depolarizing the membrane potential translates to a shift in the dose–inhibition curve towards larger antagonist concentrations. Accordingly, full blockade was reached at all studied potentials, with IC_{50} values between $0.36 \pm 0.04\ \mu$M at +20 mV and $0.78 \pm 0.08\ \mu$M at +100 mV. In the case of SKF96365 (Fig. 3*F*), together with the shift in the dose–inhibition curve (IC_{50}, 0.5–0.9 μM), membrane depolarization appeared to be coupled to a decline in maximum effect of the antagonist.

The inhibition of the cold-evoked current by 1,10-phenanthroline was also voltage dependent (not shown), exhibiting weaker inhibition at more positive potentials. The effect was quantified for 600 μM 1,10-phenanthroline, which blocked $92 \pm 2\%$ of the cold-evoked current at +40 mV, and $70 \pm 2\%$ at +100 mV ($P < 0.001$, Student's paired t test, $n = 3$).

BCTC and SKF96365 shift the activation curve of TRPM8 towards more positive potentials

The voltage-dependent antagonism by BCTC and SKF96365, together with the fact that both compounds are electroneutral at pH 7.4, led us to think that they are not acting as typical pore blockers driven by the transmembrane voltage (Hille, 2001). Recently it was shown that low temperature and menthol activate TRPM8 channels by producing a shift in the voltage-dependence of activation towards more negative potentials (Voets *et al.* 2004; Brauchi *et al.* 2004). We hypothesized that the mechanism of inhibition exerted by the studied TRPM8 antagonists involved an opposite effect on the voltage dependence of activation (i.e. a shift in gating towards more depolarized potentials). Consequently, TRPM8 activation was probed with 525 ms duration voltage ramps from −100 to +200 mV in whole-cell voltage-clamp mode both in CR#1 HEK293 cells stably expressing rat TRPM8 channels (Brauchi *et al.* 2004) and in transiently transfected HEK293 cells (Fig. 4*A*, *B, D* and *E*).

Figure 4*A* shows the effects of 3 μM BCTC on currents evoked by cold and/or menthol at −80, +80 and +160 mV. The I–V curves from the same experiment are shown in Fig. 4*B*. As can be seen, in this cell cooling to 20°C produced a clear augmentation of the outward current at depolarized potentials only, while co-application of the cold stimulus with 100 μM menthol also produced a potentiation of the inward current at negative potentials. Application of 3 μM BCTC in the continuous presence of both agonists (cold and menthol) produced an incomplete inhibition of outward currents but a full inhibition of inward currents. To estimate the midpoint of activation ($V_{1/2}$), a measure of changes in channel gating, the ramp I–V data obtained in the presence and absence of antagonists were fitted (red lines in Fig. 4*B*) with eqn (6) described in the Methods, which consists of a Boltzmann activation term combined with a linear conductance. The assumption of a linear conductance was shown to be reasonable by Voets *et al.* (2004).

A summary of the mean values obtained for the fitting variables under different experimental conditions is shown in Table 1. As reported previously, cooling and menthol produced marked leftward shifts in $V_{1/2}$ (Voets *et al.* 2004; Brauchi *et al.* 2004). By contrast, application of 3 μM BCTC produced a positive shift in $V_{1/2}$ and a reduction in g but no apparent change in the slope factor s ($P > 0.05$ when comparing conditions with and without BCTC). For conditions of 33°C, 20°C, 100 μM menthol at 33°C, and 100 μM menthol at 20°C, application of 3 μM BCTC shifted $V_{1/2}$ by 34 ± 9 mV ($n = 6$); 67 ± 11 mV ($n = 8$); 78 ± 6 mV ($n = 21$), and 97 ± 11 mV ($n = 15$), respectively ($P < 0.05$ for all shifts, paired t test). These data indicate that the inhibitory effects of BCTC increase under conditions of high open probability of the TRPM8 channel.

To better illustrate the bidirectional shifts in the voltage activation of TRPM8 induced by BCTC, menthol and temperature, we constructed a summary histogram (Fig. 4*C*) where the mean $V_{1/2}$ values of the various experimental conditions are presented relative to the value obtained for cold in the same cells. As can be seen in Fig. 4*C*, cooling to 20°C alone produced a significantly smaller negative shift than applying 100 μM menthol at 33°C ($P < 0.01$, $n = 12$, paired t test). In the presence of both agonists, 3 μM BCTC completely cancelled the effect of 100 μM menthol and restored $V_{1/2}$ to the value obtained in the presence of cold alone ($P = 0.54$, $n = 14$, paired t test). In summary, under the various experimental conditions (see also Table 1), the effect of 1–3 μM BCTC was to produce a significant positive shift in $V_{1/2}$ with only a modest reduction in g, particularly at lower concentrations of antagonist.

We subsequently studied whether a similar effect on the voltage activation of TRPM8 was induced by SKF96365 and 1,10-phenanthroline. Figure 4*D* and *E* shows the time course of whole-cell current development and I–V data of a TRPM8-positive cell where 3 μM SKF96365 was applied during a cold stimulation. As summarized in Fig. 4*F*, application of 3 μM SKF96365 during cooling induced a positive shift on $V_{1/2}$ that averaged 24 ± 3 mV ($n = 6$; $P < 0.001$, paired t test). For 300 μM 1,10-phenanthroline, the mean value of the shift was 35 ± 5 mV ($n = 5, P < 0.01$, paired t test).

The functional consequence of the bidirectional shift in channel gating is a displacement in the apparent temperature-response threshold of TRPM8-expressing cells

The observation that the antagonists and menthol shift the activation curve of TRPM8 in opposite directions prompted us to investigate whether the same holds true for the apparent response threshold during a temperature stimulus.

Figure 5*A* shows the whole-cell current (holding potential, −60 mV) in a TRPM8-expressing cell as the bath temperature was cooled in the absence and presence of 0.6 μM BCTC. Comparing the current responses during the cooling ramp (Fig. 5*B*), we found that the apparent response threshold was shifted by an average of $-4.3 \pm 0.5^{\circ}$C ($P < 0.01$, $n = 4$, paired t test). The shifts observed in four individual cells are shown in Fig. 5*C*. The effects of BCTC on apparent TRPM8 response thresholds obtained from calcium-imaging experiments (Fig. 5*D*) were analysed in terms of relative response curves (Fig. 5*E*). Briefly, for each cell, the relative response at a temperature T was calculated as the fluorescence response normalized to the expected maximum response of the cell (i.e. the response to cold in control solution corrected with the desensitization coefficient (eqn (1)). The relative responses of the individual cells ($n = 16$–19 for each condition) were averaged, yielding the curves seen in Fig. 5*E*. Whereas

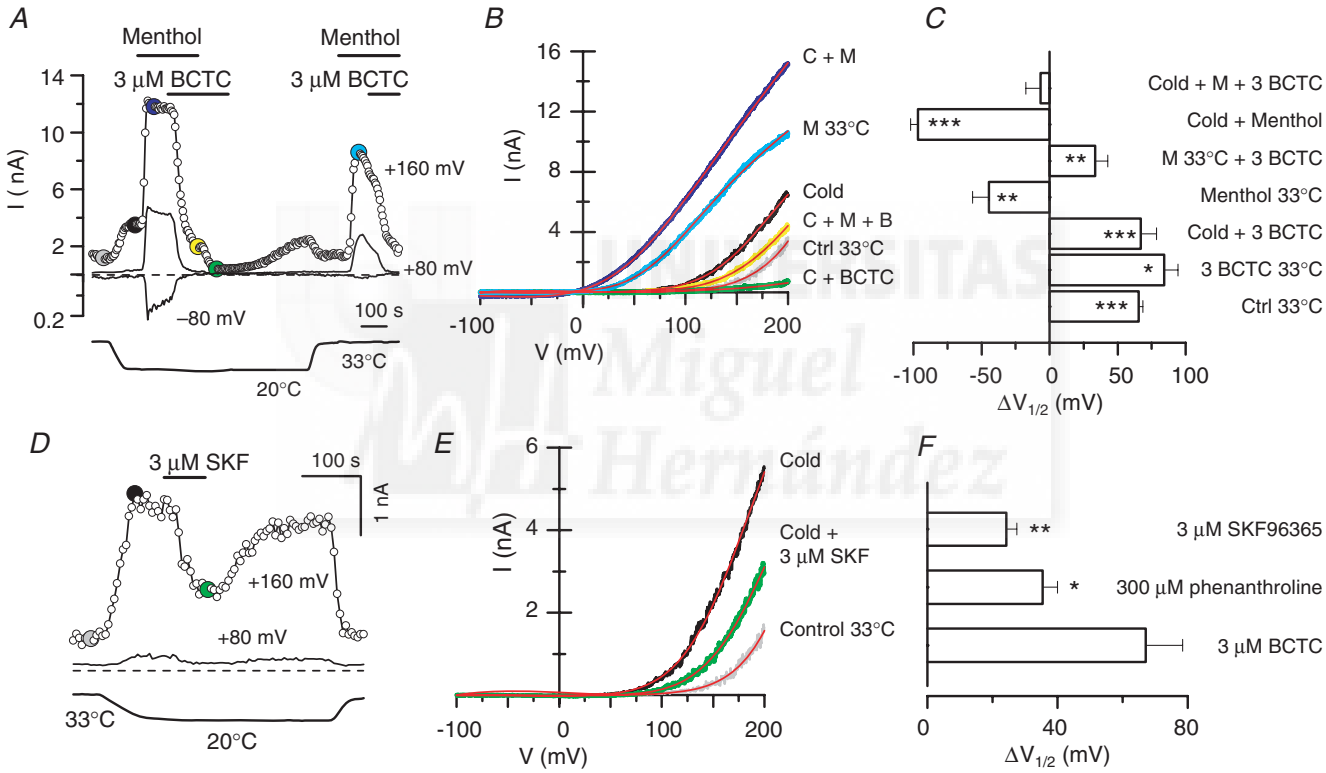

Figure 4. BCTC and SKF96365 shift the activation curve of TRPM8 towards more positive potentials
A, time course of current development at +160, +80 and −80 mV in a CR#1 HEK293 cell under various experimental conditions. Voltage ramps (−100 to +200 mV) of 525 ms duration were delivered every 5 s and the current traces for the time points marked with filled dots are presented in *B*. The dashed line indicates the zero current level; lower trace is bath temperature. *B,* whole-cell ramp *I–V* relationships corresponding to the different conditions shown in *A*. The red lines, superimposed on each trace, represent the fit of the current to eqn (6). *C,* summary histogram of the effects of BCTC on the midpoint of voltage activation ($V_{1/2}$) of TRPM8 channels ($n = 3$–22). The data are represented as shifts in $V_{1/2}$ with respect to the value obtained for cold. Statistical significance was assessed with the unpaired t test and is indicated $^{***}P < 0.001$, $^{**}P < 0.01$ and $^{*}P < 0.05$. *D,* time course of the blockade caused by SKF96365 on cold-evoked whole-cell currents at +160 and +80 mV. Current traces for the time points marked with filled dots are presented in *E*. The dashed line indicates the zero current level; lower trace is bath temperature. *E,* whole-cell ramp *I–V* relationships corresponding to the experiment shown in *D*. The red lines represent the fits to eqn (6). *F,* shifts in $V_{1/2}$ induced by 3 μM BCTC, 3 μM SKF96365 and 300 μM 1,10-phenanthroline with respect to the value in cold. The average values for $V_{1/2}$ during cold application in control solution were 156 ± 7 mV (BCTC), 158 ± 6 mV (SKF96365) and 146 ± 5 mV (1,10-phenanthroline). Statistical significance was assessed with one-way ANOVA ($P < 0.01$) in combination with Dunnett's *post hoc* test using 3 μM BCTC as the reference, and is indicated $^{**}P < 0.01$ and $^{*}P < 0.05$.

Table 1. Summary of the effects of temperature, menthol and BCTC on TRPM8 activation in HEK293 cells

	Control 33°C		Cold 20°C			100 μM menthol 33°C			Cold + 100 μM menthol		
	no drug	3 BCTC	no drug	1 BCTC	3 BCTC	no drug	1 BCTC	3 BCTC	no drug	1 BCTC	3 BCTC
s (mV^{-1})	36 ± 2	54 ± 8	35 ± 1	40 ± 3	45 ± 4*	38 ± 2	33 ± 3	36 ± 1	40 ± 2	48 ± 5	41 ± 1
g (nS)	38 ± 3	25 ± 11	52 ± 5	48 ± 14	19 ± 6‡	78 ± 7	60 ± 10	43 ± 7†	86 ± 7	64 ± 19	56 ± 5†
$V_{1/2}$ (mV)	215 ± 4	229 ± 11	153 ± 5	193 ± 19*	223 ± 10‡	89 ± 6	112 ± 16	172 ± 7‡	58 ± 4	122 ± 33	153 ± 9‡
n	39	6	26	3	8	29	8	21	24	3	15

The absolute values of the parameters s, g and $V_{1/2}$ obtained from the fits of the ramp (−100 to +200 mV) I–V curves to eqn (6) in the Methods. The data are given as means ± S.E.M. and are grouped according to the different experimental conditions (control or agonist) onto which BCTC was applied. To assess statistical significance, unpaired t test was performed between the parameters obtained in the absence ('no drug') and presence of BCTC for each antagonist condition, and significance indicated: *$P < 0.05$; †$P < 0.001$; ‡$P < 0.001$.

10 μM BCTC produced a complete inhibition of the current, lower concentrations of the drug reduced the peak amplitude and shifted the response towards lower temperatures. The control curve was obtained in an identical manner from experiments where the second cooling application was also performed in the absence of drug; this confirmed that the observed shifts in the response curves is not an artefact of applying subsequent cooling applications.

For SKF96365 we found, similarly, that the apparent response threshold was shifted to lower temperature values in the presence of antagonist. From whole-cell

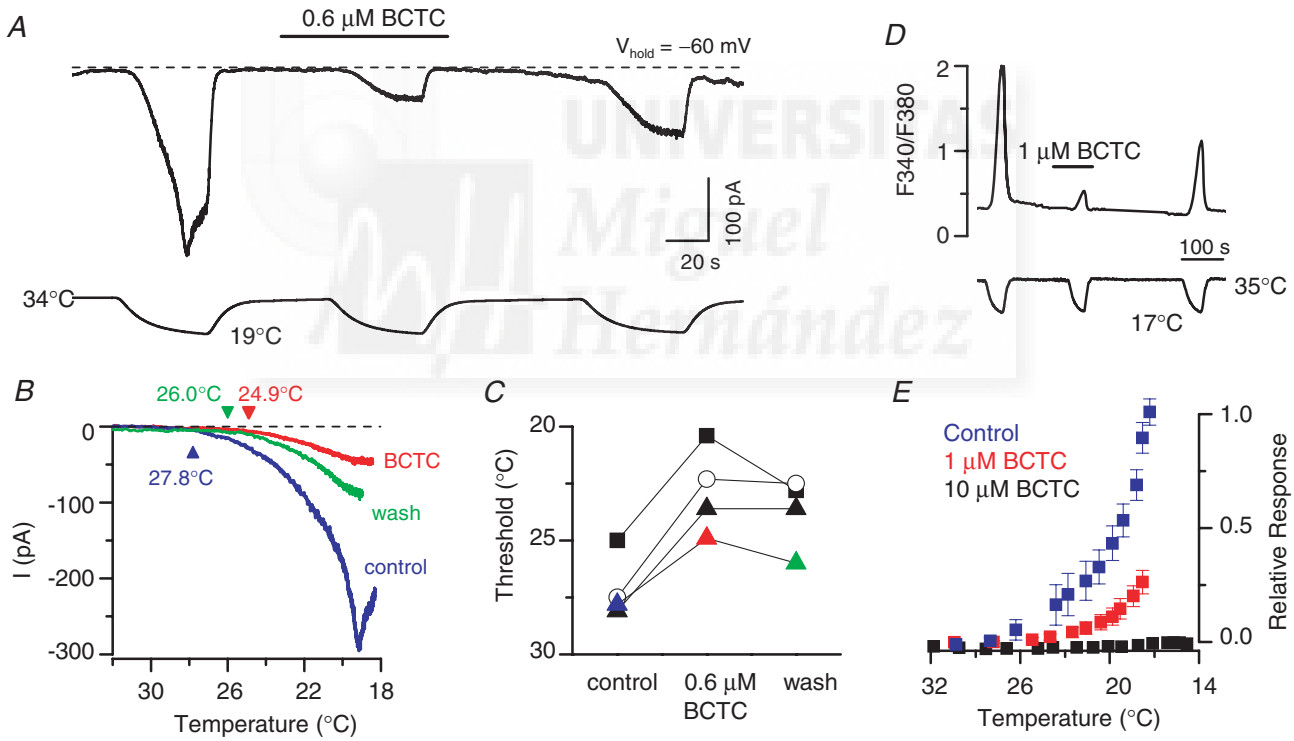

Figure 5. BCTC lowers the response-threshold temperature during cooling
A, simultaneous recording of whole-cell membrane current (top trace) and bath temperature (bottom trace) during application of three consecutive cooling ramps to a TRPM8-transfected HEK293 cell (holding potential, −60 mV). Application of 0.6 μM BCTC produced a reversible reduction in I_{cold} amplitude. The dashed line indicates the zero current level. *B,* close-up and superposition of the cold-evoked responses shown in *A* in the absence and presence of 0.6 μM BCTC. The current traces were corrected to yield a 0 pA baseline; holding potential, −60 mV. *C,* response-threshold temperatures of four cells during cold applications in control solution, 0.6 μM BCTC and after washing. The coloured symbols correspond to the cell in *A* and *B*. *D,* fluorescence ratiometric (F_{340}/F_{380}) calcium-imaging recording of cold-evoked responses in the absence and presence of 1 μM BCTC. *E,* relative response *versus* temperature curves constructed from cooling ramps in the presence of 1 and 10 μM BCTC. For each cell, the relative response at each temperature was calculated as the fluorescence response normalized to the expected maximum response of the cell, defined in eqn (1). The control curve was obtained in an identical manner from experiments where the second cooling application was also performed in the absence of drug. Each data point represents the average of 16–19 cells. For clarity, error bars are omitted where negligibly small.

electrophysiology experiments (Fig. 6*A* and *B*) we determined an average shift of -2.6 ± 0.5°C ($P < 0.01$, $n = 6$, paired t test) for 1 μM SKF96365. The shifts for six individual cells are shown in Fig. 6*C*. As observed for BCTC, SKF96365 shifted the relative response curves during cooling towards lower temperatures in a concentration-dependent manner (Fig. 6*D* and *E*). However, whereas 10 μM BCTC was capable of completely blocking the responses evoked by cooling to 14°C (Fig. 5*E*), in the presence of 20 μM (Fig. 6*E*) or 40 μM (not shown) SKF96365, a fraction of the response remained when the cooling was continued below 20°C. Thus, the capacity of SKF93653 to modulate TRPM8 gating seems to be both weaker (requires higher antagonist concentration) and more limited (restricted threshold shift range) than that of BCTC.

Expressing the average threshold-temperature shifts as divided by unit concentration, one obtains -7.2 and -2.6°C μM^{-1} for BCTC and SKF96365, respectively, yielding a ratio of potency of 2.8 in favour of BCTC. It is intriguing that by comparing the shifts in $V_{1/2}$ induced by the two antagonists (8.1 and 22.4 mV μM^{-1}), one obtains exactly the same ratio, suggesting that the two phenomena are strongly coupled.

These results indicate that, with regard to cold sensing, the main functional effect of the antagonists is a dose-dependent shift in the apparent temperature activation threshold of the cell.

The modulation of cold-evoked responses of TRPM8-expressing cells by menthol and antagonists is additive

Considering the opposite shifts in activation curves and apparent temperature thresholds induced by menthol and

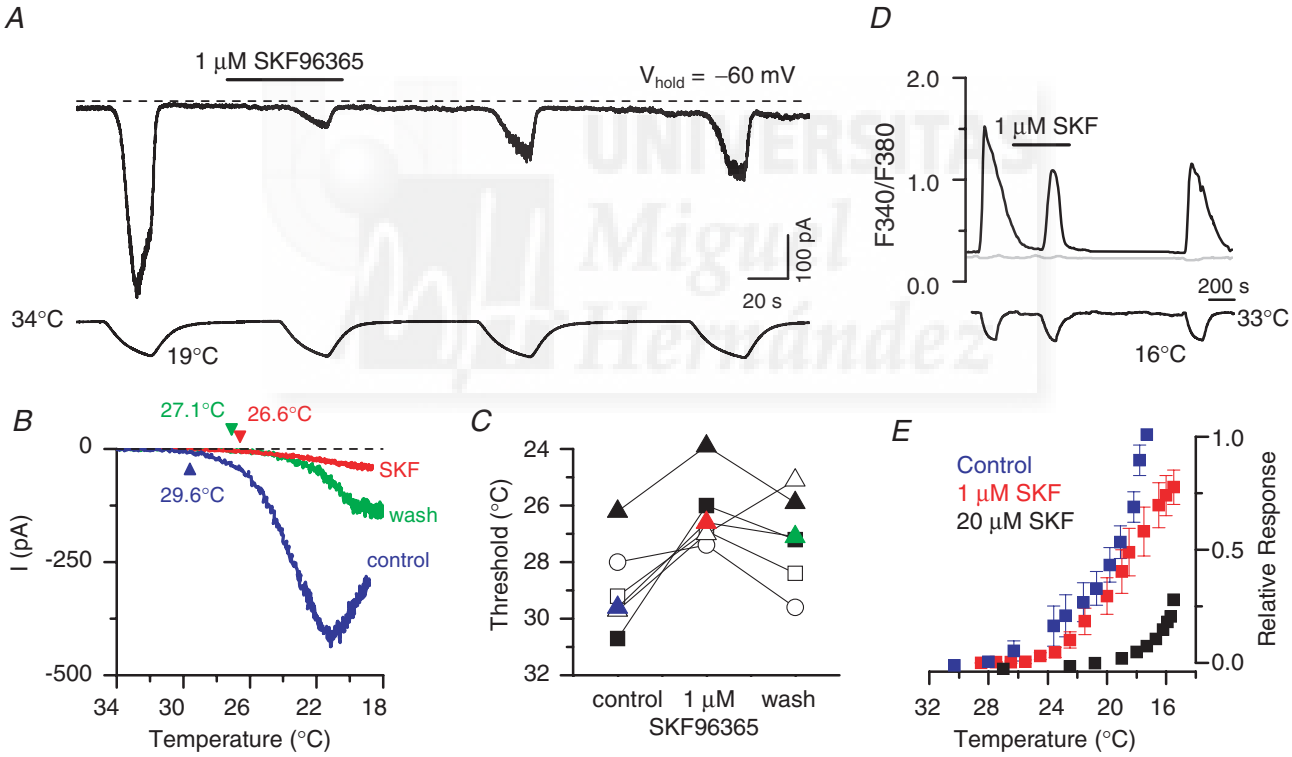

Figure 6. SKF96365 shifts the response-threshold temperature towards lower values in a concentration-dependent manner

A, simultaneous recording of whole-cell membrane current (top trace) and bath temperature (bottom trace) during application of four consecutive cooling ramps to a TRPM8-transfected HEK293 cell (holding potential, −60 mV). Application of 1 μM SKF96365 produced a reversible reduction in I_{cold} amplitude. The dashed line indicates the zero current level. *B*, superimposed current–temperature relationships in control, in the presence of 1 μM SKF96365, and after washout of the drug. Same traces as in *A*. Note the marked shift in threshold temperature induced by SKF96365. The current traces were corrected to yield a 0 pA baseline; holding potential, −60 mV. *C*, response-threshold temperatures of six TPRM8-expressing HEK293 cells during cold applications in control solution, in 1 μM SKF96365 and after washout of the drug. The coloured symbols correspond to the cell in *A* and *B*. *D*, fluorescence ratiometric (F_{340}/F_{380}) calcium-imaging recording of cold-evoked responses in the absence and presence of 1 μM SKF96365. A TRPM8-negative cell in the same field is shown in grey. *E*, relative response–temperature curves constructed from cooling ramps in the presence of 1 and 20 μM SKF96365. Each data point represents the average of 9–16 cells. For clarity, error bars are omitted where negligibly small.

the antagonists, we were curious to investigate the effects of joint applications of agonists (thermal and chemical) and antagonists on TRPM8 channel activity. Menthol-evoked responses of TRPM8 have previously been shown to be blocked by BCTC (Behrendt *et al.* 2004; Weil *et al.* 2005; Madrid *et al.* 2006). We confirmed the same to be true for SKF96365 (not shown), with 20 μM of the antagonist blocking 99.5 ± 3% of the calcium response evoked by 100 μM menthol ($n = 12$, $P < 0.001$, paired t test). To obtain quantitative information on the menthol-induced shifts in temperature sensitivity of TRPM8, we constructed a dose–threshold shift curve (Fig. 7*A* and *B*), which

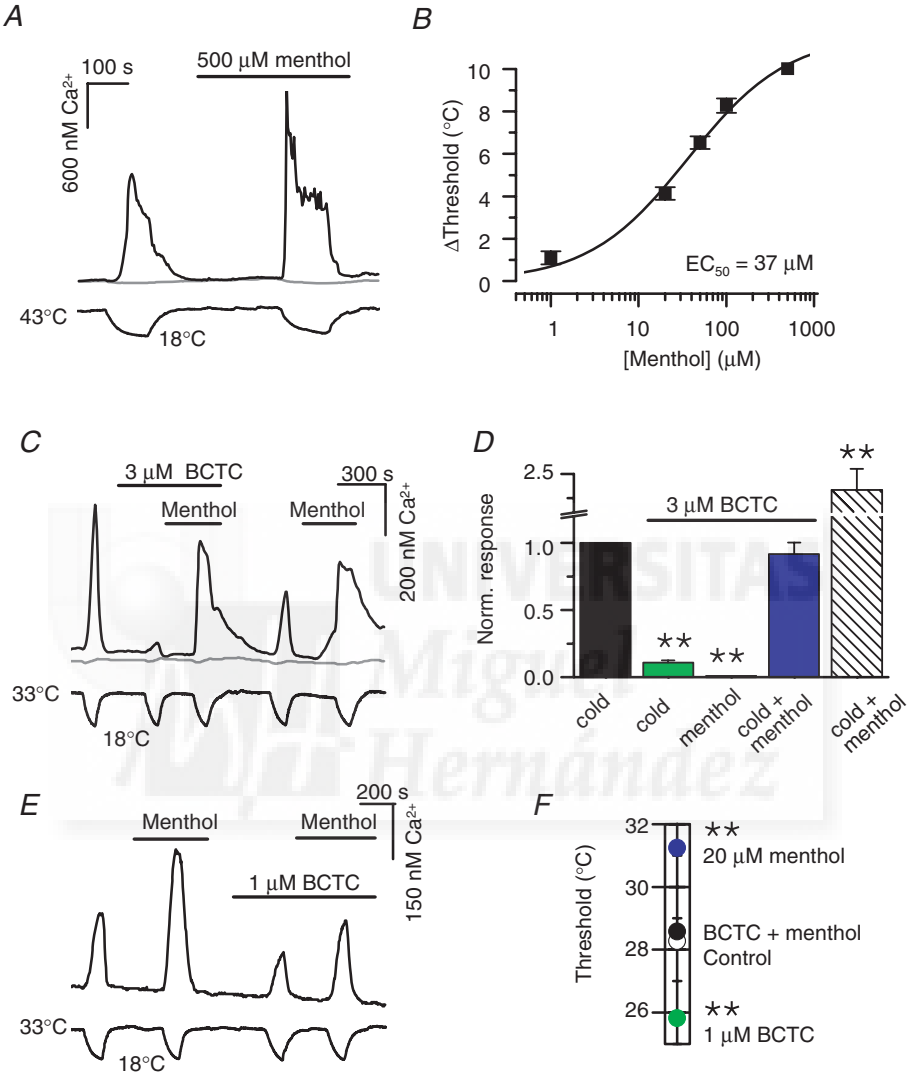

Figure 7. Bidirectional shifts of TRPM8 activity by chemical antagonists and menthol in TRPM8-transfected HEK293 cells

A, time course of ratiometric $[Ca^{2+}]_i$ response in a TRPM8-positive HEK293 cell (black trace) in the absence and presence of 500 μM menthol. The starting temperature was 43–45°C to prevent the 'spontaneous' response to menthol at the usual baseline temperature. The grey trace corresponds to a GFP-negative cell. *B*, correlation between menthol concentration and temperature threshold shift based on experiments shown in *A* ($n = 11$–19). The solid line is the fit to the Hill equation. *C,* experimental recording of the effect of 3 μM BCTC on $[Ca^{2+}]_i$ responses to cold and/or 100 μM menthol. Upper trace is intracellular Ca^{2+} and lower trace is bath temperature. The unresponsive cell (grey trace) did not express GFP. *D,* summary histogram of effects of 3 μM BCTC on cold- and menthol-evoked changes in $[Ca^{2+}]_i$. Note that BCTC effectively blocks calcium responses to cold (86 ± 2% inhibition, $P < 0.01$) or 100 μM menthol (100% inhibition, $P < 0.01$), but not to a combination of the two agonists (92 ± 9% of control response, $P > 0.05$). Each response was normalized to the amplitude of the nearest preceding cold response in control solution; $n = 22$. *E,* experimental recording of the effects of 1 μM BCTC plus 20 μM menthol on cold-evoked responses of TRPM8. Upper trace is intracellular Ca^{2+} and lower trace is bath temperature. *F,* average response-threshold temperatures in control solution, 20 μM menthol, 1 μM BCTC and 1 μM BCTC + 20 μM menthol ($n = 19$). In all panels statistical significance was assessed with Dunnett's *post hoc* test in combination with one-way repeated-measures ANOVA ($P < 0.001$ for all) with respect to the response in control solution, and indicated ***$P < 0.001$, **$P < 0.01$ and *$P < 0.05$.

exhibited a maximum threshold shift of $11.6 \pm 0.9^{\circ}$C and a half-maximum concentration of $37 \pm 9\ \mu$M. Remarkably, this EC_{50} value is very similar to the dose-dependent shift in $V_{1/2}$ produced by menthol (Voets *et al.* 2004). The cooling ramps in these experiments were initiated from 39–45°C to allow for the detection of the menthol-modified temperature thresholds in the absence of a baseline response (see Fig. 7*A*). It should be noted that the briefly applied higher baseline temperature did not modify *per se* the sensitivity of the channel to temperature changes. This was confirmed by an experiment carried out in control solution, where the thresholds to the first cold application (base temperature 32–33°C) and the second cold application (after 200 s of base temperature 39°C) were not statistically different ($n = 5$, $P = 0.7$, paired t test).

Figure 7*C* demonstrates the experimental calcium-imaging protocol where 3 μM BCTC was applied over stimuli of cold, 100 μM menthol and cold combined with menthol. During analysis, each response was normalized to the response to cold in control solution, yielding the graph shown in Fig. 7*D*. Although 3 μM BCTC was capable of nearly abolishing the response to cold, and all of the response to menthol at 33°C, the combination of the two agonists restored the response amplitude to the same level as observed for cold in the absence of chemical agents.

We subsequently searched our data for menthol and antagonist concentrations for which matching threshold temperature shifts, but in the opposite direction, had been observed during individual applications, to see whether these shifts could be cancelled out during the combined application of both agents. Figure 7*E* shows a calcium-imaging experiment, where the joint effects of 1 μM BCTC and 20 μM menthol on apparent response-threshold temperatures were investigated. Notably, analysis of the results (Fig. 7*F*) revealed that the individually observed shifts (i.e. the opposite shifts produced by menthol and BCTC) indeed cancel each other out when the compounds are co-applied during cooling. Another antagonist with similar cancelling effects when combined with 20 μM menthol was 4 μM SKF96365 (not shown). The fact that simple algebraic operations can explain the opposite effects of agonists (cold and menthol) and antagonists on the TRPM8 temperature-response threshold suggests that a common mechanistic principle underlies the actions of the various modulators.

Bidirectional modulation by menthol and blocking agents on cold-evoked responses are maintained in trigeminal thermoreceptors

We investigated whether similar bidirectional shifts in channel function can be observed in native cold thermoreceptors, the sensory neurons responsible for the transduction and coding of temperature signals in the peripheral nervous system (Hensel, 1981). Cold-sensitive trigeminal ganglion neurons were identified by calcium imaging as previously described (de la Pena *et al.* 2005). During rapid reductions in bath temperature from a baseline of 34°C to approximately 18°C, cold-sensitive neurons responded with an average $[Ca^{2+}]_i$ elevation of 247 ± 44 nM ($n = 20$) exhibiting a mean apparent threshold of $30.2 \pm 0.9^{\circ}$C with a range of 10°C. This threshold temperature is significantly higher than the one we obtained in TRPM8-expressing HEK293 cells ($P < 0.001$, Student's unpaired t test). All cold-sensitive neurons identified in this particular calcium-imaging screen were also activated by menthol, which suggests they all expressed endogenous TRPM8 channels. We note here that in a previous similar screen with a higher number of neurons, we also identified a cold-sensitive but menthol-insensitive population that represented ~8% of the total number of cold-sensitive neurons (Madrid *et al.* 2006).

In these neurons, 3 μM BCTC strongly suppressed $[Ca^{2+}]_i$ increases evoked by cold and completely abolished the responses to 100 μM menthol at 34°C (Fig. 8*A* and *C*). As was the case with recombinant TRPM8 channels, applying a cold stimulus in the presence of both menthol and BCTC provoked $[Ca^{2+}]_i$ increases with very similar amplitude to the control response(change in $[Ca^{2+}]_I$, 262 ± 54 nM, $P = 0.29$, $n = 20$). As seen previously for heterologously expressed TRPM8, BCTC application shifted the apparent threshold temperatures of the cold-sensitive neurons towards lower values. In 10 neurons, the cold-induced response was completely abolished; in the other 10 cold-sensitive cells, the effect was partial and the threshold was shifted by an average of $-7.6 \pm 0.6^{\circ}$C ($P < 0.01$). In addition, co-application of menthol and cold completely reversed the negative shift in threshold temperature produced by BCTC, yielding a mean apparent threshold temperature of $31.9 \pm 0.7^{\circ}$C. The mean shifts in threshold temperature for the 10 neurons in which some amount of response remained in the presence of BCTC are shown in Fig. 8*B*.

Finally, the effects of agonists and antagonists on native I_{cold} activation were also investigated. As shown in Fig. 8*D*, cooling produced a reversible inward current at a holding potential of −60 mV, which exhibited an apparent threshold of $30.9 \pm 0.4^{\circ}$C ($n = 29$). Analysis of the current amplitudes under the various conditions confirmed the observations from the calcium-imaging experiments in both trigeminal neurons and TRPM8-expressing HEK293 cells: 3 μM BCTC effectively inhibited responses to separate applications of cold or 100 μM menthol, but co-application of the two agonists restored the response to the level of the control response (Fig. 8*E*).

The effects of BCTC on the voltage activation of I_{cold} were further studied with application of −100 to +200 mV ramps from a holding potential of −60 mV (Fig. 9*A*). An *I–V* plot of the cold-evoked current in the absence and presence of chemical modulators is shown in Fig. 9*C*. I_{cold} displays strong outward rectification and reversal close to 0 mV (0.5 ± 1.0 mV; $n = 8$), which is similar to the properties of current conducted by TRPM8 (I_{TRPM8}) in HEK293 cells. As observed for recombinant TRPM8 channels above, application of a cooling stimulus in the presence of BCTC produced an incomplete inhibition of outward currents but a full inhibition of inward currents in trigeminal neurons. This is illustrated in Fig. 9*D*, where I_{BCTC} represents the part of I_{cold} that was blocked by 3 μM BCTC (i.e. the difference between traces I_{cold} and of the cold current of trigeminal neurons in the presence of 3μM BCTC ($I_{cold+3BCTC}$ in Fig. 9*C*). Note that I_{BCTC} only begins to deviate from I_{cold} at potentials more positive than +70 mV, indicating a complete block by 3 μM BCTC below this value. A similar result was obtained by analysing the blockade of I_{cold} in cold-sensitive trigeminal neurons by 3 μM BCTC over various potentials (Fig. 9*B*).

To estimate $V_{1/2}$, the ramp *I–V* data obtained in the presence and absence of antagonists were fitted (red lines in Fig. 9*C*) with eqn (6). A summary of the mean values obtained for the fitting variables under different experimental conditions is shown in Table 2. Comparing the values in Tables 1 and 2, one can see a notable difference between the mean value of $V_{1/2}$ measured from native I_{cold} and cold-induced I_{TRPM8} in transfected cells; $V_{1/2}$ was significantly more negative in the former (15 *versus* 153 mV, $P < 0.001$, unpaired *t* test). Furthermore, despite the qualitatively similar effect of BCTC on the voltage activation of the cold current in TRPM8-expressing

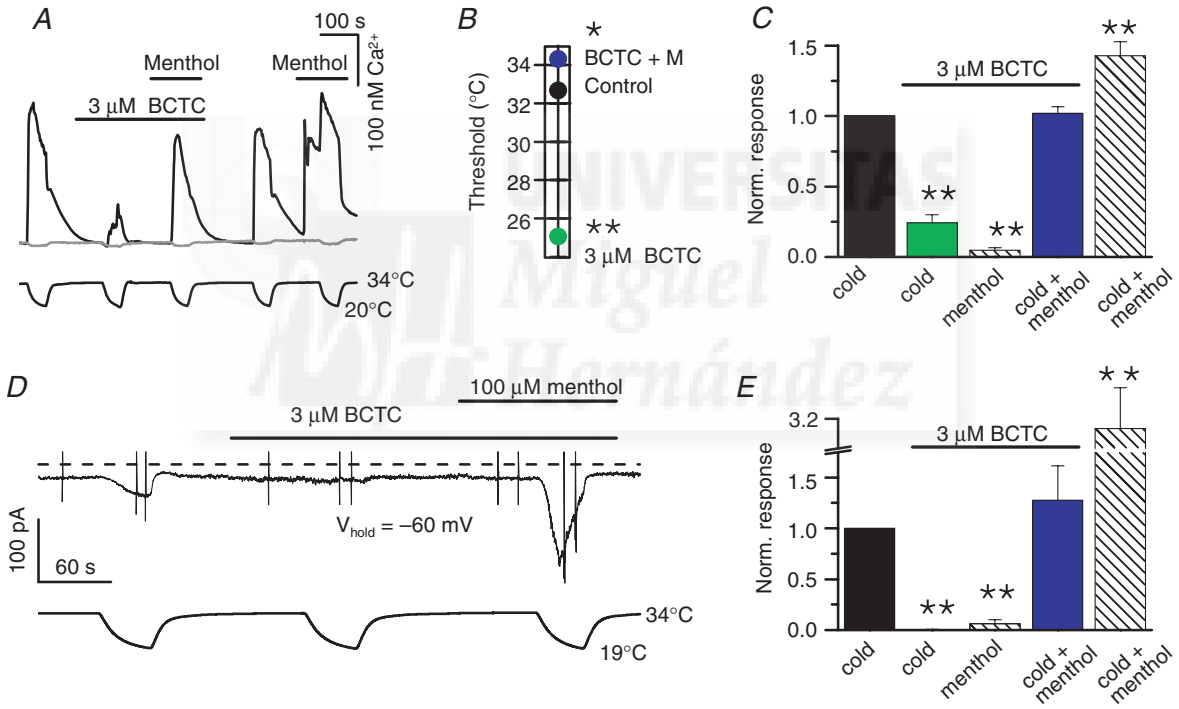

Figure 8. Menthol and the antagonists modulate cold-evoked responses in cold-sensitive trigeminal neurons

A, calcium-imaging recording of the effect of 3 μM BCTC on responses to cold and/or 100 μM menthol. Upper trace is intracellular Ca^{2+} and lower trace is bath temperature. The grey trace shows the simultaneous response in a cold-insensitive neuron for comparison. Note the full inhibition of the menthol-evoked response at 34°C. *B,* average response-threshold temperatures of cold-sensitive trigeminal neurons in control solution, 3 μM BCTC and 3 μM BCTC + 100 μM menthol ($n = 10$). *C*, 3 μM BCTC effectively blocks calcium responses to cold or 100 μM menthol, but not to a combination of the two agonists. Each response was normalized to the nearest preceding cold response in control solution ($n = 20$). *D,* simultaneous recording of whole-cell membrane current (top trace) and bath temperature (bottom trace) during application of three consecutive cooling ramps, showing the effects of 3 μM BCTC and 100 μM menthol on cold responses in a cold-sensitive trigeminal neuron. The holding potential was −60 mV. The dashed line indicates the zero current level and the vertical lines mark clipped current responses to voltage ramps (see Figure 9). *E*, summary histogram of current responses at −60 mV from experiments shown in *D* ($n = 3$–8). In all panels statistical significance was assessed with Dunnett's *post hoc* test in combination with one-way repeated-measures ANOVA ($P < 0.001$ for all) with respect to the response in control solution, and indicated ***$P < 0.001$, **$P < 0.01$ and *$P < 0.05$.

Table 2. Summary of the effects of menthol and BCTC on I_{cold} activation in cold-sensitive trigeminal neurons

	Cold 20°C	Cold 20°C 1 μM BCTC	Cold 20°C 3 μM BCTC	Cold 20°C 100 μM menthol
s (mV^{-1})	40 ± 5	42 ± 5	46 ± 8	32 ± 9
g (nS)	19 ± 4	19 ± 5	5 ± 1*	23 ± 4
$V_{1/2}$ (mV)	15 ± 8	76 ± 14†	137 ± 28*	−101 ± 23†
n	6	4	4	5

The absolute values of the parameters s, g and $V_{1/2}$ obtained from the fits of the ramp (−100 to +200 mV) I–V curves to eqn (6) in the Methods (see text for definitions). The data are given as means ± S.E.M. Statistical significance was assessed with Student's unpaired t test using cold as the reference condition, and is significance indicated: *$P < 0.05$; †$P < 0.01$.

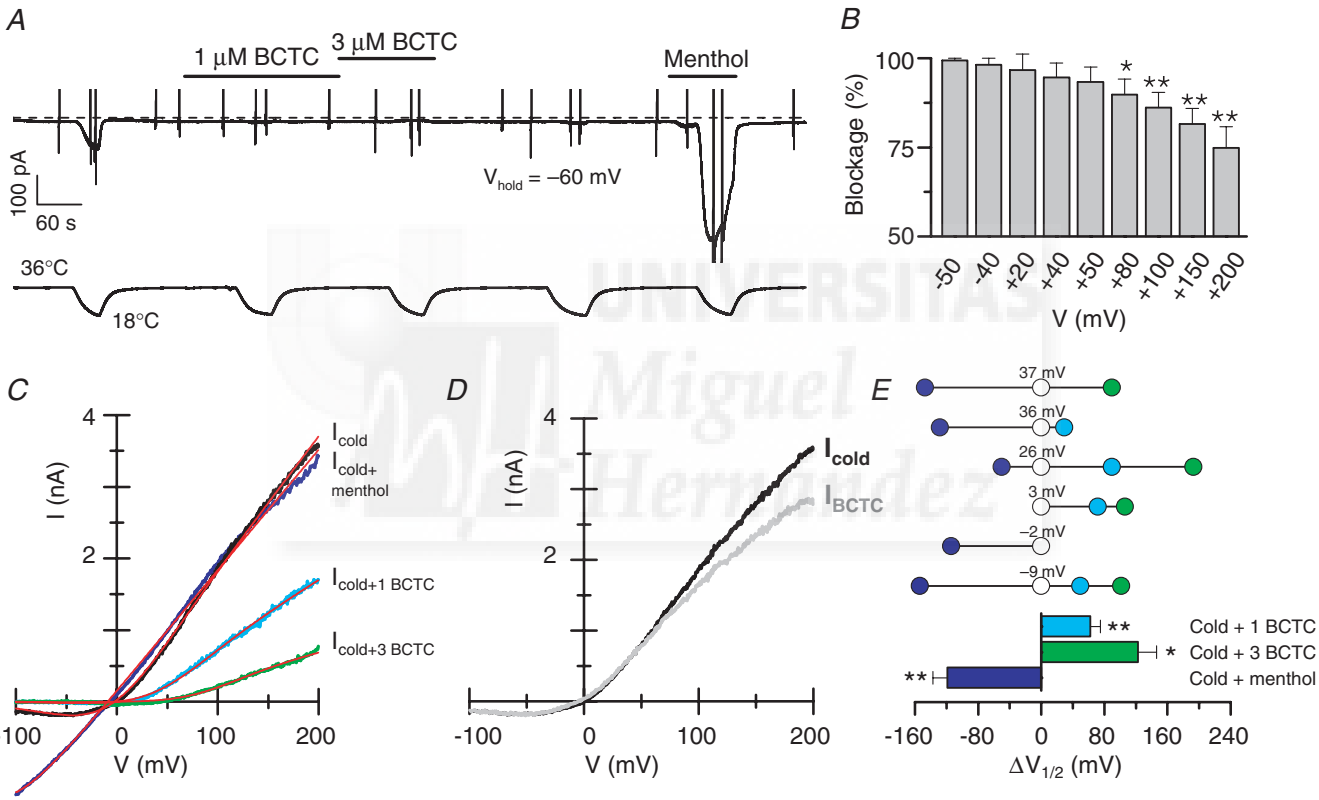

Figure 9. BCTC and menthol produce opposite shifts in the voltage activation curve of I_{cold} in cold-sensitive trigeminal neurons

A, time course of current development at −60 mV in a cold-sensitive trigeminal neuron during cooling ramps. Voltage ramps (−100 to +200 mV) of 1500 ms duration were applied under the various experimental conditions (they appear as vertical bars in the current trace). *B*, blockade of I_{cold} in seven cold-sensitive trigeminal neurons by 3 μM BCTC analysed over various membrane potentials. Dunnett's *post hoc* test in combination with one-way repeated-measures ANOVA ($P < 0.001$) was employed to assess statistical significance between the blockade at each of the studied potentials and at −50 mV. *C*, whole-cell ramp I–V relationships of the experiment shown in *A* at 18°C in the presence and absence of BCTC (1 and 3 μM) and 100 μM menthol. The red lines, superimposed on the recorded I–V relationships, represent the fits of the current to eqn (6). *D*, the grey trace (I_{BCTC}) represents the part of I_{cold} that was blocked by 3 μM BCTC ($I_{cold} - I_{cold+3BCTC}$). Note that I_{BCTC} only begins to deviate from I_{cold} at potentials more positive than +70 mV, indicating a complete block by 3 μM BCTC below this value. *E,* effects of BCTC and menthol on the midpoint of voltage activation during cooling in six cold-sensitive trigeminal neurons. The data are represented as shifts in $V_{1/2}$ with respect to the value obtained for cold (the absolute value for each neuron is indicated above the open symbol). Below a summary histogram of the average shifts in $V_{1/2}$ with respect to cold ($n = 4$–6). Statistical significance was assessed with the unpaired t test and is indicated ***$P < 0.001$, **$P < 0.01$ and *$P < 0.05$.

HEK293 cells and cold-sensitive trigeminal neurons, the magnitude of the shift in $V_{1/2}$ induced by BCTC was significantly larger in the trigeminal neurons: 122 ± 24 ($n = 4$) *versus* 67 ± 11 mV ($n = 8$); $P < 0.05$ (unpaired t test).

These results indicate that native cold-sensitive channels with similar biophysical properties to TRPM8 (e.g. similar reversal potential and rectification properties) are activated by temperature at more negative membrane potentials. The native channels are blocked by BCTC in a similar manner to recombinant TRPM8 in terms of amplitude, but the biophysical modulation (shifts in $V_{1/2}$ and temperature threshold) underlying the inhibition is notably stronger in the trigeminal neurons.

Discussion

At present very little is known about the pharmacological and biophysical properties of TRPM8 channel antagonists (Desai & Clapham, 2005; Dhaka *et al.* 2006; Voets *et al.* 2007). This information is essential to better understand the role of TRPM8 channels in temperature transduction at peripheral thermoreceptors (Madrid *et al.* 2006).

In this study, we provide a thorough characterization of the responses of recombinant TRPM8 channels to their physiological stimulus, cold temperature, and describe in mechanistic terms the effects of substances that increase and decrease the temperature sensitivity of the channel. We identified a common modulatory action of three chemical antagonists (BCTC, SKF96365 and 1,10-phenanthroline) on TRPM8 function that involves marked shifts in their voltage-dependent gating. Furthermore, we describe important differences between the properties of recombinant TRPM8 channels and native currents in trigeminal cold thermoreceptors that underlie their high thermal sensitivity.

Cold-induced responses in TRPM8-expressing HEK293 cells and trigeminal neurons

In our experiments, rat TRPM8-transfected HEK293 cells responded to cooling with apparent threshold temperatures of 26.8°C and 27.6°C as measured by calcium imaging and electrophysiology, respectively. These values, although among the highest reported for heterologously expressed rodent TRPM8 (McKemy *et al.* 2002; Peier *et al.* 2002; Andersson *et al.* 2004), are clearly lower than observed for cold-sensitive trigeminal and dorsal root ganglion neurons (Reid *et al.* 2002; Viana *et al.* 2002; Thut *et al.* 2003; Madrid *et al.* 2006). Such differences suggest that the cellular environment (e.g. membrane lipid composition and presence of auxiliary subunits) may be an important factor in the modulation of TRPM8 function, and/or that other mechanisms of cold transduction are present in sensory neurons, making them more sensitive to temperature decreases (de la Pena *et al.* 2005).

BCTC is the most potent antagonist of cold-evoked responses in TRPM8 channels

Arranging the blockers from our study by their IC_{50} values yielded the following sequence of potency: BCTC > SKF96365 >> 1,10-phenanthroline, with the first two compounds exhibiting concentrations of half-maximum TRPM8 inhibition below or close to 1 μM. Comparison with previously reported values revealed that SKF96365 is a slightly more potent antagonist of TRPM8 than of other TRP channels (e.g. TRPC3 and TRPC6) studied to date (Zhu *et al.* 1998; Inoue *et al.* 2001). By contrast, SKF96365 was not an effective blocker of the epithelial calcium channel TRPV5 (Nilius *et al.* 2001).

Here, 1,10-phenanthroline was equally effective in blocking cold-evoked TRPM8 responses in the presence as in the absence of Cu^{2+}. This finding is in contrast with a previous report on TRPV1, where heat-evoked currents were only blocked in the presence of the Cu–Phe complex (Tousova *et al.* 2004) suggesting a different mechanism of block for these two TRP channels.

BCTC produced full antagonism of cold-evoked TRPM8 activity in the temperature range studied, with similar IC_{50} values to those determined using menthol as the stimulus (Behrendt *et al.* 2004; Weil *et al.* 2005; Madrid *et al.* 2006). These IC_{50} values, although one to two orders of magnitude larger than observed for TRPV1 (Valenzano *et al.* 2003; Correll *et al.* 2004), make BCTC the most potent and most effective antagonists of TRPM8 channels to date.

In conclusion, although none of the blockers studied here are specific for TRPM8, the potent and reversible TRPM8 antagonism by BCTC and SKF96365 should make them useful for further functional characterization of thermoreceptor fibres and the role of TRPM8 channels in cold transduction.

Menthol and the blockers act as TRPM8 modulators in opposite directions

TRPM8 is a voltage-dependent channel (Voets *et al.* 2004; Brauchi *et al.* 2004; Rohacs *et al.* 2005). Low temperature, cooling agents (such as menthol) and the inositide phospholipids (such as phosphatidylinositol 4,5-bisphosphate (PIP_2)) are known to shift the activation curve towards more physiological membrane potentials. However, the mechanisms and sites of action of these stimuli on the TRPM8 protein remain unclear. The voltage and temperature sensors are situated on separate structural domains (Brauchi *et al.* 2006). Furthermore, the

menthol binding site and the cold sensor are structurally separate entities (Bandell *et al.* 2006). Whether the menthol molecule acts directly on the voltage sensor of TRPM8 or has a separate binding site on the protein remains to be resolved.

In the present work, we identify three new gating modifiers of TRPM8. On basis of the apparent voltage dependence of block and the shifts in the voltage activation of the channel towards more depolarized potentials, BCTC, SKF96365 and 1,10-phenanthroline should be considered negative allosteric modulators of the channel. In agreement with this view, recent reports on the effects of ethanol (albeit at a high concentration) on TRPM8 were also ascribed to a rightward shift in voltage-dependent gating (Benedikt *et al.* 2007). These agents may become useful tools in the ongoing quest for the molecular determinants of TRPM8 gating and regulation (Chuang *et al.* 2004; Nilius *et al.* 2005; Rohacs *et al.* 2005; Bandell *et al.* 2006). It is also of interest to find out whether the heat-sensitive TRPV1 channel can be modulated in a similar way by these chemical agents.

The main functional consequence of the dynamic voltage-dependent gating of TRPM8 is a shift in the apparent temperature activation threshold of the cell. Consequently, the studied antagonists exert an opposite effect to cooling and menthol on the thermosensitivity of the channel. Furthermore, the effects induced separately by menthol and the antagonists appear to be additive (i.e. they cancel each other during joint application of the compounds). The above findings raise the question of whether menthol and the antagonists studied here share the same site of action, or act through separate receptors. We find indications suggesting that the antagonists may be acting on different sites from which they exert their competitive, opposite effects on the voltage gating of TRPM8. Because the functional and biophysical effects of the antagonists on cold-evoked responses – shifts in apparent temperature thresholds and $V_{1/2}$ – take place both in the absence and presence of menthol, and the antagonist-induced shifts in the voltage-dependent activation are in fact stronger during activation by menthol than by cold, it seems likely that the inhibitory effect is independent of the occupation of the menthol-binding site. This issue can only be completely settled with a direct analysis of ligand binding, with *ad hoc* designed radioactive probes.

The fact that none of the inhibitors acted as a pure pore blocker (i.e. reducing channel activity without affecting channel gating) indicates that some caution should be taken when interpreting the lack of inhibitory actions of these agents on cold-evoked responses at nerve terminals (Madrid *et al.* 2006): the negative modulatory effects on the native channel may be insufficient to prevent cold-evoked activity. However, when we compared the effects of BCTC on channel gating observed in TRPM8-expressing HEK293 cells and in cold-sensitive trigeminal neurons, we found that the opposite was true: the neurons were, in fact, more sensitive to modulation by BCTC than the HEK293 cells. Together with the fact that in the study by Madrid *et al.* (2006) the effects of menthol – a more potent agonist of recombinant TRPM8 channels than cold temperature – were fully suppressed at the nerve terminals, the new observations from this work argue for alternative explanations, such as the presence of additional, TRPM8-independent, cold sensors at nerve endings (Viana *et al.* 2002).

Native I_{cold} channels have distinct properties

The bidirectional modulation of the voltage-dependent activation and the resulting shift in temperature threshold caused by menthol and antagonists is also conserved in cold-sensitive trigeminal neurons expressing native TRPM8 protein subunits. We found a remarkable difference in the $V_{1/2}$ of TRPM8 activation between native and recombinant channels, with a much higher open probability at negative potentials in the former case. Thus, despite lower values of cold- and menthol-sensitive conductance in neurons (i.e. lower density of TRPM8 channels), their higher open probability gives rise to larger inward currents at physiological membrane potentials. In functional terms, this difference translates into a much higher apparent threshold temperature in native thermoreceptors compared to recombinant TRPM8 channels (see Supplementary Fig. 1). In both cases, response thresholds can be shifted bidirectionally by more than 15°C, directly illustrating the dynamic nature of the apparent temperature threshold of TRPM8 channels. Although our results were obtained with exogenous agents, it is very likely that endogenous modulators of the channel operate upon the same general principles, and in the process give rise to the wide range of threshold temperatures exhibited by recombinant TRPM8 channels in various expression systems (de la Pena *et al.* 2005) and cold-sensitive thermoreceptors (Reid *et al.* 2002; Viana *et al.* 2002; Thut *et al.* 2003). One such endogenous modulator could be the membrane lipid PIP_2, which is known to potentiate the activity of TRPM8 (Liu & Qin, 2005; Rohacs *et al.* 2005; Benedikt *et al.* 2007) and that of other TRP channels (Hardie, 2003; Nilius *et al.* 2006). Notably, PIP_2 modulates TRPM8 by shifting the $V_{1/2}$ of activation of the channels (Rohacs *et al.* 2005). Additional factors that may contribute to the response plasticity of thermoreceptors are changes in TRPM8 channel density, modulation of TRPM8 by intracellular Ca^{2+} levels (McKemy *et al.* 2002; Reid *et al.* 2002; Rohacs *et al.* 2005), phosphorylation status of TRPM8 (Premkumar *et al.* 2005; Abe *et al.* 2006) and the variable expression of potassium channels acting as temperature-dependent excitability brakes (Viana *et al.* 2002).

References

Abe J, Hosokawa H, Sawada Y, Matsumura K & Kobayashi S (2006). Ca^{2+}-dependent PKC activation mediates menthol-induced desensitization of transient receptor potential M8. *Neurosci Lett* **397**, 140–144.

Andersson DA, Chase HW & Bevan S (2004). TRPM8 activation by menthol, icilin, and cold is differentially modulated by intracellular pH. *J Neurosci* **24**, 5364–5369.

Aziz QH, Partridge CJ, Munsey TS & Sivaprasadarao A (2002). Depolarization induces intersubunit cross-linking in a S4 cysteine mutant of the Shaker potassium channel. *J Biol Chem* **277**, 42719–42725.

Bandell M, Dubin AE, Petrus MJ, Orth A, Mathur J, Hwang SW & Patapoutian A (2006). High-throughput random mutagenesis screen reveals TRPM8 residues specifically required for activation by menthol. *Nat Neurosci* **9**, 493–500.

Bautista DM, Jordt SE, Nikai T, Tsuruda PR, Read AJ, Poblete J, Yamoah EN, Basbaum AI & Julius D (2006). TRPA1 mediates the inflammatory actions of environmental irritants and proalgesic agents. *Cell* **124**, 1269–1282.

Behrendt HJ, Germann T, Gillen C, Hatt H & Jostock R (2004). Characterization of the mouse cold-menthol receptor TRPM8 and vanilloid receptor type-1 VR1 using a fluorometric imaging plate reader (FLIPR) assay. *Br J Pharmacol* **141**, 737–745.

Benedikt J, Teisinger J, Vyklicky L & Vlachova V (2007). Ethanol inhibits cold-menthol receptor TRPM8 by modulating its interaction with membrane phosphatidylinositol 4,5-bisphosphate. *J Neurochem* **100**, 211–224.

Brauchi S, Orio P & Latorre R (2004). Clues to understanding cold sensation: thermodynamics and electrophysiological analysis of the cold receptor TRPM8. *Proc Natl Acad Sci U S A* **101**, 15494–15499.

Brauchi S, Orta G, Salazar M, Rosenmann E & Latorre R (2006). A hot-sensing cold receptor: C-terminal domain determines thermosensation in transient receptor potential channels. *J Neurosci* **26**, 4835–4840.

Caterina MJ, Leffler A, Malmberg AB, Martin WJ, Trafton J, Petersen-Zeitz KR, Koltzenburg M, Basbaum AI & Julius D (2000). Impaired nociception and pain sensation in mice lacking the capsaicin receptor. *Science* **288**, 306–313.

Chuang HH, Neuhausser WM & Julius D (2004). The super-cooling agent icilin reveals a mechanism of coincidence detection by a temperature-sensitive TRP channel. *Neuron* **43**, 859–869.

Clapham DE (2003). TRP channels as cellular sensors. *Nature* **426**, 517–524.

Correll CC, Phelps PT, Anthes JC, Umland S & Greenfeder S (2004). Cloning and pharmacological characterization of mouse TRPV1. *Neurosci Lett* **370**, 55–60

de la Pena E, Malkia A, Cabedo H, Belmonte C & Viana F (2005). The contribution of TRPM8 channels to cold sensing in mammalian neurones. *J Physiol* **567**, 415–426.

Desai BN & Clapham DE (2005). TRP channels and mice deficient in TRP channels. *Pflugers Arch* **451**, 11–18.

Dhaka A, Viswanath V & Patapoutian A (2006). TRP ion channels and temperature sensation. *Annu Rev Neurosci* **29**, 135–161.

Fleig A & Penner R (2004). The TRPM ion channel subfamily: molecular, biophysical and functional features. *Trends Pharmacol Sci* **25**, 633–639.

Garcia-Martinez C, Humet M, Planells-Cases R, Gomis A, Caprini M, de la Viana FPE *et al.* (2002). Attenuation of thermal nociception and hyperalgesia by VR1 blockers. *Proc Natl Acad Sci U S A* **99**, 2374–2379.

Hardie RC (2003). Regulation of TRP channels via lipid second messengers. *Annu Rev Physiol* **65**, 735–759.

Hensel H (1981). Thermoreception and temperature regulation. *Monogr Physiol Soc* **38**, 1–321.

Hille B (2001). *Ion Channels of Excitable Membranes*, 3rd edn, pp. 1–814. Sinauer Associates, Sunderlad, MA.

Hofmann T, Chubanov V, Gudermann T & Montell C (2003). TRPM5 is a voltage-modulated and Ca^{2+}-activated monovalent selective cation channel. *Curr Biol* **13**, 1153–1158.

Inoue R, Okada T, Onoue H, Hara Y, Shimizu S, Naitoh S, Ito Y & Mori Y (2001). The transient receptor potential protein homologue TRP6 is the essential component of vascular α_1-adrenoceptor-activated Ca^{2+}-permeable cation channel. *Circ Res* **88**, 325–332.

Jordt SE, McKemy DD & Julius D (2003). Lessons from peppers and peppermint: the molecular logic of thermosensation. *Curr Opin Neurobiol* **13**, 487–492.

Krause JE, Chenard BL & Cortright DN (2005). Transient receptor potential ion channels as targets for the discovery of pain therapeutics. *Curr Opin Investig Drugs* **6**, 48–57.

Kwan KY, Allchorne AJ, Vollrath MA, Christensen AP, Zhang DS, Woolf CJ & Corey DP (2006). TRPA1 contributes to cold, mechanical, and chemical nociception but is not essential for hair-cell transduction. *Neuron* **50**, 277–289.

Liu B & Qin F (2005). Functional control of cold- and menthol-sensitive TRPM8 ion channels by phosphatidylinositol 4,5-bisphosphate. *J Neurosci* **25**, 1674–1681.

Liu HS, Jan MS, Chou CK, Chen PH & Ke NJ (1999). Is green fluorescent protein toxic to the living cells? *Biochem Biophys Res Commun* **260**, 712–717.

Liu Y, Jurman ME & Yellen G (1996). Dynamic rearrangement of the outer mouth of a K^+ channel during gating. *Neuron* **16**, 859–867.

McKemy DD (2005). How cold is it? TRPM8 and TRPA1 in the molecular logic of cold sensation. *Mol Pain* **1**, 16.

McKemy DD, Neuhausser WM & Julius D (2002). Identification of a cold receptor reveals a general role for TRP channels in thermosensation. *Nature* **416**, 52–58.

Madrid R, Donovan-Rodriguez T, Meseguer V, Acosta MC, Belmonte C & Viana F (2006). Contribution of TRPM8 channels to cold transduction in primary sensory neurons and peripheral nerve terminals. *J Neurosci* **26**, 12512–12525.

Merritt JE, Armstrong WP, Benham CD, Hallam TJ, Jacob R, Jaxa-Chamiec A, Leigh BK, McCarthy SA, Moores KE & Rink TJ (1990). SK&F 96365, a novel inhibitor of receptor-mediated calcium entry. *Biochem J* **271**, 515–522.

Montell C, Birnbaumer L & Flockerzi V (2002). The TRP channels, a remarkably functional family. *Cell* **108**, 595–598.

Nealen ML, Gold MS, Thut PD & Caterina MJ (2003). TRPM8 mRNA is expressed in a subset of cold-responsive trigeminal neurons from rat. *J Neurophysiol* **90**, 515–520.

Nilius B, Mahieu F, Prenen J, Janssens A, Owsianik G, Vennekens R & Voets T (2006). The Ca^{2+}-activated cation channel TRPM4 is regulated by phosphatidylinositol 4,5-biphosphate. *EMBO J* **25**, 467–478.

Nilius B, Owsianik G, Voets T & Peters JA (2007). Transient receptor potential cation channels in disease. *Physiol Rev* **87**, 165–217.

Nilius B, Prenen J, Droogmans G, Voets T, Vennekens R, Freichel M, Wissenbach U & Flockerzi V (2003). Voltage dependence of the Ca^{2+}-activated cation channel TRPM4. *J Biol Chem* **278**, 30813–30820.

Nilius B, Prenen J, Vennekens R, Hoenderop JG, Bindels RJ & Droogmans G (2001). Pharmacological modulation of monovalent cation currents through the epithelial Ca^{2+} channel ECaC1. *Br J Pharmacol* **134**, 453–462.

Nilius B, Talavera K, Owsianik G, Prenen J, Droogmans G & Voets T (2005). Gating of TRP channels: a voltage connection? *J Physiol* **567**, 35–44.

Okazawa M, Takao K, Hori A, Shiraki T, Matsumura K & Kobayashi S (2002). Ionic basis of cold receptors acting as thermostats. *J Neurosci* **22**, 3994–4001.

Owsianik G, Talavera K, Voets T & Nilius B (2006). Permeation and selectivity of TRP channels. *Annu Rev Physiol* **68**, 685–717.

Pedersen SF, Owsianik G & Nilius B (2005). TRP channels: an overview. *Cell Calcium* **38**, 233–252.

Peier AM, Moqrich A, Hergarden AC, Reeve AJ, Andersson DA, Story GM, Earley TJ, Dragoni I, McIntyre P, Bevan S & Patapoutian A (2002). A TRP channel that senses cold stimuli and menthol. *Cell* **108**, 705–715.

Popa MO & Lerche H (2006). $Cu^{2+}(1,10\ phenanthroline)_3$ is an open-channel blocker of the human skeletal muscle sodium channel. *Br J Pharmacol* **147**, 808–814.

Premkumar LS, Raisinghani M, Pingle SC, Long C & Pimentel F (2005). Downregulation of transient receptor potential melastatin 8 by protein kinase C-mediated dephosphorylation. *J Neurosci* **25**, 11322–11329.

Reid G (2005). ThermoTRP channels and cold sensing: what are they really up to? *Pflugers Arch* **451**, 250–263.

Reid G, Babes A & Pluteanu F (2002). A cold- and menthol-activated current in rat dorsal root ganglion neurones: properties and role in cold transduction. *J Physiol* **545**, 595–614.

Reid G & Flonta ML (2001). Physiology. Cold current in thermoreceptive neurons. *Nature* **413**, 480.

Rohacs T, Lopes CM, Michailidis I & Logothetis DE (2005). $PI(_{4,5})P_2$ regulates the activation and desensitization of TRPM8 channels through the TRP domain. *Nat Neurosci* **8**, 626–634.

Schwarz G, Droogmans G & Nilius B (1994). Multiple effects of SK&F 96365 on ionic currents and intracellular calcium in human endothelial cells. *Cell Calcium* **15**, 45–54.

Thut PD, Wrigley D & Gold MS (2003). Cold transduction in rat trigeminal ganglia neurons in vitro. *Neuroscience* **119**, 1071–1083.

Tousova K, Susankova K, Teisinger J, Vyklicky L & Vlachova V (2004). Oxidizing reagent copper-o-phenanthroline is an open channel blocker of the vanilloid receptor TRPV1. *Neuropharmacology* **47**, 273–285.

Tsavaler L, Shapero MH, Morkowski S & Laus R (2001). Trp-p8, a novel prostate-specific gene, is up-regulated in prostate cancer and other malignancies and shares high homology with transient receptor potential calcium channel proteins. *Cancer Res* **61**, 3760–3769.

Valenzano KJ, Grant ER, Wu G, Hachicha M, Schmid L, Tafesse L *et al.* (2003). *N*-(4-tertiarybutylphenyl)-4-(3-chloropyridin-2-yl) tetrahydropyrazine -1(2*H*)-carbox-amide (BCTC), a novel, orally effective vanilloid receptor 1 antagonist with analgesic properties: I. in vitro characterization and pharmacokinetic properties. *J Pharmacol Exp Ther* **306**, 377–386.

Viana F, de la Pena E & Belmonte C (2002). Specificity of cold thermotransduction is determined by differential ionic channel expression. *Nat Neurosci* **5**, 254–260.

Voets T, Droogmans G, Wissenbach U, Janssens A, Flockerzi V & Nilius B (2004). The principle of temperature-dependent gating in cold- and heat-sensitive TRP channels. *Nature* **430**, 748–754.

Voets T, Owsianik G & Nilius B (2007). TRPM8. *Handb. Exp. Pharmacol* **179**, 329–344.

Weil A, Moore SE, Waite NJ, Randall A & Gunthorpe MJ (2005). Conservation of functional and pharmacological properties in the distantly related temperature sensors TRPV1 and TRPM8. *Mol Pharmacol* **68**, 518–527.

Wissenbach U, Niemeyer BA & Flockerzi V (2004). TRP channels as potential drug targets. *Biol Cell* **96**, 47–54.

Zhang L & Barritt GJ (2006). TRPM8 in prostate cancer cells: a potential diagnostic and prognostic marker with a secretory function? *Endocr Relat Cancer* **13**, 27–38.

Zhu X, Jiang M & Birnbaumer L (1998). Receptor-activated Ca^{2+} influx via human Trp3 stably expressed in human embryonic kidney (HEK) 293 cells. Evidence for a non-capacitative Ca^{2+} entry. *J Biol Chem* **273**, 133–142.

Acknowledgements

The authors thank E. Quintero, A. Miralles and A. Pérez Vegara for excellent technical assistance. The TRPM8 cDNA and pcINeo-IRES-GFP vector were generous gifts from Drs David Julius and Jan Eggermont, respectively. The HEK293 CR#1 cell line was supplied by Dr Ramón Latorre. The authors thank Diego Muñoz for performing some preliminary experiments concerning effects of BCTC. During the course of this work A.M. was supported by the Spanish Ministry of Foreign affairs (MAE)/Spanish Agency for International Cooperation (AECI), the Osk Huttunen Foundation and the Academy of Finland (grant no. 107866), R.M. was supported by a postdoctoral fellowship of the Spanish Fundación Marcelino Botín and V.M and M.V. by predoctoral fellowships from the Generalitat Valenciana. The work was also supported by funds from the Spanish Ministry of Education and Science: projects SAF2004-01011 to F.V. and BFI2002-03788 to C.B.

Supplemental material

Online supplemental material for this paper can be accessed at:
http://jp.physoc.org/cgi/content/full/jphysiol.2006.123059/DC1
and
http://www.blackwell-synergy.com/doi/suppl/10.1113/jphysiol.2006.123059

Behavioral/Systems/Cognitive

Contribution of TRPM8 Channels to Cold Transduction in Primary Sensory Neurons and Peripheral Nerve Terminals

Rodolfo Madrid, Tansy Donovan-Rodríguez, Victor Meseguer, Mari Carmen Acosta, Carlos Belmonte, and Félix Viana
Instituto de Neurociencias de Alicante, Universidad Miguel Hernández–Consejo Superior de Investigaciones Científicas, 03550 San Juan de Alicante, Spain

Transient receptor potential melastatin 8 (TRPM8) is the best molecular candidate for innocuous cold detection by peripheral thermoreceptor terminals. To dissect out the contribution of this cold- and menthol-gated, nonselective cation channel to cold transduction, we identified BCTC [*N*-(4-*tert*-butylphenyl)-4-(3-chloropyridin-2-yl)piperazine-1-carboxamide] as a potent and full blocker of recombinant TRPM8 channels. In cold-sensitive trigeminal ganglion neurons of mice and guinea pig, responses to menthol were abolished by BCTC. In contrast, the effect of BCTC on cold-evoked responses was variable but showed a good correlation with the presence or lack of menthol sensitivity in the same neuron, suggesting a specific blocking action of BCTC on TRPM8 channels. The biophysical properties of native cold-gated currents (I_{cold}), and the currents blocked by BCTC were nearly identical, consistent with a role of this channel in cold sensing at the soma. The temperature activation threshold of native TRPM8 channels was significantly warmer than those reported in previous expression studies. The effect of BCTC on native I_{cold} was characterized by a dose-dependent shift in the temperature threshold of activation.

The role of TRPM8 in transduction was further investigated in the guinea pig cornea, a peripheral territory densely innervated with cold thermoreceptors. All cold-sensitive terminals were activated by menthol, suggesting the functional expression of TRPM8 channels in their membrane. However, the spontaneous activity and firing pattern characteristic of cold thermoreceptors was totally immune to TRPM8 channel blockade with BCTC or SKF96365 (1-[2-(4-methoxyphenyl)-2-[3-(4-methoxyphenyl)propoxy]ethyl-1*H*-imidazole hydrochloride). Cold-evoked responses in corneal terminals were also essentially unaffected by these drugs, whereas responses to menthol were completely abolished. The minor impairment in the ability to transduce cold stimuli by peripheral corneal thermoreceptors during TRPM8 blockade unveils an overlapping functional role for various thermosensitive mechanisms in these nerve terminals.

Key words: **somatosensory; trigeminal ganglion; nociceptor; cornea; BCTC; SKF96365**

Introduction

The activation by low temperatures of specific receptors located on the surface of the body gives rise to a rich spectrum of sensations that range from pleasantly cool to outright painful (Yarnitsky and Ochoa, 1991; Chen et al., 1996; Craig et al., 2000; Acosta et al., 2001). The transduction of temperature stimuli into propagated nerve impulses occurs in free endings of thin sensory axons (Hensel and Zotterman, 1951; Hensel, 1981; Heppelmann et al., 1990). At normal skin temperatures, innocuous cold thermoreceptors exhibit spontaneous, periodic activity that is augmented by cooling and silenced by warming (Hensel and Zotterman, 1951; Brock et al., 2001). In contrast, cold nociceptors are quiescent at rest firing only in response to low temperatures (LaMotte and Thalhammer, 1982; Simone and Kajander, 1997).

The recent identification of several ion channels with marked sensitivity to cooling provides a molecular framework to understand the transduction mechanisms for cold temperatures by sensory endings (for review, see Jordt et al., 2003; Patapoutian et al., 2003; Reid, 2005). So far, transient receptor potential melastatin 8 (TRPM8), a nonselective cation channel of the transient receptor potential superfamily (McKemy et al., 2002; Peier et al., 2002), is the best molecular candidate to explain the transduction of moderate cold. Recombinant TRPM8 channels are activated by low temperatures (threshold of ~25°C) and by exposure to cooling compounds such as menthol. These channels are expressed selectively in a subpopulation of cold-sensitive (CS) primary sensory neurons (McKemy et al., 2002; Peier et al., 2002) with specific electrophysiological properties (Reid et al., 2002; Viana et al., 2002). In these neurons, cooling opens a cation current (I_{cold}) with properties consistent with those of TRPM8-dependent currents in transfected cells (Okazawa et al., 2002; Reid et al., 2002). The same neurons are also excited by menthol (McKemy et al., 2002; Reid et al., 2002; Viana et al., 2002; Nealen et al., 2003; Thut et al., 2003).

Nonetheless, a significant percentage of CS neurons in culture

Received Feb. 22, 2006; revised Oct. 24, 2006; accepted Oct. 24, 2006.

This work was supported by Spanish Ministry of Education and Science Projects SAF2004-01011 (F.V.) and BFU2005-08741 (C.B.). R.M. is a postdoctoral fellow of the Spanish Fundación Carolina, T.D.-R. is a fellow of the Fundación Marcelino Botín, and V.M. holds a predoctoral fellowship from the Generalitat Valenciana. We thank E. Quintero and A. Pérez Vegara for excellent technical assistance. Elvira de la Peña performed the experiments shown in supplemental Figure 3*A* (available at www.jneurosci.org as supplemental material), and Carolina Luna contributed preliminary data on SKF96365 effects in corneal terminals. The rat TRPM8 and the mouse TRPA1 cDNA were a generous gift from David Julius and Ardem Patapoutian, respectively. We thank Elvira de la Peña, Annika Mälkiä, Patricio Orio, María Dominguez, and Roberto Gallego for comments on this manuscript.

Correspondence should be addressed to Dr. Félix Viana, Instituto de Neurociencias de Alicante, Universidad Miguel Hernández–Consejo Superior de Investigaciones Científicas, Apartado 18, 03550 San Juan de Alicante, Spain. E-mail: felix.viana@umh.es.

DOI:10.1523/JNEUROSCI.3752-06.2006

 0270-6474/06/2612512-14$15.00/0

are insensitive to menthol and lack TRPM8 transcripts (Nealen et al., 2003; Babes et al., 2004). Moreover, other studies have revealed that menthol-insensitive channels also contribute to I_{cold} (Reid and Flonta, 2001; Viana et al., 2002). Additional evidence for TRPM8-independent cold transduction mechanisms has been reported in damaged sensory endings (Cabanes et al., 2003; Roza et al., 2006). Thus, despite significant advances in our understanding of cold thermotransduction (Brauchi et al., 2004; Voets et al., 2004; McKemy, 2005; Reid, 2005), the role of TRPM8 channels in defining the sensory modality, temperature activation threshold, and spontaneous discharge of native cold receptors is not well established.

Recently, the compound BCTC [*N*-(4-*tert*-butylphenyl)-4-(3-chloropyridin-2-yl)piperazine-1-carboxamide] has been identified as a blocker of menthol-evoked responses in TRPM8 channels (Behrendt et al., 2004; Weil et al., 2005). Here we show that BCTC is also a potent and rather selective blocker of cold-activated responses in TRPM8 channels. Thereafter, we used BCTC to explore the contribution of TRPM8 to cold-evoked electrical activity in the soma and peripheral nerve terminals of trigeminal ganglion (TG) neurons. Peripheral studies were performed in the cornea, a tissue with a dense innervation of cold thermoreceptors (Gallar et al., 1993; Carr et al., 2003). We conclude that, in the soma of the large majority of cultured trigeminal neurons, activation of TRPM8 channels is the major player in establishing cold-evoked responses. In contrast, TRPM8 channels mediate only the response to menthol of peripheral cold thermoreceptors but not their ongoing activity or the increased impulse discharges evoked by cooling, indicating that thermal sensitivity of innocuous cold thermoreceptors is determined by additional ionic mechanisms.

Materials and Methods

Rat TRPM8 cDNA (a gift from Dr. David Julius, University of California, San Francisco, CA) was subcloned in the bicistronic vector pcINeo/internal ribosomal entry site–green fluorescent protein (GFP), as described previously, and used for transient transfection in HEK293 cells (de la Pena et al., 2005). Mouse ankyrin-repeat TRP subtype 1 (TRPA1) in pCDNA5 (a gift from Dr. Ardem Patapoutian, Scripps Research Institute, La Jolla, CA) was cotransfected with pGreen Lantern-1 GFP (Invitrogen, Carlsbad, CA)at a 1:1 ratio. Transfected cells were identified by their green fluorescence emission during excitation with 470 nm light.

Culture of HEK293 cells and trigeminal ganglion neurons. HEK293 cells were obtained from The European Collection of Cell Cultures (Salisbury, UK). Cells were cultured in DMEM containing 10% of fetal bovine serum and plated on 2 cm^2 wells at 400,000 cells per well and grown for 18–48 h before transfection. Cells were transiently transfected with plasmid DNA using Lipofectamine 2000 (Invitrogen): 2 μg of DNA and 3 μl of Lipofectamine per well. At 0–24 h after transfection, cells were trypsinized and replated on laminin-coated round coverslips (6 mm diameter) at 30,000 cells per coverslip. At 24–48 h after transfection, GFP-positive (GFP^+)cells were selected for intracellular calcium measurements and electrophysiological recordings.

Trigeminal ganglion neurons from neonatal mice were cultured as described previously (Viana et al., 2001). In brief, trigeminal ganglia were isolated from anesthetized newborn Swiss OF1 mice [postnatal days 1 (P1) to P5], incubated with 1 mg/ml collagenase type IA (Sigma, St. Louis, MO) for 45 min at 37°C in 5% CO_2, and cultured in medium: 45% DMEM, 45% F-12, and 10% fetal bovine serum (Invitrogen), supplemented with 4 mM L-glutamine (Invitrogen), 200 μg/ml streptomycin, 125 μg/ml penicillin, 17 mM glucose, and nerve growth factor (NGF) (mouse 7S, 100 ng/ml; Sigma). Cells were plated on poly-L-lysine-coated glass coverslips and used after 1–3 d in culture.

To culture trigeminal ganglion neurons from young adult mice (P25–P28) and neonatal (P5–P10) guinea pigs (Hartley strain), the protocol was similar to the one used for neonatal mice except in the following details. Before dissection, mice were anesthetized with 100% CO_2 and guinea pigs with sodium pentobarbital (90 mg/kg) intraperitoneally, followed by rapid decapitation. After removal, ganglia were incubated in a mixture of collagenase type XI (0.66 mg/ml) and dispase (3 mg/ml) for 1 h. After mechanical dissociation, cells were cultured in media containing 89% MEM and 10% fetal bovine serum (Invitrogen), supplemented with 1% MEM vitamins (Invitrogen), 100 μg/ml penicillin/streptomycin, and NGF.

Trigeminal ganglion neurons and HEK293 electrophysiology. Cell-attached and whole-cell voltage/or current recordings were performed simultaneously with temperature recordings. The standard bath solution contained the following (in mM): 140 NaCl, 3 KCl, 1.3 $MgCl_2$, 2.4 $CaCl_2$, 10 HEPES, and 10 glucose, pH 7.4 adjusted with NaOH (297 mOsm/kg). Standard patch pipettes (3–5 MΩ for HEK293 cells; 5–8 MΩ for whole-cell recordings in neurons; 10–12 MΩ for cell-attach recordings) were fabricated from borosilicate glass capillaries (Harvard Apparatus, Edenbridge, Kent, UK) and contained the following (in mM): for TG neurons, 140 KCl, 6 NaCl, 1 EGTA, 0.6 $MgCl_2$, 1 NaATP, 0.1 Na-GTP, and 10 HEPES, pH 7.4 adjusted with KOH (282 mOsm/kg); and for HEK293 cells, 140 CsCl, 0.6 $MgCl_2$, 1 EGTA, and 10 HEPES, pH 7.4, adjusted with CsOH (276 mOsm/kg).

To measure the reversal potential of the cold-sensitive current (I_{cold}) in sensory neurons, the bath solution contained the following (in mM): 140 NaCl, 3 KCl, 1.3 $MgCl_2$, 0.1 $CaCl_2$, 10 HEPES, 10 glucose, and 0.5×10^{-3} TTX, pH 7.4 adjusted with NaOH. The pipette solution contained the following (in mM): 140 CsCl, 0.6 $MgCl_2$, 1 EGTA, 10 HEPES, 1 $ATPNa_2$, and 0.1 GTPNa, pH 7.4 adjusted with CsOH. These modifications were necessary to minimize large voltage-dependent currents.

Current and voltage signals were recorded with an Axopatch 200B or a Multiclamp patch-clamp amplifier (Molecular Devices, Sunnyvale, CA). Stimulus delivery and data acquisition were performed using pClamp 9 software (Molecular Devices). Analysis was performed with pClamp 9 and WinASCD software (Guy Droogmans, Katholieke Universiteit Leuven, Leuven, Belgium).

Temperature stimulation. Coverslips with cultured cells were placed in a microchamber and continuously perfused (~0.8 ml/min) with solutions warmed at 34 ± 1°C. The temperature was adjusted with a water-cooled RDTC-1 Peltier device (ReidDan Electronics) placed directly on the cell field and controlled by a feedback device (Reid et al., 2001). Cold sensitivity was investigated with a 50 s temperature drop to 18 ± 1°C. Temperature decreased and recovered in a quasi-exponential manner with a time constant of ~8 s.

Fluorescence Ca^{2+} imaging. Neurons were incubated with 5 μM fura-2 AM dissolved in standard extracellular solution and 0.02% pluronic (both from Invitrogen) for 40 min at 37°C in darkness. Fluorescence measurements were made with a Leica (Nussloch, Germany) DM IRE2 inverted microscope fitted with a 12-bit cooled CCD camera (Imago QE Sensicam; T.I.L.L. Photonics, Graefelfing, Germany). Fura-2 was excited at 340 and 380 nm with a Polychrome IV monochromator (T.I.L.L. Photonics), and the emitted fluorescence was filtered with a 510 nm long-pass filter. Calibrated ratios (0.5 Hz) were displayed on-line with T.I.L.L. Vision software version 4.01 (T.I.L.L. Photonics). Bath temperature was sampled simultaneously (see below), and threshold temperature values for $[Ca^{2+}]_i$ elevation were estimated by linearly interpolating the temperature at the midpoint between the last baseline point and the first point at which a rise in $[Ca^{2+}]_i$ deviated by at least four times the SD of the baseline

Cold nerve terminals electrophysiology. The action of BCTC on cold- and menthol-evoked nerve impulse activity was tested on single nerve terminals of cold thermoreceptors innervating the cornea of the eye in an *in vitro* preparation adapted following Brock et al. (1998). A total of 32 terminals were recorded from the surface of the cornea, five of which were used for the menthol dose–response study, 17 for BCTC experiments, and 10 for investigating SKF96365 effects. Male Dunkin Hartley guinea pigs (Harlan, Borchen, Germany) weighing 250–400 g were anesthetized with sodium pentobarbitone (20 mg/kg; Dolethal) and killed by decapitation. Corneas were cut at the limbus and pinned to the Sylgard-coated (Dow Corning, Midland, MI) base of a recording chamber, which was superfused continuously with physiological solution of the following

composition (in mM): 133.4 NaCl, 1.3 NaH_2PO_4, 16.3 $NaHCO_3$, 4.7 KCl, 2 $CaCl_2$, 1.2 $MgCl_2$, and 9.8 glucose. This solution was gassed with carbogen (95% O_2, 5% CO_2) to pH 7.4 and maintained at 34–36°C.

Glass micropipette electrodes (tip diameter of ~20 μm), filled with the physiological solution and applied to the cornea with light suction, were used to record nerve terminal impulses (NTIs). Electrical signals were recorded with respect to an Ag/AgCl pellet placed in the chamber. The electrical activity was recorded through an alternate current amplifier (gain 2000×, high-pass filter 0.1 Hz; Neurolog NL103; Digitimer, Welwyn Garden City, UK). Data were captured and analyzed using a CED 1401 interface coupled to a computer running Spike 2 software (Cambridge Electronics Design, Cambridge, UK). Only NTIs originating from single cold-sensitive receptors were recorded, identifiable by their relatively high level of spontaneous discharge (in this study, 4–15 Hz), sometimes in a bursting pattern, which was increased by cooling and decreased by warming of the superfusion solution (Brock et al., 1998, 2001).

Spontaneous NTI activity at 34–36°C was recorded for at least 1 min before cooling the cornea to 22–25°C by perfusing it with cold solution during 30 s, followed by rewarming to the baseline temperature of 34–36°C. Basal mean spontaneous activity (in hertz) was calculated during the 20 s before cooling. Temperature response threshold was taken as the temperature at which firing frequency increased to a value higher than 2 SDs above the mean basal spontaneous activity, and maximum response was defined as the highest firing frequency reached during cooling.

After two stable, consecutive cooling–rewarming cycles (defined by <10% variation in spontaneous activity, threshold, and maximum response between trials), 10 μM BCTC was added to the bath solution and allowed to perfuse for 3 min; then, a new cooling–rewarming cycle was applied. The process was repeated in the presence of BCTC and menthol, 10 and 100 μM, respectively, and finally, with 100 μM menthol alone. The dose–response curve of menthol effects on background activity was obtained in five additional corneas that were not exposed to BCTC.

Animal experiments were approved by the local veterinarian authority and were in accordance with the European Union legislation on the use of experimental animals.

Data analysis. To compare the effects of BCTC on cold- or menthol-evoked currents in individual cells, data were normalized to percentage of control using the following equation: Relative block (%) = $((\{\text{Response}\}_{\text{control}} - \{\text{Response}\}_{\text{blocker}})/\{\text{Response}\}_{\text{control}}) \times 100$. Smooth curves shown in the dose–response relationships are fits to the Hill equation: Relative block (RB) (%) = $RB_{min} + (RB_{max} - RB_{min})/[1 + (X/EC_{50}))^N]$, where EC_{50} is the concentration of half-maximal blockage, X is the blocker concentration, and N is the Hill coefficient.

Unless noted, all dose–response curves of current block were measured at +80 mV. For estimates of BCTC block during cooling, leak currents were measured at 35°C, thus minimizing TRPM8 activation, and temperature-corrected by a factor $Q_{\Delta T}$ according to the following expression: $Q_{\Delta T} = (Q_{10}) \times \exp(\Delta T/10)$, where ΔT is the difference between the baseline temperature (35°C) and the temperature of the cold stimulus. The value of Q_{10} was fixed at 1.5, a reasonable value for "cold-insensitive" (CI) channels (Hille, 2001).

Data are presented as means ± SEM. Statistical analyses were performed with Excel 2001 (Microsoft, Seattle, WA) or SigmaStat 3.0 software (Systat Software, Port Richmond, CA). Significance was set at $p < 0.05$.

Reagents. BCTC was a generous gift from Dr. H. Behrendt and Dr. R. Jostock (Grünenthal AG, Aachen, Germany). L-Menthol was purchased from Scharlau Chemie (Barcelona, Spain). Cinnamon aldehyde, clotrimazole [(1-(o-chloro-α,α-diphenylbenzyl)-imidazole)], phenanthroline (1-10-phenanthroline monohydrate), 4-aminopyridine, and nickel chloride were from Sigma. SKF96365 (1-[2-(4-methoxyphenyl)-2-[3-(4-methoxyphenyl)propoxy]ethyl-1*H*-imidazole hydrochloride] was purchased from Tocris Bioscience (Bristol, UK).

Results

BCTC blocks $[Ca^{2+}]_i$ responses to cold and menthol in TRPM8-transfected HEK293 cells

BCTC is a novel blocking agent of transient receptor potential vanilloid receptor 1 (TRPV1) channels (Valenzano et al., 2003) and of mouse and human TRPM8 channels activated by menthol (Behrendt et al., 2004; Weil et al., 2005). Using fura-2 calcium imaging in rat TRPM8-transfected HEK293 cells, we confirmed the blocking effects of BCTC on menthol-evoked responses. As shown in Figure 1*A*, BCTC produced a reversible suppression of $[Ca^{2+}]_i$ elevations to menthol application. In nontransfected cells, menthol had no effect on $[Ca^{2+}]_i$ levels. At 3 μM BCTC, the inhibition was complete, with an EC_{50} value of 647 nM (Fig. 1*D*). Next, we tested the effects of BCTC on cold-evoked calcium signals in TRPM8-transfected HEK293 cells. As was the case for menthol responses, BCTC produced a dose-dependent and reversible inhibition of $[Ca^{2+}]_i$ elevations evoked by cooling down to ~18°C from a baseline temperature of 35°C (Fig. 1*E*). Inhibition was also complete at 3 μM with an EC_{50} of 685 nM (Fig. 1*H*).

BCTC blocks currents evoked by menthol and cold in TRPM8-transfected HEK293 cells

The blockade of TRPM8 channels by BCTC was verified directly, testing its effect on menthol-evoked whole-cell currents ($I_{menthol}$). Current development was monitored with periodic injections of voltage ramps from −100 to +100 mV. Application of 100 μM menthol at 33–34°C activated a current characterized by a reversal potential near 0 mV (−3.5 ± 0.7 mV; $n = 21$) and strong outward rectification ($I_{+80\ mV}/I_{-80\ mV}$ of 110 ± 32; $n = 21$) (Fig. 1*C*). As shown in Figure 1, *B* and *C*, 3 μM BCTC produced a complete inhibition of menthol-gated TRPM8 currents that recovered to a large extent during wash. The time constant of current inhibition by 3 μM BCTC was 6.7 ± 1.1 s ($n = 4$). The full dose–response curve of BCTC blockade of $I_{menthol}$ is shown in Figure 1*D*, with an estimated EC_{50} of 475 nM.

The actions of BCTC on cold-evoked currents (I_{cold}) were also tested in whole-cell recordings of TRPM8-transfected HEK293 cells, using identical protocols. From a baseline temperature of 33–35°C, cooling to ~18°C activated a current (Fig. 1*G*) with similar outward rectification ($I_{+80\ mV}/I_{-80\ mV}$ of 103 ± 27; $n = 23$) and reversal potential of −1.5 ± 0.9 mV ($n = 24$) as after applying menthol. BCTC produced a dose-dependent reduction in the current that reversed rapidly during wash (Fig. 1*F*,*G*). At 3 μM, the inhibition was complete and the time constant of inhibition was 11.0 ± 1.6 s ($n = 8$). A full dose–response curve of BCTC effects on cold-evoked currents is shown in Figure 1*H*. In this case, the estimated EC_{50} was 621 nM, similar to the values obtained for $I_{menthol}$. The inhibition of $I_{menthol}$ and I_{cold} by BCTC appeared to be voltage dependent: inward currents were fully blocked at negative potentials by submaximal concentrations of BCTC, but a fraction of current remained at more positive potentials (Fig. 1*G*). The voltage dependence of block was quantified, comparing the block produced by 1 μM BCTC at +40 and +100 mV. In the case of $I_{menthol}$, mean percentage of block was 88.5 ± 4.5 and 64.5 ± 5.7% at +40 and +100 mV, respectively ($p = 0.01$; $n = 5$). For I_{cold}, the values of block produced by 1 μM BCTC were similar to those of $I_{menthol}$ (82.4 ± 3.8 and 64.3 ± 5.4%) and also significantly different at both potentials ($p = 0.04$; $n = 4$).

We also tested the effects of several other known blockers of TRP channels, such as clotrimazole, phenanthroline, and SKF96365 (Nilius et al., 2001; Hill et al., 2004), and nickel, a blocker of voltage-gated calcium channels. With the exception of nickel, which at concentrations as high as 10 mM was almost inactive against cold-evoked currents, the rest of the compounds also exhibited strong inhibitory effects on TRPM8 channels (R. Madrid, V. Meseguer, and F. Viana, unpublished observations). BCTC and SKF96365 were the two most potent compounds

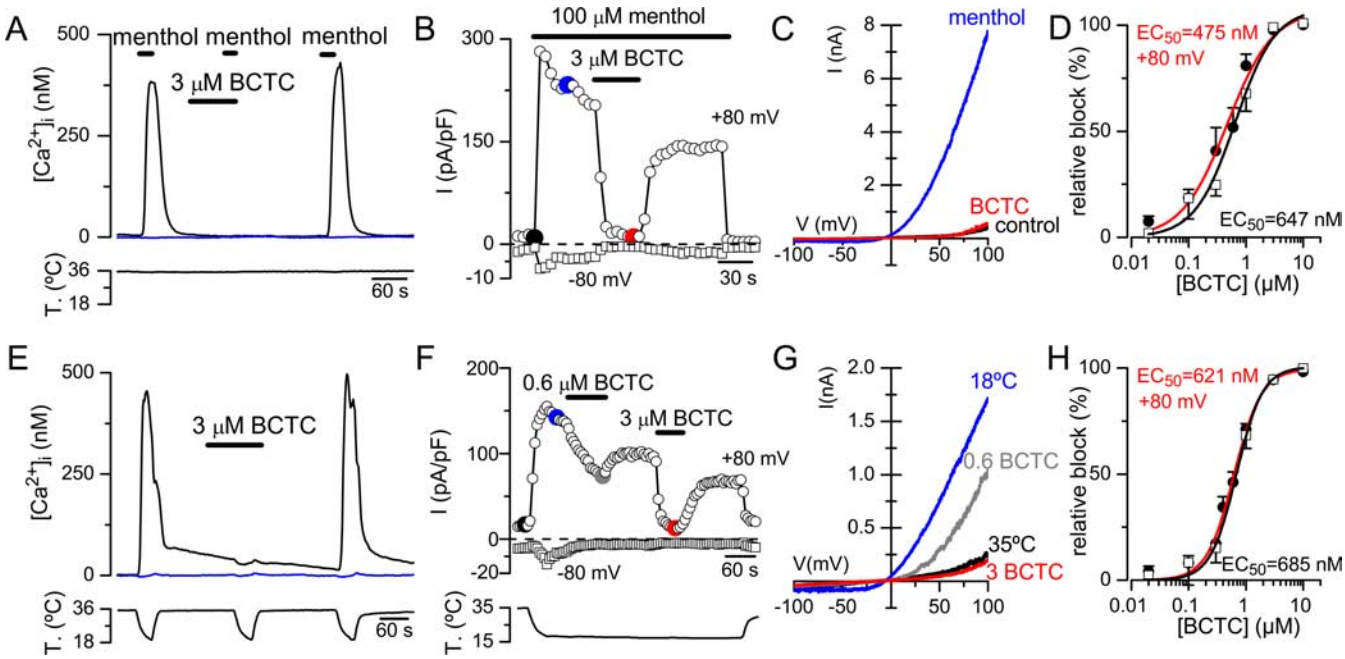

Figure 1. BCTC blocks TRPM8-mediated responses to cold and menthol in transfected HEK293 cells. ***A***, Ratiometric $[Ca^{2+}]_i$ response of a TRPM8$^+$ HEK293 cell (black trace) to 100 μM menthol in control solution, in the presence of 3 μM BCTC, and after washout of BCTC. In the same field, a TRPM8-negative (TRPM8$^-$) cell (blue trace) did not respond to menthol. ***B***, Time course of current development at +80 and −80 mV in a TRPM8$^+$ HEK293 cell, recorded at 33°C, by the application of 100 μM menthol. In the continuous presence of menthol, 3 μM BCTC produced a full suppression of the current. Currents were evoked by a 1-s-duration −100/+100 mV voltage ramp delivered every 5 s. The negative current axis is expanded fivefold to show the very small inward currents. ***C***, Whole-cell ramp *I–V* relationship at 33°C in control solution (black trace), during 100 μM menthol (blue trace), and during 100 μM menthol plus 3 μM BCTC (red trace). ***D***, Relative block of calcium response (open squares) and menthol-evoked currents (filled circles) to cooling pulses as a function of BCTC concentration ($n = 5$–10 cells for calcium data and 2–5 cells for current data). Solid lines correspond to dose–response fits to the Hill equation, in black for menthol data (EC_{50} of 647 nM and a Hill coefficient of 1.9), and in red for current data (EC_{50} of 475 nM and Hill coefficient of 1.1). ***E***, Ratiometric $[Ca^{2+}]_i$ response in a TRPM8$^+$ HEK293 cell (same as in ***A***) during a cooling stimulus in control solution and in the presence of 3 μM BCTC. Note the lack of response in a TRPM8$^-$ cell (blue trace) recorded simultaneously. ***F***, Time course of current at +80 and −80 mV in a TRPM8$^+$ HEK293 cell during a cooling stimulus and effect of 0.6 and 3 μM BCTC. Same voltage protocol as in ***B***. The negative current axis is expanded twofold. ***G***, *I–V* relationship of currents at 35°C (black trace), during cooling at 18°C (blue trace), and during cooling in the presence of 0.6 (gray trace) and 3 μM BCTC (red trace). ***H***, Normalized block of cold-evoked calcium signals (open squares) and currents (filled circles) in TRPM8$^+$ HEK293 cells by different concentrations of BCTC. The smooth curves are fits of the Hill equation to the data with an EC_{50} of 685 nM and a Hill coefficient of 1.9 for calcium data (black line; $n = 5$–10 cells) and an EC_{50} of 621 nM and $N = 1.8$ for current data at +80 mV (red line; $n = 2$–8 cells).

Table 1. Electrophysiological properties of cold-sensitive neurons recorded in control solution and in the presence of 3 μM BCTC

	V_{rest} (mV)	R_{in} (MΩ)	IR_{index} (%)	$I_{rheobase}$ (pA)	*I*-evoked firing (Hz)	AP amplitude (mV)	AP duration (ms)
Control	−49.5 ± 1.4 ($n = 18$)	544 ± 103 ($n = 8$)	28.3 ± 5.8 ($n = 8$)	107 ± 36 ($n = 10$)	77 ± 18 ($n = 10$)	71 ± 3 ($n = 10$)	0.9 ± 0.1 ($n = 10$)
3 μM BCTC	−46.6 ± 1.6 ($n = 18$)	573 ± 129 ($n = 5$)	22.1 ± 5.4 ($n = 5$)	89 ± 30 ($n = 10$)	76 ± 15 ($n = 10$)	60 ± 5 ($n = 10$)	0.9 ± 0.1 ($n = 10$)
t test	$p = 0.17$	$p = 0.87$	$p = 0.45$	$p = 0.71$	$p = 0.83$	$p = 0.08$	$p = 0.63$

V_{rest}, Resting membrane potential; R_{in}, input resistance; IR_{index}, inward rectification index (percentage), measured as $[((V_{m\ peak} - V_{m\ steady\text{-}state})/V_{m\ peak}) \times 100]$ during hyperpolarizing voltage responses induced by −100 pA (250 ms) current pulses under current clamp from I_{hold} of 0 pA; $I_{rheobase}$, rheobase current; *I*-evoked firing frequency was calculated from the number of AP evoked by a 1 s depolarizing current ramp of 500 pA, in a time interval of 250 ms from the first spike evoked. AP amplitude was measured from base to pick of the first spike during the depolarizing ramp. AP duration was measured at half-amplitude. *t* test, Two-tailed Student's *t* test.

tested and were subsequently used to dissect the functional activity of native TRPM8 channels in cold-sensitive neurons and corneal thermoreceptor terminals.

Identification and properties of cold-sensitive trigeminal ganglion neurons

Calcium imaging techniques were used for a fast and reliable identification of the subpopulation of CS mouse trigeminal ganglion neurons (McKemy et al., 2002; Viana et al., 2002). During rapid reductions in bath temperature from a baseline temperature of 33–35°C to ~18°C, a small fraction (~10%) of neurons responded with an elevation in their $[Ca^{2+}]_i$. The average increase in $[Ca^{2+}]_i$ produced by cooling was 205 ± 20 nM ($n = 88$). As reported previously, CS trigeminal neurons had a small round- or ovoid-shaped soma (average diameter of 15.7 ± 0.3 μm; $n = 88$) and a mean whole-cell capacitance of 10.3 ± 0.4 pF ($n = 42$). CS neurons had variable temperature thresholds ranging from 35.2 to 21.1°C ($n = 88$). Nearly all CS neurons identified in calcium imaging screens were also activated by menthol (94.9% of all neonatal CS tested; $n = 59$). Furthermore, in CS neurons, we observed the development of robust inward currents during brief applications of menthol (see below), strongly suggesting a contribution of TRPM8 channels to their depolarizing response during cooling. The membrane properties of these neonatal CS trigeminal neurons are summarized in Table 1.

BCTC markedly reduced cold and menthol $[Ca^{2+}]_i$ responses in a large fraction of cultured cold-sensitive trigeminal ganglion neurons

At a concentration of 3 μM, BCTC produced a complete suppression of the $[Ca^{2+}]_i$ rise evoked by application of 100 μM menthol in neonatal CS trigeminal neurons (Fig. 2*A*,*B*). On its own, BCTC did not modify resting $[Ca^{2+}]_i$ levels in CS or CI neurons. The inhibition by BCTC was fully reversible in all neurons tested ($n = 12$) (Fig. 2*B*,*C*). This effect of BCTC on menthol-evoked

responses in the soma of trigeminal sensory neurons is entirely consistent with the actions on expressed TRPM8 channels described above.

In contrast, the effects of the drug on cold-evoked responses varied from neuron to neuron, from full suppression to no effect. This variability is illustrated in Figure 2*D*, which shows the effect of 3 μM BCTC on $[Ca^{2+}]_i$ responses to cooling in three CS trigeminal neurons recorded simultaneously. In the neuron with the largest initial $[Ca^{2+}]_i$ response (blue trace), BCTC produced a complete suppression of the $[Ca^{2+}]_i$ rise. In the neuron with the smallest initial response (green trace), the inhibition was incomplete, and, in the third cell (red trace), the effect of BCTC was negligible. As shown also in Figure 2*D*, the effects of BCTC were fully reversible after only a few minutes wash. In 52% of the neurons with a response to cooling ($n = 88$), the $[Ca^{2+}]_i$ rise was fully blocked, in 40% the inhibition was partial, and in seven cells (8%) BCTC had no blocking action. Interestingly, all cold-sensitive but BCTC-insensitive TG neurons tested were also menthol unresponsive ($n = 3$) (note the red trace in Fig. 2*D*). In contrast, all BCTC-sensitive neurons tested were also activated by menthol ($n = 56$). These results strongly support the view that BCTC is acting preferentially on TRPM8 channels. The effects of BCTC on cold-evoked responses were dose dependent and are summarized in Figure 2*E* for the entire population of neonatal CS neurons.

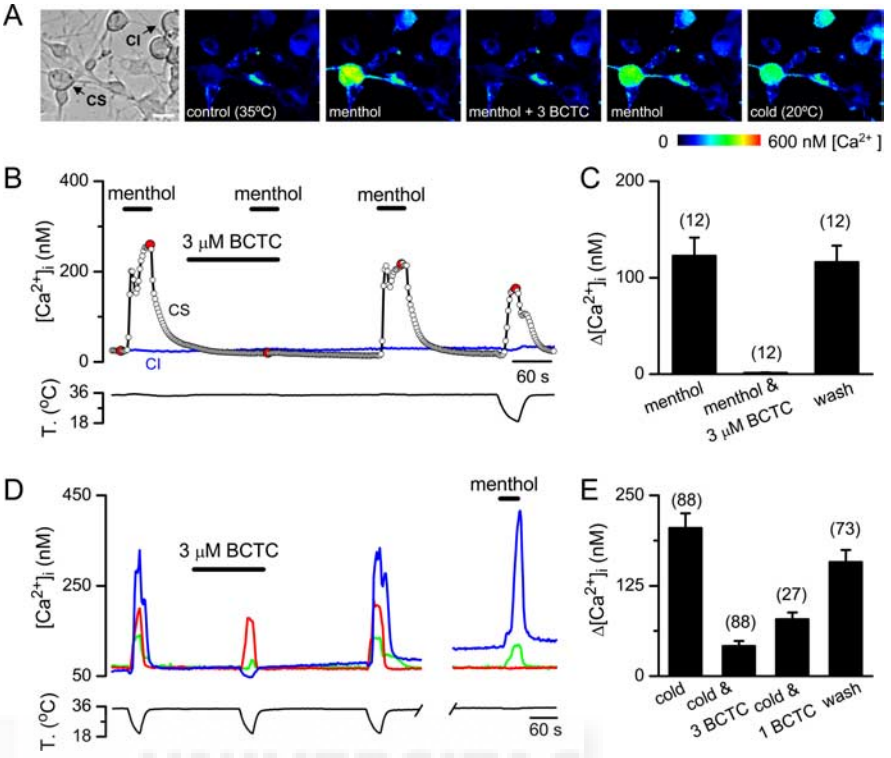

Figure 2. BCTC blocks menthol- and cold-induced $[Ca^{2+}]_i$ responses in neonatal mice trigeminal sensory neurons. ***A***, Transmitted (left) and pseudocolor ratiometric $[Ca^{2+}]_i$ images showing the effects of BCTC on menthol-evoked $[Ca^{2+}]_i$ signals in cultured trigeminal neurons. The fluorescence images correspond with the time points marked in red in ***B***. Scale bar, 15 μm. ***B***, Ratiometric $[Ca^{2+}]_i$ response of a CS and a CI trigeminal sensory neuron to 100 μM menthol in control solution, in the presence of 3 μM BCTC, and after washout of BCTC. ***C***, Mean evoked $[Ca^{2+}]_i$ elevation by menthol, by menthol in the presence of 3 μM BCTC, and after wash of BCTC. ***D***, Ratiometric $[Ca^{2+}]_i$ responses to cooling in three CS trigeminal sensory neurons, recorded simultaneously, in control solution, in the presence of 3 μM BCTC, and after washout. A response to 100 μM menthol in the same three neurons is also shown. The time gap equals 550 s. ***E***, Mean evoked $[Ca^{2+}]_i$ elevation by cooling in control solution, in the presence of 1 and 3 μM BCTC, and after wash in mouse CS trigeminal neurons.

In adult mouse CS trigeminal neurons, the effects of BCTC were very similar to those found in neonates. As shown in supplemental Figure 1 (available at www.jneurosci.org as supplemental material), BCTC also produced a powerful, fully reversible, inhibition of cold- and menthol-evoked $[Ca^{2+}]_i$ responses. Of 19 CS neurons tested (all were activated by 100 μM menthol), 3 μM BCTC fully suppressed menthol-evoked responses in 15 of them (79%). In contrast, cold-evoked responses were fully blocked in nine neurons (47%), whereas in the remaining 10 cells the inhibition was only partial, decreasing from 153 ± 19 nM in control solution to 86 ± 9 nM in 3 μM BCTC ($p < 0.001$).

BCTC shifted the temperature threshold of cold-sensitive trigeminal ganglion neurons

To pinpoint the role of TRPM8 channels in CS trigeminal neurons during cold sensing, we performed simultaneous recordings of $[Ca^{2+}]_i$ signals and electrical activity from their soma (Fig. 3*A*) using the cell-attached mode of the patch-clamp technique, a recording configuration that preserves the intracellular milieu of the cell, thus minimizing alterations in modulatory factors. With the use of subsaturating doses of BCTC, we were able to reduce the functional density of active TRPM8 channels in the cell membrane and asked how this reduction affected the threshold temperature for excitation.

As shown in Figure 3*B*, cooling evoked a $[Ca^{2+}]_i$ response in parallel with the onset of action potential (AP) firing. In the presence of 1 μM BCTC, the reduction in the amplitude of the $[Ca^{2+}]_i$ signal correlated with reduced impulse firing and was accompanied by a shift in threshold to lower temperatures: in this particular neuron, the firing threshold shifted from 33.7°C in control conditions to 28.4°C in the presence of 1 μM BCTC. In 3 μM BCTC, the cell fired a single action potential at 20.2°C and the $[Ca^{2+}]_i$ elevation was completely abolished. The effects of BCTC on cold-evoked firing and $[Ca^{2+}]_i$ signals were reverted during wash. As summarized in Figure 3*C*, in neurons recorded in control solution (filled circles), there was a tight correspondence between temperature threshold for firing of action potentials and for $[Ca^{2+}]_i$ elevations in each individual cell. The correlation between both thresholds had a slope of 0.98 and an *r* value of 0.99 ($n = 11$). When repeating this experiment after applying 1 μM (triangles) or 3 μM (stars) BCTC, this tight correlation was maintained (Fig. 3*C*), and the absolute difference in threshold between $[Ca^{2+}]_i$ signals and AP firing was only 0.1 ± 0.14°C. This result indicates that the onset of $[Ca^{2+}]_i$ signals can be used as a reliable marker of electrical activity and of the effects of BCTC on temperature threshold in individual CS neurons.

Figure 4*A* summarizes the effects of applying 1–3 μM BCTC on cold-evoked activity in the 88 neonatal CS neurons analyzed (see above). In the graph, individual neurons have been plotted according to their initial temperature threshold (black circles). In all but seven cells (8%) (green circles), 3 μM BCTC produced marked increases in temperature threshold (i.e., the temperature for activation decreased). In fact, as already mentioned, in 52% of

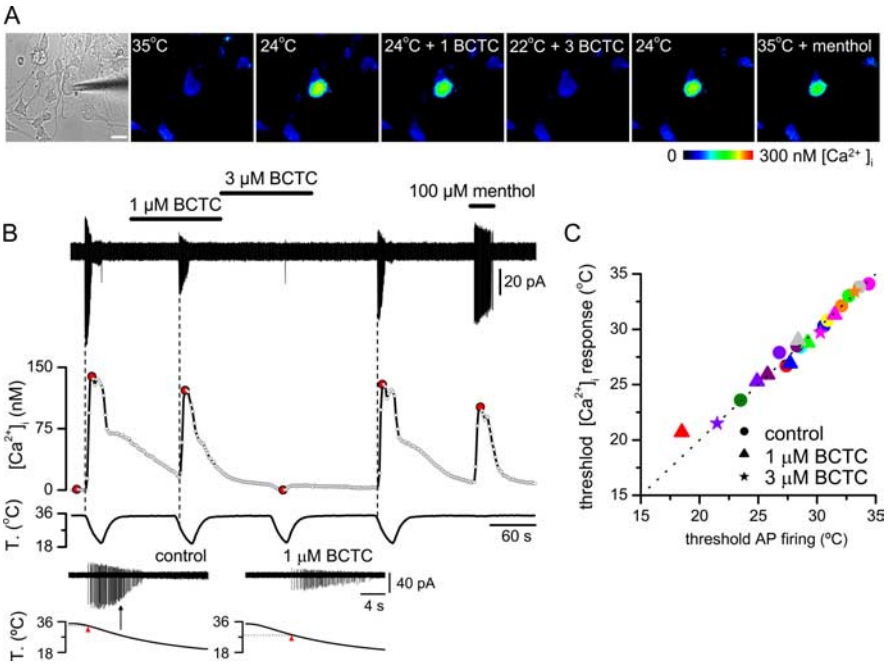

Figure 3. BCTC reduces firing and shifts temperature threshold in cold-sensitive trigeminal ganglion neurons. ***A***, Transmitted (left) and pseudocolor ratiometric $[Ca^{2+}]_i$ images showing the effects of BCTC on cold-evoked $[Ca^{2+}]_i$ signals in a CS trigeminal neuron. Note also the response to menthol. A patch pipette has been positioned in close apposition to the CS cell before initiating the sequence of cell-attach recordings. The fluorescence images correspond with the time points marked in red in ***B***. ***B***, Simultaneous recording of action currents (top trace), $[Ca^{2+}]_i$ signals (middle), and bath temperature (bottom) during four consecutive cooling ramps. The two insets at the bottom show the action currents and the temperature change on an expanded timescale, in control (left) and 1 μM BCTC (right). The temperature threshold is marked by a pink arrowhead. The black arrow marks, on the control trace, the temperature threshold in 1 μM BCTC. Note the decline in action current amplitude with low temperature. ***C***, Scatter plot of thresholds for action potential and $[Ca^{2+}]_i$ signals in response to cooling in 11 neurons (each neuron has been color coded) recorded in control solution (circles) and 1 μM (triangles) and 3 μM (stars) BCTC. The dotted line represents the unity line.

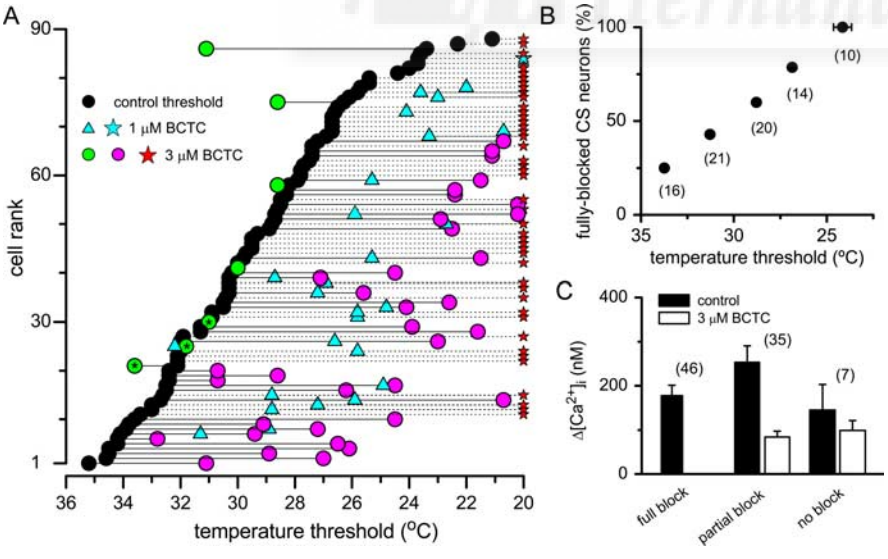

Figure 4. BCTC shifts temperature threshold in mouse cold-sensitive trigeminal ganglion neurons in a dose-dependent manner. ***A***, Dot plot summarizing the effect of 1 and 3 μM BCTC on cold-evoked temperature threshold in 88 cold-sensitive TG neurons. Threshold was estimated from the ratiometric $[Ca^{2+}]_i$ responses to cooling. The 88 neurons have been plotted according to initial temperature threshold in control solution (black circles) from lowest to highest threshold. The threshold measured in 1 and 3 μM BCTC is represented by cyan triangles and magenta circles, respectively. Those neurons fully inhibited by 3 μM BCTC during a cooling ramp to 20–18°C are represented by a red star. The green circles mark the threshold in 3 μM BCTC for those neurons whose temperature threshold were not augmented by BCTC: 100 μM menthol was tested in three of these neurons (asterisk) and had no effect. ***B***, Diagram representing the percentage of CS neurons fully inhibited by 3 μM BCTC of the total population with responses to cooling affected by BCTC ($n = 81$). Neurons have been grouped according to initial temperature threshold. The horizontal error bars in four groups overlap with symbol size. ***C***, Bar histogram summarizing the effect of 3 μM BCTC on cold-evoked $[Ca^{2+}]_i$ responses in the three subpopulations of neurons grouped according to blocking effect of BCTC.

cells, 3 μM BCTC completely suppressed the $[Ca^{2+}]_i$ response during cooling down to 20–18°C (red stars). In neurons showing a partial blockade (40%), 3 μM BCTC shifted the threshold by 6.3 ± 0.4°C toward the colder range (magenta circles). In comparison, 1 μM BCTC eliminated the $[Ca^{2+}]_i$ elevation induced by cold in just one neuron (cyan star) and shifted the temperature threshold to intermediate values (cyan triangles) with a mean shift of 4.1 ± 0.3°C ($n = 27$). The shift in threshold produced by BCTC was accompanied by a reduction in the amplitude of the $[Ca^{2+}]_i$ attributable to a decrease in the firing frequency of action potentials (Fig. 4*C*). The effects of BCTC on temperature threshold and $[Ca^{2+}]_i$ elevation were almost fully reversible (Fig. 3*B*).

It is noteworthy that BCTC produced these inhibitory effects in CS neurons with widely different initial temperature thresholds, from the innocuous to the noxious range, and including those with very low threshold. As shown in Figure 4*B*, the high-threshold cells were much more likely to be silenced by 3 μM BCTC than low-threshold CS neurons. In contrast, the few BCTC-insensitive neurons (green circles) were not clustered in any particular threshold temperature range. Figure 4*C* shows the mean $[Ca^{2+}]_i$ elevation evoked by cold in trigeminal neurons grouped according to their sensitivity to BCTC. There was a notable variability in the amplitude of cold-evoked $[Ca^{2+}]_i$ responses in individual cells, without significant difference between the means of the three groups ($p = 0.16$, Kruskall–Wallis ANOVA).

Altogether, these results indicate that TRPM8 channels are expressed in the soma of a majority of mouse cultured CS trigeminal neurons and that these channels are critical determinants of their cold temperature threshold.

BCTC eliminates cold- and menthol-evoked transduction currents

To examine directly the effects of BCTC on native I_{cold} currents, we performed whole-cell recordings on CS trigeminal neurons voltage clamped at a potential of −60 mV. Figure 5*A* shows current responses to three consecutive cooling ramps to ~18°C from a starting temperature of 35°C. In control solution, cooling induced an inward current that faded rapidly during rewarming. In the presence of 3 μM BCTC, the cold-induced inward current was fully blocked, recovering partially during wash. To monitor the characteristics and the reversal potential of the cold-sensitive current in trigeminal neurons, we applied 1-s-duration

voltage ramps (−100 to +100 mV) at different temperatures. As shown in Figure 5*B*, the native cold-sensitive current reversed close to 0 mV (−4.0 ± 2.3 mV; $n = 4$) and had notable outward rectification ($I_{+80\ mV}/I_{-80\ mV}$ of 10.6 ± 6.1; $n = 4$), similar to the properties of I_{TRPM8} in HEK293 cells. Furthermore, the current blocked by BCTC had similar rectification properties ($I_{+80\ mV}/I_{-80\ mV}$ of 7.1 ± 4.0; $n = 4$; $p = 0.65$) and identical reversal potential as I_{cold} (V_{rev} of −4.0 ± 1.8 mV; $n = 4$; $p = 0.99$). Only at very positive potentials did both currents deviate, indicating incomplete block of I_{cold} by BCTC at these voltages. These results strongly support the tenet that both currents are carried by the same type of nonselective, cold-sensitive channels, most likely TRPM8.

The bar histogram in Figure 5*C* summarizes the effects of 1 and 3 μM BCTC on the amplitude of native I_{cold}. In 16 of 17 cells tested, 3 μM BCTC reduced I_{cold} from 164 ± 31 to 6 ± 2 pA ($p < 0.001$, paired *t* test). In one neuron, the amplitude of the current was unaffected by 3 μM BCTC. We hypothesized that cold-sensitive but BCTC-insensitive neurons may represent a distinct population of thermosensitive neurons lacking TRPM8 expression. To test this possibility, we performed a second calcium imaging screen in cultured TG neurons derived from neonatal animals, looking for cold-sensitive neurons insensitive to 100 μM menthol. Only 12 of 203 (6%) were insensitive to the stimulating and/or sensitizing effect of menthol. During patch-clamp recordings, these cells displayed small inward currents during cooling that lacked the increase in membrane noise at low temperatures characteristic of BCTC-sensitive currents (Fig. 5*D*). In agreement with our hypothesis, in three of these neurons in which 3 μM BCTC was tested, I_{cold} was unaffected by the drug.

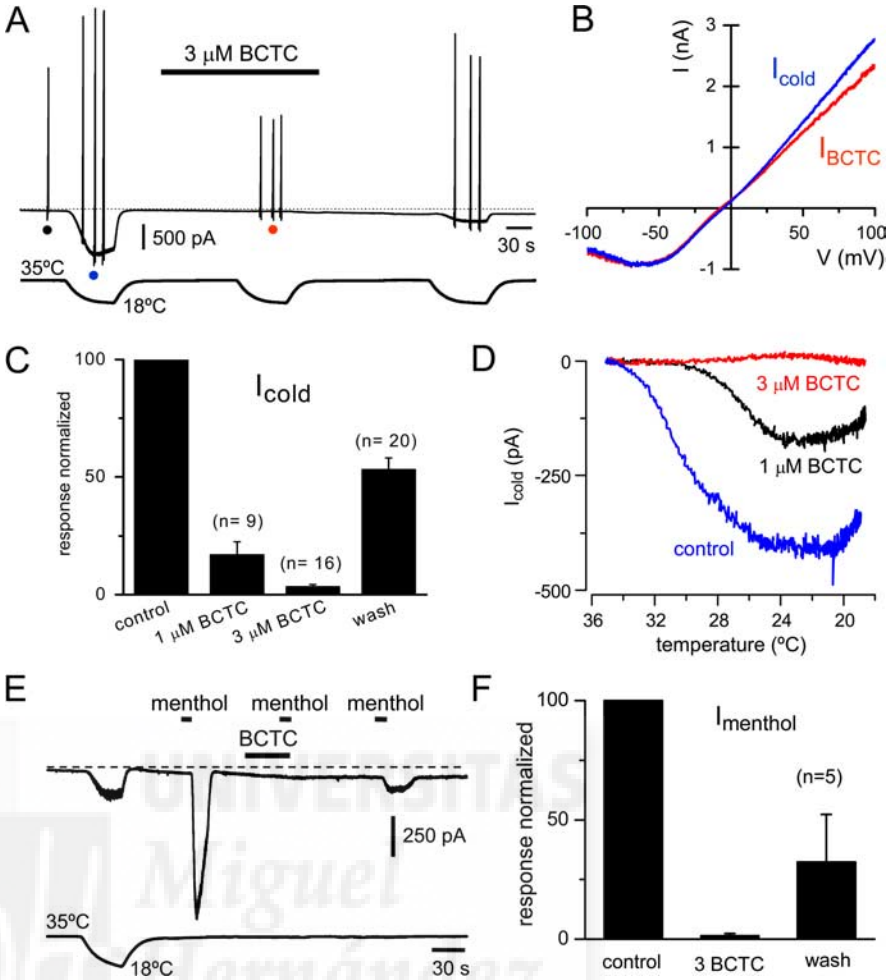

Figure 5. BCTC blocks currents induced by cooling and menthol in cold-sensitive trigeminal ganglion neurons. ***A***, Simultaneous recording of membrane current (top trace) and bath temperature (bottom trace) during application of three consecutive cooling ramps to a CS neuron (V_{hold} of −60 mV). The spike-like currents are the responses to voltage ramps (−100 to +100 mV). Application of 3 μM BCTC fully blocked I_{cold}. The dotted line represents the 0 holding current. ***B***, Current–voltage relationship of the cold-sensitive (blue trace) and BCTC-sensitive (red trace) current obtained during the voltage ramps. To derive the cold-sensitive current, the ramp current at 35°C (black dot) was subtracted from the current at 20°C (blue dot). To derive the BCTC-sensitive current, the ramp current at 20°C in BCTC (red dot) was subtracted from the current at 20°C in control solution (blue dot). ***C***, Bar histogram summarizing the block of I_{cold} by 1 and 3 μM BCTC. ***D***, Current–temperature relationships for a different neuron in control (blue trace) and in the presence of 1 μM (black trace) and 3 μM (red trace) BCTC. Note the marked shift in temperature threshold. ***E***, Simultaneous recording of membrane current (top trace) and bath temperature (bottom trace) during thermal and chemical (500 μM menthol) activation of a CS neuron (V_{hold} of −60 mV). ***F***, Bar histogram summarizing the block of $I_{menthol}$ by 3 μM BCTC.

Figure 5*D* shows the temperature dependence of the inward current (V_h of −60 mV) in a CS trigeminal neuron. The current had a threshold of 34.5°C, reaching a maximum at ~21°C and inactivating partially during the ramp. The mean threshold temperature of I_{cold} was 31.1 ± 0.4°C in trigeminal neurons recorded in control solution ($n = 25$). In the presence of 1 μM BCTC, the cold-evoked inward current was reduced and the threshold shifted to colder temperatures (Fig. 5*D*). In six neurons with measurable currents, threshold temperature shifted from 32.9 ± 0.7°C in control to 27.3 ± 1.5°C in 1 μM BCTC ($p = 0.012$). Finally, in 3 μM BCTC, the amplitude of the current was nearly abolished in this cell (Fig. 5*D*).

In an additional set of trigeminal CS neurons, the effect of BCTC was tested on currents evoked by 500 μM menthol ($I_{menthol}$) at a temperature of 34–35°C. In control solution, a brief application of menthol produced a robust inward current (V_{hold} of −60 mV) (Fig. 5*E*). In all cells tested ($n = 5$), 3 μM BCTC produced a complete suppression of $I_{menthol}$ (Fig. 5*E*). In this case, reversibility was more variable, in part attributable to a more pronounced desensitization during repeated applications of menthol at high concentration. Thus, these data show that 3 μM BCTC also produced a complete blockade of temperature-gated or chemically gated currents in a large fraction of trigeminal cold thermoreceptor neurons.

Effects of BCTC on cold-evoked transduction currents are specific

To rule out the possibility that the effects of BCTC resulted of a nonspecific action on spike generation conductances rather than on cold-evoked transduction currents, we compared the effects of BCTC on current-evoked (500 pA ramp in 1 s) and cold-evoked electrogenesis during current-clamp recordings in the same cells. As shown in Figure 6*A*, cooling depolarized CS neurons reversibly, with a mean threshold of 30.4. ± 0.4°C ($n = 13$). The average depolarization was 11.1 ± 0.9 mV ($n = 13$), and all

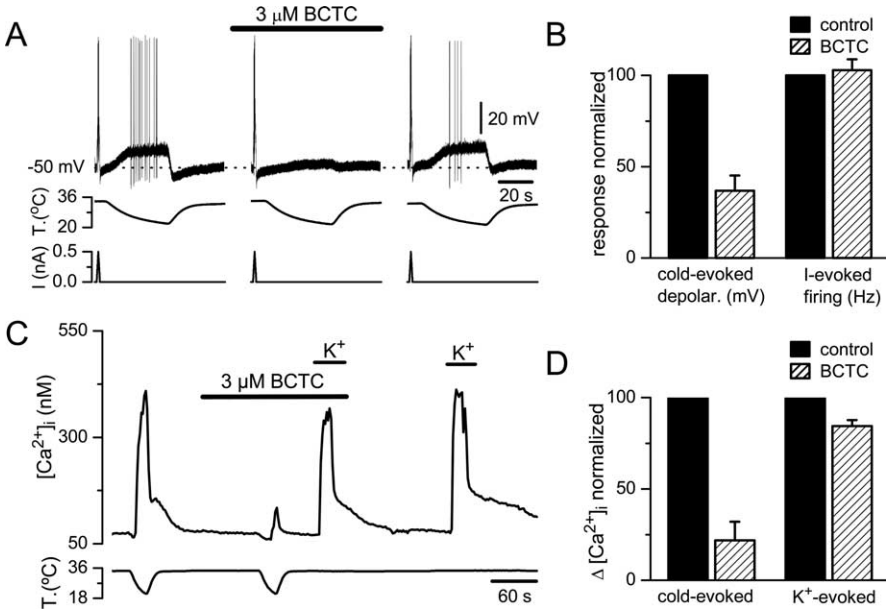

Figure 6. BCTC blocks cold-induced generator potentials in cold-sensitive trigeminal ganglion neurons. ***A***, Simultaneous recording of membrane potential (top trace), bath temperature (middle trace), and membrane current (bottom trace) during three consecutive cooling ramps to a cold-sensitive TG neuron recorded in current-clamp mode (I_{hold} of 0 pA). Application of 3 μM BCTC produced a reversible reduction in the cold-induced depolarization without affecting the voltage response to a 500 pA ramp. The dotted line represents the initial resting membrane potential. ***B***, Bar histogram of normalized responses to cooling and to *I*-evoked firing in control solution (black bars) and in 3 μM BCTC (stripped bars). ***C***, Simultaneous recording of $[Ca^{2+}]_i$ (top trace) and bath temperature (bottom trace) during two consecutive cooling steps to a cold-sensitive TG neuron. BCTC at 3 μM produced a large reduction in the cold-induced response with only minor effects on the depolarization-induced response produced by a 30 mM elevation in extracellular K^+. ***D***, Bar histogram of normalized $[Ca^{2+}]_i$ responses to cooling and to elevated K^+ in control solution (black bars) and in 3 μM BCTC (striped bars). The reduction in BCTC is significant in both cases ($p < 0.0001$ for cold-evoked responses and $p < 0.001$ for K^+-evoked responses).

neurons reached the firing of action potentials at an average threshold of 26.5 ± 0.7°C. In the same population of cells, depolarization by cold in the presence of BCTC was reduced to 4.9 ± 0.9 mV ($p < 0.001$), and only three cells reached AP threshold. The effects of BCTC were reversible. Notably, spiking responses to depolarizing intracellular current pulses were essentially unaffected by BCTC (Fig. 6*B*). Moreover, as shown in Table 1, 3 μM BCTC had no effect on the duration and amplitude of the action potential, input resistance, rheobase, and current-evoked firing frequency of CS neurons.

The specific nature of BCTC blockade on cold-evoked activity was also verified during calcium imaging experiments. Figure 6*C* shows the effect of 3 μM BCTC on $[Ca^{2+}]_i$ responses evoked by two consecutive cold ramps and two brief applications of elevated extracellular K^+ (30 mM). Whereas the cold-evoked activity was almost fully suppressed by BCTC, the depolarization-evoked $[Ca^{2+}]_i$ increase was well preserved. The bar diagrams in Figure 6*D* summarize the results obtained in 10 CS neurons using this protocol.

Altogether, these results indicate that the effects of 3 μM BCTC are selective and complete on cold transduction currents, with minor blocking effects on voltage-gated ion channels.

BCTC does not block activity of TRPA1 channels

TRPA1 is the second TRP channel postulated to be activated by cold temperatures, with a reported threshold of 18°C (Story et al., 2003). In addition, TRPA1 is activated by a number of pungent compounds, such as cinnamaldehyde, allycin, and mustard oil (Bandell et al., 2004; Jordt et al., 2004). Unexpectedly, 3 μM BCTC produced a robust activation of TRPA1 channels expressed in HEK293 cells (supplemental Fig. 2, available at www.jneurosci.org as supplemental material). This effect of BCTC was observed during both $[Ca^{2+}]_i$ imaging experiments (supplemental Fig. S*A*, available at www.jneurosci.org as supplemental material) and whole-cell recordings (supplemental Fig. 2*C*,*D*, available at www.jneurosci.org as supplemental material). In contrast to the powerful blocking effects on TRPM8 channels, BCTC had no significant blocking effects on TRPA1 activity evoked by application of cinnamaldehyde (supplemental Fig. 2*F*,*G*, available at www.jneurosci.org as supplemental material). The stimulatory actions of BCTC on TRPA1 activity were not apparent on native channels: we never observed $[Ca^{2+}]_i$ elevations in the soma of cultured sensory neurons or increased firing in corneal nerve terminals with BCTC, even in those activated by cinnamaldehyde (data not shown).

Functional characteristics of cold-sensitive corneal thermoreceptor endings

To examine the effects of BCTC on cold-evoked activity in sensory nerve terminals, we turned to an *in vitro* preparation of the guinea pig cornea (Brock et al., 1998). These types of recordings have been unsuccessful in mice. Therefore, to exclude potential species differences in pharmacological properties of TRPM8 channels, we verified first the effects of BCTC on menthol- and cold-evoked activity in cultured guinea pig trigeminal sensory neurons loaded with fura-2. As shown in Figure 7*A–C*, menthol responses in cold-sensitive neurons of guinea pig were also fully and reversibly blocked by 3 μM BCTC ($n = 7$; $p < 0.001$). Next we investigated the sensitivity of cold-evoked responses to BCTC in 20 guinea pig trigeminal neurons. The findings were qualitatively similar to those obtained in mice in that we identified the same three phenotypes of sensory neurons. In 25%, cold-evoked responses were fully and reversibly blocked by 3 μM BCTC (Fig. 7*D*). Furthermore, in three of three of these neurons, cold-evoked responses were potentiated by 100 μM menthol (Fig. 7*D*), suggesting that they are mediated by activation of TRPM8 channels. In 20% of the neurons, cold-evoked $[Ca^{2+}]_i$ responses were unaffected by BCTC (Fig. 7*E*). In this subpopulation ($n = 4$), menthol produced no activation or potentiation of the cold-evoked response, suggesting that it is independent of TRPM8 activity (Fig. 7*E*). Finally, in a third group comprising 55% of neurons, the cold-evoked response was partially blocked by BCTC. In five of six cells tested, there was an excitatory effect of menthol. These findings indicate a clear correlation between menthol responsiveness and BCTC blocking action, full or partial, among cold-sensitive neurons. The principal difference with mouse was a larger proportion (20 vs 8%) of cold-sensitive but BCTC- and menthol-insensitive neurons ($p = 0.089$, Fisher's exact test).

Figure 8*A* shows a typical example of the effects of temperature decrease on the occurrence of NTIs in a single CS receptor fiber of the eye cornea recorded extracellularly with a patch pi-

pette. These cold receptors were characterized by the spontaneous, regular firing of NTIs at resting temperatures of 34–36°C and the accelerating increase in firing frequency, often in bursts, when cooling pulses were applied (Fig. 8*B*). Rewarming silenced transiently the receptor terminal discharge, which resumed gradually during the recovery to the initial resting temperature (Fig. 8*A*). Table 2 shows different parameters of NTI frequency discharge at resting temperature, during cooling and during various pharmacological manipulations (see below) in corneal cold thermoreceptor fibers.

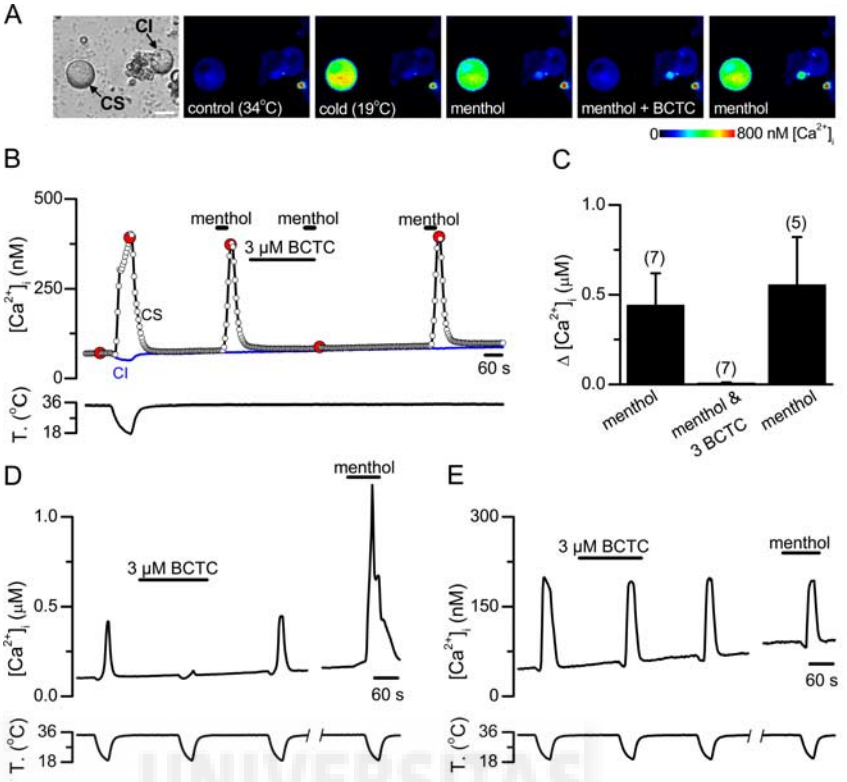

Figure 7. BCTC blocks menthol- and cold-induced $[Ca^{2+}]_i$ responses exclusively in the menthol-sensitive subpopulation of guinea pig cold-sensitive trigeminal sensory neurons. ***A***, Transmitted (left) and pseudocolor ratiometric $[Ca^{2+}]_i$ images showing the response to low temperature and 100 μM menthol and the effects of BCTC on menthol-evoked $[Ca^{2+}]_i$ signals in a CS trigeminal neuron. Note the lack of response in the CI neuron. The fluorescence images correspond with the time points marked in red in ***B***. ***B***, Time course of ratiometric $[Ca^{2+}]_i$ responses of a CS and a CI trigeminal sensory neuron (same experiment as in ***A***). The recording starts with a cooling ramp to identify the CS neurons in the imaging field. ***C***, Mean evoked $[Ca^{2+}]_i$ elevation by menthol, by menthol in the presence of 3 μM BCTC, and after wash of BCTC. ***D***, Ratiometric $[Ca^{2+}]_i$ responses to cooling in a CS trigeminal sensory neurons in control solution, in the presence of 3 μM BCTC, and after washout. After a brief interruption, a fourth cooling ramp was applied in the presence of 100 μM menthol. ***E***, Ratiometric $[Ca^{2+}]_i$ responses to cooling in a CS trigeminal sensory neurons in control solution, in the presence of 3 μM BCTC, and after washout. Note the lack of effect of BCTC and the lack of response to 100 μM menthol.

Lack of effect of BCTC on spontaneous and cold-evoked activity in corneal sensory terminals

We next tested the effect of perfusing BCTC on NTI activity in 17 corneal terminals. Curiously, the mean spontaneous NTI firing frequency at 35°C was not significantly modified by perfusion with high concentration (10 μM) of BCTC (Fig. 8*A*,*B*). The mean NTI frequency was 8.5 ± 0.9 Hz in control and 8.6 ± 0.9 Hz in BCTC ($p = 0.8$); firing rate was reduced >20% in only 2 of the 17 terminals, the majority showing a modest increase of 5–10% in rate. Furthermore, effects of BCTC on cold-evoked increases in activity were also very modest in the cornea. In 65% of the terminals ($n = 17$), BCTC had no effect on NTI discharge, including maximum response, cooling threshold, and temperature required to silence the cold-induced NTI discharge during rewarming (warming threshold) (Fig. 8*A*, Table 2). The typical burst pattern of NTI discharge during cooling was also unaffected by BCTC (Fig. 8*B*). In the remaining six cold-sensitive endings, the spontaneous activity at 35°C was equally not altered, but the peak frequency value evoked by the cold ramp was reduced between 25 and 50% of the pretreatment values and the mean cold temperature threshold shifted (0.9 ± 0.3°C) to cooler values. The endings exhibiting some degree of sensitivity to BCTC in their response to cooling were undistinguishable from insensitive endings in their mean spontaneous firing frequency, cold threshold temperature, or peak frequency of the cold response before treatment (Table 2).

Expression of TRPM8 channels in corneal thermoreceptor nerve endings and effects of BCTC on menthol-evoked NTI activity

The modest effect of BCTC on cold-evoked activity in corneal endings cannot be attributed to the lack of expression of TRPM8 channels. Indeed, application of menthol to the bath solution at 35°C produced a dose-dependent increase in the basal activity in single cold nerve terminals (Fig. 9*A*). At a concentration of 5 μM, menthol already evoked a significant increase in firing frequency, whereas at 100 μM, its application resulted in a robust effect in all of the CS terminals tested ($n = 22$), with the mean basal frequency more than doubling (Fig. 9*A*,*B*). The EC_{50} of the response to menthol, computed as percentage increase over baseline activity, had a value of 20 μM (Fig. 9*B*). In addition, menthol produced an increase in the maximal cold-evoked response (Fig. 9*C*) and a deviation to warmer temperatures of the threshold temperature required to evoke a cold response (Table 3). These results strongly suggest that TRPM8 channels are functional in all CS nerve terminals of the cornea.

In contrast to the modest inhibition of BCTC on cold-evoked responses in corneal endings, menthol-evoked activity was completely abrogated by BCTC. As shown in Figure 9*A*, the inhibitory effects of BCTC on menthol-evoked NTI activity were fully reversible. In 17 additional nerve endings tested, exposure of the cornea to 10 μM BCTC completely abolished the increase in spontaneous firing, the shift in temperature threshold to cooling pulses, and the enhanced response to cooling evoked by 100 μM menthol (Table 3). After washout of BCTC, the typical potentiating effects of menthol on cold-evoked activity were apparent (Fig. 9*C*). Figure 9*D* summarizes the effects of BCTC on cold-evoked responses in control solution and in the presence of menthol. It is evident that BCTC prevents the sensitizing effects of menthol on the terminal. In addition, this result indicates that the insensitivity of the terminals to BCTC effects during cooling is not attributable to a poor access of the drug or a different pharmacological profile of the receptor at the endings.

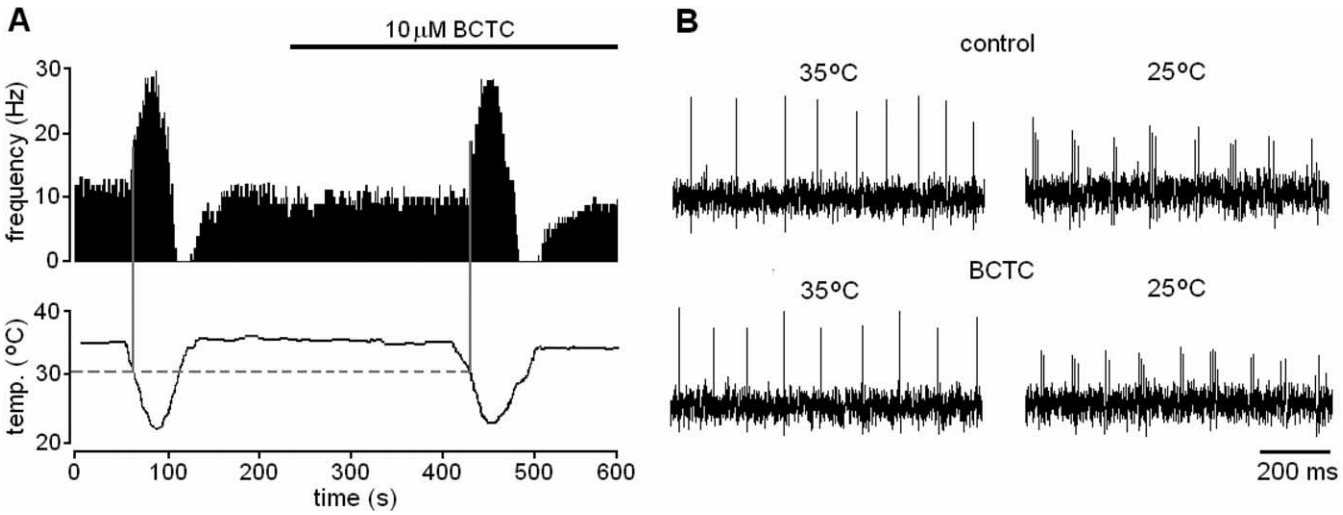

Figure 8. Lack of effect of BCTC on spontaneous and cold-evoked activity in corneal sensory endings. ***A***, Activity in a corneal CS receptor during two consecutive cooling cycles, in control solution, and during perfusion with 10 μM BCTC. The bottom trace shows the temperature of the bathing solution recorded close to the corneal surface. The top trace shows the effect of changing temperature on the frequency of NTIs. The gray vertical bars mark the cold threshold, projected as a dotted line on the temperature scale. Note the lack of effect of 10 μM BCTC on spontaneous and cold-evoked activity. ***B***, Each trace represents a 1 s original record of the terminal shown in ***A***, at the baseline temperature (35°C), and at the peak of the cold response (25°C). Note the complete lack of effect of BCTC, on neither the mean firing frequency nor the pattern of discharge.

Table 2. Effects of 10 μM BCTC on responses to cooling of cold-sensitive nerve terminals

	Baseline activity (Hz)		Cooling threshold (°C)		Maximum response (% of baseline)		Warming threshold (°C)	
	Control	BCTC	Control	BCTC	Control	BCTC	Control	BCTC
All terminals ($n = 17$)	8.5 ± 0.9	8.6 ± 0.9	31.9 ± 0.3	31.2 ± 0.4	272 ± 18	240 ± 20	28.5 ± 1.6	30.0 ± 1.1
Low BCTC sensitivity ($n = 11$)	8.8 ± 1.0	9.2 ± 1.1	31.7 ± 0.3	31.1 ± 0.5	279 ± 25	271 ± 25	29.6 ± 1.7	30.1 ± 1.3
High BCTC sensitivity ($n = 6$)	7.8 ± 1.4	7.5 ± 1.6	32.3 ± 0.4	31.5 ± 0.4*	260 ± 19	182 ± 14*	28.6 ± 0.9	29.3 ± 1.3

Modest effect of SKF96365 on spontaneous and cold-evoked activity in corneal sensory terminals

SKF96365 is another drug with blocking actions on several TRP channels (Clapham et al., 2005; Wang and Poo, 2005), including cold-sensitive currents in primary sensory neurons (Reid et al., 2002). On rat recombinant TRPM8 channels, we found an inhibition of I_{cold} by SKF96365, with an EC_{50} of 0.8 ± 0.1 μM at +80 mV (our unpublished data), indicating that SKF96365 is also a potent blocker of TRPM8 channels. Therefore, we tested the effects of SKF96365 on NTI activity during cooling and menthol application in an additional set of 10 corneal terminals. These results are summarized in Table 4. Qualitatively, the findings were nearly identical to those obtained with BCTC. In 7 of the 10 terminals, application of 20 μM SKF96365 produced no effect on the spontaneous or cold-evoked activity. A representative example is shown in Figure 10*A*. In the remaining three terminals, we observed modest but significant reductions in spontaneous and cold-evoked activity but no shifts in cooling or warming threshold (Table 4). A summary of mean effects of SKF96365 on normalized peak cold response is shown in Figure 10*B*. In contrast, and in full agreement with results obtained with BCTC, the enhancement in activity produced by 100 μM menthol at baseline temperature (~32°C) was fully blocked by 20 μM SKF96365 (Fig. 10*C*). A summary of effects of SKF96365 on normalized menthol-evoked response is shown in Figure 10*D* for 10 corneal terminals.

BCTC does not affect 4-AP-induced cold sensitivity

Micromolar doses of 4-AP can render cold sensitive a large fraction of trigeminal sensory neurons by a mechanism that appears to be independent of TRPM8 expression (Viana et al., 2002). Indeed, as shown in supplemental Figure 3 (available at www.jneurosci.org as supplemental material), this subpopulation of sensory neurons remained insensitive to cold, even if cooling was applied in the presence of 100 μM menthol ($n = 27$). In the absence of 4-AP, the amplitude of cold-evoked signals $[Ca^{2+}]_i$ in these neurons was −4.1 ± 1.2 nM. We asked whether BCTC could affect the 4-AP-induced cold sensitivity of this class of neurons. Thus, after turning these neurons cold sensitive by treatment with 4-AP (75 μM), we tested the effects of 3 μM BCTC on cold-evoked $[Ca^{2+}]_i$ signals. As shown in supplemental Figure 3*D* (available at www.jneurosci.org as supplemental material), 3 μM BCTC had no effect on the amplitude of cold-evoked responses: the $[Ca^{2+}]_i$ increase was 283 ± 46 nM in the presence of 4-AP and 301 ± 59 nM in 4-AP plus BCTC ($p > 0.9$; $n = 28$). Temperature thresholds were also unaffected, with mean values of 27.5 ± 0.6 and 28.0 ± 0.6°C in the absence and presence of BCTC, respectively ($p > 0.4$; $n = 28$). These results indicate that effects of BCTC on cold sensitivity appear to be highly selective for neurons expressing TRPM8 channels in their membrane.

Discussion

In the present study, we explored the contribution of TRPM8 channels to cold sensing in trigeminal ganglion neurons and in corneal receptor endings. First, we characterized the blocking effects of BCTC on cold- and menthol-activated currents in recombinant TRPM8 channels. Subsequently, we used BCTC to probe native TRPM8 channels in the soma and endings of cold thermoreceptors. The results obtained with BCTC were validated with SKF96365, a broader-spectrum TRP channel blocker. We reach the

following main conclusions. First, BCTC is a potent blocker of recombinant and native TRPM8 channels. Second, in the soma of the majority of cultured mouse cold-sensitive trigeminal ganglion neurons, activation of BCTC-sensitive channels, presumably TRPM8 channels, participate in the depolarizing responses, firing, and secondary intracellular calcium elevations evoked by cold. Third, the contribution of TRPM8 to cold responses in sensory neurons spans a wide range of temperatures, with thresholds significantly warmer than those reported in previous expression studies. Fourth, in trigeminal corneal cold receptor endings, TRPM8 plays no role in the spontaneous discharge activity typical of cold thermoreceptors. Fifth, blockade of TRPM8 channels at corneal sensory endings produces a selective reduction of menthol-mediated activation, with only a minor impairment in their ability to transduce cold stimuli.

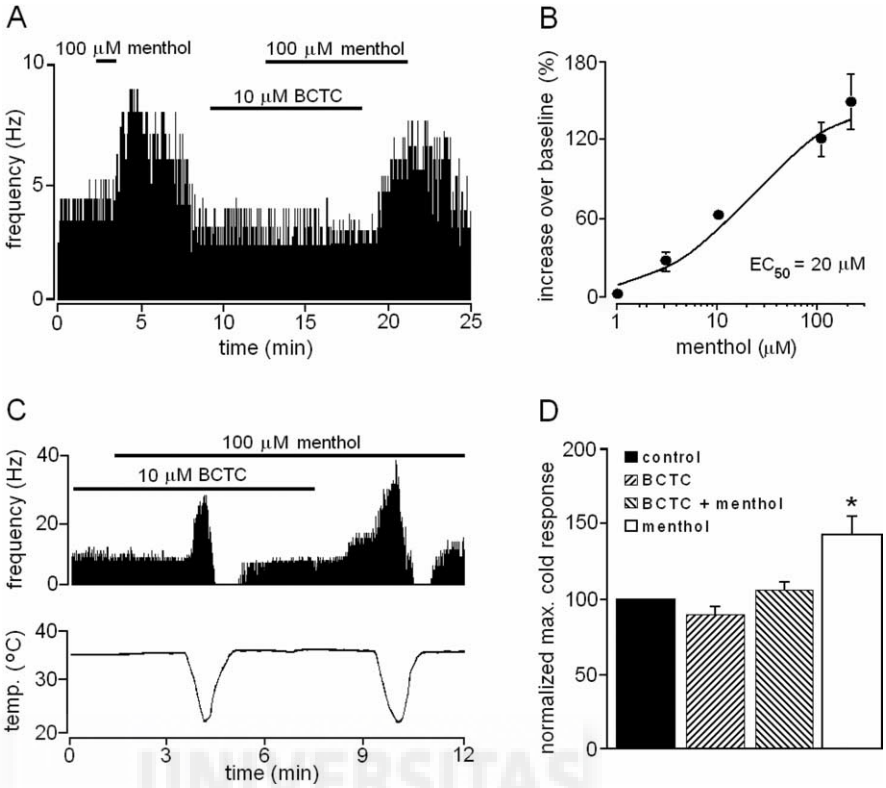

Figure 9. Effect of BCTC on menthol-evoked NTI activity in corneal cold thermoreceptor nerve endings. ***A***, Application of 10 μM BCTC blocks the enhancement in NTI activity produced by 100 μM menthol. ***B***, Dose–response curve of menthol effects on the frequency of ongoing NTI activity in corneal cold-sensitive receptors. Data have been fitted to the Hill equation (EC_{50} of 20 μM; Hill coefficient of 0.9). ***C***, Illustrative example of the effect of 10 μM BCTC on menthol-evoked NTI activity in a CS receptor. In the presence of BCTC, application of menthol did not augment ongoing NTI activity. After BCTC removal, the spontaneous NTI discharge nearly doubled, and the cold-evoked activity also increased. ***D***, Summary of menthol (100 μM) and BCTC (10 μM) effects on cold-evoked responses ($n = 17$). Results have been normalized to those obtained in control solution. Only the response in menthol is significantly different from the rest (ANOVA test, $^*p < 0.05$).

Specific effects of BCTC on TRPM8 channels

The conclusions of this study are critically dependent on the postulate that BCTC effects on cold sensing are attributable to a specific blockade of TRPM8 channels. This view is supported by several independent pieces of evidence. BCTC was identified as a potent and selective blocker of TRPV1 channels (Valenzano et al., 2003). Subsequent work showed that BCTC is also a full blocker of menthol-evoked responses in mouse (Behrendt et al., 2004) and human (Weil et al., 2005) TRPM8 channels. We confirmed the effects of BCTC on menthol-evoked signals in mouse and guinea pig TRPM8 channels and extended these results to cold-evoked currents. According to the present data, BCTC is the most potent blocker of TRPM8 channels reported to date. Other TRPV1 blockers, such as capsazepine, also block TRPM8 channels, albeit less potently (Reid et al., 2002; Behrendt et al., 2004; Weil et al., 2005), suggesting a partial overlap in ligand actions on these two TRP channels. The blocking action of BCTC on TRPV1 channels should not affect our interpretation because their threshold temperature (~42°C) (Caterina et al., 1997) is much higher than the temperatures reached during our stimulation protocol.

In an extensive screen of BCTC effects on ion channels and receptors performed by Valenzano et al. (2003), BCTC proved to be a highly specific TRPV1 antagonist (actions on TRPM8 were not tested in that study). Furthermore, BCTC does not block agonist-evoked (α-phorbol 12,12-didecanoate) $[Ca^{2+}]_i$ signals in TRPV4-transfected cells (Behrendt et al., 2004). Additionally, we show that BCTC has minimal effects on the intrinsic excitability and action potential parameters of CS trigeminal ganglion neurons and nerve terminals. Finally, in our experiments, cold sensitivity depending on the activation of ion channels other than TRPM8 was completely unaffected by BCTC. In summary, the specificity and reversibility of BCTC blockade of certain thermoTRP channels (i.e., TRPV1 and TRPM8) make this drug a very useful tool to analyze their role in temperature transduction and nociception.

The molecular mechanism of action of BCTC still needs to be fully identified. BCTC produces an apparent dose-dependent shift in temperature activation threshold of menthol- and cold-evoked currents. At neutral pH, the ionization of BCTC is very low (with an estimated ratio between charged vs neutral forms <0.0002). This suggests that the apparent voltage dependence of TRPM8 block is not attributable to a direct interaction of BCTC with charged particles within the membrane electric field.

Contribution of TRPM8 to cold sensing in the soma of cultured primary sensory neurons

BCTC produced a powerful inhibition of cold-evoked responses in the soma of the majority (>90%) of mouse CS trigeminal ganglion neurons in culture, and this inhibition was specific to the $TRPM8^+$ subpopulation of neurons. This percentage appeared to be somewhat lower in guinea pigs. The inhibition by BCTC of the response to cooling was manifested even in the case of neurons activated by very small temperature decreases (i.e., low-threshold cold thermoreceptors). This strongly suggests that the functional operating range of native TRPM8 channels in CS neurons is far warmer (i.e., they have a lower threshold) than inferred by measurements obtained in expression studies (for review, see McKemy, 2005; Reid, 2005), spanning the entire physiological temperature range of native cold receptors (Hensel, 1981). Recently, we showed that the temperature threshold of menthol- and cold-sensitive, $TRPM8^+$ cultured trigeminal ganglion neurons was much lower than that of hippocampal neurons

Table 3. Effects of 10 μM BCTC on responses to cooling of cold-sensitive nerve terminals in the presence of 100 μM menthol

	Baseline activity (Hz)		Cooling threshold (°C)		Maximum response (% of baseline)		Warming threshold (°C)	
	Control	BCTC	Control	BCTC	Control	BCTC	Control	BCTC
All terminals ($n = 17$)	12.9 ± 1.5	7.9 ± 0.9*	33.3 ± 0.2	28.5 ± 1.6	262 ± 19	300 ± 19	32.9 ± 0.9	30.1 ± 1.0*
Low BCTC sensitivity ($n = 11$)	13.3 ± 1.9	9.4 ± 1.4*	33.2 ± 0.2	29.7 ± 1.8	276 ± 26	308 ± 22	32.9 ± 1.0	30.4 ± 0.9*
High BCTC sensitivity ($n = 6$)	12.2 ± 2.2	7.1 ± 1.5*	33.4 ± 0.3	28.6 ± 0.9	240 ± 16	274 ± 31	32.9 ± 0.9	29.4 ± 1.1*

Table 4. Effects of 20 μM SKF96365 on responses to cooling of cold-sensitive nerve terminals

	Baseline activity (Hz)		Cooling threshold (°C)		Maximum response (% of baseline)		Warming threshold (°C)	
	Control	SKF	Control	SKF	Control	SKF	Control	SKF
All terminals ($n = 10$)	7.8 ± 0.8	7.0 ± 0.9	30.1 ± 0.5	29.2 ± 0.8	295 ± 27	291 ± 35	27.1 ± 1.1	25.7 ± 1.1
Low SKF sensitivity ($n = 7$)	7.0 ± 0.9	7.1 ± 1.3	30.5 ± 0.7	29.1 ± 1.1	317 ± 35	349 ± 28	27.6 ± 1.5	25.8 ± 1.4
High SKF sensitivity ($n = 3$)	9.6 ± 0.8	6.8 ± 1.0*	29.4 ± 0.8	29.4 ± 1.0	245 ± 22	155 ± 6*	25.8 ± 0.8	25.5 ± 1.9

Baseline temperature, 32.0 ± 0.6°C (29.0–35.8°C). Minimum temperature during cooling, 22.1 ± 0.3°C (20.8–23.5°C). *$p < 0.05$, paired t test.

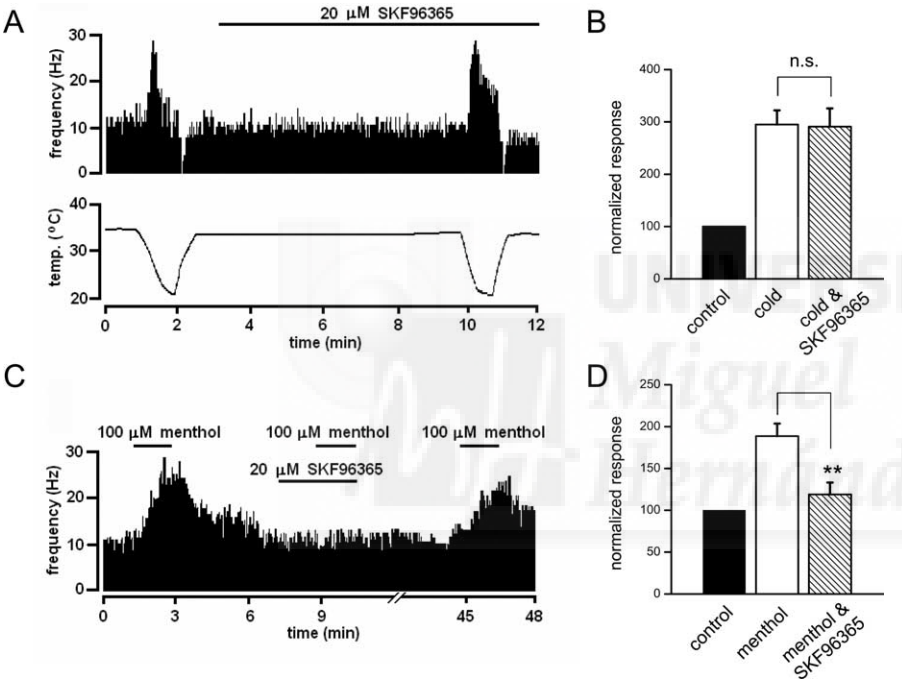

Figure 10. Effect of SKF96365 on cold and menthol-evoked NTI activity in corneal cold thermoreceptor nerve endings. ***A***, Activity in a corneal CS receptor during two consecutive cooling cycles, in control solution, and during perfusion with 20 μM SKF96365. The bottom trace shows the temperature of the bathing solution recorded close to the corneal surface. The top trace shows the effect of changing temperature on the frequency of NTIs. Note the lack of effect of 20 μM SKF96365 on spontaneous and cold-evoked activity. ***B***, Summary histogram of effects of 20 μM SKF96365 on cold-evoked activity ($n = 10$). For each terminal, cold-evoked activity has been normalized to the mean frequency at static temperature (32–34°C) before application of SKF96365. The drug did not produce a significant inhibition of the cold-evoked response. ***C***, Application of 20 μM SKF96365 blocks reversibly the enhancement in NTI activity produced by 100 μM menthol at a baseline temperature of 34°C. ***D***, Summary histogram of effects of 20 μM SKF96365 on menthol-evoked activity ($n = 10$). For each terminal, menthol-evoked activity has been normalized to the mean frequency at static temperature (32–34°C) in control solution, before application of SKF96365. The drug produce a highly significant inhibition of the menthol-evoked response (**$p < 0.001$).

transiently transfected with recombinant TRPM8 channels (de la Pena et al., 2005) and hypothesized that TRPM8 channels could be modulated intrinsically to shift their activation threshold. Thus far, very little is known about sensitizing agents of native TRPM8 channels. Elevated intracellular phosphatidylinositol-4, 5-biphosphate levels increase the amplitude of TRPM8 currents in transfected cells (Liu and Qin, 2005; Rohacs et al., 2005). Also, acute application of nerve growth factor to DRG neurons shifts their cold thresholds to warmer values (Reid et al., 2002). Another modulatory mechanism of TRPM8 channels is their PKC-dependent phosphorylation state (Premkumar et al., 2005).

Nonessential role of TRPM8 channels in cold-sensitive nerve terminals of the cornea

The basal activity of cold thermoreceptor fibers has been attributed to a rhythmic oscillation of membrane potential in their endings that generates repetitive firing of action potentials (Braun et al., 1980). The identification of TRPM8 as a thermosensitive channel expressed by cold- and menthol-sensitive primary sensory neurons led to the proposal that cooling increases the opening probability of TRPM8, thus generating a depolarizing inward current that augments the firing frequency of cold thermoreceptor terminals (for review, see McKemy, 2005; Reid, 2005).

Our work in the isolated cornea confirms previous studies showing that this tissue is innervated by cold- and menthol-sensitive sensory fibers (Gallar et al., 1993; Brock et al., 2001; Acosta et al., 2001; Carr et al., 2003) that exhibit rhythmic ongoing activity and response characteristics typical of innocuous cold receptor fibers previously described in the trigeminal territory (Hensel and Wurster, 1970; Schafer et al., 1988). BCTC did not affect the spontaneous activity of corneal cold receptor endings. The inhibitory effects of SKF96365 were also very modest. Such static discharge encodes the absolute temperature of the exposed surface (Carr et al., 2003). Therefore, our data indicate that TRPM8 channels present in the endings are not responsible for their background impulse activity, suggesting that activity in the basal oscillator is essentially independent of TRPM8 channels. Cold-sensitive neurons have a strong expression of other inward currents that could play a role in spontaneous firing, including pacemaker channels of the HCN family and low-threshold calcium channels (Viana et al., 2002).

In approximately two-thirds of the corneal cold receptor end-

ings, increases in NTI firing frequency evoked by cooling pulses were not modified by saturating concentrations of BCTC or SKF96365. In the remaining endings, both drugs caused a very modest reduction of the peak firing frequency evoked by cooling. In contrast, the strong stimulating effect of menthol on NTI discharges, observed in all cold receptor endings of the cornea, was fully blocked by BCTC and SKF96365. This indicates first that the endings express TRPM8 channels that are fully accessible to the drug and also that these channels play at best a minor role in the generation of the augmented impulse discharges evoked by mild temperature reductions.

It is unlikely that the resistance of guinea pig cold-sensitive terminals to blockade by BCTC can be attributed to species differences in the pharmacological profile of TRPM8 channels. Menthol-evoked responses in cold-sensitive neurons were abrogated by even lower concentrations of BCTC, also in guinea pigs. Furthermore, all cold-sensitive endings in the cornea are excited by menthol, and this sensitivity is also fully blocked by BCTC and SKF96365, strongly suggesting that TRPM8 activity in the terminals is also abrogated. Remarkably, nearly all BCTC-insensitive neurons were also insensitive to menthol, strongly suggesting the presence of a TRPM8-independent cold-sensing mechanism. Thus, the most parsimonious explanation of our results is that, in the corneal terminals, other molecular cold sensors coexpress with TRPM8, operating in the same temperature range and overlapping in function. Several background K^+ channels are extremely temperature sensitive, are functional in the same temperature range, and are expressed in sensory neurons, making them obvious candidates to function as additional cold sensors (Maingret et al., 2000; Reid and Flonta, 2001; Viana et al., 2002; Kang et al., 2005).

We consider an alternative explanation for the low sensitivity of cold-sensitive corneal terminals to the blocking actions of BCTC and SKF96365. Native TRPM8 channels in the terminal may occur in a molecular configuration that renders them highly temperature sensitive but resistant to pharmacological blockade. The existence of splice variants with different functional properties has already been reported for other thermoTRP channels in trigeminal neurons (Lu et al., 2005). These alternative explanations can only be addressed with other experimental paradigms, such as the analysis of TRPM8 knock-out mice, specially those lines with spatially restricted and/or temporally conditioned gene inactivation. According to our first hypothesis (coexpression of molecular cold sensors), these animals would show functional deficits in peripheral cold sensing much milder than predicted from results derived from cultured cells, whereas the alternative hypothesis predicts a full inhibition at terminals as well.

Role of TRPM8 channels in cold transduction

We find that TRPM8 is expressed in CS neurons across the entire spectrum of temperature thresholds, including those into the noxious range. The low-threshold neurons were less likely to be silenced by BCTC, suggesting the presence of an additional population of temperature-sensitive channels in the soma of these neurons. The expression of TRPM8 channels in higher-threshold neurons is consistent with several psychophysical studies suggesting that TRPM8 channels may play a role in human cold nociception. Thus, acute application of menthol to the skin or mucosae can produce a painful sensation in addition to a cold sensation (Cliff and Green, 1994; Acosta et al., 2001; Wasner et al., 2004; Namer et al., 2005). In addition, a large percentage of sensory neurons have a dual response to TRPV1 and TRPM8 agonists (McKemy et al., 2002; Reid et al., 2002; Viana et al., 2002; Xing et al., 2006).

In summary, our results show that the peripheral receptor endings of CS neurons contain TRPM8 channels but that inhibition of these channels does not impair significantly their capacity to transduce or encode cold stimuli. A similar paradox between effects of ion-channel disruption at the level of soma and terminals for temperature sensitivity is also apparent for another thermoTRP. In studies with TRPV1 null mice, deficits in heat sensitivity are only apparent in the soma of cultured sensory neurons (Caterina et al., 2000; Davis et al., 2000), in contrast to the persistence of normal heat responses in afferent C-fibers in skin–nerve preparations (Woodbury et al., 2004; Zimmermann et al., 2005), and the lack of differences in behavioral tests of acute thermal nociception between wild-type and TRPV1$^{-/-}$ animals (Caterina et al., 2000; Davis et al., 2000; Almasi et al., 2003).

As pointed out by Gerald Edelman, "multiple genes contribute in an overlapping manner to the construction of each phenotypic feature undergoing selection" (Edelman and Gally, 2001). Thermal sensing is a conserved attribute of all animal species, playing an essential role in their behavior, and must be under strong evolutionary pressure. Thus, from an evolutionary perspective, it is understandable and meaningful to have an overlapping functional role of various thermosensitive channels in individual peripheral thermoreceptors as suggested by our findings.

References

Acosta MC, Belmonte C, Gallar J (2001) Sensory experiences in humans and single-unit activity in cats evoked by polymodal stimulation of the cornea. J Physiol (Lond) 534:511–525.

Almasi R, Petho G, Bolcskei K, Szolcsanyi J (2003) Effect of resiniferatoxin on the noxious heat threshold temperature in the rat: a novel heat allodynia model sensitive to analgesics. Br J Pharmacol 139:49–58.

Babes A, Zorzon D, Reid G (2004) Two populations of cold-sensitive neurons in rat dorsal root ganglia and their modulation by nerve growth factor. Eur J Neurosci 20:2276–2282.

Bandell M, Story GM, Hwang SW, Viswanath V, Eid SR, Petrus MJ, Earley TJ, Patapoutian A (2004) Noxious cold ion channel TRPA1 is activated by pungent compounds and bradykinin. Neuron 41:849–857.

Behrendt HJ, Germann T, Gillen C, Hatt H, Jostock R (2004) Characterization of the mouse cold-menthol receptor TRPM8 and vanilloid receptor type-1 VR1 using a fluorometric imaging plate reader (FLIPR) assay. Br J Pharmacol 141:737–745.

Brauchi S, Orio P, Latorre R (2004) Clues to understanding cold sensation: thermodynamics and electrophysiological analysis of the cold receptor TRPM8. Proc Natl Acad Sci USA 101:15494–15499.

Braun HA, Bade H, Hensel H (1980) Static and dynamic discharge patterns of bursting cold fibers related to hypothetical receptor mechanisms. Pflügers Arch 386:1–9.

Brock J, Pianova S, Belmonte C (2001) Differences between nerve terminal impulses of polymodal nociceptors and cold sensory receptors of the guinea-pig cornea. J Physiol (Lond) 533:493–501.

Brock JA, McLachlan EM, Belmonte C (1998) Tetrodotoxin-resistant impulses in single nociceptor nerve terminals in guinea-pig cornea. J Physiol 512:211–217.

Cabanes C, Viana F, Belmonte C (2003) Differential thermosensitivity of sensory neurons in the guinea pig trigeminal ganglion. J Neurophysiol 90:2219–2231.

Carr RW, Pianova S, Fernandez J, Fallon JB, Belmonte C, Brock JA (2003) Effects of heating and cooling on nerve terminal impulses recorded from cold-sensitive receptors in the guinea-pig cornea. J Gen Physiol 121:427–439.

Caterina MJ, Schumacher MA, Tominaga M, Rosen TA, Levine JD, Julius D (1997) The capsaicin receptor: a heat-activated ion channel in the pain pathway. Nature 389:816–824.

Caterina MJ, Leffler A, Malmberg AB, Martin WJ, Trafton J, Petersen-Zeitz KR, Koltzenburg M, Basbaum AI, Julius D (2000) Impaired nociception and pain sensation in mice lacking the capsaicin receptor. Science 288:306–313.

Chen CC, Rainville P, Bushnell MC (1996) Noxious and innocuous cold discrimination in humans: evidence for separate afferent channels. Pain 68:33–43.

Clapham DE, Julius D, Montell C, Schultz G (2005) International Union of

Pharmacology. XLIX. Nomenclature and structure-function relationships of transient receptor potential channels. Pharmacol Rev 57:427–450.
Cliff MA, Green BG (1994) Sensory irritation and coolness produced by menthol: evidence for selective desensitization of irritation. Physiol Behav 56:1021–1029.
Craig AD, Chen K, Bandy D, Reiman EM (2000) Thermosensory activation of insular cortex. Nat Neurosci 3:184–190.
Davis JB, Gray J, Gunthorpe MJ, Hatcher JP, Davey PT, Overend P, Harries MH, Latcham J, Clapham C, Atkinson K, Hughes SA, Rance K, Grau E, Harper AJ, Pugh PL, Rogers DC, Bingham S, Randall A, Sheardown SA (2000) Vanilloid receptor-1 is essential for inflammatory thermal hyperalgesia. Nature 405:183–187.
de la Pena E, Malkia A, Cabedo H, Belmonte C, Viana F (2005) The contribution of TRPM8 channels to cold sensing in mammalian neurones. J Physiol (Lond) 567:415–426.
Edelman GM, Gally JA (2001) Degeneracy and complexity in biological systems. Proc Natl Acad Sci USA 98:13763–13768.
Gallar J, Pozo MA, Tuckett RP, Belmonte C (1993) Response of sensory units with unmyelinated fibres to mechanical, thermal and chemical stimulation of the cat's cornea. J Physiol (Lond) 468:609–622.
Hensel H (1981) Thermoreception and temperature regulation. Monogr Physiol Soc 38:1–321.
Hensel H, Wurster RD (1970) Static properties of cold receptors in nasal area of cats. J Neurophysiol 33:271–275.
Hensel H, Zotterman Y (1951) The response of the cold receptors to constant cooling. Acta Physiol Scand 22:96–113.
Heppelmann B, Messlinger K, Neiss WF, Schmidt RF (1990) Ultrastructural three-dimensional reconstruction of group III and group IV sensory nerve endings ("free nerve endings") in the knee joint capsule of the cat: evidence for multiple receptive sites. J Comp Neurol 292:103–116.
Hill K, McNulty S, Randall AD (2004) Inhibition of TRPM2 channels by the antifungal agents clotrimazole and econazole. Naunyn Schmiedebergs Arch Pharmacol 370:227–237.
Hille B (2001) Ion channels of excitable membranes. Sunderland, MA: Sinauer.
Jordt SE, McKemy DD, Julius D (2003) Lessons from peppers and peppermint: the molecular logic of thermosensation. Curr Opin Neurobiol 13:487–492.
Jordt SE, Bautista DM, Chuang HH, McKemy DD, Zygmunt PM, Hogestatt ED, Meng ID, Julius D (2004) Mustard oils and cannabinoids excite sensory nerve fibres through the TRP channel ANKTM1. Nature 427:260–265.
Kang D, Choe C, Kim D (2005) Thermosensitivity of the two-pore domain K^+ channels TREK-2 and TRAAK. J Physiol (Lond) 564:103–116.
LaMotte RH, Thalhammer JG (1982) Response properties of high-threshold cutaneous cold receptors in the primate. Brain Res 244:279–287.
Liu BY, Qin F (2005) Functional control of cold- and menthol-sensitive TRPM8 ion channels by phosphatidylinositol 4,5-bisphosphate. J Neurosci 25:1674–1681.
Lu G, Henderson D, Liu L, Reinhart PH, Simon SA (2005) TRPV1b, a functional human vanilloid receptor splice variant. Mol Pharmacol 67:1119–1127.
Maingret F, Lauritzen I, Patel AJ, Heurteaux C, Reyes R, Lesage F, Lazdunski M, Honore E (2000) TREK-1 is a heat-activated background K^+ channel. EMBO J 19:2483–2491.
McKemy DD (2005) How cold is it? TRPM8 and TRPA1 in the molecular logic of cold sensation. Mol Pain 1:16.
McKemy DD, Neuhausser WM, Julius D (2002) Identification of a cold receptor reveals a general role for TRP channels in thermosensation. Nature 416:52–58.
Namer B, Seifert F, Handwerker HO, Maihofner C (2005) TRPA1 and TRPM8 activation in humans: effects of cinnamaldehyde and menthol. NeuroReport 16:955–959.
Nealen ML, Gold MS, Thut PD, Caterina MJ (2003) TRPM8 mRNA is expressed in a subset of cold-responsive trigeminal neurons from rat. J Neurophysiol 90:515–520.
Nilius B, Prenen J, Vennekens R, Hoenderop JG, Bindels RJ, Droogmans G (2001) Pharmacological modulation of monovalent cation currents through the epithelial Ca^{2+} channel ECaC1. Br J Pharmacol 134:453–462.
Okazawa M, Takao K, Hori A, Shiraki T, Matsumura K, Kobayashi S (2002) Ionic basis of cold receptors acting as thermostats. J Neurosci 22:3994–4001.
Patapoutian A, Peier AM, Story GM, Viswanath V (2003) ThermoTRP channels and beyond: mechanisms of temperature sensation. Nat Rev Neurosci 4:529–539.
Peier AM, Moqrich A, Hergarden AC, Reeve AJ, Andersson DA, Story GM, Earley TJ, Dragoni I, McIntyre P, Bevan S, Patapoutian A (2002) A TRP channel that senses cold stimuli and menthol. Cell 108:705–715.
Premkumar LS, Raisinghani M, Pingle SC, Long C, Pimentel F (2005) Downregulation of transient receptor potential melastatin 8 by protein kinase C-mediated dephosphorylation. J Neurosci 25:11322–11329.
Reid G (2005) ThermoTRP channels and cold sensing: what are they really up to? Pflügers Arch 451:250–263.
Reid G, Flonta M (2001) Cold transduction by inhibition of a background potassium conductance in rat primary sensory neurones. Neurosci Lett 297:171–174.
Reid G, Amuzescu B, Zech E, Flonta M (2001) A system for applying rapid warming or cooling stimuli to cells during patch clamp recording or ion imaging. J Neurosci Methods 111:1–8.
Reid G, Babes A, Pluteanu F (2002) A cold- and menthol-activated current in rat dorsal root ganglion neurones: properties and role in cold transduction. J Physiol (Lond) 545:595–614.
Rohacs T, Lopes CM, Michailidis I, Logothetis DE (2005) PI(4,5)P2 regulates the activation and desensitization of TRPM8 channels through the TRP domain. Nat Neurosci 8:626–634.
Roza C, Belmonte C, Viana F (2006) Cold sensitivity in axotomized fibers of experimental neuromas in mice. Pain 120:24–35.
Schafer K, Braun HA, Kurten L (1988) Analysis of cold and warm receptor activity in vampire bats and mice. Pflügers Arch 412:188–194.
Simone DA, Kajander KC (1997) Responses of cutaneous A-fiber nociceptors to noxious cold. J Neurophysiol 77:2049–2060.
Story GM, Peier AM, Reeve AJ, Eid SR, Mosbacher J, Hricik TR, Earley TJ, Hergarden AC, Andersson DA, Hwang SW, McIntyre P, Jegla T, Bevan S, Patapoutian A (2003) ANKTM1, a TRP-like channel expressed in nociceptive neurons, is activated by cold temperatures. Cell 112:819–829.
Thut PD, Wrigley D, Gold MS (2003) Cold transduction in rat trigeminal ganglia neurons in vitro. Neuroscience 119:1071–1083.
Valenzano KJ, Grant ER, Wu G, Hachicha M, Schmid L, Tafesse L, Sun Q, Rotshteyn Y, Francis J, Limberis J, Malik S, Whittemore ER, Hodges D (2003) *N*-(4-tertiarybutylphenyl)-4-(3-chloropyridin-2-yl)tetrahydropyrazine −1(2*H*)-carbox-amide (BCTC), a novel, orally effective vanilloid receptor 1 antagonist with analgesic properties. I. in vitro characterization and pharmacokinetic properties. J Pharmacol Exp Ther 306:377–386.
Viana F, de la Pena E, Belmonte C (2002) Specificity of cold thermotransduction is determined by differential ionic channel expression. Nat Neurosci 5:254–260.
Viana F, de la Pena E, Pecson B, Schmidt RF, Belmonte C (2001) Swelling-activated calcium signalling in cultured mouse primary sensory neurons. Eur J Neurosci 13:722–734.
Voets T, Droogmans G, Wissenbach U, Janssens A, Flockerzi V, Nilius B (2004) The principle of temperature-dependent gating in cold- and heat-sensitive TRP channels. Nature 430:748–754.
Wang GX, Poo MM (2005) Requirement of TRPC channels in netrin-1-induced chemotropic turning of nerve growth cones. Nature 434:898–904.
Wasner G, Schattschneider J, Binder A, Baron R (2004) Topical menthol–a human model for cold pain by activation and sensitization of C nociceptors. Brain 127:1159–1171.
Weil A, Moore SE, Waite NJ, Randall A, Gunthorpe MJ (2005) Conservation of functional and pharmacological properties in the distantly related temperature sensors TRPV1 and TRPM8. Mol Pharmacol 68:518–527.
Woodbury CJ, Zwick M, Wang S, Lawson JJ, Caterina MJ, Koltzenburg M, Albers KM, Koerber HR, Davis BM (2004) Nociceptors lacking TRPV1 and TRPV2 have normal heat responses. J Neurosci 24:6410–6415.
Xing H, Ling J, Chen M, Gu JG (2006) Chemical and cold sensitivity of two distinct populations of TRPM8-expressing somatosensory neurons. J Neurophysiol 95:1221–1230.
Yarnitsky D, Ochoa JL (1991) Warm and cold specific somatosensory systems. Psychophysical thresholds, reaction times and peripheral conduction velocities. Brain 114:1819–1826.
Zimmermann K, Leffler A, Fischer MM, Messlinger K, Nau C, Reeh PW (2005) The TRPV1/2/3 activator 2-aminoethoxydiphenyl borate sensitizes native nociceptive neurons to heat in wildtype but not TRPV1 deficient mice. Neuroscience 135:1277–1284.

UNIVERSITAS
Miguel
Hernández

UNIVERSITAS
Miguel
Hernández